



INNERVATION OF THE TEMPOROMANDIBULAR JOINT
AN EXPERIMENTAL ANIMAL MODEL USING
AUSTRALIAN MERINO SHEEP

ABDOLGHAFAR TAHMASEBI-SARVESTANI, B.Sc, M.Sc.

Thesis submitted for the degree of
DOCTOR OF PHILOSOPHY

In

The Department of Anatomical Sciences
The University of Adelaide (Faculty of Medicine),
Adelaide, South Australia, 5005

April, 1997

*This thesis is dedicated to my wife Roghyeh and our
three children Taherah, Raziieh and Marzieh*

STATEMENT

This work contains no material which has been accepted for the award of any other degree or diploma in any University or other tertiary institution and, to the best of my knowledge and belief, contains no material previously published or written by another person, except where the due reference has been made in the text.

I give consent to this copy of my thesis, when deposited in the University library, being available for loan and photocopying.

Signed

Date

30/4/97

ACKNOWLEDGMENTS

I am greatly indebted to my supervisors Dr. Ray Tedman and Professor Alastair Goss who first introduced me to this field of study and providing me with the opportunity to carry out this work. I wish to thank them for their constant interest and guidance throughout the course of this study.

I am also indebted to the scholarship committee of the Shiraz Medical Science University and Ministry of Health and Medical Education, Iran for granting me a 4 year scholarship to study at the University of Adelaide.

I thank Professor Goss and the Japanese Surgical Research team for their expertise in surgical animal models, and Professor July Polak and Dr Mika Hukkanen, Royal Postgraduate Medical School London University for their expertise in immunohistochemistry and for providing some of the antisera used in the neuropeptide studies. I would also like to thank Professor Ian Gibbins, Department of Anatomy and Histology of the Flinders Medical Centre for, without the use of his laboratories, materials, and expertise, the double and triple labelling parts of the immunocytochemical work would not have occurred. I also owe many thanks to Susan Matthew, a senior laboratory officer for her skilful technical assistance in double and triple immunocytochemistry. I am grateful to Dr S Robinson and Mr Don Bigham, Department of Obstetrics and Gynaecology, for permitting use of their Image Analysis equipment. I also thank the team of the Feto-Maternal Physiology group, Department of Physiology, for providing me fetal sheep used for Chapter 4. I thank Sandra Powel, for her advice in the histological preparations of some of the tissues and Patricia Little and Alma Bennett, Institute of Medical and Veterinary Research for their help in the animal handling.

My warmest thanks go to many people in the Department of Anatomical Science, University of Adelaide for their skilful technical advice and guidance, especially Mrs, G Hermanis, Mrs, N Gagliardi, Mr C Leigh and Mr R Murphy. I thank Associate Professor WG Breed for permitting the use of his fluorescence microscope, Dr M Ghabriel and Mrs G Hermanis for reading various parts of this thesis. I thank Professor M Henneberg for his constructive criticism and encouragement during preparation and submission of this thesis. I would also like to thank Ms R Norris for her computing advice, Mrs J Haynes and Mrs E Peirce for organising casual teaching for me.

My sincere thanks also go to Mr John Cecchin, the Laboratory Manager, Department of Anatomical Sciences for his quick response in providing laboratory materials and equipment whenever needed. I thank Mrs Julia Brazier the department secretary for unfailing assistance involving her secretarial skills throughout the time of my study in the Department of Anatomical Sciences.

My thanks also go to Dr Bruce Firth for his kindness and his openness to me from the beginning to the end of this study in the department. I also thank him for permitting me the use of his computer whenever I needed. Thanks are extended to Professor J Priedkalns, Dr R A Barbour Dr Adam Locket, Dr J Trahair, Dr J Kumaratilake, Dr B Callaghan, Dr N Edwin and Mr C Jones for their encouragement.

I am also indebted to my fellow Ph.D students for trusting me and selecting me as their representative in the Department throughout the 1995 and 1996 academic years. I thank them for their inspiration and encouragement throughout the course of this study. These people include, Dr Lillian Soon, Ms Susan Rehorek and Mr Robert Moyer. I am truly grateful for their friendship and happiness during this study.

My warmest thanks again go to my supervisor Dr Ray Tedman for his patience in correcting and reviewing this thesis. His invaluable help made it possible to finish this work.

Finally, my special thanks go to my wife Roghyeh and our three children, Taherah, Razieh and Marzieh for their patience and understanding during our busy student life period in Adelaide.

ABSTRACT

The present study provides a detailed account of the anatomical and neurohistological structure of the temporomandibular joint (TMJ) in foetal and adult Australian Merino sheep. The purpose is to describe the innervation of the joint and to determine the possible roles of both afferent receptor structures and neuropeptides in the pathophysiology of experimentally induced osteoarthritis.

A total of 33 adult and 7 fetal Australian Merino sheep were used for this investigation. The surgical procedure developed by Professor Goss and his Japanese colleagues was used to induce osteoarthritis. Gold chloride and glyoxylic acid as well as single, double, and triple labelling immunocytochemical techniques were used to localise nerves and their peptide distribution in normal, experimental and in late gestation fetal TMJ. Transmission electron microscopy was employed to examine the ultrastructural details of the morphology of nerves supplying the normal adult TMJ. Scanning electron microscopy was applied to study the surface topography of normal and arthritic joints. In addition, laser scanning confocal microscopy was used whenever more specific details of neural structures were required. Nerve fibre densities were quantified using image analysis of immunofluorescent staining and tested statistically using a general linear model.

Except for some differences in the shape of the mandibular condyle and glenoid fossa, the macroscopic and microscopic appearance of the sheep TMJ was generally similar to that described for other mammals. The mandibular condyle separated from the glenoid fossa of the temporal bone by an articular disc. The peripheral part of the disc merged with the capsule, thus separating upper and lower joint compartments. The condylar head and temporal surface of the joint consisted of a relatively acellular fibrous articular surface and underlying cartilage.

The auriculotemporal, deep temporal, and masseteric branches of the mandibular division of the trigeminal nerve contributed branches to the TMJ. Nerve fibres supplying the joint covered almost the entire range of diameters from large myelinated (A alpha-), through small myelinated (A delta-) to small unmyelinated (C-) fibres. The majority of fibres were myelinated with diameters $<6 \mu\text{m}$. The capsule, synovial membrane and peripheral part of the disc contained nerve fibres immunoreactive (IR) to antisera for PGP 9.5, and neuropeptides SP and CGRP. Noradrenergic fibres were also demonstrated mainly in the capsule. In addition, Ruffini, paciniform-type and Golgi organ nerve endings were located in the capsule with the highest density of nerve endings occurring at the site of attachment of the disc to the capsule. The highest density of autonomic fibres was in the anterior capsule and the highest density of sensory fibres was in the synovium and capsule of the anterior region of the TMJ in normal adult sheep.

The fetal sheep TMJ at 140 days gestation age (full term=157) was not fully developed. The superior joint compartment was present but the inferior joint cavity was incomplete and confined to a narrow region anteriorly, near the capsule/disc junction, but over most of the mandibular condyle the disc was continuous with the cellular fibrous tissue on the superior surface of the condyle. Some small clefts indicated the location of the developing inferior joint cavity.

The study showed that the pattern of neuropeptide-immunoreactive fibre distribution in the fetal sheep TMJ disc differed from that of the adult TMJ disc. At 140 days gestation the entire disc was innervated by SP-, CGRP- and PGP 9.5-IR fibres, while in adult sheep the disc was innervated only in the peripheral part at the site of attachment to the capsule. This supported the view that the TMJ disc is innervated during fetal development but at later ages these nerves degenerate and persist only in the peripheral disc. Furthermore, CGRP- and SP- immunoreactivity suggested that these nerve fibres

in fetal sheep TMJ disc were sensory, for nociception and perhaps mechanoreception, and might also have had a role in regulation of vascular supply to joint tissues through the release of SP and CGRP in joint tissues. The lack of receptor endings, other than free nerve endings in the late gestation of fetal sheep used in this study might have been a reflection of anatomical and perhaps functional immaturity of the TMJ, as reflected in the gross and microscopic appearance of the disc, the inferior joint compartment and articular surface of the condyle at this stage. Thus the present findings support the view that weight bearing postnatally might influence the distribution of receptor endings in joints and that mechanical stimuli might be necessary for the maturation of receptor endings postnatally.

The arthritic TM joints were characterised by abnormalities mainly in condylar surfaces. Macroscopically, the articulating surface of the temporal fossa appeared normal. Erosions and outgrowths were observed on all condylar surfaces, but these deformities were different from one animal to another, even between the left and right joints of the same animal. Peripheral osteophyte formation, fibrosis and sub-cortical cysts were obvious. The osteoarthritic changes were commonly seen in the anterior and lateral regions of the condyle. Microscopically, fibrosis of bone marrow and trabecular remodelling were obvious. Subcortical cysts were also the common feature in all condylar surfaces. No disc perforation was present in all joints examined. However, the peripheral parts of the lateral and anterior parts of the discs were either folded or sharply thinned.

The qualitative assessment of the effect of experimentally-induced degenerative disease on the TMJ in the present study suggested that the density of nerve fibres immunoreactive to antisera for PGP 9.5, CGRP and SP was less in the arthritic TMJ capsule than in the normal capsule. In addition, there seemed to be fewer nerve fibres in parts of the sheep TMJ that were most affected by the degenerative changes. Nevertheless, the quantitative data showed no statistically significant effect ($P > 0.01$) of

induced osteoarthritis on the percentage surface areas or number of PGP 9.5- or CGRP-IR nerve fibres in the capsule.

The results of this investigation show that while the development of TMJ in human and sheep fetuses follows a similar sequence, there are differences in the timing of neural and morphological development. In addition, this study suggests that while inflammatory arthritis has a marked influence on the density of sensory and autonomic nerve fibres in synovium, the experimentally induced non-inflammatory osteoarthritis in the sheep TMJ broadly maintains a nerve supply similar to normal joints.

PUBLICATIONS ARISING FROM THIS THESIS

PAPERS

Tahmasebi-Sarvestani A, Tedman RA and Goss A (1996). Neural structures within the sheep temporomandibular joint. *Journal of Orofacial Pain* 10: 217-231.

Tahmasebi-Sarvestani A, Tedman RA and Goss AN (1997) Distribution and co-existence of neuropeptides in nerve fibres in the temporomandibular joint of late gestation fetal sheep. *Journal of Anatomy* (accepted for publication).

Tahmasebi-Sarvestani A, Tedman RA and Goss AN (1997) The influences of osteoarthritis on articular nerve endings through experimental manipulation of the sheep temporomandibular joint (preparation).

ABSTRACTS

Sarvestani, AT-S, Tedman RA and Goss A (1994). Demonstration of nerve endings in the sheep temporomandibular joint by using a modified gold chloride technique. *Proceedings Anatomical Society of Australia and New Zealand Conference, Sydney*.

Tahmasebi-Sarvestani A, Tedman RA and Goss A. (1995). Neural structures within the sheep temporomandibular joint. *Proceedings of the first Asia-Pacific anatomical conference*. p 135. Singapore.

Tahmasebi-Sarvestani A, Tedman RA and Goss A. (1995). The innervation of the normal sheep temporomandibular joint. In: *The Sheep as a Model for Temporomandibular Joint Disorders*. eds Goss A, Kurita K and McMahon L. p17. Department of Dentistry, University of Adelaide, Adelaide.

Sarvestani, AT-S, Tedman RA and Goss A (1996). Distribution of PGP 9.5-, substance P- and CGRP-immunoreactive nerve fibres in the temporomandibular joint of late gestation fetal sheep. *Journal of Medicine*. 26:475.

Tahmasebi-Sarvestani A, Tedman RA and Goss A. (1996). Sensory and autonomic nerves within the sheep temporomandibular joint. *Proceedings of the Australian Neurosciences Society* 7: 231.

TABLE OF CONTENTS

Statement	i
Acknowledgements	ii
Abstract	v
Publications arising from this thesis	ix
List of figures	xvii
List of tables	xxiii

CHAPTER 1

LITERATURE REVIEW

1.1. INTRODUCTION	3
1.2. EMBRYOLOGY	3
1.2.1. Neurogenesis	6
1.3. MORPHOLOGY	8
1.3.1. Temporomandibular Joint Components	8
1.3.1.1. The condyle	9
1.3.1.2. The mandibular fossa (glenoid fossa)	10
1.3.1.3. Disc	11
1.3.1.4. Capsule	12
1.3.1.5. Synovial membrane	13
1.3.1.6. Muscle	15
1.4. NEURAL SUPPLY OF ARTICULAR TISSUES	16
1.4.1. Classification of peripheral nerve fibres	16
1.4.2. Classification of articular sensory receptors	18
1.4.2.1. Type I receptors (Ruffini endings)	18
1.4.2.2. Type II receptors (Pacinian corpuscles)	19

1.4.2.3. Type III receptors (Golgi tendon organs)	21
1.4.2.4. Type IV receptors (free nerve endings)	22
1.5. NERVE SUPPLY OF TEMPOROMANDIBULAR JOINT	22
1.5.1. Mandibular nerve	25
1.5.1.1. Auriculotemporal nerve	25
1.5.1.2. Masseteric nerve	27
1.5.1.3. Deep temporal nerve	27
1.5.2. Regional distribution of nerve fibres in temporomandibular joint	27
1.6. NEUROPEPTIDES	28
1.6.1. Substance P	29
1.6.2. Calcitonin gene-related peptide	30
1.6.3. Neuropeptide Y	31
1.6.4. Vasoactive intestinal polypeptide	32
1.7. NEUROSPECIFIC PROTEINS AS GENERAL MARKERS	33
1.7.1. Protein gene product 9.5	34
1.8. ARTHRITIS	35
1.8.1. Osteoarthritis	35
1.8.2. Rheumatoid arthritis	37
1.8.3. Neuropeptides and arthritis	39
1.8.4. Ageing and osteoarthritis	39
1.9. ANIMAL AS A MODEL FOR TMJ RESEARCH	41
1.9.1. Induced arthritis	42
1.10. AIMS OF THIS STUDY	44

CHAPTER 2	
TEMPOROMANDIBULAR JOINT MORPHOLOGY	
2.1. SUMMARY	2
2.2. INTRODUCTION	3
2.3. MATERIALS AND METHODS	3
2.3.1. Animals	3
2.3.2. Macroscopic morphology	3
2.3.4. Microscopic morphology	4
2.3.5. Scanning electron microscopy	4
2.4. RESULTS	5
2.4.1. General features	5
2.4.2. Articular surfaces	5
2.4.3. Capsule	6
2.4.4. Articular disc	7
2.4.5. Synovium	8
2.5. DISCUSSION	8
2.5.1. Articular surfaces	9
2.5.2. Articular disc	10
2.5.3. Capsule	11
2.5.4. Synovium	12

TEMPOROMANDIBULAR JOINT INNERVATION

3.1. SUMMARY	2
3.2. INTRODUCTION	3
3.3. MATERIALS AND METHODS	4
3.3.1. Animals and tissues	4
3.3.2. Macroscopic anatomy	6
3.3.3. Gold chloride histochemistry	6
3.3.4. Fluorescence histochemistry	7
3.3.5. Immunohistochemistry	8
3.3.5.1. Immunoperoxidase histochemistry	8
3.3.5.2. Immunofluorescence histochemistry	9
3.3.6. Transmission electron microscopy	10
3.3.7. Relative density of nerve fibres	11
3.4. RESULTS	11
3.4.1. Gross morphology of nerves supplying the TMJ	11
3.4.2. Microscopic appearance of nerves supplying the TMJ.	12
3.4.3. Gold Chloride	13
3.4.4. Fluorescence histochemistry	14
3.4.5. Immunoperoxidase histochemistry	15
3.4.6. Immunofluorescence histochemistry	15
3.5. DISCUSSION	17
3.5.1. Gross morphology of the nerves	17
3.5.2. Gold chloride histochemistry	18
3.5.3. Fluorescence histochemistry	21
3.5.4. Immunohistochemistry	21

**INNERVATION OF THE PRENATAL SHEEP
TEMPOROMANDIBULAR JOINT**

4.1. SUMMARY	2
4.2 INTRODUCTION	3
4.3 MATERIALS AND METHODS	4
4.3.1. Animals and tissue processing	4
4.3.2. Immunocytochemistry	6
4.3.2.1. Single labelling	6
4.3.2.2. Double and triple labelling	7
4.3.3. Laser scanning confocal microscopy	9
4.3.4. Quantification and statistical analysis	10
4.4. RESULTS	11
4.4.1. General observations	11
4.4.2. Immunohistochemical observations	12
4.4.2.1. Disc	12
4.4.2.2. Capsule	13
4.4.2.3. Synovium	13
4.4.2.4. Bone and periosteum	14
4.4.2.5 Double and triple labelling	14
4.4.2.6. Confocal immunofluorescence microscopy	14
4.4.3. Quantitative data	15
4.5. DISCUSSION	15

**THE INFLUENCE OF OSTEOARTHRITIS ON THE
INNERVATION OF THE SHEEP
TEMPOROMANDIBULAR JOINT**

5.1 SUMMARY	2
5.2. INTRODUCTION	3
5.3. MATERIALS AND METHODS	4
5.3.1. Animals	4
5.3.2. Surgical procedures	5
5.3.3. Sample collection	6
5.3.4. Immunocytochemistry	7
5.3.4.1. Tissue processing	7
5.3.4.2. Single labelling	8
5.3.4.3. Double- and triple-labelling	8
5.3.5. Quantification and statistical analysis	9
5.4. RESULTS	10
5.4.1. Morphology of osteoarthrotic temporomandibular joint	10
5.4.2. Immunocytochemical observations	11
5.4.2.1. Normal sheep TMJ tissue	11
5.4.2.2. Arthritic joints	12
5.4.3. Quantitative observations	13
5.5. DISCUSSION	15

CHAPTER 6**GENERAL DISCUSSION**

6.1. INTRODUCTION	2
6.2. MORPHOLOGY OF THE SHEEP TMJ	2
6.3. DISTRIBUTION OF NERVES IN SHEEP TMJ	3
6.4. INNERVATION OF THE PRENATAL SHEEP TMJ	5
6.5. THE EFFECTS OF ARTHRITIS ON THE INNERVATION OF THE TMJ	8
6.6. USING SHEEP AS AN ANIMAL MODEL IN THE PRESENT WORK	10
6.7. CONCLUDING REMARKS AND FUTURE DIRECTIONS	12

CHAPTER 7**REFERENCES****CHAPTER 8****APPENDICES**

LIST OF FIGURES

		AFTER PAGE
Figure 1.1	Drawing of human TMJ components.	1.9
Figure 1.2	A Ruffini type nerve ending in the human TMJ capsule.	1.19
Figure 1.3	A Pacinian corpuscle in the human TMJ capsule.	1.20
Figure 1.4	A Golgi tendon organ in the human TMJ capsule.	1.21
Figure 1.5	A type of free nerve ending in the human TMJ capsule.	1.22
Figure 1.6	Dorsal view of spinal cord, brain stem, thalamic and cortical pain pathway.	1.23
Figure 1.7	Diagrammatic representation of the mandibular nerve and its branches.	1.26
Figure 1.8	Drawing of TMJ with degenerative arthritis (TMJ arthrosis).	1.36
Figure 1.9	Drawing of TMJ with rheumatoid arthritis.	1.38
Figure 2.1	Lateral aspect of the skull of an adult Australian Merino sheep.	2.5
Figure 2.2a	Sagittal section of decalcified, silver impregnated, right TMJ of an adult sheep	2.5
Figure 2.2b	Lateral aspect of the right TMJ of an adult sheep.	2.5
Figure 2.2c	Anterior aspect of the articular surface of the condyle.	2.6
Figure 2.3	Macroscopic and scanning electron microscopic appearance of the articular surfaces of the condyle.	2.6

Figure 2.4	Light micrographs of adult TMJ tissues stained with Masson's trichrome and light green.	2.6
Figure 2.5	Scanning electron microscopic appearance of the anterior capsule(a),lateral capsule (b), peripheral disc (c) and central disc (d).	2.7
Figure 2.6	Light micrographs of toluidine blue stained sections of adult TMJ tissues to show the synovium.	2.7
Figure 3.1	Subdivision of disc and attached capsule of TMJ to show the four regions used for microscopic examination.	3.4
Figure 3.2a	Lateral aspect of the left TMJ of an adult sheep.	3.5
Figure 3.2b	Temporomandibular joint of sheep and its innervation.	3.5
Figure 3.3 a	Macroscopic appearance of nerves in sheep TMJ.	3.11
Figure 3.3 b	Lateral aspect of the TMJ of an adult sheep.	3.11
Figure 3.3 c	Light micrograph of transverse section of the masseteric nerve.	3.11
Figure 3.3 d	Light micrograph of transverse section of the masseteric nerve. Toluidine blue stain.	3.11
Figure 3.4	Transmission electron microscopic appearance of the masseteric nerve.	3.12
Figure 3.5	Transmission electron microscopic appearance of the masseteric nerve.	3.12

Figure 3.6	Light micrographs of gold chloride stained sections of capsule of the TMJ of adult sheep.	3.13
Figure 3.7	Light micrographs of (a) free nerve endings (b) a clew-type Ruffini ending	3.13
Figure 3.8	Light micrographs of (a) Paciniform and (b) a Golgi-Mazzoni corpuscle	3.13
Figure 3.9	Fluorescence photomicrographs of sections of capsule of the TMJ of adult sheep after treatment with glyoxylic acid showing adrenergic nerve fibres.	3.14
Figure 3.10	CGRP-immunoreactive nerve fibres in the TMJ of adult sheep.	3.15
Figure 3.11	PGP 9.5-immunoreactive nerve fibres in the TMJ of adult sheep as revealed by immunofluorescence confocal microscopy.	3.15
Figure 3.12	PGP 9.5-immunoreactive nerve receptors (a) Ruffini ending, (b) Golgi organ ending, and (c) free nerve endings.	3.15
Figure 4.1a,c	Sagittal section of the temporomandibular joint of a fetal sheep at 140 days gestation.	4.11
Figure 4.1d,e	Temporomandibular joint of a fetal sheep at 140 days gestation.	4.11
Figure 4.1f,g	Temporomandibular joint of a fetal sheep at 140 days gestation.	4.11
Figure 4.2	CGRP-IR fibres (a,b,c), PGP 9.5-IR fibres (d,e) and substance P-IR fibres (f,g) in fetal sheep TMJ disc.	4.12

Figure 4.3	CGRP-IR fibres (a,b,c), PGP 9.5-IR fibres (d,e) and substance P-IR fibres (f,g) in fetal sheep TMJ capsule.	xx 4.13
Figure 4.4	CGRP-IR fibres (a,b), PGP 9.5-IR fibres (c,d) and substance P-IR fibres (e,f) in synovium and adjacent capsule of fetal sheep at 140 days gestation.	4.13
Figure 4.5	CGRP-IR fibres (a,b), PGP9.5-IR fibres (c) and SP-IR fibres (e) in condyle of fetal sheep at 140 days gestation.	4.14
Figure 4.6	Triple labelled section of synovium and capsule of the TMJ of a fetal sheep at 140 days gestation.	4.14
Figure 4.7	Double labelled section of capsule of the TMJ of a 140-days-old sheep fetus. (a) SP-IR and (b) NPY-IR.	4.14
Figure 4.8	Immunoreactive nerve fibres in the TMJ of adult sheep as revealed by immunofluorescence confocal microscopy. (a) CGRP-IR, (b) PGP 9.5-IR and (c) SP-IR.	4.14
Figure 4.9	Widths of nerves in capsule of TMJ of fetal sheep.	4.14
Figure 5.1	Sagittal section of the central part of a decalcified TMJ from a normal adult sheep.	5.6
Figure 5.2	Sample collection from different regions of TMJ.	5.7
Figure 5.3	Articular surfaces of the condyle (a) and temporal (glenoid) fossa (b) from arthritic TMJ.	5.10
Figure 5.4	Lateral (a) and superior (b,c) aspects of the condyle of arthritic TMJ.	5.10
Figure 5.5	Light micrographs of normal (a) and arthritic (b) TMJ stained with Masson's trichrome and Light Green.	5.11

Figure 5.6	Light micrographs of arthritic TMJ tissues stained with Masson's trichrome.	5.11
Figure 5.7	Light micrographs of normal (a) and arthritic condyle (b,c) stained with Alcian Blue and showing the articular surface.	5.11
Figure 5.8	Immunofluorescence micrographs of normal adult TMJ tissues showing PGP 9.5-IR (a,c) and CGRP-IR (b).	5.11
Figure 5.9	Immunofluorescence micrographs of normal adult TMJ tissues showing VIP-IR (a,) and NPY-IR (b).	5.11
Figure 5.10	Immunofluorescence micrographs of arthritic adult TMJ tissues showing PGP 9.5-IR (a,) and CGRP-IR (b).	5.12
Figure 5.11	Immunofluorescence micrographs of arthritic adult TMJ tissues showing PGP 9.5-IR.	5.12
Figure 5.12	Immunofluorescence micrographs of arthritic adult TMJ tissues showing CGRP-IR.	5.13
Figure 5.13	Immunofluorescence micrographs of arthritic adult TMJ tissues showing PGP 9.5-IR in capsule near osteophytes.	5.13
Figure 5.14	Immunofluorescence micrographs of arthritic adult TMJ tissues showing a section of capsule double labelled with SP antiserum (a) and CGRP antiserum (b).	5.13
Figure 5.15	Relative distribution of nerve fibres showing PGP 9.5-IR in different regions of the capsule of TMJ in adult sheep (normal and arthritic data combined).	5.13
Figure 5.16	Relative distribution of nerve fibres showing CGRP-IR in different regions of the capsule of TMJ in adult sheep (normal and arthritic data combined).	5.14
Figure 5.17	Mean plus standard error (SE) percentage surface area in capsule of TMJ of adult sheep.	5.14

- Figure 5.18** Mean plus standard error (SE) number of nerve fibres
in capsule of TMJ. 5.14
- Figure 5.19** Widths of nerves in capsule of TMJ. 5.14

LIST OF TABLES

Table 1.1	Classification of peripheral nerve fibres.	1.17
Table 1.2	Classification of articular sensory receptors	1.18
Table 1.3	Regional distribution of nerve fibres.	1.28
Table 1.4	Characteristics of some neuropeptides.	1.29
Table 1.5	The incidence of human TMJ osteoarthritis (OA) and its correlation with age.	1.40
Table 3.1	Number of animals, joints and applied procedure.	3.5
Table 3.2	Relative density of neural structures in four regions of the capsule of TM joints from adult male Merino sheep.	3.17
Table 4.1	Primary antibody characteristics.	4.7
Table 4.2	Antibody combinations used for double-labelling immunofluorescence.	4.8
Table 4.3	Antibody combinations used for triple-labelling immunofluorescence.	4.9
Table 5.1	Number of animals, joints and applied procedure.	5.5
Table 5.2	Primary antibody characteristics.	5.9
Table 5.3	Antibody combinations used for triple-labelling immunofluorescence.	5.10
Table 5.4	Antibody combinations used for double-labelling immunofluorescence.	5.10

Table 5.5	Mean percentage surface area (plus standard error) for all adults (normal and arthritic data combined).	5.15
Table 5.6	Mean number of nerve fibres (plus standard error) for all adults (normal and arthritic data combined).	5.15

CHAPTER 1

LITERATURE REVIEW

1.1. INTRODUCTION	3
1.2. EMBRYOLOGY	3
1.2.1. Neurogenesis	6
1.3. MORPHOLOGY	8
1.3.1. Temporomandibular joint components	8
1.3.1.1. The condyle	9
1.3.1.2. The mandibular fossa (glenoid fossa)	10
1.3.1.3. Disc	11
1.3.1.4. Capsule	12
1.3.1.5. Synovial membrane	13
1.3.1.6. Lateral pterygoid muscle	15
1.4. NEURAL SUPPLY OF ARTICULAR TISSUES	16
1.4.1. Classification of peripheral nerve fibres	16
1.4.2. Classification of articular sensory receptors	18
1.4.2.2. Type II receptors (Pacinian corpuscles)	19
1.4.2.3. Golgi tendon organs (type III receptors)	21
1.4.2.4. Type IV receptors (free nerve endings)	22
1.5. NERVE SUPPLY OF TEMPOROMANDIBULAR JOINT	22
1.5.1. Mandibular nerve	25
1.5.1.1. Auriculotemporal nerve	25
1.5.1.2. Masseteric nerve	27
1.5.1.3. Deep temporal nerve	27
1.5.2. Regional distribution of nerve fibres in the temporomandibular joint	27
1.6. NEUROPEPTIDES	28
1.6.1. Substance P	29

1.6.2. Calcitonin gene-related peptide	30
1.6.3. Neuropeptide Y	31
1.6.4. Vasoactive intestinal polypeptide	32
1.7. NEUROSPECIFIC PROTEINS AS GENERAL MARKERS	33
1.7.1. Protein gene product 9.5	34
1.8. ARTHRITIS	35
1.8.1. Osteoarthritis	35
1.8.2. Rheumatoid arthritis	37
1.8.3. Neuropeptides and arthritis	39
1.8.4. Ageing and osteoarthritis	39
1.9. ANIMAL MODELS FOR TMJ RESEARCH	41
1.9.1. Induced arthritis	42
1.10. AIMS OF THIS STUDY	44



1.1. INTRODUCTION

Articular neurology is that branch of the neurological sciences that concerns itself with the study of the anatomical, physiological and clinical features of the nerve supply of the joint systems in various parts of the body (Wyke, 1972). The functions of joints are controlled by the central nervous system, which receives information from peripheral nerves and ganglia that are connected to it.

Joint innervation has attracted the interest of not only clinicians studying the pathology of the joint but also neurophysiologists investigating the fine structure of articular nerves in order to analyse the responses of nerves to various movements.

Before the innervation of the temporomandibular joint can be discussed it is necessary first to describe its embryology, gross anatomy and microscopic appearance.

1.2. EMBRYOLOGY

Phylogenetically the temporomandibular joint is a relatively new structure, which can be found only in mammals (Moffett, 1957). The initial development of temporomandibular joint and its associated structures follows a number of morphological events in an embryo. In humans and other mammals, the embryology of this synovial joint has been described by many authors, for example, Scott (1951), Symons (1952), Moffett (1957), Baume (1962), Yuodelis (1966), Liven (1993), Ogutcen-Toller and Juniper (1993) and Avery and Bernik (1994).

In mammals, the first pharyngeal arch is remodelled to form a cranial maxillary swelling and a caudal mandibular swelling (Larsen, 1993). These processes give rise to the upper

and lower jaws, respectively. Each process contains a central cartilaginous element. The central cartilages are produced by neural crest cells arising in the regions of the embryonic midbrain (mesencephalon) and cranial portion of the hindbrain (metencephalon). The central cartilage of the mandibular swelling is called Meckel's cartilage. In humans and other mammals, the jaws consist of membrane bones that form a sheath around some of the cartilages of the first arch. The first-arch cartilages of mammals give rise mainly to two ossicles (incus and malleus) of the middle ear. The maxillary cartilage forms the incus, and the mandibular cartilage forms the malleus (Larsen, 1993).

There is some dispute as to how the temporomandibular joint develops in the embryo. Some researchers like Moffett (1957) believe that, in humans and other mammals, the temporomandibular joint develops from the membranous portion of the temporal bone, from skeletal, muscular and mesenchymal derivatives of the first branchial arch, and from a mesenchymal interzone. Other workers (Baume, 1962; Levy, 1964) report that the elements of the temporomandibular joint originate from two separate blastemata (condylar and temporal) that develop and grow at different rates. The condylar blastema gives rise to the inferior part of the capsule, the anterior part of the articular disc, the condylar cartilage and the aponeurosis of the lateral pterygoid muscle. The temporal blastema gives rise to the posterior part of the articular disc, and other articular structures of the superior part of the future temporomandibular joint (Bauma, 1962).

According to Yuodelis (1966) the temporomandibular joint in the human forms between the 6th and 12th weeks of gestation. In a study on human embryos and fetuses between age six weeks to full term, Yuodelis (1966) showed that the ossification of the mandibular element of the temporomandibular joint first appeared during the sixth week of gestation, whereas, in the temporal element, ossification appeared during the eighth week. He also indicated that the greatest changes in the joint region occurred between the 10th and 12th weeks.

The muscles of mastication also originate from the first pharyngeal arch. In the first arch, the paraxial mesoderm of the fourth cranial somitomere gives rise to the muscles of mastication: (the masseter, temporalis, and medial and lateral pterygoids) as well as to the anterior belly of the digastric, tensor tympani, and tensor veli palatini muscles (Larsen, 1993).

Despite several theories proposed by investigators such as Symons (1952) and Moffett (1957), regarding the role of the lateral pterygoid muscle in the formation of articular disc and the important role of this muscle or its tendon or both, played in the temporomandibular joint's prenatal development, Yuodelis (1966) found no evidence at any stage of development to show that this muscle has any contribution to the articular disc formation. He demonstrated that the primordial articular disc was distinct long before skeletal element approximation, thus ruling out that possibility of a direct formation by compression of intra-articular tissue. Ogutcen-Toller and Juniper (1993) have supported Yuodelis's finding and argued that the attachment of lateral pterygoid muscle fibres to both the disc and the condyle is indirect and suggested that the temporomandibular joint structures develop in a block of mesenchymal cells independent of lateral pterygoid muscle formation.

The differences between the embryologic development of the temporomandibular joint and other joints of human beings and animals have been described by many authors: Scott (1951) in sheep; Baume (1969) in rat and man; Durkin et al (1979) in rat and guinea pig; Liven (1993) in humans and mice. According to Liven's (1993) findings, there are two major differences between the temporomandibular joint and other joints, and both relate to early embryogenesis. First, the condylar cartilage develops during the third trimester of embryonic life, when the body of the mandible has already been established. The mandibular cartilage of humans and mice is referred to as being a secondary cartilage. In

contrast, other joints consist of primary cartilages which develop earlier. Secondly, during embryogenesis the mandibular cartilage develops from the first pharyngeal arch elements that include, aside from mesenchymal derivatives, also neural crest-derived cells that migrate during the fourth week of gestation.

Baume (1969), in a comparison of the embryologic events in both rats and humans, observed that the newborn rat corresponded to a 16-week-old human fetus in terms of skeletal development. A study of the postembryonic development of the rat mandibular condyle (Durkin et al, 1979) demonstrated a stage in development of the mandibular condyle at birth which appeared morphologically to coincide with human development somewhere in the range of the 12-14th week.

Scott (1951) examined the temporomandibular joint of fetal sheep 36-70 days of gestation and found no evidence of temporomandibular joint formation up to the 40th day of gestation, but he observed the muscles of mastication including the tensor tympani of the middle ear at the 40th day of gestation. The first indication of a joint cavity and articular disc at the mandibular joint was found about the 47th day of gestation, when the fetus was about 60mm crown-rump length. Scott also showed that the Meckel's cartilage began to show breaks in its continuity with the anterior process of the malleus to the inner side of the mandibular joint at about the 60th day of gestation. The full term or total gestation period for the sheep is 157 days (Barcroft, 1941 cited by Scott, 1951).

1.2.1. Neurogenesis

One of the derivatives of the three embryonic germ layers in the embryo is the neural crest. During the fourth week of gestation, neural crest cells detach from the neural folds and migrate to numerous locations in the body, where they differentiate to form a wide range of structures and tissues (Atkinson and White, 1992; Larsen, 1993). The principal derivatives

of the neural crest are the sensory and autonomic parts of the peripheral nervous system. With the exception of some cranial nerve sensory ganglia, ganglia of the peripheral nervous system are also derived from neural crest. The trigeminal ganglion of the trigeminal nerve has a mixed origin. The proximal portion arises mainly from caudal diencephalic and cranial mesencephalic neural crest, whereas the neurons of the distal portions arise mainly from the diffuse trigeminal placode (Larsen, 1993).

The cranial nerve nuclei of the brain stem are organised into seven columns on the basis of function. The branchial efferent neurons of the basal columns serve the striated muscles derived from the pharyngeal arches and general afferent association neurons of the alar columns in the brain subserve "general sensation" (touch, temperature, pain, etc) (Larsen, 1993). The trigeminal nerve nuclei appear in the brain stem in the middle of the fifth week and all nuclei are distinguishable by the end of the fifth week (Larsen, 1993). The trigeminal nerve is a mixed sensory and motor nerve. The sensory nuclei arise in the metencephalon and myelencephalon but are later displaced partly into the mesencephalon. The trigeminal motor nucleus arises in the metencephalon and remains there (Larsen, 1993).

The information regarding prenatal and postnatal development of neural elements in the temporomandibular joint is limited. The nerve elements in the temporomandibular joint may be detectable from the end of the eighth week and the full development of nerves in different components of the human temporomandibular joint are seen between the third and the fifth month of gestation (Thilander, 1963; Kitamura, 1974; Doyle, 1982; Ramieri et al, 1996). There are differences in the timing of nerve development in the temporomandibular joints of human and animals. Tahmasebi-Sarvestani et al (1997) showed that the fetal sheep temporomandibular joint is well innervated at 17 days before birth. Ichikawa et al (1989) found no calcitonin gene-related peptide (CGRP)-immunoreactive (IR) nerve fibres in the temporomandibular joint of rats at birth, but they found some CGRP-IR nerve fibres in the

disc and capsule at day 3 postpartum. By day 10 postpartum, there were increased numbers of nerves in the disc and fibrous tissue of the capsule.

1.3. MORPHOLOGY

The gross morphology of the human temporomandibular joint (TMJ) has been reported by many investigators, for example, Angel (1948), Rees (1954), Choukas and Sicher (1960), Toller (1961), Dixon (1962), Öberg and Carlsson (1979), Dubrul, 1980, Bell (1983), McKay et al (1992), Avery and Bernick (1994), Melfi (1994), Wilkinson and Crowley (1994), Crowley et al (1996) and Tuomiren et al (1996). This joint is unique compared with other joints in both structure/function and embryological development. It is a diarthroidal sliding-hinge articulation between the condyle of the mandible and the squamous portion of the temporal bone (Figure 1.1).

The temporomandibular joint is a true synovial joint which, besides having much in common with other synovial joints, has certain anatomical features that distinguish it (Sicher, 1951; Wight, 1974). The articulating surfaces of the condyle and mandibular fossa are covered by fibrocartilaginous tissue and not by hyaline cartilage, unlike most other articulations. The joint has an articulating disc that separates the head of the condyle from the temporal bone. Therefore the disc completely divides the joint into superior and inferior joint compartments with different but interrelated functions (Bell, 1983; Avery and Bernick, 1994).

1.3.1. Temporomandibular joint components

The primary components of the TMJ are the head of the condyle, the mandibular or glenoid fossa of the squamous part of the temporal bone, the fibrous capsule, disc and the synovial

membrane. The lateral pterygoid muscle can also be regarded as part of the joint, since it is attached to the condyle and the intermediate part of the disc (Öberg and Carlsson, 1979).

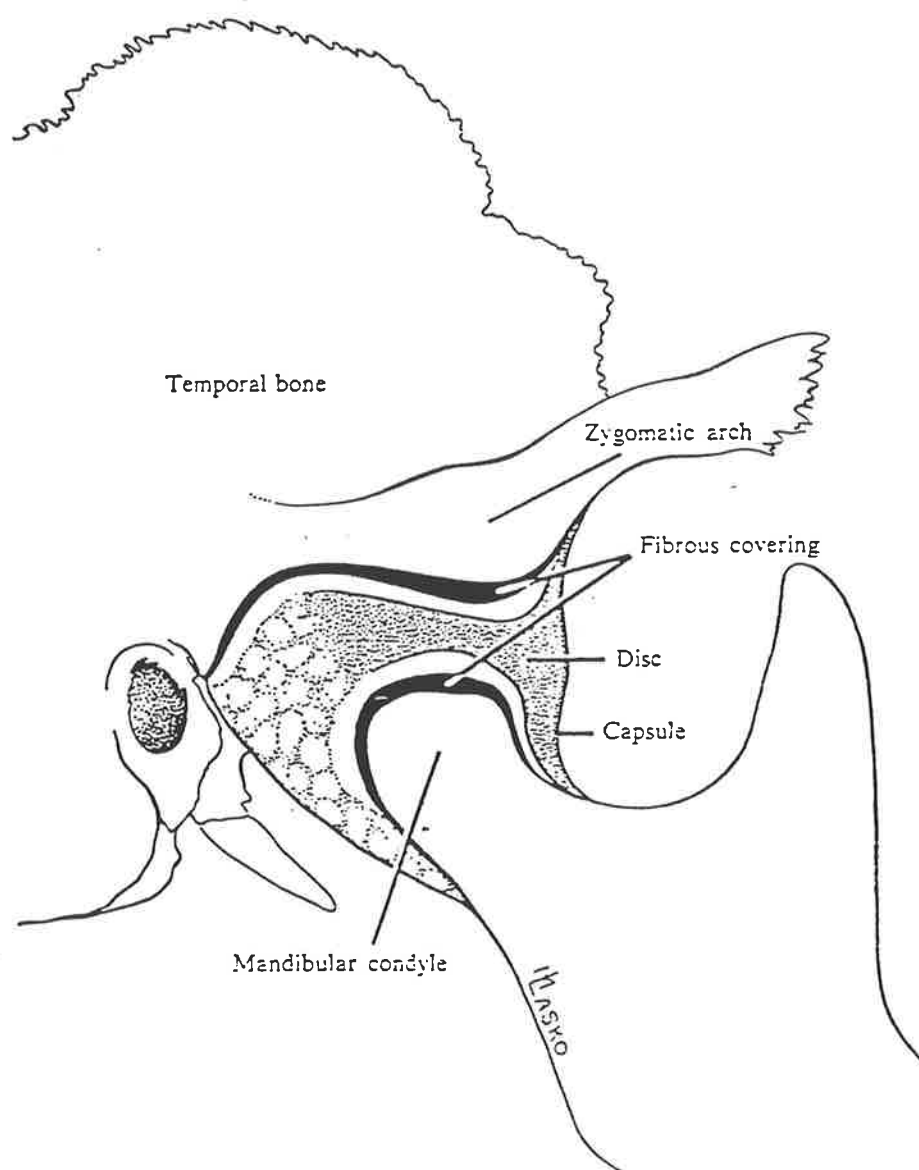


Figure 1.1 Drawing of human TMJ components (adapted from Melfi, 1994).

1.3.1.1. The condyle

The mandibular condyle consists of spongy bone, compact bone, and soft articular tissue. The condyle in the adult human is perpendicular to the ramus of the mandible. The average

length of the condyle in the mediolateral direction is 20 mm and the average width in the anteroposterior direction is 10 mm (Öberg and Carlsson, 1979). However these authors stated that the measurements of the condyle vary widely from one individual to another. Therefore the form and the shape of the condyle can be rounded, convex, flat or straight in the mediolateral plane (Öberg et al, 1971). In young animals the articulating surface of the condyle is covered by fibrous connective tissue which is replaced by fibrocartilage with increasing age (Sharpe et al, 1965; Griffin et al, 1975; Solberg, 1986). In humans, as in the other mammals including cats, rats, rabbits, dogs, sheep, goats, cows and pigs, the articular surface of the mandibular condyle is convex and joins the lower articular surface of the disc, which is concave (May, 1970; Bosanquet and Goss, 1987; Bermejo et al, 1993).

1.3.1.2. The mandibular fossa (glenoid fossa)

The mandibular fossa in humans is a depression on the inferior aspect of the temporal bone just posterior and medial to the posterior end of the zygomatic arch. It is slightly broader mediolaterally (23 mm) than anteroposteriorly (19 mm) respectively (Öberg and Carlsson, 1979) and is divided into anterior and posterior portions by the petrotympanic fissure. Solberg (1986) described the mandibular fossa as a dense, thin, plate of compact bone which is covered by a thin periosteum. The articulating surface of the mandibular fossa is covered with fibrous connective tissue similar to that covering the articulating surface of mandibular condyle (Melfi, 1994).

The articular eminence, which is the anterior border of the articular fossa in humans, is aligned mediolaterally (Melfi, 1994). According to Melfi (1994) and Avery and Bernick (1994), both the articular fossa and the articular eminence are the parts of the temporal bone that make up the cranial articulation of the temporomandibular joint. In humans, pigs, dogs, cats, rabbits and rats the articular surface of the temporal bone is concavoconvex (Bermejo et al, 1993), while the articular surface of the temporal bone of cows, sheep, and

goats is slightly convex (Bosanquet and Goss, 1987; Ström et al, 1988; Bermejo et al, 1993; Ishimaru et al, 1993). The articular eminence is poorly developed or absent in sheep.

1.3.1.3. Disc

Hanky (1954), Dixon (1962) and Griffin and Sharpe (1962) found general similarities between the morphological structure of the temporomandibular joint disc of humans and animals. Bellinger (1948) described the interarticular disc of the human temporomandibular joint as an oval, biconcave structure of dense fibrous connective tissue that is interspersed with a few cartilaginous cells. In human beings, pigs, dogs, cats, rabbits and rats the upper articular surface of the disc is concavoconvex while the lower articular surface of the disc in cows, sheep and goats is slightly concave (Bermejo et al, 1993). Bermejo et al (1993) also observed that the lower articular surface of the disc in cows, sheep, and goats is concavoconvex, whereas, Bosanquet and Goss (1987) described the sheep temporomandibular joint disc as a biconcave structure in the sagittal plane.

Markowitz and Gerry (1949) noted the loose attachment of the disc to the posterior part of the joint capsule and observed that this region bled freely during surgical removal of the disc. The disc of the human temporomandibular joint has certain morphological characteristics which are related to its function (Rees, 1954). According to Rees (1954) the interarticular disc consists of a sheet of dense fibrous connective tissue that can be subdivided into an anterior, moderately thick band, an intermediate thin band, a posterior thick band and a bilaminar zone which consists of loose neurovascular connective tissue. He also found that the posterior portion of the disc exhibited a superior stratum attached to the squamotympanic fissure and an inferior stratum attached to the inferior margin of the posterior articular slope of the condyle. Choukas and Sicher (1960) criticized Rees' (1954) work and described the posterior portion of the disc as fibrous tissue not elastic as Rees believed. In 1962, Dixon observed that the interarticular disc of the human temporomandibular joint was not a homogenous structure, and divided the disc into two

parts. These were the extremely dense, avascular, plate-like anterior portion and a posterior part of loose connective tissue which merged with the posterior region of the joint capsule. Dixon (1962) also found several muscle fasciculi, derived from the upper head of the lateral pterygoid muscle, inserting into the anterior part of the disc. Dixon (1962) divided the posterior part of the disc into an upper zone which was rich in elastic tissue and a lower zone which possessed little elastic tissue but a plexus of large endothelium-lined spaces. Elastic fibres have been reported in the articular disc of the mouse (Frommer and Monroe, 1966), guinea pig (Silva, 1969), rat, sheep and dog (Gillbe, 1973), and rabbit (O'Dell et al, 1989). The disc of the sheep temporomandibular joint is composed of dense fibrous connective tissue with scattered clumps of chondroblasts in the central layer (Bosanquet and Goss, 1987). These authors also found that both the condylar and temporal aspects of the disc in the sheep are covered by a thin synovial membrane. According to these authors, in the sheep, the anterior attachment of the disc contains multiple vascular sinusoids, whereas the posterior attachment is fibrous and avascular. This is different from the human where the posterior portion of the disc is loose connective tissue and the anterior part is a very dense avascular tissue (Rees, 1954; Dixon, 1962).

1.3.1.4. Capsule

The capsule, ligaments and tendons are the three main elements in the periarticular tissue that provide for joint stability and limit range of motion (Rocubado, 1983). In the temporomandibular joint the articular capsule is made of fibrous tissue that is attached to the entire articular disc about its circumference thus creating superior and inferior joint cavities (Carlsson et al, 1979). Most authors have subdivided the articular capsule into anterior, posterior, medial and lateral parts (Ishibashi, 1974; Öberg and Carlsson, 1979; Bermejo-Fenoll, et al 1992). Rees (1954) has been the only author who found no articular capsule in the anterior part of the human temporomandibular joint, whereas others like Choukas and Sicher (1960), Ishibashi (1974) and Griffin et al (1975) demonstrated that the anterior part of the human temporomandibular joint is covered by capsule and attached to

the articular eminence. Posteriorly, the capsule is attached to the margin of mandibular fossa superiorly and to the neck of the condyle inferiorly. A pad of loose connective tissue is located in the posterior aspect of the temporomandibular joint to separate the disc from the capsule (Melfi, 1994). Melfi (1994) suggested that this pad of loose connective tissue between the capsule and disc permitted freedom of anterior movement of the disc. Medially, the capsule is attached to the medial region of the neck of the condyle and the medial rim of the mandibular fossa (Griffin et al, 1975). It is thicker near its bony insertion and thinner around the inner portion of the disc (Yung et al, 1990). Laterally the capsule is strengthened to form the lateral (temporomandibular) ligament (Choukas and Sicher, 1960; Griffin et al, 1975). The lateral ligament or the lateral capsule in humans consists of a horizontal band and an oblique band. The horizontal band acts to restrict posterior condyle movement while the oblique band serves to stabilise the joint in translation (Solberg, 1986). In addition, there are two accessory ligaments, the stylomandibular and the sphenomandibular ligaments, associated with the temporomandibular joint. The former attaches to the styloid process and the posterior border of the ramus of the mandible. The sphenomandibular ligament extends between the spine of the sphenoid bone and the lingula of the mandible (Avery and Bernik, 1994). These ligaments have little influence on the movement of the mandible (Solberg 1986).

May (1970) described the articular capsule of sheep as consisting of an outer fibrous layer and an inner synovial layer. Sison and Grossman (1961) and May (1970), reported that the synovial membrane or the inner layer of articular capsule is a thin layer of connective tissue which lines the joint cavity but does not cover the articulating surfaces.

1.3.1.5. Synovial membrane

The histology, histochemistry and electronmicroscopy of the synovial membrane has been extensively investigated by many authors. The synovial membrane covers the entire inner layer of the articular capsule of all synovial joints (Lever and Ford, 1958). It secretes

synovial fluid, which fills the synovial cavity, lubricates the joint and provides nourishment to joint parts that are without a blood supply such as the fibrous part of the articular surfaces of the bones and the central region of the disc in the temporomandibular joint (Melfi, 1994).

Synovial membrane may be of the areolar, fibrous or adipose type (Griffin et al, 1975). The areolar type covers the internal surfaces of the capsule as well as the surfaces of the anterior part of the disc in humans (Griffin et al, 1975). The presence of loose connective tissue in the subintimal layer is characteristic of areolar synovial membrane (Henderson and Edwards, 1987). The fibrous synovial membrane covers the ligaments, tendons and other areas where the synovial lining is subject to pressure. The presence of dense connective tissue in the subintimal layer is characteristic of this type of synovial membrane (Griffin et al, 1975; Dijkgraaf et al, 1996). Adipose synovial membrane is characterised by the presence of fat pads directly adjacent to the joint space (Dijkgraaf et al, 1996). This type of synovial membrane is not characteristic of the normal temporomandibular joint, but in abnormal situations it is possible to see an increase in fat droplets in the subintimal tissue (Dijkgraaf et al, 1996).

Öberg and Carlsson (1979) suggested that the synovial tissue can be divided into two layers, one adjacent to the joint space called the 'intima' and a deeper layer, the subsynovial or subintimal layer. The synovial intimal cells may be spindle-shaped or rounded in appearance and occur as one to four layers of cells (Helmy et al, 1990; Dijkgraaf et al, 1996). The surface of the synovial membrane may often have synovial folds or villi which project into the joint cavities. The number and appearance of these processes varies in individuals and may change with age (Dixon, 1962; Ghadially, 1983). According to Ghadially no fundamental morphologic differences exist in the matrix of synovial intima within a joint, or from one joint to another. The subintimal tissue, however does show morphological differences in matrix structure. The subintimal tissue contains fibroblasts,

macrophages and mast cells, and is richly supplied with blood vessels and lymphatics. The amount of blood vessels in the normal synovial membrane appears to be different from one type of synovial membrane to another (Dixon 1962; Henderson and Edwards, 1987). The areolar synovial membrane has extensive capillaries in the subintimal tissue. The fibrous synovial membrane is less vascularised and has a core of fibrous tissue containing blood vessels.

An electronmicroscopic study by Helmy et al in 1990, revealed two types of synovial cells in the lining layer of the synovium. These were called type A and type B cells. The type A cells had well developed Golgi complexes with numerous vesicles and vacuoles, whereas type B cells had more rough endoplasmic reticulum (RER) and only a few Golgi complexes (Ghadilly, 1983; Dijkgraaf et al, 1996). According to Ghadially (1983) the amount of RER is the main factor used to differentiate between the type A and type B cells in the intimal layer of synovial membrane.

The extracellular matrix of the synovial intima contains little collagen (Ghadially, 1983; Henderson and Edwards, 1987). However, the subsynovial tissue of a fibrous synovial membrane contains numerous collagen fibres whereas the subsynovial tissue of an areolar synovial membrane has only a few collagen fibrils that are scattered in matrix. These authors also reported that there are no collagen fibres in subsynovial tissue of an adipose type.

The general morphological features of the synovial membrane in the human temporomandibular joint correlates well with the appearance of the tissue reported in other animals (Toller, 1961; Cutlip and Cheville, 1973; and Dijkgraaf et al, 1996).

1.3.1.6. Lateral pterygoid muscle

Muscles which act directly upon the temporomandibular joint (the masticatory muscles) are lateral pterygoid, medial pterygoid, masseter, temporalis and anterior belly of digastric.

Among the masticatory muscles, the lateral pterygoid muscle plays an important role in structure, function and dysfunction of the temporomandibular joint (Juniper, 1984).

The lateral pterygoid muscle has two distinct heads. The superior head has a direct insertion to the disc of the temporomandibular joint while the inferior head is inserted into the pterygoid fovea on the anterior surface of the neck of the condyle (Scott and Dixon, 1972; Atkinson and White, 1992). A more detailed study by Ogutcen-Toller and Juniper (1993) on human fetuses, demonstrated that the lateral pterygoid muscle attaches to the posterior as well as anterior parts of the temporomandibular joint disc. One of the functions of the temporomandibular joint during jaw opening is translation of the condylar head onto the articular eminence which is achievable by the action of the lateral pterygoid muscle (McKay et al, 1992).

1.4. NEURAL SUPPLY OF ARTICULAR TISSUES

Articular tissues in the human body are supplied by sensory receptors, commonly called 'proprioceptors' or 'mechanoreceptors' and 'nociceptors'. Decision making by the brain is possible because of the information it is constantly receiving from these sensory receptors about joint position and movements and about the tensions and strains of skeletal muscles and other external stimuli. These sensory receptors are scattered throughout joints and can be divided into several groups according to their morphological, topographical and functional properties (Hromada and Polacek (1958).

1.4.1. Classification of peripheral nerve fibres

Peripheral nerve fibres have a wide range of diameters; from large myelinated to small myelinated and unmyelinated fibres, and there is some correlation between the fibre

Table 1.1 Classification of peripheral nerve fibres (modified from Notle, 1993)

Ruman numeral classification	Diameter (μm)	Letter classification	Conduction velocity (m/sec)	Myelinated	Function and types of structures innervated
Ib	12-20	A α	70-120	yes	Proprioception: muscle spindle, annulospiral endings
Ib	12-20	A α	70-120	yes	Proprioception: Golgi tendon organs
II	6-12	A β	30-70	yes	Proprioception: muscle spindle and other encapsulated endings (flower spray endings; Ruffini endings; Pacinian corpuscles)
III	1-6	A δ	5-30	yes	Free-ending nociceptors: sharp pain, temperature, hair receptors
—	<3	B	3-15	yes	Preganglionic autonomic efferents
IV	0.4-1.2	C	0.5-2.5	no	Free-ending nociceptors: pain, itch, temperature, postganglionic autonomic efferents and some visceral receptors

diameter, conduction velocity and function of the target organ which a given fibre innervates (Nolte, 1993). According to Nolte (1993) there are two major classification systems for peripheral nerve fibres. The first system is based on conduction velocity whereby the speed of conduction of an action potential is related to the diameter of the fibres (see Table 1.1). The compound action potential of a peripheral nerve contains several peaks (referred to as A, B and C) that relate to different types of nerve fibres within the peripheral nerve. The fibres responsible for the A peaks are myelinated sensory and motor fibres and can be subdivided into alpha (α), beta (β) gamma (γ) and delta (δ) types. The A-alpha fibres are the largest and most rapidly conducting myelinated fibres and the A-delta fibres are the smallest and slowest conducting myelinated fibres. Preganglionic autonomic fibres and some visceral afferents are in the 'B' category of myelinated fibres. Unmyelinated fibres fall into the 'C' category. According to Nolte (1993) the A-beta and A-delta are two common terminologies that are used for proprioceptive fibres. The A-alpha fibres are the larger axons innervating the extrafusal fibres of muscles and the A-gamma fibres are the smaller axons innervating intrafusal muscle fibres of muscle spindles. In the literature the "A" is commonly dropped, and these are simply called alpha (α) and gamma (γ) motor neurons.

The second classification system is based on direct microscopic measurement of axonal diameter. There are four major groups in this classification system. Group I, II and III are myelinated and group IV consists of unmyelinated fibres. The size, conduction velocities, and functional correlates involved in both systems are listed in Table 1.1.

Myelinated afferents found in muscle nerves innervate the primary endings of muscle spindles or Golgi tendon organs. To distinguish between them, spindle primary fibres are called Ia and Golgi tendon organ fibres are called Ib. Group II, corresponding to A- fibres, is quite diverse and includes the fibres that form the secondary endings of muscle spindles and those that form all the encapsulated receptors of skin and joints. Group III consists of

Table 1.2. Classification of articular sensory receptors (adapted from Hukkanen 1994)

Type	Average diameter (μm)	Location	Function
I (Ruffini ending)	100x40	superficial joint capsule	low threshold, slowly adapting, mechanoreceptors
II (Pacinian corpuscles)	280x120	deeper layer of the fibrous capsule	low threshold, rapidly adapting, mechanoreceptors
III (Golgi tendon organs)	600x100	ligament	low threshold, slowly adapting, mechanoreceptors
IV (free endings)	<1.5	capsule, synovium, bone, menisci, ligament	High threshold, non-adapting, nociceptors

small myelinated afferents that form free nerve endings and includes mechanoreceptors, cold sensitive thermoreceptors, and some nociceptors (Nolte, 1993).

Investigators such as Wyke (1967), Warwick and Williams (1973), Hukkanen (1994), and Gebhart (1995) subdivided muscle and joint sensory myelinated nerve axons into groups I, II, or III. The unmyelinated axons from muscles and joints are referred to as group IV (see Table 1.1). The conduction velocities of the myelinated group I through III axons range from 5 to 120 meters per second; group IV axons are like C fibres, conducting slowly at less than 2.5 meters per second (Conn, 1994).

1.4.2. Classification of articular sensory receptors

Joint receptors have been classified into four types, based on their morphological appearance. These are: Ruffini endings or type I, Pacinian corpuscles or type II, Golgi tendon organs or type III and free nerve endings or type IV (Table 1.2).

1.4.2.1. Type I receptors (Ruffini endings)

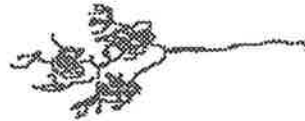
Ruffini endings are small, thinly encapsulated globular or ovoid corpuscles. They have a thin connective tissue capsule. After entering into the end organ the axon loses its myelin and arborizes freely within the capsule (Figure 1.2).

They are distributed throughout the peripheral layers of each fibrous joint capsule in clusters of up to seven corpuscles per cluster. A few corpuscles are also present at the attachment of certain joint ligaments and tendons. The mean dimensions of these receptors are 100 μm x 40 μm (Wyke, 1967; 1972; Hukkanen, 1994). Population density varies

between joints. In each individual joint capsule, they are most densely aggregated on the side subjected naturally to the greatest stress or variations in tension (Zimny and Onge, 1987; Zimny, 1988).

Figure 1.2. A Ruffini type

nerve ending in the human TMJ capsule (Redrawn from Thilander, 1961).



Wyke (1972; 1981) showed that these receptors have a higher density in posterior and anterior aspects of the knee and ankle joint capsule and relatively sparse on the lateral and medial aspects. In the hip joint the population density is much greater on the posterior and inferior than the anterior or superior aspects (Wyke, 1972; 1981). In the temporomandibular joint, the Ruffini endings occur in higher densities than any other corpuscular endings and are mostly found in superficial capsule (Thilander, 1961; Wyke, 1967; Keller and Moffett, 1968; Klineberg, 1971).

Functionally, Ruffini endings are static and dynamic mechanoreceptors, with a low threshold. They discharge continuously even at rest (Wyke, 1972). Since a proportion of these receptors are always active, they may provide awareness of joint position in immobile joints (Skoglund, 1973, cited by Hukkanen, 1994).

1.4.2.2. Type II receptors (Pacinian corpuscles)

Pacinian corpuscles are embedded in the fibrous capsule of the joint and the interarticular fat pads, but are most common in the deeper layers of the capsule and intramuscular connective tissue (Figure 1.3).

Figure 1.3. A Pacinian corpuscle found in human TMJ capsule (Redrawn from Thilander, 1961)



They are relatively large in size (280 μm x 120 μm) and thickly encapsulated, and lamellate with a central core of a single Y-shaped axon with medium myelinated nerve fibres of 9 to 12 μm diameter (Wyke, 1967). There are several variations in the shapes of these receptors. The lamellation varies between 2 and 130, depending on the tissue and joints (Hukkanen, 1994). Within individual joints, the type II receptors are relatively sparse, but are found in a higher density in the joints of hand and foot and cervical region than the shoulder and hip joints (Wyke, 1972). Kawamura et al (1967) found 85 Pacinian type corpuscles in the temporomandibular joint of cat. They were located in subsynovium and fibrous capsule. These mechanoreceptors were located in the areas of capsule that were stretched during jaw opening (anterolateral) or jaw closure (posterolateral).

In a study on the temporomandibular joint of the monkey, Keller and Moffett (1968) found paciniform endings only occasionally in the posterior capsule near its attachment to the neck of the mandible. The type II receptors behave as very low threshold

mechanoreceptors, but in contrast to the type I receptors they are inactive when the joint is at rest. They react as dynamic mechanoreceptors upon active or passive movement of the joint (Wyke, 1981).

1.4.2.3. Golgi tendon organs (type III receptors)

Type III receptors are located primarily in ligaments. They have also been found in fibrous periosteum near ligament attachments. They are the largest of the articular corpuscles, and are thinly encapsulated, flattened end organs (Figure 1.4).

Figure 1.4. A Golgi tendon organ in human

TMJ capsule (Redrawn from Thilander, 1961).



They occur singly or in clusters of 2 or 3 corpuscles and each cluster is innervated from the related articular nerve by a large myelinated afferent fibre (13 to 17 μm diameter) (Wyke, 1981). They are present in the collateral ligaments of joints, in lateral ligament, peripheral disc and disc/capsular junction of the TMJ and intrinsic joint ligaments such as the knee cruciate ligaments, but they are absent from the ligaments of the vertebral column (Thilander, 1961; Wyke, 1967; Keller and Moffett, 1968; Klineberg, 1971).

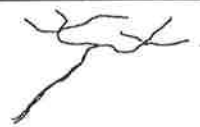
Golgi tendon organs are high threshold and very slowly adapting receptors which are active at extremes of movement when considerable stress develops in joint ligaments and may therefore prevent excessive stresses of the joints (Wyke, 1967; Zimny, 1986; Hukkanen, 1994). Wyke (1967) also stated that type III receptors are activated in immobile

joints and produce reflex inhibition of muscles operating over the joints. Therefore they are dynamic mechanoreceptors.

14.2.4. Type IV receptors (free nerve endings)

Type IV receptors are non-capsular and occur as plexuses of unmyelinated nerve fibres in the joint capsule and posterior fat pad and as free nerve endings in the lateral ligament (Wyke, 1967). They are innervated by unmyelinated and small myelinated axons less than 4 to 5 μm in diameter (Figure 1.5) and constitute the articular pain receptor system (Wyke, 1967; Clark and Wyke, 1974; Ichikawa et al 1989).

Figure 1.5. A type of free nerve ending in human TMJ capsule (Redrawn from Thilander, 1961).



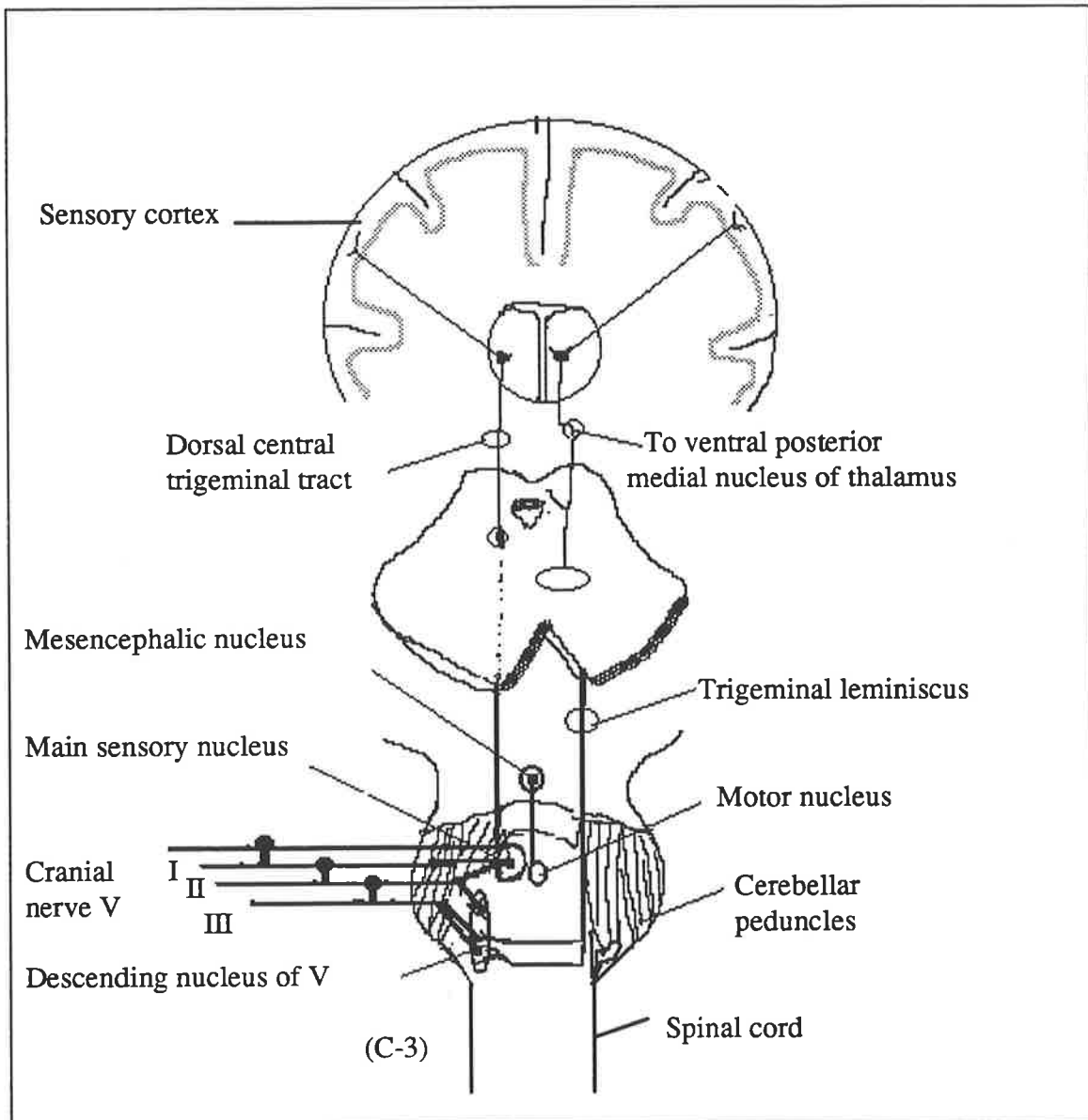
The articular pain receptors (nociceptors) have parent nerve fibres of either type C or A delta type. Type C fibres have the slowest conduction velocity (0.5 to 2 ms^{-1}) and type A delta nociceptors have a higher conduction of 12 to 30 ms^{-1} (Hukkanen, 1994). Based on the conduction velocities, it has been suggested that the C nociceptors mediate 'slow' pain and that the A-delta nociceptors are responsible for 'fast' pain (Hukkanen, 1994). (see Tables 1.1 and 1.2).

1.5. NERVE SUPPLY OF TEMPOROMANDIBULAR JOINT

The sensory innervation of the temporomandibular joint as well as motor innervation of the muscles of mastication are supplied by the trigeminal cranial nerve (Greenfield and Wyke,

1966). The trigeminal nerve is the largest of the cranial nerves. It is connected with the lateral part of the pons by a large sensory and a small motor root (Fig. 1.6).

Figure 1.6. Dorsal view of spinal cord, brain stem, thalamic and cortical pain pathway (redrawn from Mcneill, 1993)



The sensory trigeminal nerve fibres enter from the midpons, interdigitating with the fibres of the middle cerebellar peduncle, and then join the trigeminal ganglion (Conn, 1994). The

trigeminal ganglion contains most of the primary sensory cell bodies associated with the sensory trigeminal nerves. Other primary sensory cell bodies are located in the trigeminal mesencephalic nucleus. These unipolar sensory neurons vary in size, and a significant portion gives rise to myelinated axons. Several subsets of neurons have been described in a number of species based on their content of neuropeptides (Conn, 1994). The central processes of trigeminal ganglion cells make up the large sensory root of the trigeminal nerve. These fibres enter the pons and terminate in the pontine and spinal trigeminal nuclei (Fig. 1.6). The pontine trigeminal nucleus may also be called the chief, principal, or main sensory nucleus. The large diameter fibres for sensations of touch and pressure terminate in the pontine trigeminal nucleus and fibres for sensation of pain and temperature end in the spinal nucleus (descending nucleus of V). This spinal nucleus extends caudally down into the region where cervical spinal nerves 1 through 3 enter the central nervous system (McNeill, 1993). Neurons from the trigeminal as well as facial, hypoglossal and vagus cranial nerves share in the same neuron pool as neurons from cervical spinal nerves 1, 2 and 3 (McNeill, 1993). The central processes of the neurons in the pontine trigeminal (main sensory) nucleus and spinal nucleus (descending nucleus of V), cross the median plane and ascend as the trigeminal lemniscus to relay integrated sensory information to the nerve cells of the ventral posteromedial nucleus of the thalamus. The thalamus provides further integration and relays information through axons to the postcentral gyrus of the cerebral hemispheres (Snell, 1992).

The trigeminal motor nucleus, consisting of typical multipolar neurons, is situated medial to the pontine sensory nucleus. This nucleus mainly receives corticonuclear fibres from both cerebral hemispheres. It also receives fibres from the reticular formation, the mesencephalic nucleus, red nucleus, the tectum and the medial longitudinal fasciculus. The neurons of the motor nucleus give rise to the axons that form the motor root which supplies the muscles of mastication and other small muscles. The motor root fibres join sensory fibres of the mandibular nerve just distal to the trigeminal ganglion (Snell, 1992).

The peripheral processes of trigeminal ganglion cells make up the three divisions of the trigeminal nerve which are ophthalmic, maxillary and mandibular nerves (Conn, 1994). The trigeminal ophthalmic division and the trigeminal maxillary division are both purely sensory.

1.5.1. Mandibular nerve

The trigeminal mandibular division is the largest of the three branches and it consists of sensory and motor fibres. It courses inferiorly from the trigeminal ganglion and then exits the cranial cavity through the foramen ovale. It contains sensory fibres from the masticatory muscles, the lateral part of the scalp, the teeth, and the temporomandibular joint (Fig. 1.7).

According to Birgit Thilander (1961) the first person who investigated the innervation of human temporomandibular joints was Rudinger (1857). He found that in humans, the temporomandibular joint is innervated by the auriculotemporal, the masseteric and the posterior deep temporal nerves. Similar observations have been reported by Thilander (1961), Schmid (1969), Isibashi (1974), Kreutziger and Mahan (1975). The branches are derived from the mandibular nerve after its passage through the oval foramen, which is located medial to the temporomandibular joint articular eminence (Johansson et al, 1990). In various mammals, as in humans, the articular branches of the auriculotemporal, masseter and deep temporal nerves enter into the joint capsule where they divide into small branches and extend into the periphery of the articular disc (Johansson et al, 1990).

1.5.1.1. Auriculotemporal nerve

The auriculotemporal nerve is a sensory nerve with autonomic nerve contribution (Storris, 1974). After it leaves the mandibular nerve immediately below the cranial base, it passes

posteriorly close to the inner surface of the capsule of the temporomandibular joint. As it passes outwards, it usually enters the glenoid lobe of the parotid gland and here it gives off its secretomotor fibres to the gland which are derived from the glossopharyngeal nerve via the otic ganglion (see Fig. 1.7) (Scott and Dixon, 1972; Johansson et al, 1990). It then turns upwards over the posterior root of the zygomatic process immediately behind and to the outer side of the postglenoid tubercle. During its course it is closely related to the medial and posterior part of the joint capsule and gives off sensory branches to the posterior part of the articular disc and other joint structures (Thilander, 1961; Scott and Dixon, 1972; Kawamura, 1974; Johansson et al, 1986; 1990)

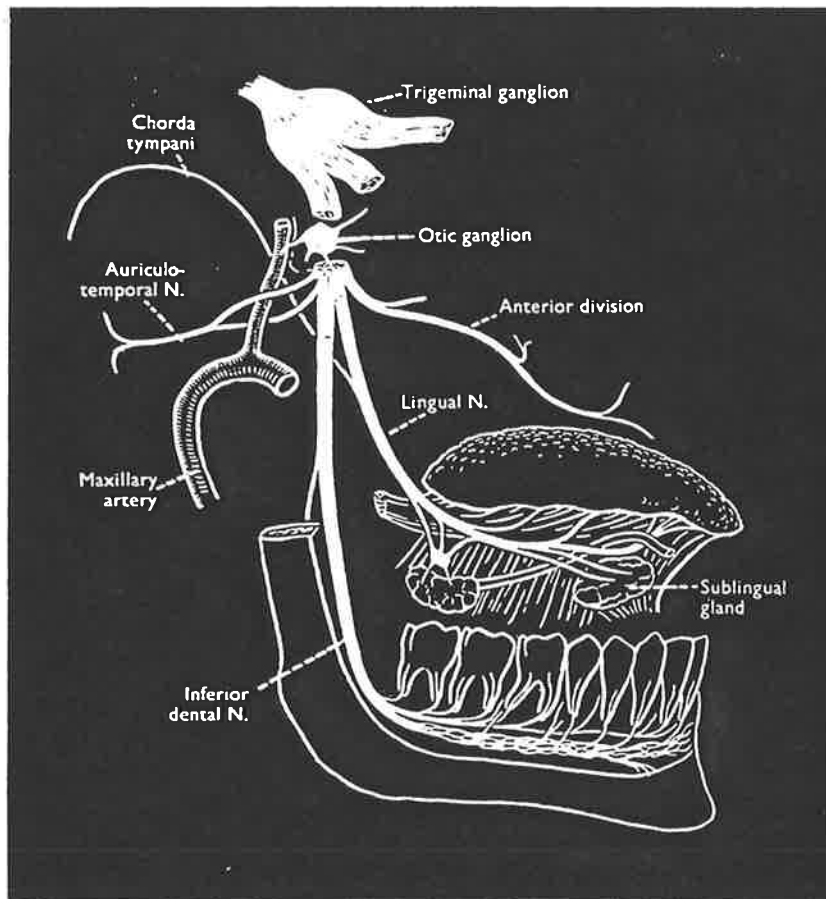


Figure 1.7 Diagrammatic representation of the mandibular nerve and its branches (adapted from Scott and Dixon, 1972).

1.5.1.2. Masseteric nerve

The masseteric nerve is mainly a motor nerve with sensory filaments distributed to the anterior part of the temporomandibular joint capsule (Thilander, 1961; Schmid, 1969). The masseteric nerve lies in close relation to the anterior attachment of the articular disc and passes laterally, close to the medial border of the lateral pterygoid muscle. The nerve reaches the masseteric muscle by passing below the zygomatic arch and emerging through the mandibular notch in its anterior part behind the tendon of the temporalis muscle. It gives branches to the anterior part of the capsule and disc (Scott and Dixon, 1972; Johansson et al, 1990).

1.5.1.3. Deep temporal nerve

The deep temporal nerve reaches the temporomandibular joint region from the anteromedial side. It follows the course of the masseteric nerve, but winds around the infratemporal crest to innervate the anterior part of temporomandibular joint capsule and temporalis muscle (Scott and Dixon, 1972; Kawamura, 1974; Johansson et al, 1990).

1.5.2. Regional distribution of nerve fibres in the temporomandibular joint

While reports on the innervation of the human temporomandibular joint by different workers (Thilander, 1961; Schmid, 1969; Ishibashi, 1974;, Kreutziger and Mahan, 1975) are broadly consistent, there are some variations. The anterior and posterior aspect of the monkey (Keller and Moffet, 1968; Johansson et al, 1986), sheep (Tahmasebi-Sarvestani et al, 1996) and cat (Klineberg, 1971) temporomandibular joints have an innervation similar to that of the human temporomandibular joint (Table 1.3).

Table 1.4. Characteristics of some neuropeptides

Neuropeptide	Amino acids	Structure	2nd messenger	References
SP	11	R-P-K-P-Q-Q-F-F-G-L-M-NH ₂	phospholipase C	Von Euler and Gaddumin, 1931; Said, 1980; Erspamer, 1981
CGRP	37	A-C-D-T-A-T-C-V-T-H-R-L-A-G-L-L- S-R-S-G-G-V-V-K-N-N-F-V-P-T-N-V- G-S-K-A-F-NH ₂	adenylate cyclase	Rosenfeld et al, 1984; Amara et al, 1985
NPY	36	Y-P-S-K-P-D-N-P-G-E-D-A-P-A-E-D- M-A-R-Y-Y-S-A-L-R-H-Y-I-N-L-I-T-R- Q-R-Y-NH	adenylate cyclase K ⁺ channel Ca ²⁺ channel	Tatemoto et al, 1982; Allen et al, 1983
VIP	28	H-S-D-A-V-F-T-D-N-Y-T-R-L-K-Q-M- A-V-K-K-Y-L-N-S-I-L-N-NH ₂	adenylate cyclase phospholipase C	Said and Mutt, 1970; Larsson et al, 1976

Table 1.3. Regional distribution of nerve fibres in the temporomandibular joint

Regions					
Species	Anterior	Posterior	Lateral	Medial	References
Human	M, PD	AT	PD	M	Thilander (1961)
Human	M, PD	AT	M, PD	M, AT	Ishibashi (1974)
Human	M, PD	AT	PD	M	Schmid (1969)
Human	M, PD	AT	AT	AT	Kreutziger & Mahan (1975)
Monkey	M	AT	M	?	Keller & Moffett (1968)
Monkey	M	AT	?	?	Johansson et al (1986)
Sheep	M, PD	AT	M	AT	Tahmasebi, et al (1996)
Cat	M, PD	AT	PD	M	Klineberg (1971)

M, masetric nerve; AT, auriculotemporal nerve; PD, posterior deep temporal nerve

1.6. NEUROPEPTIDES

Neuropeptides are biologically active peptides found throughout the central and peripheral nervous systems (Polak and Bloom, 1989). They are synthesized in the cell body of neurons and axonally transported to the nerve terminal. Neuropeptides can function as neurotransmitters or neuromodulators (Roberts and Allen, 1986 cited by Naraine, 1994).

The history of the study of neurotransmitters goes back to ancient times when, remarkably, Greeks and Romans suggested that the large nerves of the body, which could be easily visualised during dissection, carried a substance or substances that coordinated and activated the body. They called this substance 'psychic pneuma' and the Hindus called this substance 'prana', the flow of which could be increased by the practice of Yoga. The early

Chinese (3000 B.C.) called the flow of 'chi' or an energy that flowed through the body in channels that could be helped by the medical practice of acupuncture and by an exercise called 'tai chi chuan' (Conn, 1994).

The classic neurotransmitters are now thought of as small molecules, synthesized and stored in secretory granules of the axons of nerves (Conn, 1994). Chemically, these transmitters can be a biogenic amine (eg., serotonin, or histamine) or an amino acid (e.g., γ -aminobutyric acid [GABA]) or small proteins (i.e., peptides) that are synthesized in the cell body and carried to the axon by axoplasmic transport. These transmitters inhibit or stimulate the function of the target cell by combining with receptors and initiating a biochemical change in the membrane, cytoplasm, or nucleus of that cell (Conn, 1994).

More than 100 peptide transmitters have been described and isolated to date and more probably will be discovered every year. However few have been found in relation to joints. Those found within joints include substance P (SP), calcitonin gene-related peptide (CGRP), vasoactive intestinal polypeptide (VIP), neuropeptide Y (NPY), plus neurokinins A and B (NKA and NKB) (Gaywood, 1989). The characteristics of some neuropeptides are shown in Table 1.4.

1.6.1. Substance P

Substance P is an 11-amino acid protein that belongs to a family of bioactive peptides called the tachykinins (Said, 1980; Erspamer, 1981). It was first described by Von Euler and Gaddumin in 1931 and then isolated and chemically characterised by Chang and Leeman in 1970. Substance P is widely distributed in the peripheral and central nervous system of all vertebrate species from fish to mammals, including humans (Pernow, 1953). Substance P is synthesised in cell bodies in dorsal root ganglia and is axoplasmically transported toward the terminal regions of the peripheral sensory nerve branches where it is

stored in nerve endings (Brimijoin et al, 1980; Harmar et al, 1981; Payan, 1989). It plays a key role as a transmitter or modulator in the peripheral and central nervous system.

Highly sensitive immunohistochemical techniques have permitted a detailed morphological characterization of the neuronal systems containing substance P. It is found in unmyelinated nerve fibres of the primary sensory neurons that are believed to be involved in transmission of nociceptive information (Hökfelt et al, 1975; Barber et al, 1979). Release of substance P and other neuropeptides from the peripheral endings of afferent C fibres has been suggested to play multiple roles in the physiology and pathophysiology of various target organs (Fitzgerald and Gibson, 1984). Some of its neurotransmitter activities include smooth muscle contraction, vasodilation and histamine release which all contribute to local neurogenic inflammation (Serra et al, 1988).

Several studies have reported reduced density of substance P immunoreactive nerve fibres in synovia of joints affected by rheumatoid arthritis (Grönblad et al, 1985; Mapp et al, 1990; Konttinen et al, 1990, Hukkanen et al, 1991). It has been suggested that substance P increases the severity of adjuvant induced inflammatory arthritis in rats (Payan, 1989). In this animal model, the development of more severe arthritis (inflammatory) in distal limb joints (ankles) compared to proximal joints was interpreted as being related to the greater density of substance P-containing nerves in the distal joints.

1.6.2. Calcitonin gene-related peptide

The field of neuroanatomy has greatly benefited from the discovery of calcitonin gene-related peptide, an alternative expression product of the calcitonin gene (Rosenfeld et al, 1984; Amara et al, 1985, Girgis et al, 1985). Calcitonin gene-related peptide (CGRP) was accidentally discovered when the gene for calcitonin in the thyroid was sequenced and translated into protein (Conn, 1994). Molecular biological techniques revealed that the rat

calcitonin gene encoded two different messenger RNAs (m RNAs), one yielding the calcitonin precursor molecule and the other a similar sized protein, including the predicted 37-amino-acid CGRP (Amera et al, 1982; Rosenfeld et al, 1983). The synthesis of mRNA for CGRP by alternative splicing in the formation of calcitonin mRNA was shown in a human medullary thyroid carcinoma cell line (Morris et al, 1984) and several other tissues (Fischer and Born, 1984; Goodman and Iversen, 1986). Subsequently in both rats (Fisher and Born, 1985) and humans (Steenbergh et al, 1985; Alavizaki et al, 1986), a second CGRP gene has been discovered. All four CGRP genes code for highly homologous peptides that exhibit little immunochemical or pharmacological cross-reactivity with calcitonin from other species (Fischer and Born, 1984; Goodman and Iversen, 1986). Further work using both biochemical and histochemical methods has demonstrated CGRP in significant quantities throughout both the central and peripheral nervous system of a variety of mammals (Gibson et al, 1984; Goltzman and Mitchell, 1985; Goodman and Iversen, 1986; Hoheisel et al, 1994). Its release results in a multiplicity of potent biological effects including vasodilation, smooth muscle contractility, inhibition of bone resorption and modulation of carbohydrate metabolism (Brain et al, 1985; Bernard and shih, 1990). Calcitonin gene related peptide is synthesized by small and medium-sized sensory neurons in the dorsal root ganglia (Gibson et al, 1984; McCarthy and Lawson, 1990), which are known to innervate a variety of tissues including osteoarticular tissues (Bjurholm et al, 1988; 1990; 1992; Hukkanen et al, 1992b). It is co-localised with substance P or occurs separately in C-type pain fibres (Pernow, 1983).

1.6.3. Neuropeptide Y

Neuropeptide Y (NPY) has been localized in both the human central and peripheral nervous systems (Allen et al, 1983; 1984; Lundberg et al, 1983; Polak et al, 1991; Hukkanen et al, 1992; Gibbins, 1990; 1992; Gibbins and Matthew, 1996). It is a 36-amino acid structure originally isolated by Tatemoto in 1982 from porcine brain (Tatemoto et al,

1982). Neuropeptide Y-like immunoreactivity is localized to sympathetic noradrenergic neurons and is co-localized with catecholamines (Lundberg et al, 1988), cytoplasmic tyrosine hydroxylase and intravesicular dopamine-B-hydroxylase (markers for postganglionic sympathetic fibres) (Kontinen et al, 1991). High frequency stimulation of sympathetic nerve fibres causes secretion of both NPY and noradrenaline, and it has been found to coexist with VIP in non-noradrenergic neurons (Walker et al, 1991). In the synaptic cleft, NPY acts at the presynaptic level by inhibiting noradrenaline release. It acts postsynaptically on the vasculature. Neuropeptide Y acts as a vasoconstrictor and can potentiate the action of various vasoactive substances and neurotransmitters. Its contribution to cardiovascular regulation is thought to be highly significant as it also modulates myocardial contractility.

Neuropeptide Y has been found in most tissues including the cardiovascular system (Wharton et al, 1981; Gu et al, 1983), respiratory tract (Wharton et al, 1979; Sheppard et al, 1984), gastrointestinal tract (Pearse and Polak, 1975; Stjernquist et al, 1983) and articular tissues (Mapp et al, 1990; Schaible and Grubb, 1993). The vasomotor actions of NPY on microvasculature have been found to be different in different species (Hashim and Tadepalli, 1995). The density of NPY immunoreactive perivascular nerves in the synovium has been shown to be reduced in patients with rheumatoid arthritis (Mapp et al, 1990; Pereira da Silva and Carmo-Fonseca, 1990).

1.6.4. Vasoactive intestinal polypeptide

Vasoactive intestinal polypeptide (VIP) was originally isolated from porcine duodenum by Saide and Mutt (1970) and was characterized as a linear peptide of 28 amino acids. It can be found in both the central and peripheral nervous system (Larsson et al, 1976; Polak et al, 1991; Hukkanen et al, 1992; Gibbins, 1992; Gibbins and Matthew, 1996). It is structurally related to secretin, glucagon (Said, 1982), gastric inhibitory peptide (GIP) and a newly

isolated 27-amino acid-peptide, histidine isoleucine (PHI), from porcine intestine (Itoh et al, 1983). As the name implies, VIP is a potent vasodilator, but it also has a wide variety of other properties including enhancement of mucosal secretion and the relaxation of vascular and non-vascular smooth muscle of gut, respiratory tract (Piper et al, 1970; Said and Mutt, 1970; Uddmann et al, 1978) and genitourinary tract (Alm et al, 1977; Helm et al, 1981). Vasoactive intestinal polypeptide may also stimulate osteoclast-mediated bone resorption and regulate bone growth and metabolism (Hohmann et al, 1983).

Vasoactive intestinal polypeptide-immunoreactive nerves have been localised in many other tissues including the heart (Weihe et al, 1984), exocrine glands (Lundberg et al, 1980), primary sensory neurons in the dorsal root ganglia (Lundberg et al, 1979), periosteum, joints and ligaments (Eisenstein et al, 1994). Vasoactive intestinal polypeptide-IR fibres have a non-vascular distribution in ankle joint synovium and periosteum of rats (Eisenstein et al, 1994; Ahmed et al, 1995). It has been found to colocalize with acetylcholine in parasympathetic nerves (Lundberg et al, 1979).

1.7. NEUROSPECIFIC PROTEINS AS GENERAL MARKERS

Recent immunohistochemical techniques have made it possible to identify nerve components of tissues. Antibodies to neural proteins can be used as general cytoplasmic markers in all classes of nerves to provide a clear picture of the total innervation of the tissue (Hukkanen et al, 1993; Morani et al, 1994). Protein gene product 9.5 (PGP 9.5), neurofilament proteins (NFP), glia-specific protein S-100, synaptophysin and growth associated protein 43 (GAP-43/B-50) are among the most important general neural markers that have been discovered.

1.7.1. Protein gene product 9.5

Protein gene product 9.5 (PGP 9.5), is a soluble protein isolated from human brain (Jackson and Thompson, 1981). It is a major protein component of neuronal cytoplasm present in a wide range of species (Jackson et al, 1985). Protein gene product 9.5 is widely distributed in both the central and peripheral nervous system and has an extensive distribution throughout the cell from perikaryon to fine terminals (Thompson et al, 1983; Gulbenkian et al, 1987). Antisera for PGP 9.5 have been used in many studies to detect sensory and autonomic fibres in a variety of tissues. In an investigation of cardiovascular innervation of the guinea-pig, Gulbenkian et al (1987) found that PGP 9.5 was more extensively distributed amongst neuronal subtypes than neuron-specific enolase (NSE) and neurofilament triplet protein and demonstrated that it occurred in both cholinergic and adrenergic nerves. Ramieri et al (1990) and Morani et al (1994) used PGP 9.5 to study the innervation of human temporomandibular joint tissue. In another study Hukkanen (1994) used PGP 9.5 very extensively to study the central and peripheral nerves in normal and experimental rat tissues.

The widespread occurrence of PGP 9.5 during neurogenesis in the rat has proved to be a useful tool in studying the developing nervous system (Kent and Clarke, 1991). According to Gulbenkian et al (1987), PGP 9.5 is the best immunohistochemical marker for neural elements currently available.

There is some concern about the interpretation of data arising from the use of PGP 9.5 as an overall marker of neural structure in sites where extensive tissue damage has occurred (Hukkanen, 1994). This is because PGP 9.5 is a "heat shock protein", that is, it is one of proteins involved in the degradation of damaged proteins during the stress response

(Hukkanen,1994). Therefore PGP 9.5 may not represent an overall staining of all neural structures in the areas where tissue damage is involved.

1.8. ARTHRITIS

Osteoarthritis and rheumatoid arthritis are two common joint pathologies which may involve both small and large joints of the body.

1.8.1. Osteoarthritis

Osteoarthritis is a noninflammatory, progressive disorder of moveable joints, particularly weight-bearing joints. It is characterized by cartilage breakdown and by formation of new bone (proliferation) in the subchondral areas and at the margin of the joint (Moskowitz, 1984). Cartilage breakdown leads to erosion of the articular surface and perforation of the articular disc and subsequent exposure of underlying bone. Proliferation (see fig. 1.9) may lead to fibrillation and osteophyte and/or sub-cortical cyst formation (Toller and Glynn, 1976; Moskowitz, 1984).

According to Moffett et al (1964), remodelling is one of the major causes of temporomandibular osteoarthritis, and it has been classified into (a) progressive, (b) regressive and (c) circumferential types. Progressive remodelling comprises proliferation of the articular surfaces which occurs most often at the periphery or at weight-bearing areas. The cells within the proliferative zone have the potential, with suitable stimuli and conditions, to increase or renew their production of cartilage. This results in either closure of the joint space or increase in the vertical dimension of the joint. The condylar proliferative cartilage mineralizes, beginning at the subcondylar bone, and is subsequently resorbed and replaced by bone with haversian systems. In the early stages of

temporomandibular joint osteoarthritis, the connective tissue covering the condyle is reduced due to progressive remodelling. Regressive remodelling, by definition involves a decrease in tissue bulk from the articular surface. There is an osteoclastic resorption of the subcondylar bone, with replacement by vascular mesenchyme and proliferation of cartilage.

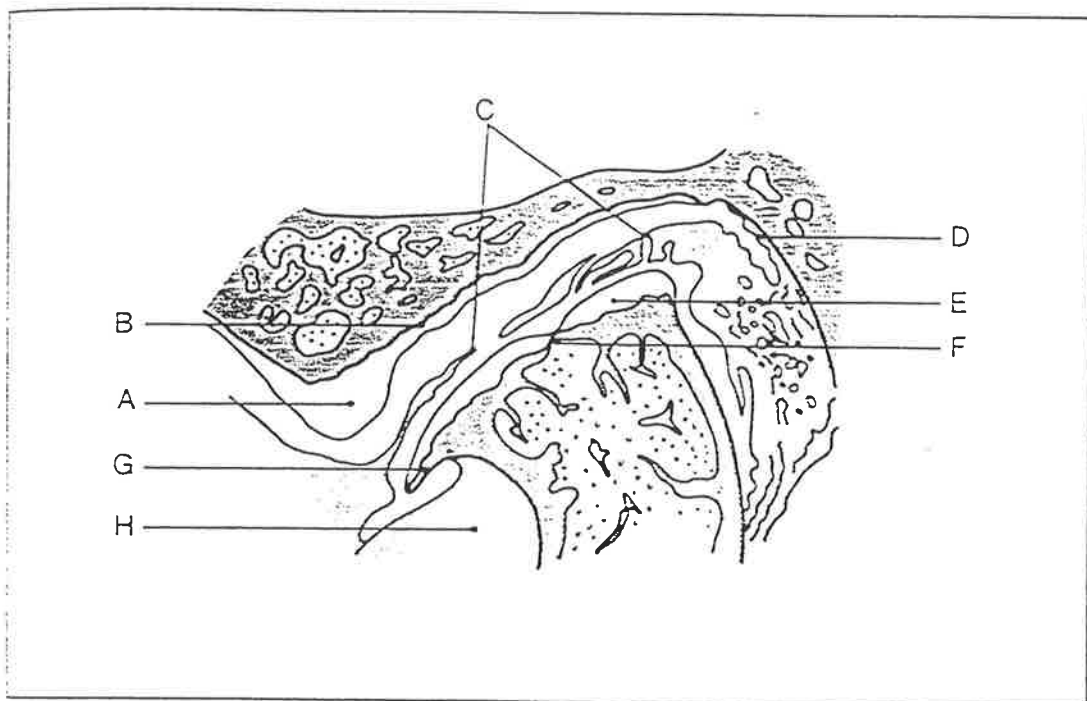


Figure 1.8. Drawing of TMJ with degenerative arthritis (TMJ arthrosis) A-Build up of collagen over articular eminence, B-Flattened and eroded articular eminence, C-Remnants of meniscus, D-Synovial membrane, E-Collagen surface of condyle, F-Degenerated articular surface of condyle, G-Osteophyte, H-fibers of lateral pterygoid inferior belly. (adapted from Mahan, 1980).

Synovial membrane, E-Collagen surface of condyle, F-Degenerated articular surface of condyle, G-Osteophyte, H-fibers of lateral pterygoid inferior belly. (adapted from Mahan, 1980).

Circumferential remodelling results in an increased diameter of the articular surfaces due to progressive remodelling. In the human temporomandibular joint, progressive, regressive, and circumferential remodelling occur simultaneously and eventually result in osteoarthritis (Johnson, 1962). Osteoarthritic changes of the temporomandibular joint appear to be directly related to the ageing process and functional abuse of the joint (Farob et al, 1992). Ishimaru et al (1991) had difficulty diagnosing patients with temporomandibular joint osteoarthritis from a clinical viewpoint, because of similarities with patients with temporomandibular pain and dysfunction syndrome, myofascial pain and dysfunction syndrome and internal derangement of the temporomandibular joint. But they stated it can be easily diagnosed in the advanced stage of osteoarthrosis when there is osteophyte or sub-cortical cyst formation.

1.8.2. Rheumatoid arthritis

Rheumatoid arthritis is characterised by inflammatory changes in joints and it tends to be chronic. In the temporomandibular joint the rheumatoid arthritis disease first affects the mandibular condyle causing destruction of the articular surface, and this may proceed either to partial or to complete fibrous ankylosis of the joint (Fig. 1.10).

In rheumatoid arthritis the synovial tissue is also affected by disease. The synovial lining cells are inflamed and various immuno-inflammatory cells are present. One of the main causes of disability in patients with chronic rheumatoid arthritis is pain. It has been suggested that chronic inflammatory disease significantly alters proprioceptive sensations in joints and this may be due to loss or distortion of afferent feedback from mechanoreceptors innervating the affected joint (Basbaum and Livene, 1991; Ferrell et al,

1992). Pain endings are common in joint capsules and they are activated by vigorous twisting and stretching of the capsule (Gibson et al, 1988; Walsh et al, 1992). Certain clinical findings are consistent with nervous system involvement in the pathogenesis of arthritis (Widenfalk, 1991). Ransjo and Thilander (1963) studied perception of mandibular position in patients with temporomandibular joint disorders and concluded that pathologic changes in the joints impaired joint receptors.

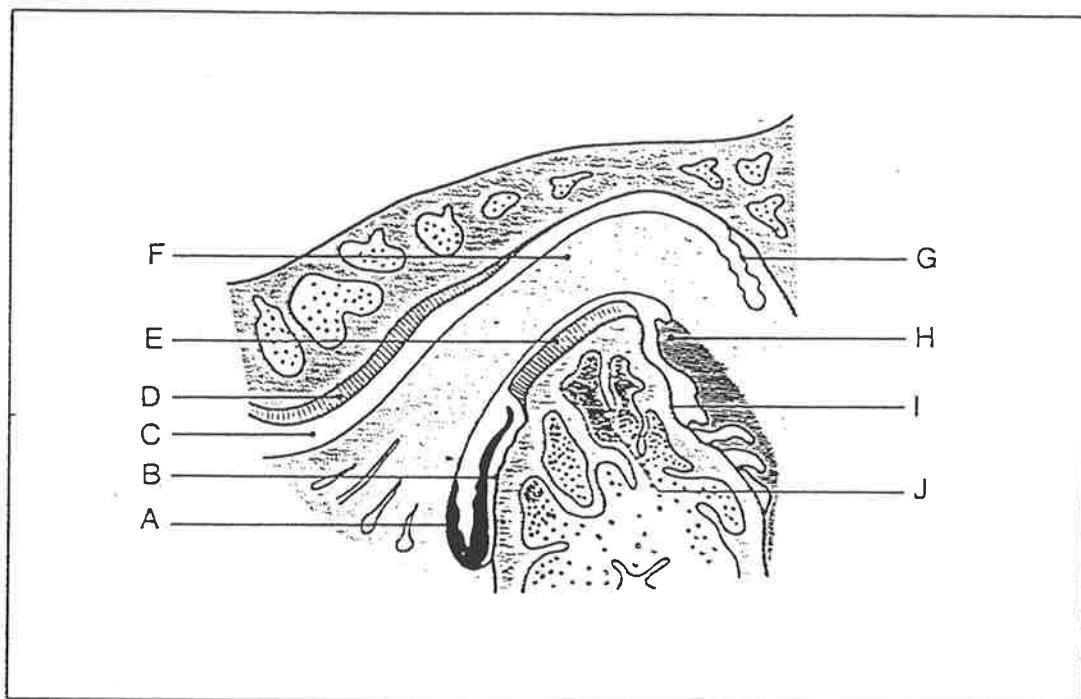


Figure 1. 9. Drawing of TMJ with rheumatoid arthritis. A-Pannus eroding condyle from the anterior, B-Eroded condyle bone, C-Superior cavity, D-Collagenous articular surface of articular eminence, E-Remaining, normal articular collagen on condyle, F-Unaffected (normal) collagen of the meniscus, G-Synovial membrane of superior cavity (not yet affected by pannus formation), H-Newly formed collagen from pannus, I-Eroded bone on posterior of condyle, J-Acute inflammation (adapted from Mahan, 1980).

1.8.3. Neuropeptides and arthritis

Joints are innervated by corpuscular mechanoreceptors and plexuses, as well as by free nerve endings of small unmyelinated afferent nerve fibres. Some of these afferent unmyelinated C-fibres and A-delta fibres contain the neuropeptides substance P and CGRP, which are involved in transmission of pain signals (Pernow, 1983). These neuropeptides have multiple proinflammatory properties (Lotz, et al, 1987; Holzer, 1988) and have been shown to increase the severity of adjuvant-induced arthritis in rats (Levine et al, 1988; Payan, 1989). The relative susceptibilities of knee and ankle joints to adjuvant arthritis are correlated with the densities of their sensory nerve fibres (Levine et al, 1984; Konttinen et al, 1989). In recent studies, several investigators have shown that substance P and CGRP synthesis is increased in experimental arthritis in the dorsal root ganglia supplying the affected joint and the sensory terminals of the spinal dorsal horn (Kuraishi et al, 1989; Marlier et al, 1991; Smith et al, 1992). In another study by Lundeberg et al (1996), there was an increase in the levels of SP, CGRP, NKA and NPY in TMJ synovial fluid of humans bilaterally, following unilateral injection of carrageenan which induced cartilage changes similar to osteoarthritis in humans.

Studies from other workers have shown a decrease in density of peptide-containing nerves of synovium in rheumatoid arthritis (Grönblad et al, 1988; Pereira da Silva and Carmo-Fonseca, 1990). In the adjuvant arthritic rat synovium a near total disappearance of nerves has been seen (Hukkanen et al, 1991).

1.8.4. Ageing and osteoarthritis

There is little information about osteoarthritic change due to ageing of the temporomandibular joint. Angel (1948) noted that with age the articular surfaces of the

temporomandibular joint tended to become flat and somewhat deformed. He called this condition osteoarthritis and considered it to be part of the normal ageing process. However, he emphasised that if the changes occur prematurely the condition can be considered pathological. Other investigators have reported that the incidence of osteoarthritis increases with age. These findings have been determined by clinical (Toller, 1973), radiological (Muir and Goss, 1990), arthroscopic (Holmlund and Hellsing, 1988) and autopsy studies (Blackwood, 1963; Öberg et al, 1971). The rate of occurrence of temporomandibular joint osteoarthritis and its correlation with age is shown in Table 1 5.

Table 1.5. The incidence of human TMJ osteoarthritis (OA) and its correlation with age.

Samples	% OA	Age	References
patients	40	over 40	Bennett et al (1971)
patients	8	adult	Toller (1973)
cadavers	40	over 40	Blackwood (1963)
cadavers	22	adult	Öberg et al (1971)

More recently, it has been suggested that ageing may be considered as the sum of all morphologic and functional alterations that occur in a subject and lead to functional impairment (Jazwinski and Rothschild, 1991). An increasing vulnerability to disease is usually superimposed on basic biologic changes occurring with age (Jazwinski and Rothschild, 1991). These findings suggest that it is important not only to look at the pathologic but also to investigate the physiologic ageing processes affecting the temporomandibular joint structure.

1.9. ANIMAL MODELS FOR TMJ RESEARCH

Use of human tissue is subject to many limitations, and studies on an animal having a temporomandibular joint that closely resembles the human temporomandibular joint are essential if appropriate observations are to be made. Various animal models have been developed for studying the temporomandibular joint, for example, mouse (Frommer and Monroe, 1966; Silberman, 1976), guinea pig (Silva, 1969), rat, sheep, dog (Gillbe, 1973), rabbit (O'Dell et al, 1989) and sheep (Bosanquet and Goss, 1987; Goss and Bosanquet, 1989; Goss et al, 1992; Ishimaru et al, 1993).

A comparative study by Bermejo et al (1993) on the temporomandibular joint of humans and of other mammals including cat, dog, cow, sheep, goat, pig, rabbit and rat revealed the presence of upper and lower joint cavities, each independent of the other. In all the animal and human specimens studied by Bermejo et al (1993) except the rabbit and the rat, the mandibular condyle extended in a lateromedial direction. In herbivores such as the rabbit the maximum diameter of the mandibular condyle extends anteroposteriorly and is suited for wide lateral movement (Hatton and Swann, 1986; Bermejo et al, 1993). In rodents the temporomandibular joint is considered to be a double anteroposterior cylindrical pivot joint that moves from back to front and vice versa (Bermejo et al, 1993). In omnivorous mammals the temporomandibular joint exhibits intermediate features (Bermejo et al, 1993) and carnivores such as lions have a rotating ball and socket temporomandibular joint (Goss, 1995).

Some investigators believed that the rabbit and rat are not suitable experimental animal models because of the small size of the animals and their marked anatomic differences with respect to human beings; instead they propose the Merino sheep because of its similarity in size and surgical anatomy with human beings (Bosanquet and Goss, 1987). The

sheep, goat, pig, rabbit and rat by Bermejo et al (1993) suggested that only the pig may be chosen as a suitable experimental animal model, because of the size of its articular structures, the shape of its meniscus, and it is omnivorous.

The function of the masticatory apparatus and the shape of the temporomandibular joint fossa varies between species. According to Goss (1995) translation (rather than rotation) and the prime site of function (anterior and superior portion of fossa) are two important characteristics in the human temporomandibular joint which can be critical for a successful animal model. He identified these two characteristics in the goat, but the translatory movement was found to be predominantly mediolateral rather than anteroposterior. Goss (1995) found sheep and goat temporomandibular joints to be similar in size to the human temporomandibular joint, thus allowing direct use of the instruments used in clinical practice. He stated that this is not possible in *Macaca* and *Papio*, nor in many other laboratory animals. Besides the morphological and functional aspects, in terms of other characteristics such as size, animal husbandry, cost, and ethical acceptance, sheep and goats are suitable animal models for temporomandibular joint research.

1.9.1. Induced arthritis

Several techniques have been developed to induce osteoarthritis and rheumatoid arthritis in animal models. Some commonly used methods for osteoarthritis include:

- (1) Intraarticular injection of antigen in rabbits (Murray, 1964; Moskowitz et al, 1970; Silberman, 1976; Merjersjo, 1984; see also review by Ishimaru et al, 1991).
- (2) Immobilization and/or compression of the joint in rabbits (Salter and Field, 1960; Trias, 1961).

Experimental models based on surgical manipulation are more widely used in the study of degenerative changes (Ghosh et al, 1983; Bosanquet et al, 1991a, b, c; Ishimaru et al, 1991; Goss et al, 1992; Ishimaru, et al, 1993). The results of using these experimental animal models have indicated that the sequence of changes to the bone and cartilage composition will vary with the model. Furthermore, each model may only reproduce certain aspects of the degenerative changes associated with osteoarthritis, such as surface matrix damage, fibrillation, flattening, erosion, subcortical cyst formation and fibrous repair.

Most of the evidence for the effect of inflammatory joint disease such as rheumatoid arthritis on the nervous system derives from experiments which have been conducted in animal models. Some authors have proposed that depletion of nerve fibres is associated with chronic synovial inflammation and can be induced by a variety of stimuli (Mapp et al, 1994). They have investigated the depletion of nerve fibres in the synovium by the induction of arthritis in the rat using hydrogen peroxide induced inflammation. According to these authors, this model of inflammation is one of acute tissue damage from the hydrogen peroxide. Synovitis can also be induced by injection of latex spheres or direct injection of antigen into the joint (Mapp et al, 1994). Other commonly used animal models for rheumatoid arthritis include: collagen-induced arthritis in rat, mouse and primate (Billingham, 1983); adjuvant-induced arthritis in rats (Hukkanen et al, 1991) and streptococcal cell wall-induced arthritis in rats and mice (Henderson et al, 1993).

1.10. AIMS OF THIS STUDY

Hypothesis

The following hypotheses were proposed:

I) There is a regional variation in the distribution of nerve fibres in the sheep TMJ which may be related to the movement characteristic of this joint in this species.

II) It has been suggested that the TMJ disc is innervated during fetal development but at later ages these nerves degenerate and persist only in the peripheral disc. Is the interarticular disc in adult and fetal sheep TMJ innervated? If so, what types of nerve fibres are present?

III) It has been shown that degenerative changes associated with inflammatory rheumatoid arthritis deplete the sensory and sympathetic nerve fibres in the synovial joints. Does this depletion of nerves occur in non-inflammatory induced degenerative joint disease in TMJ? What would be the density and distribution of nerves in various parts of the degenerated joints?

The specific aims

The main aims of the present thesis were as follows:

(1) To describe the morphology and distribution of afferent receptor structures and efferent noradrenergic nerve fibres in TMJ in normal Australian Marino sheep, using neurohistochemical techniques.

(3) To examine the morphology, distribution and co-existence of neuropeptide immunoreactive nerve fibres in the TMJ of late gestation fetal sheep.

(4) To investigate the influence of experimentally induced osteoarthritis on the innervation of the TMJ in sheep

CHAPTER 2

TEMPOROMANDIBULAR JOINT MORPHOLOGY

2.1. SUMMARY	2
2.2. INTRODUCTION	3
2.3. MATERIALS AND METHODS	3
2.3.1. Animals	3
2.3.2. Macroscopic morphology	3
2.3.4. Microscopic morphology	4
2.3.5. Scanning electron microscopy	4
2.4. RESULTS	5
2.4.1. General features	5
2.4.2. Articular surfaces	5
2.4.3. Capsule	6
2.4.4. Articular disc	7
2.4.5. Synovium	8
2.5. DISCUSSION	8
2.5.1. Articular surfaces	9
2.5.2. Articular disc	10
2.5.3. Capsule	11
2.5.4. Synovium	12

2.1. SUMMARY

The gross anatomy, light and electron microscopy of the mandibular condyle, glenoid fossa, capsule, synovial membrane and disc were examined in the normal sheep temporomandibular joint, to facilitate the understanding of its neurology and the pathological changes due to experimentally-induced osteoarthritis of the temporomandibular joint, that are presented in other parts of this thesis.

The macroscopic study of the sheep temporomandibular joint showed the capsule as a loose, thin structure which is strengthened on the anterolateral side. The capsule is attached to the periphery of the articulating surface of the glenoid (mandibular) fossa and to the neck of the mandible. The mandibular condyle is wider mediolaterally and forms an articulation with the glenoid fossa of the temporal bone by an articular disc. The articular disc was a firm oval plate that divided the joint into upper and lower compartments. The articular surfaces of the glenoid fossa and the condyle had a smooth, uniform appearance. The condylar head and temporal surface of the joint showed a relatively acellular fibrous articular surface that overlies cartilage. The fibrous tissue covering the temporal surface was thinner than that covering the condylar surface. Neither blood vessels nor nerves were found in both articular surfaces. The synovial membrane was seen to line all the internal surfaces of the joint cavity with exception of the articular surfaces. A complex of villous structures and folding were noted in both extremities of the superior and inferior joint cavities. The subsynovial tissue (subintima) was well vascularised.

2.2. INTRODUCTION

The general organisation of the temporomandibular joint of the sheep has been described by authors such as Parsons (1899), May (1970) and Miller (1988). Many other authors have contributed detailed observations on aspects of TMJ anatomy such as articular surfaces (Bosanquet and Goss, 1987; Bosanquet et al, 1991a, b, c; Gerard et al, 1992), capsule (Bosanquet and Goss, 1987), disc (Bosanquet et al, 1991a; Gerard et al, 1992), and synovium (Di Iulio, 1995) as incidental observations from various research projects. Nevertheless, there is still no single comprehensive description of the macroscopic and microscopic morphology of the sheep TMJ. Consequently, this first part of the project details the gross and microscopic appearance of the sheep TMJ to enable a good understanding of the arrangement of neural structures in this joint.

2.3. MATERIALS AND METHODS

2.3.1. Animals

The temporomandibular joints of six Australian Merino sheep were studied. The sheep were healthy, young adult animals (less than 2 years old). All sheep were killed through an overdose of sodium pentobarbital (Nembutal, Abbott, Sydney, Australia) in accordance with the ethics guidelines of the University of Adelaide, South Australia.

2.3.2. Macroscopic morphology

The joints of three animals were dissected under a magnifying lens. After removal of the skin and fascia, the heads was sectioned through the mid-sagittal plane into two halves. The right and left TMJs (including the glenoid fossa, articular eminence, condyle and mandibular neck, joint capsule, disc, as well as the surrounding soft

tissues) were removed "en bloc" with a band-saw and fixed in 10% neutral phosphate buffered formalin. The prosections were recorded photographically using a Nikon FA camera with black-and-white Pan F film.

2.3.4. Microscopic morphology

The joints of other three animals were processed for histological investigation. After the joints had been fixed, they were decalcified in a solution containing 9.5% of hydrochloric acid and 1% sodium acetate in saturated ethylenediaminetetracetate (EDTA, Sigma, Australia) for 2 weeks. Conventional plain radiographs were used to assess decalcification. Decalcified blocks were sectioned in the sagittal plane into lateral, central, and medial parts. These were then embedded in paraffin and cut at 10µm. The silver impregnation method described by Linder (1978) and routine haematoxylin and eosin, Massons trichrome and alcian blue stains (Drury and Wallington, 1967) were used for studying the general morphology of the TMJ.

2.3.5. Scanning electron microscopy

The tissues from the disc, capsule, condylar surface and glenoid fossa of the TMJ were fixed in 2% glutaraldehyde in phosphate buffer. Dehydration was carried out with increasing concentrations of acetone. The tissue was then glued to a specimen carrier and vacuum-coated with silver. The specimens were then examined in a scanning EM at 30KV and the images obtained recorded photographically.

2.4. RESULTS

2.4.1. General features

No qualitative differences could be found between left and right joints of the same animal, and between joints from different animals using the methods described in this study, consequently the observations reported are typical of all joints examined.

The skull of the sheep is characterised by long jaws in which the upper incisors do not develop. The lower jaw consists of paired mandibles, each of which has a well developed coronoid process which curves superiorly and caudally, posterior to the orbit (Figs. 2.1a, b). The mandibular ramus is long so as the condyle of the mandible, hence the temporomandibular joint lies high above the occlusal plane. A shallow mandibular notch separates the neck and condyle from the coronoid process (Figs. 2.1a, b).

The temporomandibular joint is composed of the mandibular condyle and the glenoid fossa on the ventral surface of the zygomatic process of the temporal bone (Fig. 2.2a). The articular surface of the glenoid fossa is much larger than that of the mandibular condyle. An articular disc or meniscus divides the joint into two compartments (Fig. 2.2a, b). The articular capsule presented an outer fibrous layer and an inner or synovial layer. The fibrous layer surrounded the joint, attaching to the temporal bone and mandibular condyle. On the lateral side, the capsule was thickened by additional dense fibrous tissue called the lateral ligament.

2.4.2. Articular surfaces

The articular surfaces of the glenoid fossa and the articular condyle had a smooth, uniform appearance and even margins. The temporal articular surface was slightly convex in the anterior part, with no evidence of an articular tubercle (Figs. 2.1; 2.3). Posteriorly, the glenoid fossa was limited by a vertical shelf of temporal bone, the

PLATE 1 Osteology Of The TMJ

Figure 2.1 Lateral aspect of the skull of an adult Australian merino sheep showing the condyle of the mandible (Co), coronoid process of the mandible (Cor), the external acoustic meatus (EAM), glenoid fossa (GF) and zygomatic arch (Z). Bar: 16mm (a) ; 10mm (b).

1a



1b

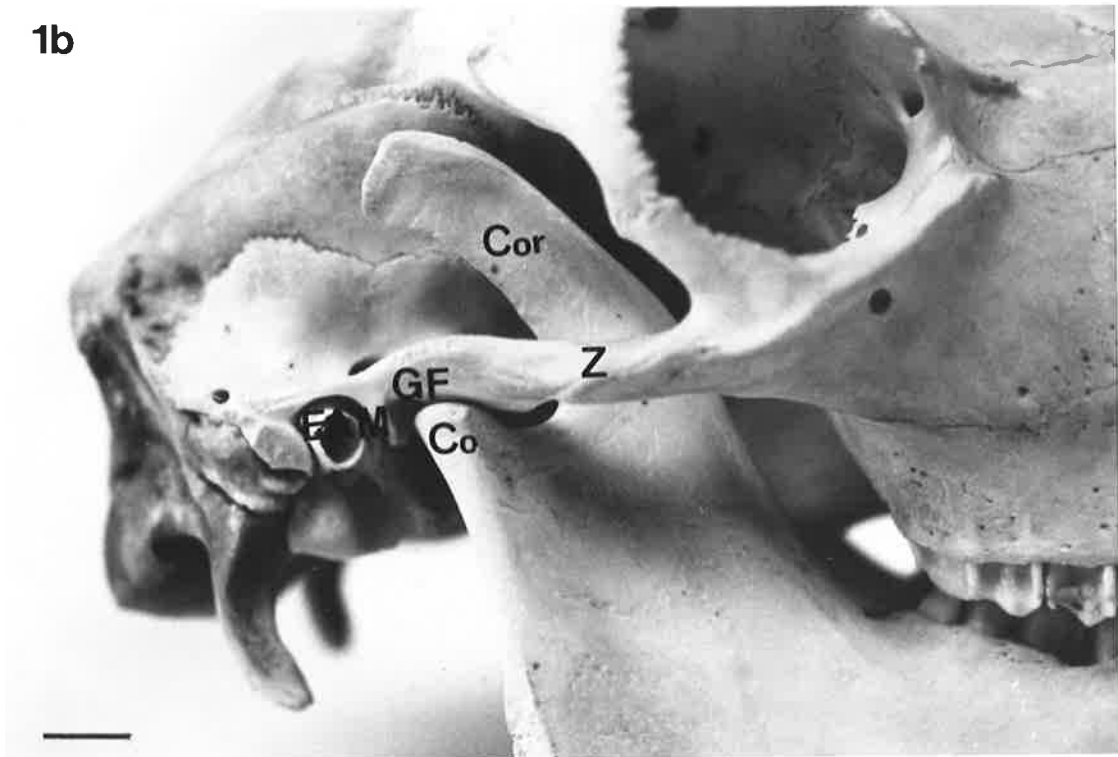
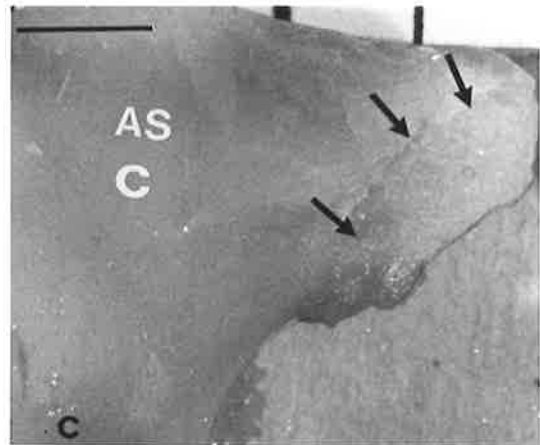
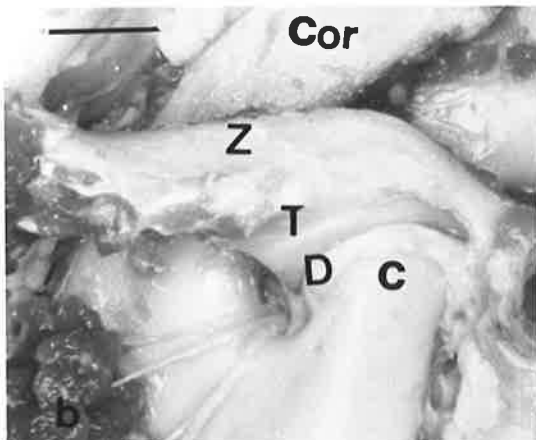


PLATE 2 Gross And Light Microscopy Of The TMJ

Figure 2.2a Sagittal section of decalcified, silver impregnated, right TMJ of an adult sheep, showing temporal fossa (T), condylar process (C), disc (D), superior joint cavity (SJ), capsule (Ca) and auriculotemporal nerve (An). Bar: 2mm.

Figure 2.2b Lateral aspect of the right TMJ of an adult sheep, showing zygomatic arch (Z), condylar process (C) and coronoid process (Cor) of the mandible, disc (D) and temporal fossa (T). Bar: 10mm.

Figure 2.2c Anterior aspect of the articular surface (AS) of the condyle (C) of the mandible showing the attachment site of the lateral pterygoid muscle (arrows). Bar: 10mm.



postglenoid tubercle that was largest medially (Fig. 2.2a). The condylar head and temporal surface of the glenoid fossa were wider lateromedially than anteroposteriorly. An elongated depression on the anteromedial aspect of the condyle marked the attachment of part of the lateral pterygoid muscle (Fig. 2.2c). The foramen ovale was located medial to the glenoid fossa and in a direct line with the anterior border of the glenoid fossa.

Histologic examination of the condyle revealed from superficial to deep: (i) a fibrous connective tissue covering that forms the articular surface, (ii) cartilage zone and (iii) trabecular bone. The articular surface of the glenoid fossa had a similar arrangement of layers except that the fibrous layer was thinner than that on the condyle (Figs. 2.2a; 2.4a, b).

Despite the smoothness of the articular surfaces of the mandibular condyle and temporal fossa under gross and light microscopic examination (Figs. 2.3a, c), when examined under the scanning electron microscope, it was revealed that the articular surfaces were quite rough (Figs. 2.3b, d). The fibrous connective tissue formed a thin sheet of parallel fibres. The underlying tissue of the condyle and the glenoid fossa formed an uneven surface of ridges and depressions (Figs. 2.3b,d).

2.4.3. Capsule

The capsule was attached to the periphery of the temporal articulating surface and the neck of the mandible. The anterior part of the capsule was attached to the cranial limb of the root of the zygomatic process, immediately cranial to the flattened articular tubercle. Posteriorly, the capsule was attached to the caudal edge of the root of the zygomatic process which protruded inferiorly as an anteroposteriorly-flattened plate of bone, the postglenoid tubercle or process, adjacent and cranial to the tympanic part of the temporal bone (Fig. 2.2a). The lateral capsule was attached to the lateral margin of the zygomatic process. On the medial side of the joint the capsule attached to the medial

PLATE 3 Articular Surfaces Of The TMJ

Figure 2.3 Macroscopic and scanning electron microscopic appearance of the articular surfaces (AS) of the condyle (C) (**a,b** respectively), and temporal (glenoid) fossa (T) (**c,d** respectively). Bar: 5mm (**a,c**); 20 μ m (**b,d**).

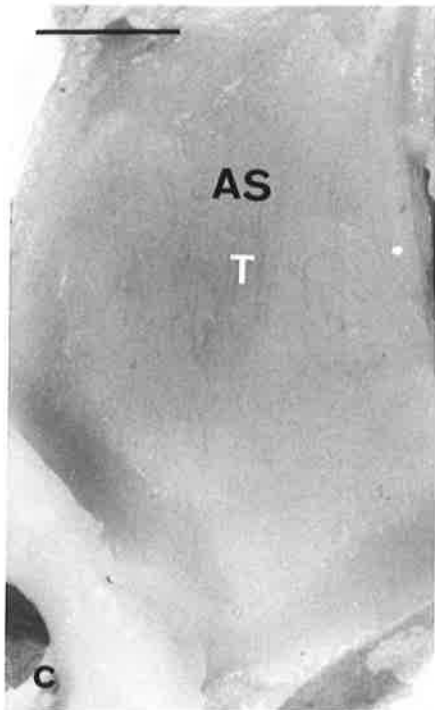
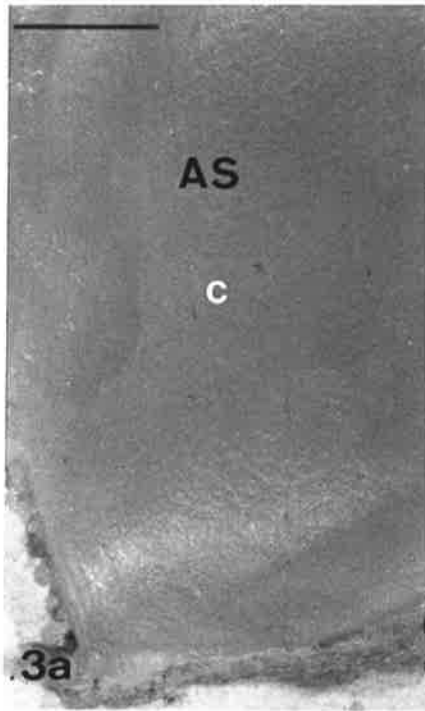
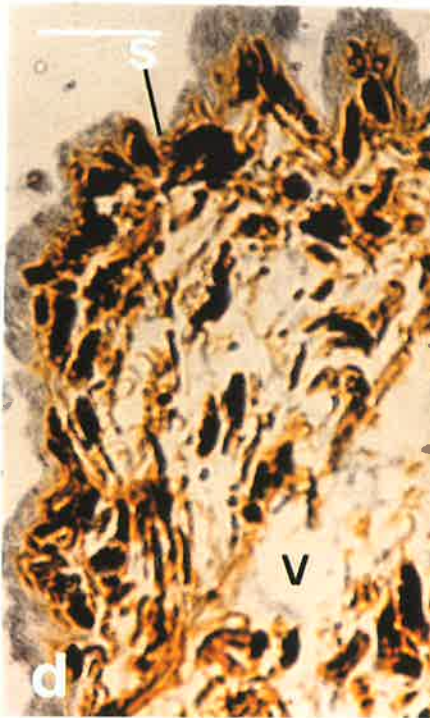
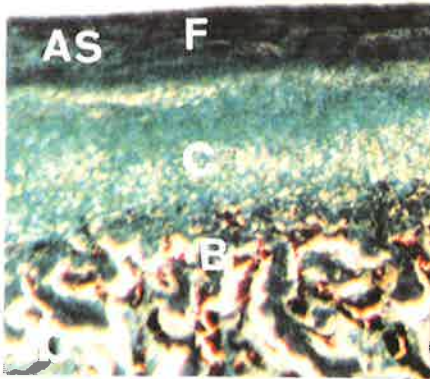
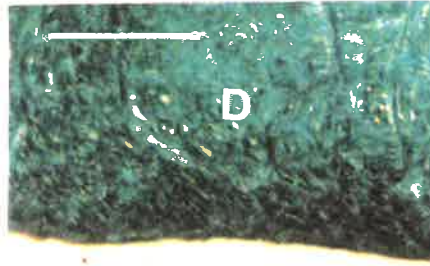
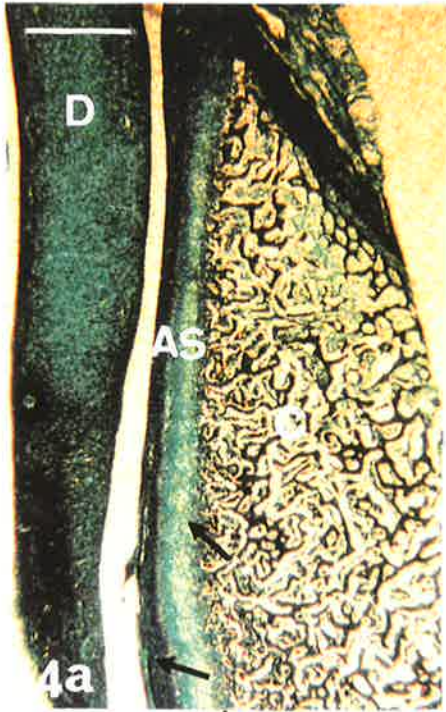


PLATE 4 Light Microscopy Of The TMJ

Figure 2.4 Light micrographs of adult TMJ tissues stained with Masson's trichrome and light green (**a,b**) to show the articular surface (AS) of the condyle (C), disc (D), bone (B), fibrous tissue (F) of the articular surface and joint cavity (Jc), or silver (**c,d**) to show the condyle (c), capsular attachment (C) of the disc (D), joint cavity (Jc), muscle (M), synovium (S) and a vessel (V). Bars: 50 μ m (**a**), 20 μ m (**b**), 60 μ m (**c**) and 30 μ m (**d**).



part of the root of the zygomatic process, adjacent to the suture between the postsphenoid and the zygomatic process.

The anterior part of the capsule consisted of highly vascular, loose connective tissue with many large nerve bundles and much adipose tissue. Posteriorly, the capsule consisted of dense connective tissue but also contained adipose tissue, many large veins, and many nerve bundles (Fig.2.2a). The medial capsule also consisted of loose connective tissue but with less adipose tissue, and fewer vessels and nerve bundles than in the anterior or posterior parts of the capsule. The lateral part of the capsule was thicker, with more collagen tissue than the other regions of the capsule.

Scanning electronmicroscopy revealed a fine, interlacing network of fibrils in the anterior capsule near the peripheral part of the articular disc. The fibrillar network gave way to uniform parallel fine fibres (Fig. 2.5a). Collagen fibres were larger and thicker in the lateral capsule (Fig.2.5b)

2.4.4. Articular disc

The articular disc was formed of a smooth, white oval plate that divided the joint into a larger superior and a smaller inferior compartments (Figs. 2.2a, b). Peripherally, the disc blended with the capsule of the joint and was attached to the margins of the articular surfaces (Fig. 2.2a). The disc did not have a uniform thickness. The anterior and posterior parts were thicker than the central part (Fig. 2.2a). While the posterior attachment of the disc to the capsule consisted of dense fibrous tissue, anteriorly there were loose connective tissue, numerous fat cells, and many blood vessels (Fig. 2.2a).

The articular surface of the disc appeared uneven and rough under the scanning electron microscope (Figs. 2.5a, c). This unevenness of the surface is probably partly caused by the shrinkage of the tissue in the drying procedure. In the peripheral part of the disc the

PLATE 5 Scanning Electron Microscopy Of The Capsule And Disc

Figure 2.5 Scanning electron microscopic appearance of the anterior capsule (a), lateral capsule (b), peripheral disc (c) and central disc (d). C: capsule; D: disc. Bar: 50 μ m (a,d); 20 μ m (b,c).

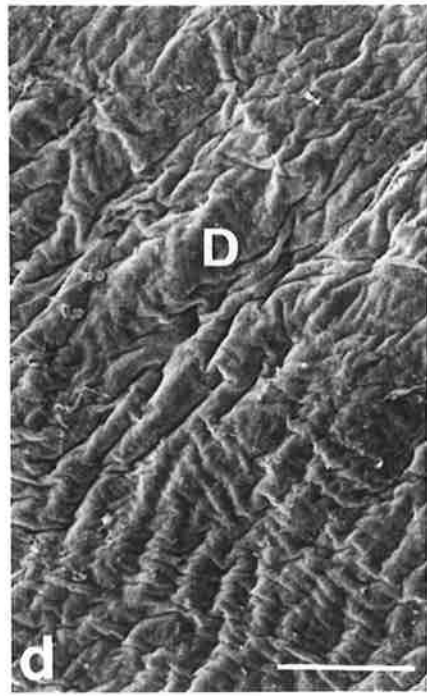
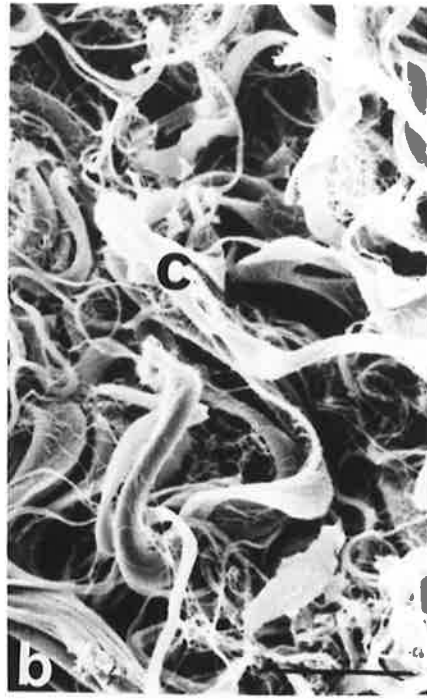
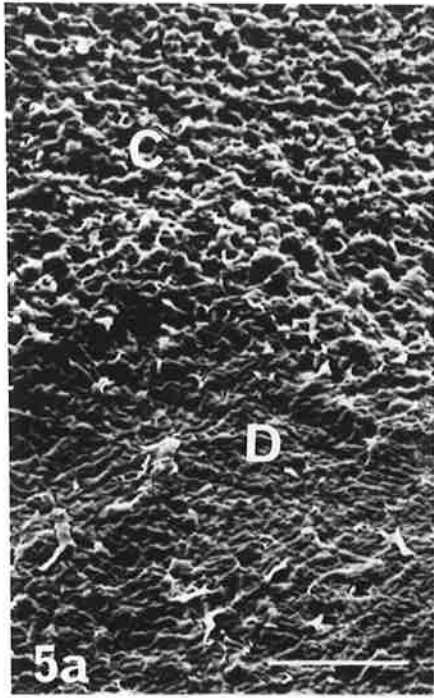
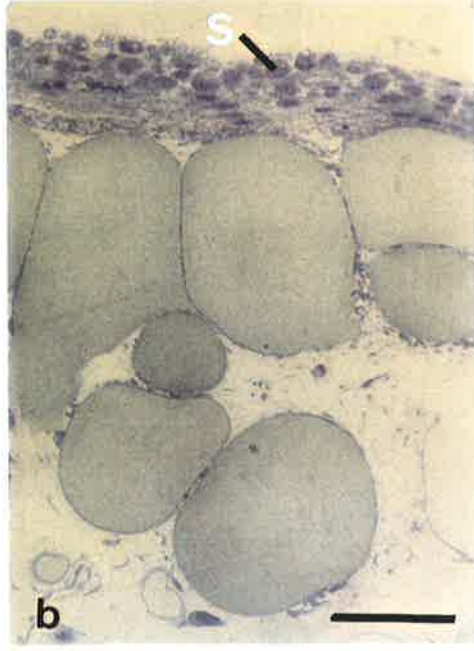
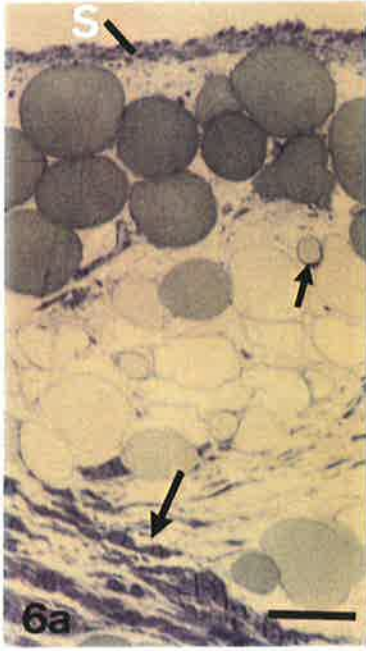


PLATE 6 Toluidine Blue Staining Of The Synovium

Figure 2.6 Light micrographs of toluidine blue stained sections of adult TMJ tissues to show the synovium (S). The small arrow shows a capillary and the large arrow shows the layer of collagen fibres deep to the adipose tissue. Bar: 30 μ m (a) and 10 μ m (b).



collagen fibres were aligned in a circular arrangement whereas in the central part of the disc the collagen fibres formed an interweaving pattern (Figs. 2.5c, d).

2.4.5. Synovium

The synovial membrane covered the peripheral parts of the articular surfaces and disc as well as the lined capsule. It formed villi and folds, in the anterior and posterior parts of the superior and inferior joint compartments near where the disc joined the capsule (Figs. 2.2a; 2.4c). The villi contained blood capillaries and nerve fibres (Figs. 2.2a; 2.4c, d; 2.6 a, b). The synovium consisted of: (i) one or more layers of cuboidal synovial cells lining the joint cavity, (ii) a thin layer of connective tissue, (iii) an adipose tissue layer that was penetrated by loose connective tissue and blood vessels, and (iv) a dense connective tissue layer composed of collagen fibres aligned parallel to the surface of the synovium (Figs. 2.6a , b).

The synovial membrane appeared to be thinner in the areas of disc attachment and thicker as it approached the areas of attachment of the capsule adjacent to the joint cavity where most of the synovial folds and villi were found (Figs. 2.4c, d).

2.5. DISCUSSION

This study showed that the temporomandibular joint of the sheep, like other mammals, is a diarthroidal articulation between the condyle of the mandible and the glenoid fossa of the temporal bone. The articulating surfaces of the condyle and glenoid fossa are covered by fibrocartilaginous tissue and not by hyaline cartilage as in other synovial joints. Each joint has an articulating disc that separates the head of the condyle from the temporal bone. Therefore the disc completely divides the joint into superior and inferior joint compartments (Goss et al, 1992).

2.5.1. Articular surfaces

In humans as in the other mammals, including cats, rats, rabbits, dogs, sheep, goats, cows and pigs the articular surface of the mandibular condyle is convex and faces the lower articular surface of the meniscus, which is concave (May, 1970; Bermejo et al, 1993). In addition, the articular surface of the condyle is characteristically covered by fibrocartilage (Griffin et al, 1975). In the sheep, the articular surface of the mandibular condyle has a layer of loose fibrous tissue overlying the fibrocartilage (Bosanquet et al, 1991a). This was confirmed in the present study on the sheep in which scanning electron microscopy revealed sheets of fibres aligned parallel to the articular surface.

In human beings, pigs, dogs, cats, rabbits and rats the articular surface of the temporal bone is concavoconvex (Bermejo et al, 1993), while the articular surface of the temporal bone of cows, sheep and goats is slightly convex (Strom et al, 1988; Bermejo et al, 1993; Ishimaru et al, 1993). The articular eminence, which is the anterior border of the articular fossa, in humans, is divided mediolaterally (Melfi, 1994). Although Noble (1979) reported that there is no articular eminence in the temporal articular surface of the sheep, Ishimaru et al (1993) referred to a flattened articular eminence. In the present study, the temporal articular surface was slightly convex over most of its surface with no evidence of an articular eminence anteriorly. There was a mediolateral concavity posteriorly, adjacent to the vertically aligned shelf of temporal bone that marked the caudal extremity of the articular surface. This posterior boundary of the temporal articular surface in the sheep TMJ is referred to as the postglenoid tubercle by Finn (1994) and Murphy (1959) and possesses a small facet for articulation with the mandibular condyle. It is well developed in the pygmy shrew to oppose the posterior movement of the condyle in response to the powerful posterior pull of the temporalis muscle (Noble, 1979). A fibrocartilaginous surface is characteristic of the glenoid fossa in sheep and other mammals (Griffin et al, 1975). In the sheep, a dense, avascular fibrous tissue layer, in which the fibres were mainly aligned parallel to the articular surface, covered a region of fibrocartilage (Bosanquet et al, 1991a). In the present

study, scanning electron microscopy confirmed the presence of an outer, fibrous layer composed of fibres aligned parallel to the articular surface and histological examination revealed the underlying cartilage.

2.5.2. Articular disc

Bellinger (1948) described the interarticular disc of the human temporomandibular joint as a structure of dense fibrous connective tissue that is interspersed with a few cartilaginous cells. In the sheep and the ox, chondrocytes are spread throughout the disc, unlike humans and animals such as dog, rabbit and guinea pig where there is little or no cartilage (Barnett et al, 1961). Barnett et al (1961) also reported a nodule of cartilage in the posterior part of the disc in the sheep. Nevertheless, this nodule of cartilage has not been reported in studies by Bosanquet and Goss (1987), Goss *et al* (1992), and it was not found in the present study.

In 1962, Dixon observed that the interarticular disc of the human temporomandibular joint was not a homogenous structure, and divided the disc into two parts. These were the extremely dense, avascular, plate-like anterior portion and a posterior part of loose connective tissue which merged with the posterior region of the joint capsule. The disc of the sheep temporomandibular joint is composed of dense fibrous connective tissue with scattered clumps of chondroblasts in the central layer (Bosanquet and Goss, 1987). According to these authors, in the sheep, the anterior attachment of the disc contained multiple vascular sinusoids, whereas the posterior attachment was fibrous and avascular. This was largely confirmed in the present study except that some vessels and adipose tissue were located in the posterior attachment. This is different from the human where the posterior portion of the disc is loose connective tissue with many large vessels and the anterior part is a very dense avascular tissue (Rees, 1954; Dixon, 1962). Gillbe (1973) also noted that the sheep's disc differed from that in rats and dogs by having vascular sinusoids in the anterior disc/capsule junction. Dixon (1962) divided the posterior part of the human disc into an upper zone which was rich in elastic tissue

and a lower zone which possessed little elastic tissue but a plexus of large endothelium-lined spaces.

Bosanquet and Goss (1987) described the disc of the sheep as having synovium on both superior and inferior surfaces. The present study also noted that synovial folds and villi were present in both superior and inferior joint compartments near the cranial and caudal disc/capsule junctions.

2.5.3. Capsule

The result of this study showed that the structural components of the temporomandibular joint capsule of the sheep are similar to those of other mammals that have been examined. The articular capsule is made of fibrous tissue that is attached to the entire articular disc about its circumference, thus creating superior and inferior joint cavities (Öberg and Carlsson, 1979). In the sheep, like other mammals, the capsule can be divided into different regions, each with a different histological appearance. The medial capsule usually consisted of loose connective tissue but with less adipose tissue, and fewer vessels and nerve bundles than in other regions. Laterally, the capsule was usually thicker, with less adipose tissue than the other regions of the capsule, with the thickening often referred to as a lateral ligament. There are differences in descriptions of the anterior and posterior regions of the capsule. In the present study, the anterior capsule consisted of highly vascular, loose connective tissue with many large nerve bundles and much adipose tissue. Posteriorly the capsule consisted of dense connective tissue but also contained adipose tissue, many large veins, and many nerve bundles. Rees (1954) has been the only author who found no articular capsule in the anterior part of the human temporomandibular joint, whereas others like Choukas and Sicher (1960), Ishibashi (1974) and Griffin et al (1975) demonstrated that the anterior part of the human temporomandibular joint is covered by capsule and attached to the articular eminence. Rats, dogs and humans feature a highly vascular region in the disc/capsule junction of the posterior TMJ and a dense, less vascular anterior disc/capsule junction

(Gillbe, 1973). The sheep TMJ characteristically has the reverse arrangement (Gillbe, 1973), and this was confirmed in the present study. Scanning electronmicroscopy also revealed a fine, interlacing network of fibrils in the anterior capsule, and larger collagen fibre bundles in the lateral capsule.

2.5.4. Synovium

The synovial membrane may be of the areolar, fibrous or adipose type (Key, 1932; Griffin et al, 1975; Henderson and Edwards, 1987). In the sheep TMJ, in the present study, four different zones of tissue could be distinguished in the synovium: lining synovial cell layer, thin connective tissue layer, adipose tissue layer and a dense connective tissue layer. In the sheep TMJ the synovial membrane lined the inner aspect of the joint capsule as well as the peripheral parts of articular surfaces of the condyle, the temporal fossa, and the bilaminar zone of the articular disc. Similar findings have been described in human TMJ by Griffin & Sharpe (1962) and McKay et al (1992). These authors found that the synovial membrane covered the inner aspect of the joint capsule as well as those articular surfaces which are not subjected to pressure or friction. These included the margins of both articular surfaces of the TMJ and the bilaminar zone of the articular disc.

Synovial membrane has been reported to be a highly vascular tissue (Knight and Levick, 1983). This vascular nature of the synovial membrane is important for joint metabolism (Knight and Levick, 1983). Nutrition of the articular surfaces of the joint occurs by diffusion from blood vessels across the synovial membrane (Knight and Levick, 1983). The present study revealed that the synovial membrane in sheep is well supplied by both blood vessels and nerves.

In conclusion this study showed that while the general histological and anatomical appearance of sheep TMJ is broadly similar to that of the human being, there are

differences in the appearance of the glenoid fossa, the vascularity of the anterior and posterior capsules and the shape of the disc.

Chapter 3

TEMPOROMANDIBULAR JOINT INNERVATION

3.1. SUMMARY	2
3.2. INTRODUCTION	3
3.3. MATERIALS AND METHODS	4
3.3.1. Animals and tissues	4
3.3.2. Macroscopic anatomy	6
3.3.3. Gold chloride histochemistry	6
3.3.4. Fluorescence histochemistry	7
3.3.5. Immunohistochemistry	8
3.3.5.1. Immunoperoxidase histochemistry	8
3.3.5.2. Immunofluorescence histochemistry	9
3.3.6. Transmission electron microscopy	10
3.3.7. Relative density of nerve fibres	11
3.4. RESULTS	11
3.4.1. Gross morphology of nerves supplying the TMJ	11
3.4.2. Microscopic appearance of nerves supplying the TMJ.	12
3.4.3. Gold Chloride	13
3.4.4. Fluorescence histochemistry	14
3.4.5. Immunoperoxidase histochemistry	15
3.4.6. Immunofluorescence histochemistry	15
3.5. DISCUSSION	17
3.5.1. Gross morphology of the nerves	17
3.5.2. Gold chloride histochemistry	18
3.5.3. Fluorescence histochemistry	21
3.5.4. Immunohistochemistry	22

3.1. SUMMARY

There is increasing interest in the interaction of disease processes such as arthritis and neural structures, including the mechanisms involved in inflammatory processes. To better understand the pathological processes associated with arthritis of the temporomandibular joint (TMJ), there is a need for detailed information on the innervation of TMJ tissues in normal as well as arthritic joints.

The macroscopic, microscopic and ultrastructural appearance plus the distribution of neural elements within the temporomandibular joint were examined using transmission electron microscopy, laser scanning confocal immunofluorescence microscopy, fluorescence histochemistry (glyoxylic acid), immunoperoxidase and gold chloride techniques. Joints from 20 mature Merino sheep were studied.

CGRP-immunoreactive nerve fibres were found in the capsule, synovial membrane and peripheral part of the disc. The capsule, synovial membrane and the disc contained fibres immunoreactive (IR) to antisera for PGP 9.5. Nerve bundles and single nerve fibres in the capsule, synovial membrane and the peripheral 2-3 mm of the disc were stained by glyoxylic acid. Ruffini, paciniform-type and Golgi organ nerve endings plus free nerve endings were located in the capsule with the highest density of nerve endings occurring at the site of attachment of the disc to the capsule. The highest density of neural structures (using gold chloride) was in the posterior part of the joint. The highest density of autonomic fibres (using glyoxylic acid) was in the anterior capsule and the highest density of sensory fibres (using CGRP) was in the synovial and subsynovial tissues of the anterior capsule. These results confirm the existence of autonomic and sensory nerves in the capsule, synovial membrane and peripheral disc in normal healthy adult sheep.

3.2. INTRODUCTION

Knowledge of the morphology of afferent and efferent nerves in the temporomandibular joint is important for a proper understanding of the normal function and pathological dysfunction of the temporomandibular joint (Clark and Wyke, 1973; Hansson, 1988; Ramieri et al, 1996). Degenerative changes associated with osteoarthritis or rheumatoid arthritis are common in temporomandibular joint (TMJ) pathology and often involve pain as well as disruption of normal joint congruity and normal joint movements (Blackwood, 1962; Ogus 1975). There is increasing interest in the interaction between disease processes such as arthritis and neural structures, including the mechanisms involved in inflammatory processes. Synovial inflammation, fibrosis and various cytoskeletal changes are features of these diseases (Kreutziger and Mahan 1975; Meek et al, 1991). Of several morphological and physiological features of synovium that may provide clues to therapeutic intervention in these diseases, innervation is one aspect which has only recently received some attention.

Antisera for protein gene product 9.5 (a neuron-specific protein) have been used in many studies to detect sensory and autonomic fibres in a variety of tissues including the TMJ (Ramieri et al, 1990; Morani et al, 1994). Decreases in the density of fine nerve fibres immunoreactive for substance P, PGP 9.5, CGRP, neuropeptide Y and its C terminal peptide (NPY/C-PON), in synovia from arthritic joints, point to some pathological influence on the innervation of this tissue (Grönblad et al, 1988; Konttinen et al, 1990; Mapp et al, 1990; Hukkanen et al, 1991).

To better understand the pathological processes associated with arthritis of the TMJ there is a need for detailed information on the innervation of TMJ tissues in normal as well as arthritic joints.

Other than the gross anatomical appearance of the nerve supplying the TMJ, nothing is known of the neural structures associated with this joint in the sheep. Consequently, this chapter describes the appearance and distribution of the neural structures of the TMJ of normal, healthy sheep using gold chloride technique; fluorescence histochemistry (glyoxylic acid); immunohistochemistry and transmission electron microscopy.

3.3. MATERIALS AND METHODS

3.3.1. Animals and tissues

Healthy adult male Australian Merino sheep approximately 60 kg body weight (less than 2 years old) were used for this investigation (n=20). The animals were divided into six groups (Table 3.1). From these animals, three were used for the macroscopic appearance of the mandibular nerve that innervated the temporomandibular joint. Seven animals were used for the microscopic visualisation of the proprioceptors and nociceptors, using confocal immunofluorescence microscopy and gold chloride techniques. Six joints from three animals were studied using fluorescence histochemistry (glyoxylic acid) to visualize autonomic nerve fibres. Three animals were used to visualise sensory nerve fibres by performing immunoperoxidase histochemistry. Finally, four animals were used for studying the ultrastructural appearance of nerves using the electron microscope. All animals were sacrificed through an overdose of sodium pentobarbital (Nembutal, Abbott, Sydney, Australia) in accordance with the ethics guidelines of the University of Adelaide and the Institute of Medical and Veterinary Science. Except for group number one, all temporomandibular

joints were removed en bloc with a band saw. The capsule and attached disc were dissected away from the condyle and glenoid fossa (temporal fossa) and cut into lateral, medial, anterior, and posterior portions for microscopic evaluation (Fig. 3.1).

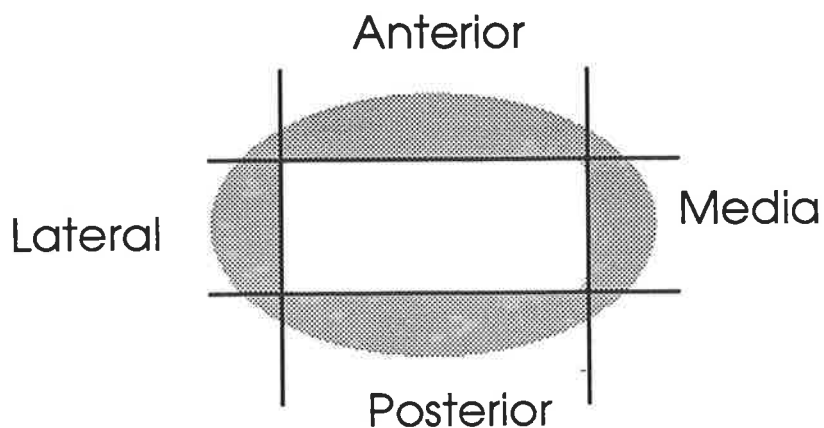


Figure 3.1 Subdivision of disc and attached capsule of TMJ to show the four regions used for microscopic examination.

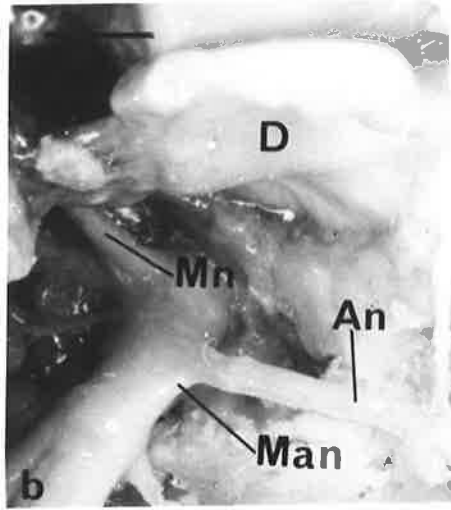
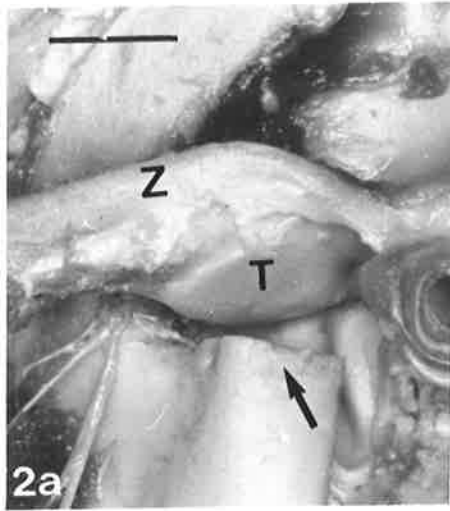
Table 3.1. Number of animals, joints and applied procedure

Group	Sheep	Joints	Procedure
I	3	6	Macroscopic study of the nerve
II	5	10	Gold chloride technique
III	3	6	Fluorescence histochemistry
IV	2	4	Immunofluorescence microscopy
V	3	6	Immunoperoxidase technique
VI	4	8	Transmission electron microscopy

PLATE 7 Gross Dissection Of The TMJ

Figure 3.2a Lateral aspect of the left TMJ of an adult sheep, showing zygomatic arch (Z) and temporal fossa (T). Arrow indicates the cut mandibular condyle. Bar: 10mm.

Figure 3.2b Lateral aspect of the disc (D) of the left TMJ of an adult sheep with the mandible removed, showing the mandibular nerve (Ma n), auriculotemporal nerve (An) and masseteric nerve (Mn). Bar: 5 mm.



3.3.2. Macroscopic anatomy

The macroscopic appearance of the branches of the mandibular nerve that innervate the TMJ was studied after the head was sectioned through the mid-sagittal plane with a band saw. An incision was made through the skin and all superficial fascia and muscles around the joint were dissected out until the whole temporomandibular joint was exposed. The head of the condyle was separated from the disc and capsular attachment, then both the condyle and zygomatic arch with glenoid fossa were removed by an electric saw in order to allow a deeper dissection to the medial aspect of the joint (Fig. 3.2a). With careful blunt dissection toward the foramen ovale, the mandibular division of the trigeminal nerve and all its branches to the temporomandibular joint were located (Fig. 3.2b). All joints were dissected under a magnifying lamp. The prosections were recorded photographically using a Nikon FA camera with black-and-white Pan F film.

3.3.3. Gold chloride histochemistry

A modified gold chloride method for the demonstration of nerve endings in frozen sections by Zimny et al (1985) was performed to visualise proprioceptor and nociceptor nerve fibres and nerve endings in temporomandibular joint. In five animals the portions of capsule and disc were immersed in a solution of one part 88% formic acid (HCOOH) and three parts filtered, freshly squeezed lemon juice for 15 minutes in the dark. Then the tissues were blotted and placed in a 1% solution of aqueous gold chloride and returned to the dark for 20 minutes. The tissues turned a uniform golden yellow colour. After this time, the gold chloride solution was decanted off and filtered for reusing.

The specimens were transferred to a 25% formic acid solution and stored at room temperature in the dark overnight. After this period, the specimens turned a purple-dark colour.

The tissues were washed in distilled water and stored in normal saline in a refrigerator at 4°C until further processing and sectioning. The pre-stained gold chloride specimens were mounted in tissue-Tek (Miles Inc, USA) on the metal cooling stub of the cryostat unit (Leitz 1720).

Frozen specimens were removed from the pre-labelled plastic embedding cassettes and mounted on a cooling platform on the sliding microtome (Reichert No 11302). Once the tissue was adequately frozen, and firmly attached to the cooling platform, sections were cut serially at 70-100 µm through the whole tissue. The sections were mounted on ATS (3-Aminopropyl-Triethoxy-Silane)-coated slides (Sigma Corporation, Australia) and allowed to dry. The slides were chemically washed by immersion in three changes of ethanol, for five minutes each, and cleared in HistoClear for five minutes and mounted in pix mounting medium and covered with coverslips.

All sections were viewed under an Olympus BH-2 light microscope. Photomicrography was done using a camera and automatic exposure unit (WILD Photoautomat system) attached to the top of the microscope.

3.3.4. Fluorescence histochemistry

Fluorescence histochemistry was performed to visualise autonomic fibres. Six joints were studied using the glyoxylic acid method described by de la Torre and Surgeon (1976). Each portion of fresh capsule and disc was placed in several drops of distilled water on a metal stub and frozen in a cryostat (Leitz 1720) at minus 30°C. Cryostat sections of 25 µm thickness were mounted on clean glass slides at room temperature.

Each slide was quickly dipped (1 dip/sec) in a solution of glyoxylic acid (GA) which consisted of 1.5 g GA in a solution of 115 ml distilled water containing 10.2 g sucrose and 4.8 g monobasic potassium phosphate adjusted to a pH of 7.4 using 35 ml of 1 N NaOH. Slides were air dried using a hair drier for five minutes and then incubated in an oven at 80°C for five minutes. The slides were cover slipped with paraffin oil and examined under an Olympus BHF fluorescence microscope with a 200 W mercury vapour lamp, 2 x BG 12 excitation filters and a K 515 emission filter. Photomicrographs were recorded on Kodak Tmax 400 film (Kodak, Rochester, NY).

3.3.5. Immunohistochemistry

The following two immunostaining methods were used to visualise immunoreactive nerve fibres.

3.3.5.1. Immunoperoxidase histochemistry

The avidin-biotin-peroxidase complex (Hsu, Raine and Fanger, 1981; Shu, Ju and Fan, 1988) technique was used to visualise sensory nerve fibres. In each of three animals, Zamboni's fixative (see appendix 1) was injected into the TMJs while the animal was unconscious (prior to sacrifice and dissection). For each joint, the disc, capsule, and attached synovial membrane were removed intact and divided into anterior, posterior, lateral and medial pieces (Fig. 3.1). These pieces were immersed in the same fixative (Zamboni's fixative) for overnight. After fixation, the tissues were washed in three changes of 80% ethanol to remove unbound picric acid, and were then cleared in dimethyl sulphoxide (DMSO) before being stored in 0.1mole/l phosphate buffer (PB; pH 7.4) containing 20% sucrose as a cryoprotectant. Pieces of tissue were mounted in Tissue Tek (Miles Inc, USA) on metal stubs and frozen in a cryostat (Leitz 1720) at minus 30°C. Serial sections (25 µm to 35 µm) were cut and mounted in ATS (3-

Aminopropyl-Triethoxy-Silane)-coated slides (Sigma Corporation, Australia) and allowed to dry overnight at room temperature. After treatment with 0.3% Triton-X 100 (Rohmand Haas, Philadelphia, PA) in phosphate-buffered saline (PBS) pH 7.4, for thirty minutes and 0.3% hydrogen peroxide in methanol for 1 hour to inactivate endogenous peroxidase, the sections were incubated for 1 hour with diluted normal blocking serum, which was prepared from the same species in which the secondary antibody was raised. After the excess serum was blotted, the sections were incubated with primary rabbit antiserum to polyclonal rat CGRP (Peninsula Laboratories, Belmont, CA) diluted 1:1,000 in a solution consisting of 1% bovine serum albumin and 0.05% sodium azide in 0.1M PBS overnight in a humid chamber at room temperature. After three washes in PBS, the sections were incubated in (1) biotinylated goat anti-rabbit IgG (Vector Laboratories, Burlingame, CA) diluted 1:50 in PBS for 1 hour at room temperature and (2) with avidin-biotin peroxidase complex (Vectastain Elite ABC Reagent, Vector Laboratories Burlingame, CA) diluted 1:50 in PBS for 1 hour at room temperature. After an additional three washes in PBS the sections were incubated in peroxidase substrate solution containing diaminobenzidine tetrahydrochloride and nickel (Vector Laboratories Burlingame, CA) for six minutes. Finally, the slides were counterstained with haematoxylin, dehydrated in ethanol, cleared in HistoClear and mounted in pix mounting medium. In control sections the primary antiserum was replaced with normal goat serum. No immunoreactivity was observed.

3.3.5.2. Immunofluorescence histochemistry

In addition to the immunoperoxidase technique, indirect immunofluorescence confocal microscopy was used to visualise the details of PGP 9.5-immunoreactive nerve fibres and receptors in different parts of the TMJ soft tissue, especially the disc and subsynovial tissue. Rabbit antiserum for PGP 9.5 (Ultraclone, Cambridge, UK) was diluted in 1% bovine serum albumin and 0.05% sodium azide in 0.1M phosphate-buffered saline (PBS, pH 7.4) containing 0.3% Triton X100 (Rohmand Haas Co,

USA). All incubation of the sections with antiserum was carried out at room temperature. The tissue sections were first preincubated for one hour with diluted normal blocking serum which was prepared from the same species as used in the secondary antibody. After the excess serum was blotted, the sections were incubated with PGP 9.5. Diluted antiserum was applied to sections overnight in a humid chamber at room temperature. After three washes in PBS, the sections were incubated in the dark for one hour with FITC-labelled anti-rabbit IgG (Sigma, Australia) diluted 1:60 in PBS, at room temperature. After a further three washes in PBS the sections were sealed with coverslips using mounting medium consisting of PBS and glycerine. Sections were viewed with a Bio-Red 1000 Laser Scanning confocal microscope. During the immunohistochemical procedures, control sections were processed in parallel, except that they were incubated in normal serum instead of primary antiserum. No immunoreactivity was observed in control sections.

3.3.6. Transmission electron microscopy

Four healthy adult male sheep, were deeply anaesthetized with sodium pentobarbitone (0.6g/1kg body weight) and the TMJ perfused by an intraarticular injection of 4% paraformaldehyde (w/v) and 0.5% glutaraldehyde solution in phosphate-buffered saline (0.1 M, pH 7.4). Small pieces of mandibular divisions of trigeminal nerves including masseteric and auriculotemoral nerve (proximal to the TMJ branches) were rapidly dissected out and immersed for four hours in the same fixative at 4°C. The tissues were then rinsed in buffer and processed for electron microscopy. After three, 5-minute washes with fresh 0.2M phosphate buffer, the tissue were post-fixed in a 1% aqueous osmium tetroxide and dehydrated in graded concentrations of alcohol. The tissues were then infiltrated with propylene oxide and embedded in epoxy resin (TK3, TAAB Embedding Materials). Semi-thin sections were cut perpendicular to the inner surface of the joint capsule and nerve trunk and stained with 0.05% toluidine blue.

Consecutive ultrathin sections 60-100 nm thick (silver to silver-grey interference colour) were cut on the ultramicrotome with a diamond knife and collected on uncoated, copper, 200 mesh grids, stained with 1% uranyl acetate and 1% lead citrate and examined with a Philips 200 electron microscope.

3.3.7. Relative density of nerve fibres

Nerve density was examined using a squared graticule eyepiece (Aherne and Dunnill, 1982; Pereira da Silva and Carmo-Fonseca, 1990). A qualitative assessment of the density of neural elements (nerve fibres and nerve endings) was made in relation to the capsule (six joints from three animals) in the following regions of the TMJ: (1) anterior; (2) posterior; (3) medial; and (4) lateral. A scale from absence (0) to high (+++++) relative density was used. Two fields from each of five sections from each region were examined at $\times 40$ magnification for each of the gold chloride, glyoxylic acid, and CGRP-immunoreactivity techniques.

3.4. RESULTS

3.4.1. Gross morphology of nerves supplying the TMJ

The mandibular division of the trigeminal nerve exits the skull via the foramen ovale medial to the temporomandibular joint in line with the anterior border of the glenoid fossa. The auriculotemporal, deep temporal and masseteric branches of the mandibular division of the trigeminal nerve contributed branches to the TMJ. The masseteric nerve arose from the anterior aspect of the mandibular nerve, a few mm distal to the foramen ovale. After passing anterolaterally, the masseteric nerve divided into two main branches. The first branch (the deep temporal nerve) passed superiorly deep to the

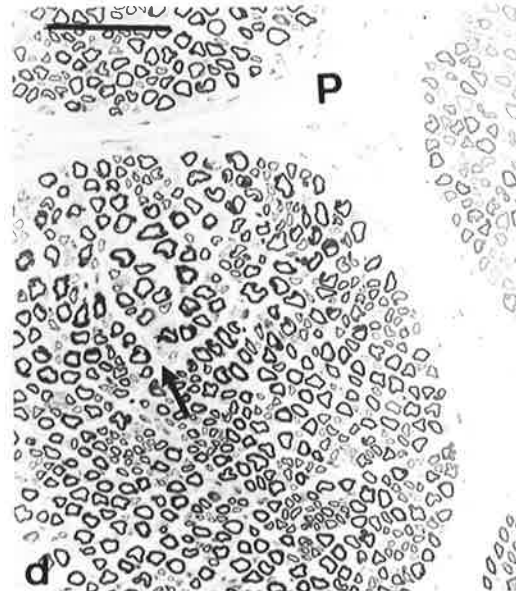
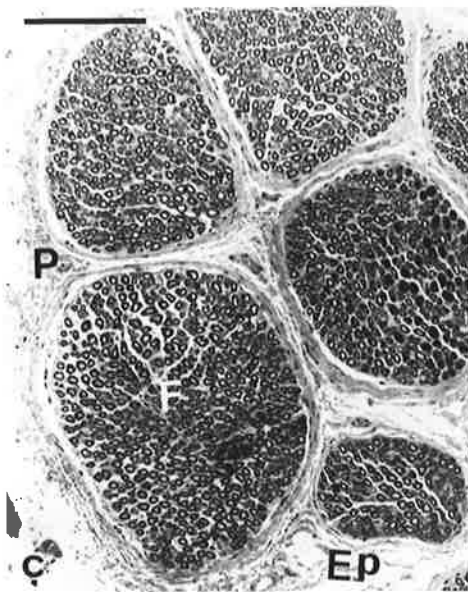
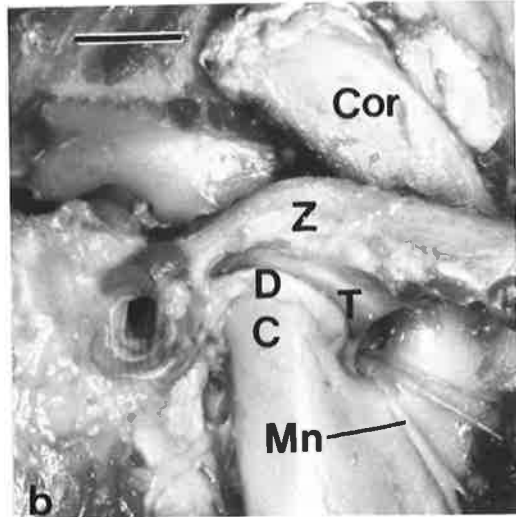
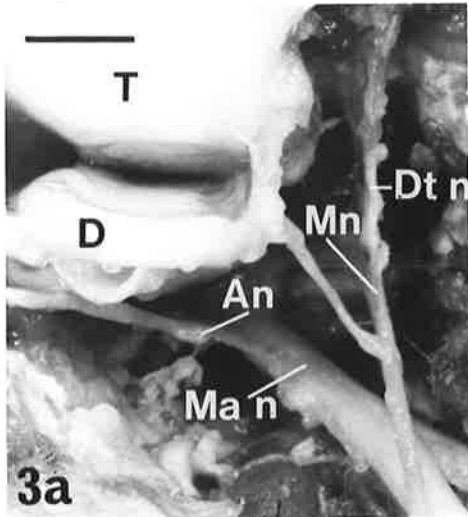
PLATE 8 Nerve Supply Of The TMJ

Figure 3.3a Lateral aspect of the disc (D) and temporal (glenoid) fossa (T) of the TMJ of an adult sheep with the mandible removed, showing the mandibular nerve (Ma n), auriculotemporal nerve (An) , masseteric nerve (Mn) and deep temporal nerve (Dtn). Bar: 5 mm.

Figure 3.3b Lateral aspect of the TMJ of an adult sheep, showing zygomatic arch (Z), coronoid process of the mandible (Cor), temporal fossa (T), condyle of the mandible (C), disc (D) and masseteric nerve (Mn). Bar: 10mm.

Figure 3.3c Light micrograph of transverse section of the masseteric nerve. P: perineurium; Ep: Epineurium. Toluidine blue stain. Bar: 30µm.

Figure 3.3d Light micrograph of transverse section of the masseteric nerve. P: perineurium. Arrow indicates the endoneurium. Toluidine blue stain. Bar: 20µm.



zygomatic process, where it contributed a branch to the medial part of the anterior capsule and then entered the deep aspect of the temporalis muscle (Fig. 3.3a). The second branch continued laterally through the mandibular notch after contributing a branch to the lateral part of the anterior capsule of the TMJ (Figs. 3.3a, b). The auriculotemporal nerve branched from the posterior aspect of the mandibular nerve, 2-3 mm distal to the origin of the masseteric nerve, and passed medial to the neck of the mandible before sending branches to the posterior part of the capsule of the TMJ (Fig. 3.3a). It then passed between the external acoustic meatus and the TMJ.

3.4.2 Microscopic appearance of nerves supplying the TMJ.

The light microscopic appearance of the toluidine blue staining of masseteric nerve before contributing branches to the TMJ are shown in (Figs. 3.3c, d). The nerve fibres supplying the joint covered almost the entire range of nerve diameters from large myelinated through small myelinated to small unmyelinated fibres. The majority of these fibres were myelinated (Fig. 3.4a).

The myelin sheath of the fibres appeared as a dark circle surrounding an electron-lucent centrum of the axon. Each myelinated axon was surrounded by Schwann cell cytoplasm (Fig. 3.4a). The network of reticular and collagen microfibrils of the endoneurial sheath was observed (Figs. 3.4a, b). The axons contained transverse sections of neurofilaments and neurotubules (Fig. 3.4b). The myelin sheath was composed of numerous myelin lamellae (Fig. 3.5a).

The ultrastructural appearance of unmyelinated nerve fibres showed several axons surrounded by cytoplasm from one Schwann cell (Figs. 3.4a and 3.5b). Similar to myelinated nerve fibres the unmyelinated fibres also have an endoneurial sheath

PLATE 9 Electron Microscopy - Masseteric Nerve

Figure 3.4 Transmission electron microscopic appearance of the masseteric nerve to show perineurium (Pn), endoneurium (En), axon (A), Schwann cell (S) and collagen microfibrils (C). Large arrow in **4a** shows an unmyelinated nerve fibre, while the small arrow in this figure shows the myelin sheath of a myelinated nerve fibre. The arrows in **4b** show neurofilaments and neurotubules in an axon of a myelinated nerve fibre. Bar: 5 μ m.

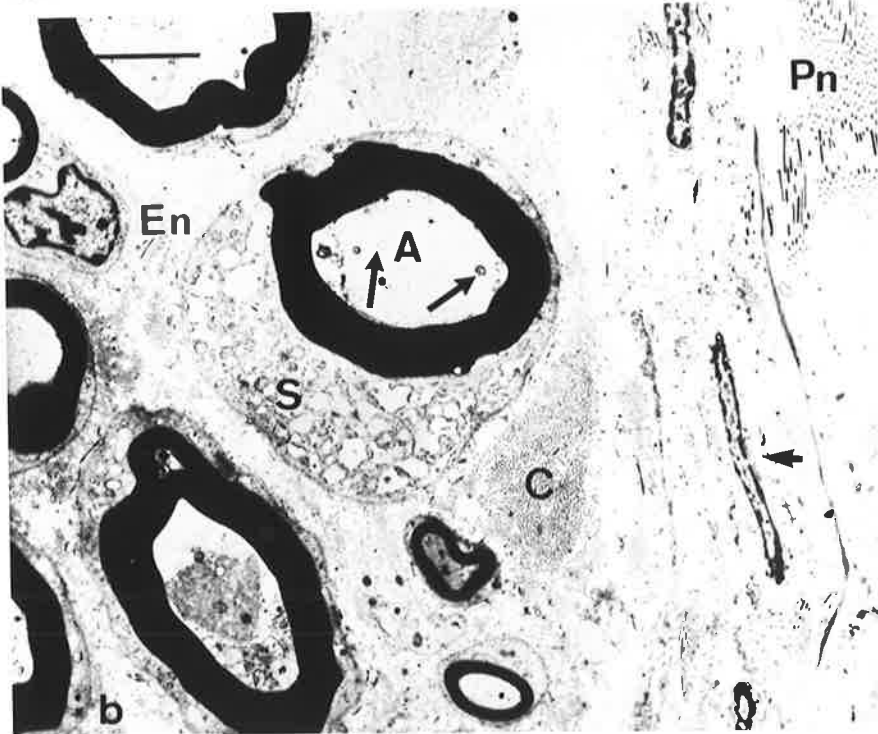
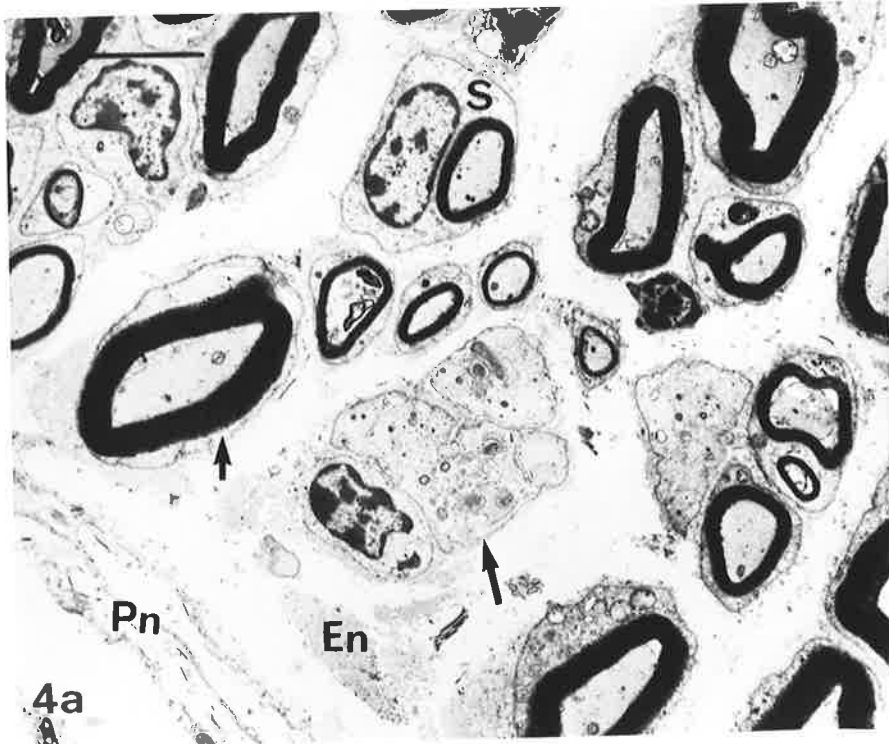
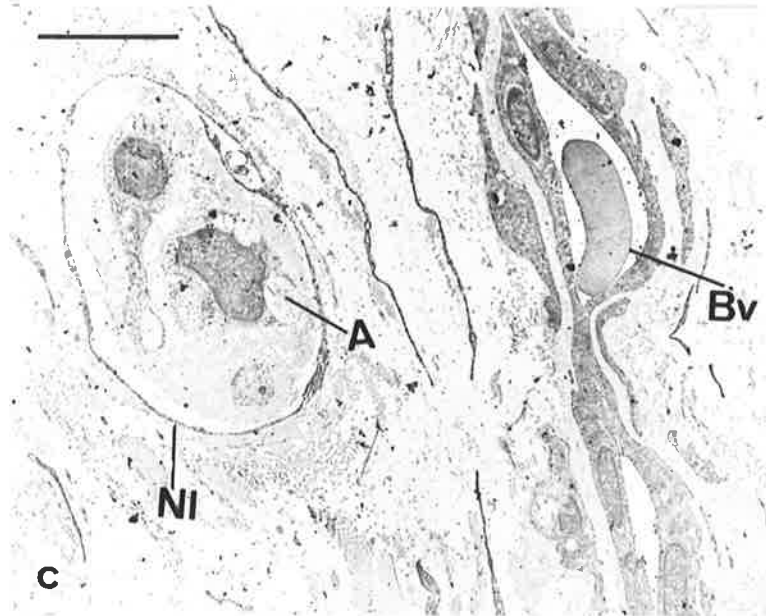
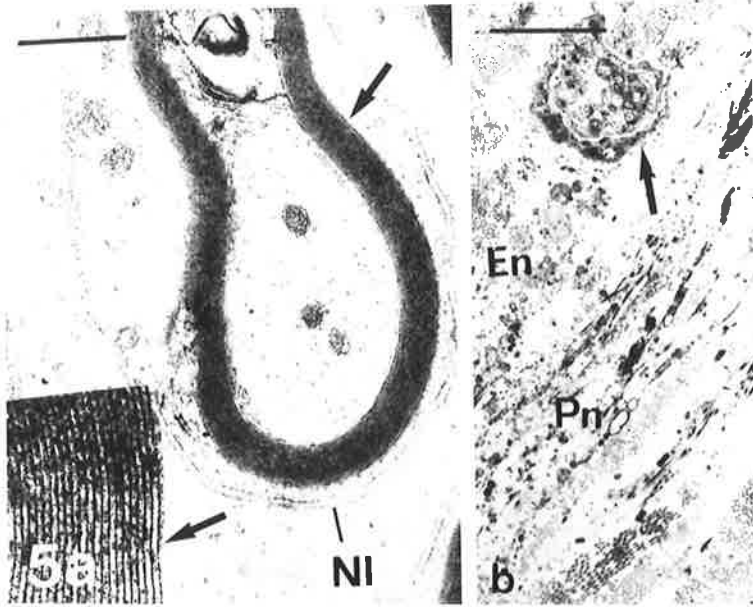


PLATE 10 Electron Microscopy - Myelinated And Unmyelinated Nerve Fibres

Figure 3.5 Transmission electron microscopic appearance of myelinated (**5a**) and unmyelinated nerves (**5b, c**) to show perineurium (Pn), endoneurium (En), axon (A), neurolemma (NI) and a blood vessel (Bv). Arrows in **5a** show the lamellated myelin sheath. The arrow in **5b** shows an unmyelinated nerve fibre. Bar: 2 μ m (**a**); 10 μ m (**b**); 5 μ m (**c**).



consisting of a basal lamina and interlaced collagen and reticular microfibrils (Fig. 3.5c).

3.4.3. Gold Chloride

Nerve fascicles, single nerve fibres and nerve endings were demonstrated by this gold chloride technique. Bundles of nerve fibres usually accompanied blood vessels passing through the capsule. Free nerve endings were seen as either unbranched fibres or simple arborizations from narrow, myelinated and unmyelinated axons (<5 μm diam.). They were found in the capsule, peripheral 3 mm of the disc and synovial membrane (Fig. 3.6a). No neural structures were found in the thicker, central part of the disc.

More complicated arborizations branching from bundles of myelinated axons (5-10 μm diam.) appeared as simple or complex sprays. The branches within the sprays often contained small swellings or varicosities. These endings were included in the Ruffini category (Figs. 3.6b; 3.7a). They did not appear to be encapsulated and were present in the capsule and peripheral disc. A simple ending that resembled a 'ball of threads' attached to a single axon or bundle of two axons was called a 'clew' type of spray or Ruffini ending (see Figs. 3.6c, d; 3.7b) following the description given by Polacek (1966). Spray or Ruffini endings were found in all parts of the capsule and although relatively more endings were found in the lateral capsule the endings were still sparsely distributed.

Golgi organs were complex spray endings arising from nerve bundles about 15 μm diameter (Figs. 3.6e; 3.7c). These were found in the peripheral disc near the attachment to the capsule.

PLATE 11 Nerve Receptors In TMJ - Using Gold Chloride Technique

Figure 3.6 Light micrographs of gold chloride stained sections of capsule of the TMJ of adult sheep showing (a) free nerve endings (small arrow) in the synovium, (b) a simple, branched Ruffini ending, (c) a clew-type Ruffini ending, (d) an enlargement of the Ruffini ending shown in 6c and (e) part of a Golgi ending. Bars: 60 μ m (a), 10 μ m (b), 50 μ m (c), 30 μ m (d) and 30 μ m (e).

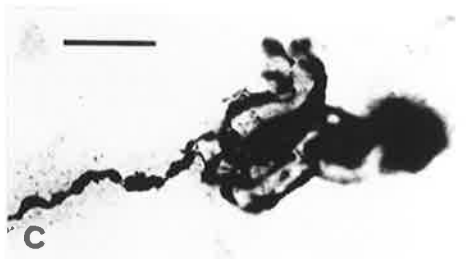
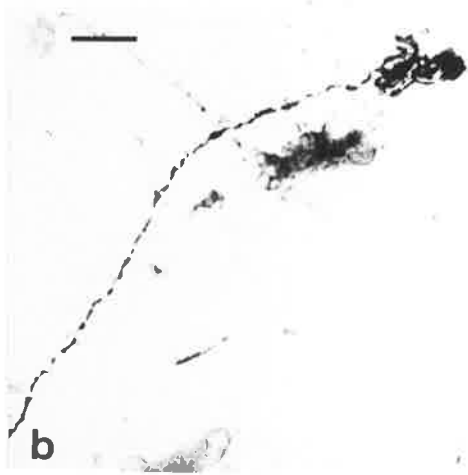


PLATE 12 Nerve Receptors In TMJ - Using Gold Chloride Technique

Figure 3.7 Light micrographs of gold chloride stained sections of capsule of the TMJ of adult sheep showing (a) free nerve endings from a simple arborization, (b) a clew-type Ruffini ending (counterstained with Light Green), and (c) part of a Golgi ending (counterstained with van Gieson's). Bars: 25 μ m (a), 15 μ m (b) and 6 μ m (c).

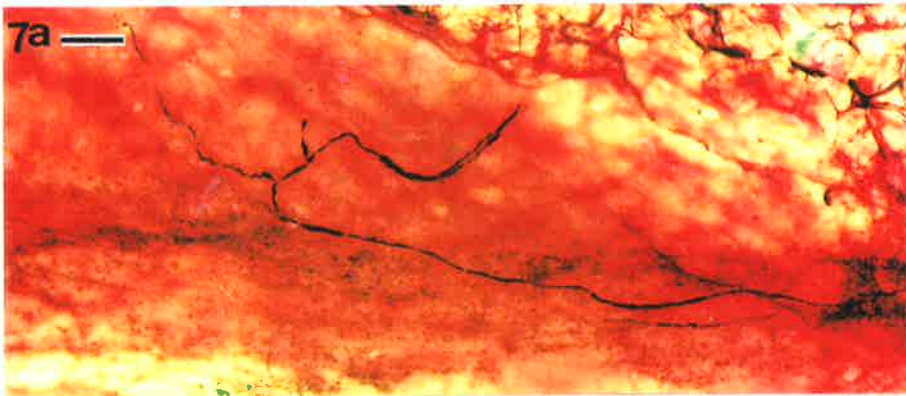
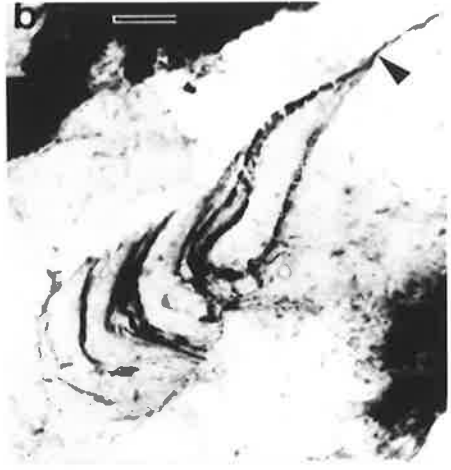
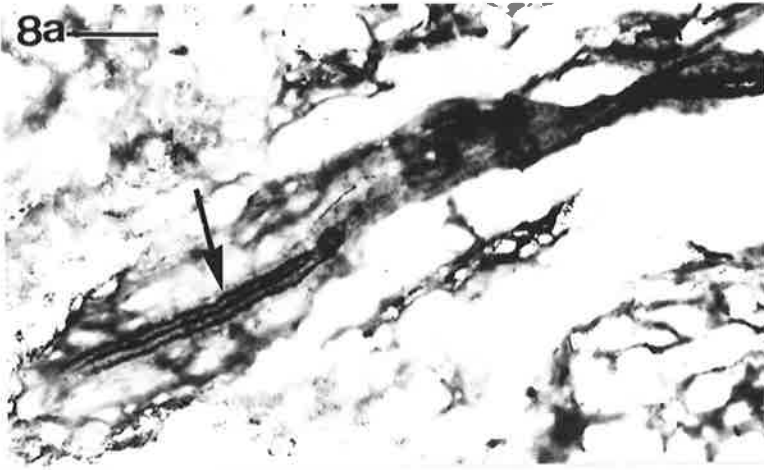


PLATE 13 Nerve Receptors In TMJ - Using Gold Chloride Technique

Figure 3.8 Light micrographs of gold chloride stained sections of capsule of the TMJ of adult sheep showing (a) a Paciniform corpuscle (arrow indicates central core of corpuscle), and (b) a Golgi-Mazzoni corpuscle (arrow head indicates axon leading to the corpuscle). Bars : 40 μ m (a) and 10 μ m (b).



Encapsulated nerve endings were rare. The paciniform-type in which the myelinated axon terminated in a dense, elongated central core surrounded by a lamellated capsule was only found in the lateral capsule (Fig. 3.8a). The Golgi-Mazzoni-type containing a branched central core surrounded by a lamellated capsule, was only found in the lateral disc-capsule junction (Fig. 3.8b). An encapsulated spray-type ending was seen in the lateral capsule in only one specimen. Free nerve endings extended up to 3 mm into the disc, but no neural structures were found in the thicker, central part of the disc.

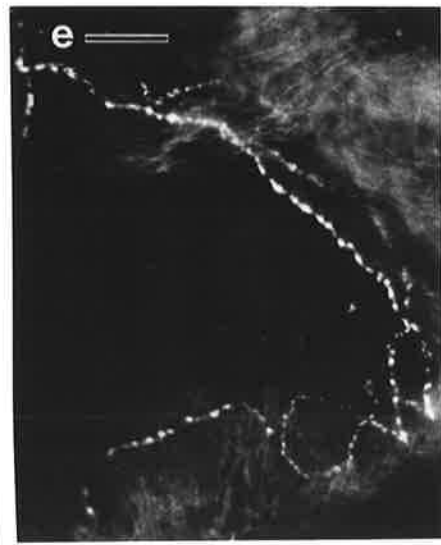
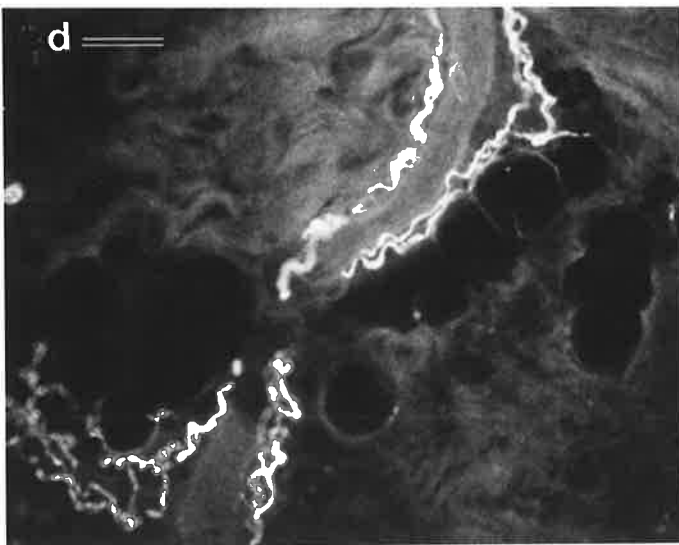
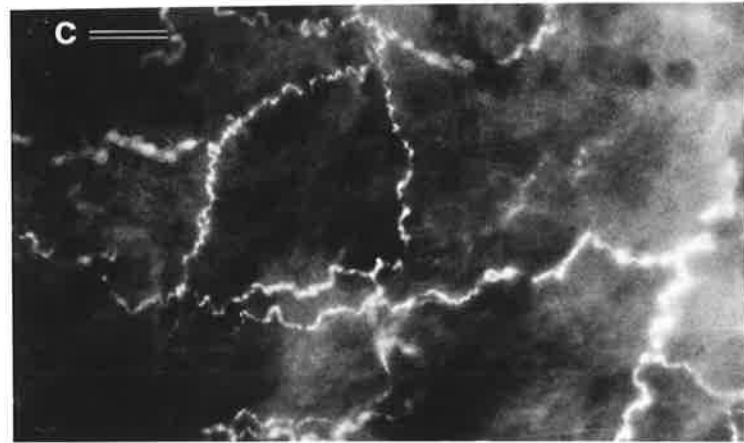
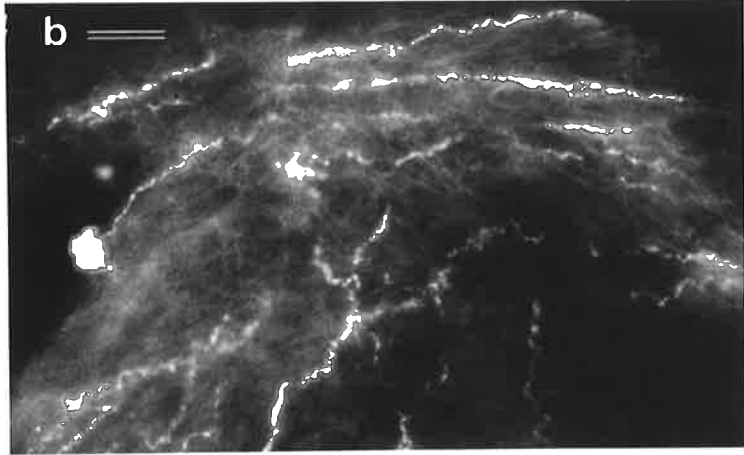
All proprioceptive-type sensory endings were more evenly distributed and more dense in the disc-capsule junction than the adjacent capsule. The disc/capsule junction in the lateral and posterior regions had more endings than the medial and anterior regions respectively.

3.4.4. Fluorescence histochemistry

Glyoxylic acid-induced fluorescence of nerve fibres was demonstrated in the capsule, synovial membrane and peripheral disc. Single nerve fibres plus nerve plexuses were localized around blood vessels and in interstitial tissue. Numerous varicosities were revealed along the fluorescent axons (Figs. 3.9a-c). Transverse sections of large arteries showed plexiform varicosities embedded in the adventitial sheath (Figs. 3.9a; d). Fluorescent axons with varicosities were present in the inner part of the tunica media. Some nerve fibres penetrated the disc to a depth of 3mm, but no nerve fibres could be seen in the central part of the disc. Large nerve bundles (branches of the masseteric nerve) did not exhibit any fluorescence.

PLATE 14 Adrenergic Nerve Fibres In TMJ - Using Glyoxylic Acid Technique

Figure 3.9 Fluorescence photomicrographs of sections of capsule of the TMJ of adult sheep after treatment with glyoxylic acid showing adrenergic nerve fibres associated with blood vessels (**a** and **d**) or forming a network in the connective tissue (**b** and **c**) or located in the junction between synovial membrane and capsule (**e**). Bars : 35 μ m (**a**), 50 μ m (**b**), 50 μ m (**c**), 40 μ m (**d**) and 40 μ m (**e**).



3.4.5. Immunoperoxidase histochemistry

The majority of CGRP-immunoreactive (IR) nerve fibres were found in the anterior capsule (Table 3.2). Except where a section of capsule contained a large bundle of nerve fibres, the immunoreactive nerve fibres were mostly single axons less than 5 μm diameter. Many axons were less than 3 μm diameter. Only small numbers of fascicles containing 2 to 5 axons were seen. Nerve fibres mostly accompanied blood vessels but were spread unevenly throughout the fibrous tissue. The CGRP-IR fibres had a wavy appearance with varicose swellings.

Many CGRP-IR nerve fibres and free nerve endings extended into the synovium (Figs 3.10a-d). Neural structures in the synovium were located interstitially and displayed numerous varicosities.

Small numbers of CGRP-IR nerve fibres penetrated the peripheral disc. Varicosities were present. In one section, the CGRP-immunoreactivity revealed a nerve terminal resembling a Ruffini receptor in the peripheral disc (Fig. 3.10e)

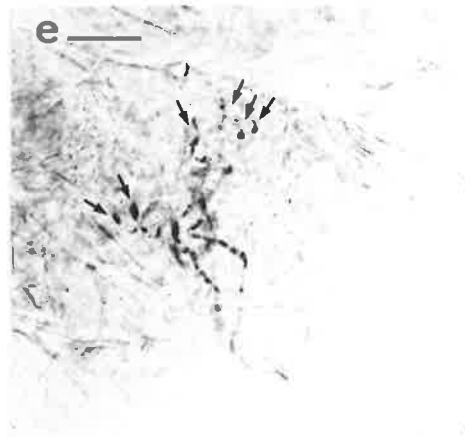
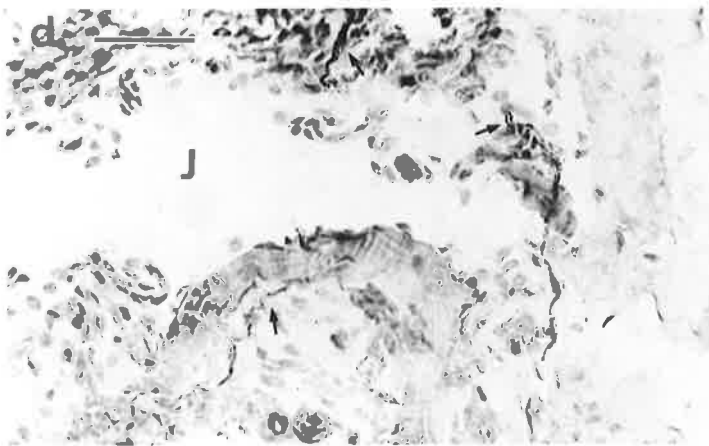
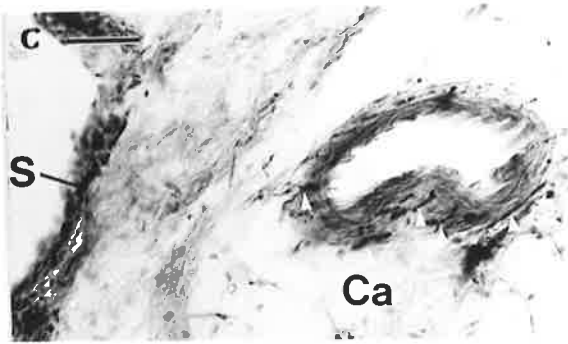
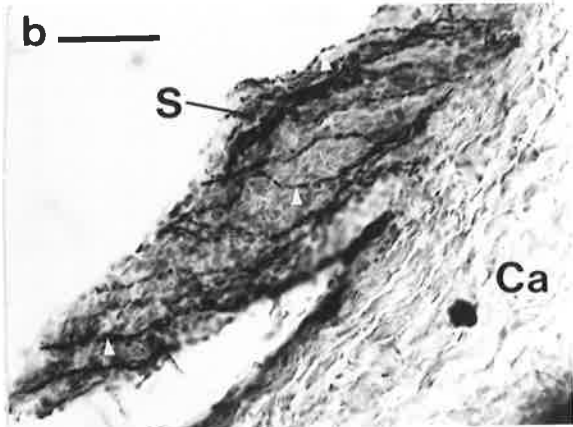
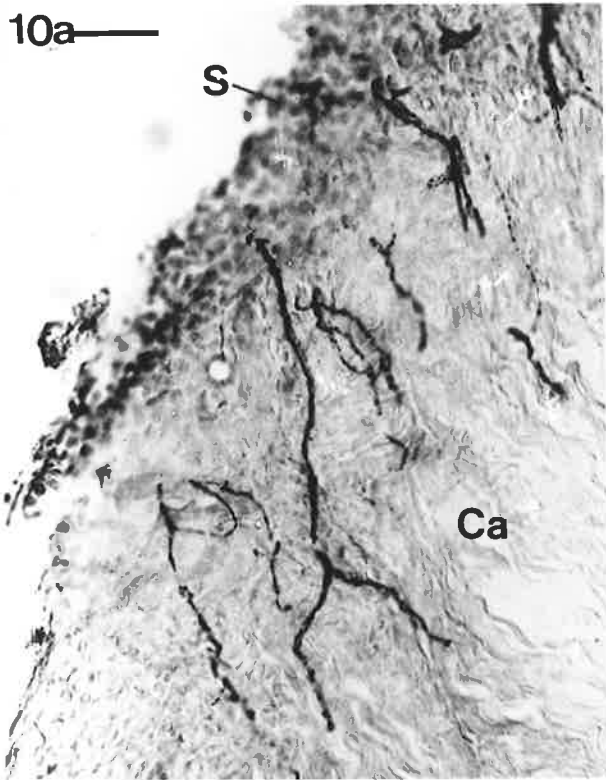
3.4.6. Immunofluorescence histochemistry

With conventional immunofluorescence microscopy the appearance and distribution of CGRP-IR fibres resembled that described previously by the immunoperoxidase staining. However the demonstration of nerve fibres was greatly improved by the use of immunofluorescence confocal microscopy (Figs. 3.11; 12). Using this method, PGP 9.5-immunostaining showed a combination of thick and thin varicose fluorescent fibres. The anterior part of the capsule and subsynovial tissue contained complex networks of PGP 9.5-IR nerve fibres (Fig. 3.11b). Plexiform arrangements of thin fibres having branched from single nerve fibres, were located adjacent to the synovial

PLATE 15 CGRP-Immunoreactive nerve Fibres In TMJ - Using Immunoperoxidase Technique

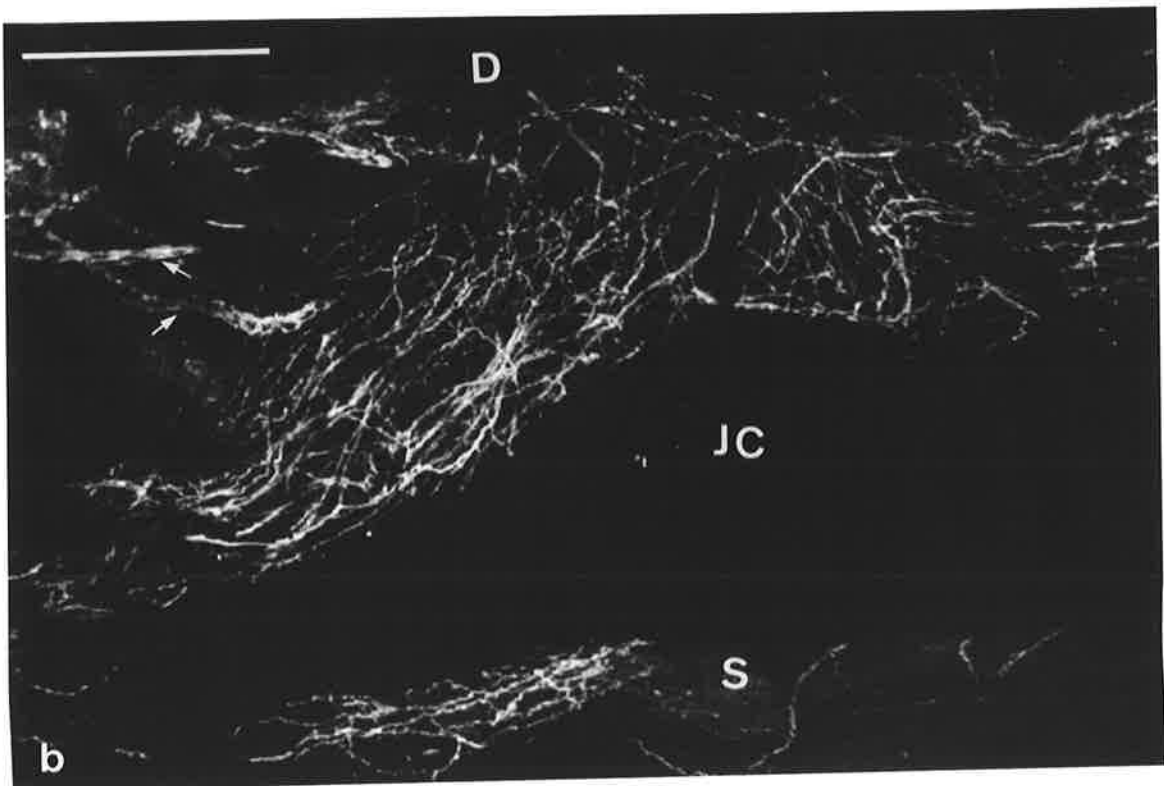
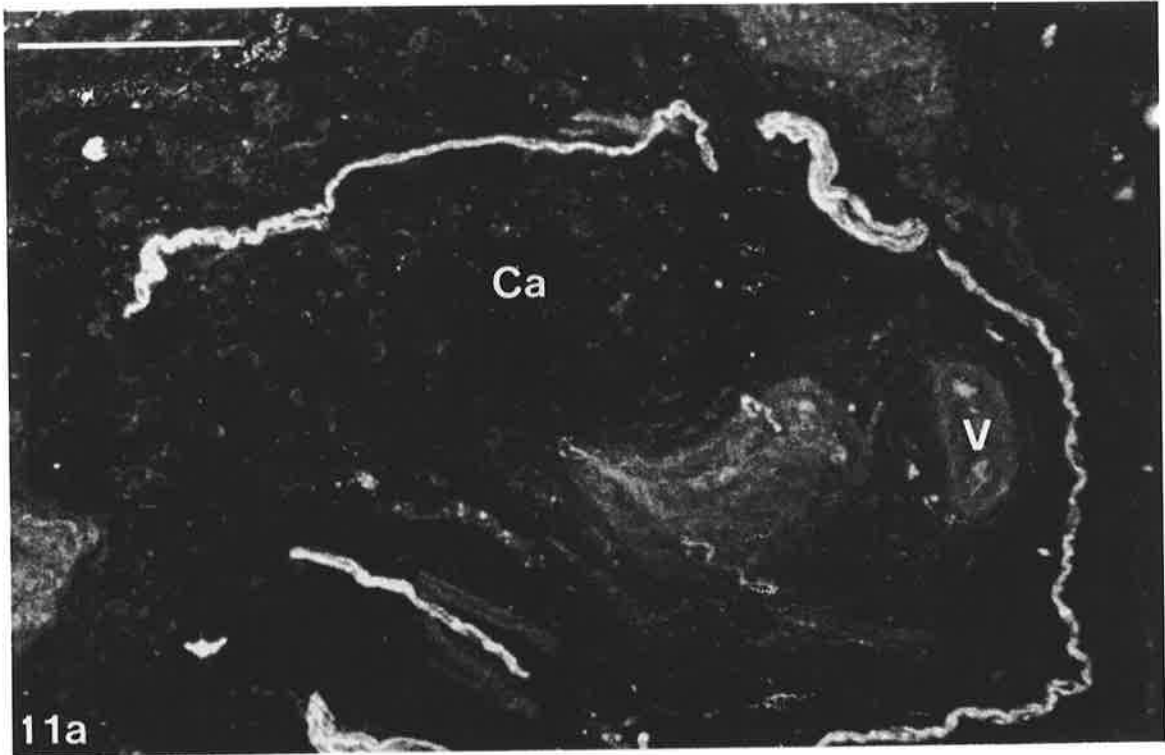
Figure 3.10 CGRP-immunoreactive nerve fibres in the TMJ of adult sheep. (a) shows nerve fibres in the capsule (Ca) and synovial membrane (S), (b) shows nerve fibres in a synovial fold, (c) shows nerve fibres in the wall of an artery, (d) shows nerve fibres entering the synovial membrane lining a lumen and (e) shows nerve terminal resembling a Ruffini receptor in the peripheral disc.

Bars : 15 μ m (a) and 20 μ m (b to d).



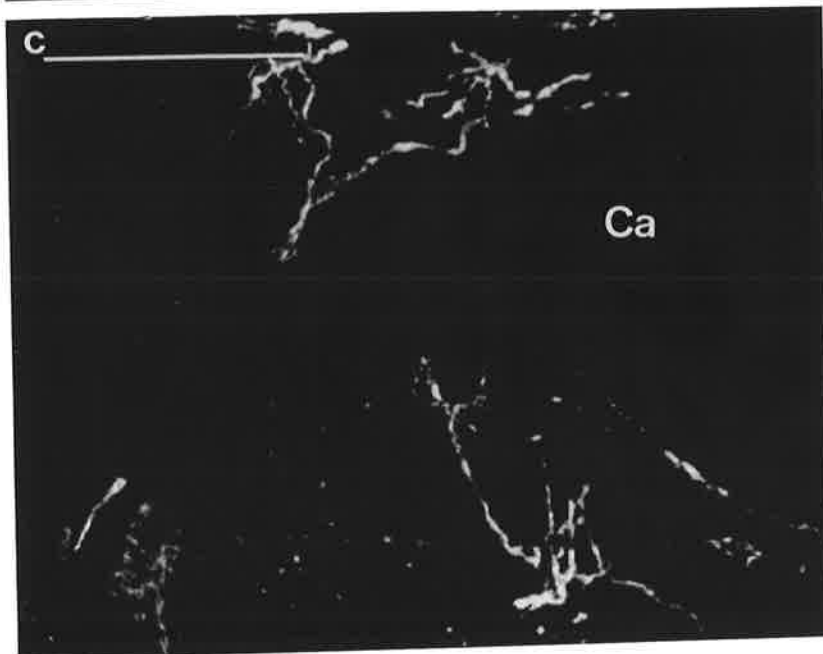
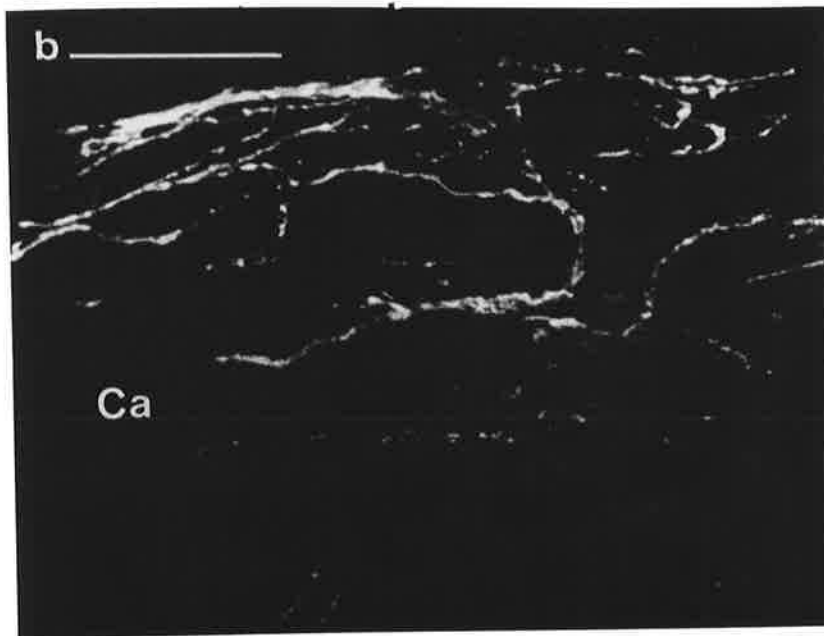
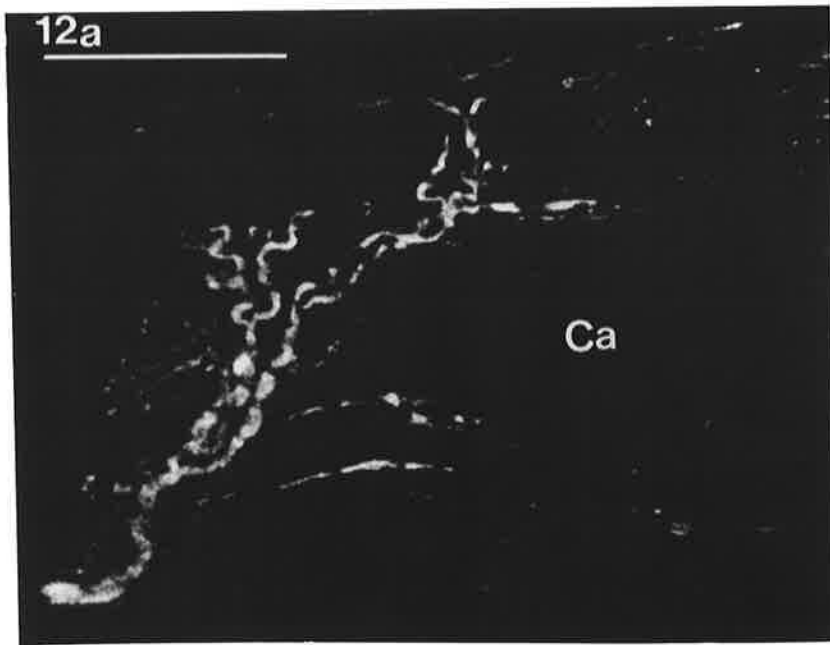
**PLATE 16 PGP 9.5 Immunoreactive Nerve Fibres In
TMJ - Using Laser Scanning Confocal
Microscopy**

Figure 3.11 PGP 9.5-immunoreactive nerve fibres in the TMJ of adult sheep as revealed by immunofluorescence confocal microscopy. **(a)** Capsule (Ca) showing a vessel (V) and **(b)** disc (D) showing synovium (S) and joint cavity (JC). Bars: 100 μ m **(a)** and 250 μ m **(b)**.



**PLATE 17 PGP 9.5 Immunoreactive Nerve Receptors In
TMJ - Using Laser Scanning Confocal
Microscopy**

Figure 3.12 PGP 9.5-immunoreactive nerve receptors in the TMJ of adult sheep as revealed by immunofluorescence confocal microscopy. (a) Ruffini ending, (b) Golgi organ ending, and (c) free nerve endings. Ca: capsule. Bar: 100 μ m.



membrane (Fig. 3.11b). The peripheral part of the disc was also innervated by PGP 9.5-IR nerve fibres. These fibres entered the disc from adjacent capsule. Very few fibres were found in medial aspect of the TMJ.

A variety of nerve receptors (Ruffini, Golgi tendon organs and free nerve endings) were labelled with antiserum to PGP 9.5 (Figs. 3.12a-c). The majority of these receptors resembled Golgi tendon organs and were located in the lateral and anterior aspects of the capsule adjacent to disc (Figs. 3.12a,b).

3.4.7 Density of nerve endings

Neural structures (nerve fibres and nerve endings) were found in decreasing density in the capsule, synovial membrane and disc. In the capsule, neural structures were most dense in the posterior part and least dense in the medial part using gold chloride (Table 3.2).

The highest density of fluorescent nerve fibres (using glyoxylic acid) was in the anterior part of the TMJ with few fibres visible in the lateral capsule (Table 3.2).

CGRP-IR fibres were most dense in the anterior capsule and least dense in the medial capsule (Table 3.2).

Table 3.2. Relative Density of Neural Structures in Four Regions of the Capsule of TM Joints from Adult Male Merino Sheep

Regions	Anterior	Posterior	Medial	Lateral
Gold chloride technique	++	++++	+	+++
Glyoxylic acid technique	++++	++	+++	+
CGRP immunoreactivity	+++	++	+	++

+ indicates low ; ++++ indicates high.

3.5. DISCUSSION

3.5.1. Gross morphology of the nerves

The TMJ of the sheep is innervated by auriculotemporal, masseteric and deep temporal branches of the mandibular division of the trigeminal nerve. Similar observations have been made for the human (Kreutziger and Mahan, 1975; Thilander, 1961; Helland, 1986) rhesus monkey (Keller and Moffett, 1968) and cat TMJ (Romph et al, 1979). Schmid (1969) found that autonomic nerve fibers (a branch of the otic ganglion) entered the medial side of the capsule in the human TMJ. It was presumed that sympathetic fibres came from a sympathetic plexus of the internal maxillary artery that joined the otic ganglion. Several authors have found nerve fibres in association with blood vessels in the TMJ (Schmid, 1969; Johansson et al, 1986). Ishibashi (1974) noted that nerve fibre bundles penetrated the capsule accompanied by small arteries in the human TMJ. While a branch of the otic ganglion to the TMJ was not found in the sheep, and sympathetic fibres could not be detected in major nerves entering the joint, the present study detected sympathetic fibres accompanied by blood vessels, in the

capsule, synovial membrane and disc (see discussion of glyoxylic acid). It is most likely that the sympathetic fibres entered the joint accompanying branches of the maxillary artery.

3.5.2. Gold chloride histochemistry

Within joint tissues, articular nerve fibres terminate in four types of endings, three of which are of the encapsulated variety (Wyke, 1967). All three types of encapsulated nerve endings (type I, II and III receptors or Ruffini endings, paciniform endings and Golgi organs respectively), are found in temporomandibular joints of rat, rabbit, guinea pig (Franks, 1975), cat (Skoglund, 1956; Greenfield and Wyke, 1964; Kawamura and Majima, 1964; Klineberg, 1971; Kawamura et al, 1990), monkey (Keller and Moffett, 1968; Johansson et al, 1986;) and humans (Davies, 1946; Thilander, 1961; Wink et al, 1992). The gold chloride technique utilised in the present study revealed all three types of endings in the sheep TMJ, although the Ruffini, or spray-type ending, were the most frequently encountered type. Most of the Ruffini endings in the sheep TMJ lacked a capsule, thus they resembled the unencapsulated spray endings described by Polacek (1966). Polacek (1966) described a series of endings which formed a continuum from simple free nerve endings to simple sprays, and more complicated encapsulated sprays to the encapsulated corpuscles of the Golgi-Mazzoni type with an inner core. This series of receptors was presumed to represent an evolutionary line with the three well-defined types of receptors occurring in the joint capsules of mammals with transitional forms occurring rarely and each species of mammal having a particular, clearly distinguishable triad of receptors.

Ruffini or type I articular receptors are numerous in all joints including the TMJ where they are usually found in superficial parts of the capsule and outnumber the other types

of corpuscular endings in cats (Wyke, 1967; Greenfield and Wyke, 1964; Klineberg, 1971), monkeys (Keller and Moffett, 1968) and humans (Thilander, 1961). The TMJ usually contains few paciniform-type receptors (Thilander, 1961; Keller and Moffett, 1968; Klineberg, 1971). The Golgi-type receptors are mostly located in the deeper parts of the capsule (Wyke, 1967; Klineberg, 1971; Klineberg et al, 1971). In the sheep TMJ the majority of corpuscular endings were located in the posterior and lateral capsule and were concentrated at the capsule-disc junction. In all parts of the TMJ this junction was more richly innervated by receptors than adjacent capsular areas. Thus the posterior/lateral capsule and all disc/capsule junction areas must play an important role in static and dynamic mechanoreception (Franks, 1975). Corpuscular endings are usually much less densely distributed in the medial/lateral parts of the TMJ capsule than the anterior/posterior parts (Kawamura and Majima, 1964; Klineberg, 1971; Johansson et al, 1986; Wink et al, 1992).

Type IV receptors (Wyke 1967) are noncorpuscular endings that belong to small myelinated (<5µm diam.) A-delta or unmyelinated C-type nerve fibres. They are the most numerous of the four categories of receptors found in the temporomandibular joint in humans (Thilander, 1961), cats (Wyke, 1967), rhesus monkey (Keller and Moffett, 1968), mouse (Dreessen et al, 1990) rat, guinea pig and rabbit (Franks, 1975). Gold chloride staining revealed numerous free nerve endings (type IV receptors) in the capsule, disc/capsule junction, synovial membrane and peripheral disc in the sheep TMJ. Freeman and Wyke (1967) divided type IV receptors into IVa or afferent pain fibres found in capsule, ligaments, synovium, menisci and bone, and IVb or efferent vasomotor fibres found in walls of small vessels. These endings exist as networks throughout the fibrous capsule, adjacent periosteum, articular fat pads and the adventitia sheaths of articular blood vessels (Wyke, 1967). Wyke (1967) reported that in the cat, free nerve endings were sparse, and largely confined to ligaments. Klineberg (1971) described plexuses of type IV nerve endings in fibrous capsule and fat pads of

cat TMJ while free nerve endings existed in small numbers in the fibrous capsule and more frequently in ligaments. However, many authors refer to free nerve endings without distinguishing networks of these type IV endings from separate so called 'free' endings. Most free nerve endings are sensitive to chemical, thermal, and mechanical stimuli (Storey, 1976; Zimny, 1988). They have a nociceptive role and may perhaps serve also polymodal mechanoreceptive functions (Dreessen et al, 1990).

Numerous studies have shown that the central region of the adult temporomandibular joint disc is invariably lacking in neural and vascular structures (Sharawy et al, 1984; Wink et al, 1992; Kido et al, 1993). While some studies have failed to find nerve endings in any part of the temporomandibular joint disc, for example in the cat (Greenfield and Wyke, 1964) and mouse (Dreessen et al, 1990), most studies report that the peripheral disc is innervated. The most detailed of these were the immunocytochemical studies by Ichikawa et al (1989) and Kido et al (1993) in which free nerve endings were restricted to the peripheral parts of the disc.

Corpuscular endings have been reported in the TMJ of human being (Zimny et al, 1985, Wink et al, 1992), monkey (Keller and Moffett, 1968; Johansson et al, 1986) and rats (Kido et al, 1993). In the present study of sheep TMJ, Golgi-Mazzoni endings were found only in the peripheral part of the disc. Corpuscular receptors have been reported in the subsynovial layers of the capsule (Kawamura et al, 1990) as well as the synovial membrane and villi (Davies, 1946). However the methods used by Davies (1946) were not described and the description of innervation was not detailed. There are no other reports of corpuscular endings in TMJ synovial membrane, although several studies have demonstrated free nerve endings and nerve fibres within the membrane and in the disc, as was noted in the present study of the sheep TMJ.

3.5.3. Fluorescence histochemistry

Glyoxylic acid can be used to demonstrate the localization of noradrenalin-containing fibres (autonomic fibres) using fluorescence histochemistry (Furness and Costa, 1975; de la Torre and Surgeon, 1976). In the sheep TMJ in the present study, adrenergic nerve fibres were demonstrated in the capsule, synovial membrane and the peripheral parts of the disc. Transverse sections of large arteries showed plexiform varicosities embedded in the adventitial sheath.

Schmid (1969) found that autonomic nerve fibres (a branch of the otic ganglion) entered the medial side of the capsule in the human TMJ. He presumed that sympathetic fibres came from a sympathetic plexus of the internal maxillary artery that joined the otic ganglion. Recently, Casatte and Bauer (1996) used a fluorescent retrograde neuronal tracer to demonstrate that the otic ganglion contained nerve cells whose axons entered the TMJ of rats. Autonomic nerve fibres characteristically form plexuses in the walls of arteries and accompany arterioles and capillaries in joint capsules. Plexuses which are separate from vessels in the capsule and synovial membrane are also formed (Samuel, 1952). A retrograde tracing study by Widenfalk and Wiberg (1990) revealed a large number of sympathetic efferents to the rat TMJ originating from the superior cervical ganglion. These authors hypothesised that nociceptive input from the TMJ could modulate activity in sympathetic efferents, which normally have a vasomotor role (Davies, 1946; Samuel, 1952; Ichikawa et al, 1989).

3.5.4. Immunohistochemistry

Immunohistochemical techniques can allow a convenient means to understand the distribution of neural elements in general by using protein gene product 9.5 (Ramieri et al, 1990; Karanth et al, 1991) as well as distinction between sensory nerves using substance P and CGRP (Ichikawa et al, 1989; Domeij et al, 1991; Kido et al, 1991; Kido et al, 1993; Karanth et al, 1991; Hukkanen et al, 1992b; Kobayashi et al, 1995) and autonomic nerves using neuropeptide Y, and vasoactive intestinal peptide (Lundberg et al, 1982; Ekblad et al, 1984; Uddmann et al, 1986) by using specific antibodies raised against these neural epitopes.

Recent immunocytochemical studies have demonstrated sensory nerve fibres and free nerve endings in the TMJ. Substance P-IR nerve endings have been demonstrated in the capsule, periosteum and adventitia of arteries of monkey TMJ (Johansson et al, 1986). Substance P and/or CGRP-IR nerve fibres have also been demonstrated in capsule, synovial membrane and disc of rats (Ichikawa et al, 1989, Hukkanen et al, 1992b, Kido et al, 1993). Substance P and CGRP are neuropeptides characteristically located in unmyelinated C-type and thinly myelinated A-delta pain fibres (Pernow, 1983). They may be present interstitially or perivascularly (Pereira da Silva and Carmo-Fonseca, 1990). These peptides may occur separately or together in articular sensory nerves (Hukkanen et al, 1992b). Ichikawa et al (1989) suggested that the CGRP-immunoreactive nerves in the rat TMJ might be associated with mediation of pain and/or proprioceptive sensations. Perivascular nerve fibres containing SP and CGRP have been given a putative involvement in the transmission of intracranial pain, and both peptides also influence vascular tone (Pernow, 1983; Fischer et al, 1983). Thus the CGRP nerve fibres demonstrated in the present study, in the synovial

membrane, adjacent capsule and disc of the sheep TMJ are probably nociceptive and perhaps proprioceptive in function.

The perivascular nerves, staining for NPY and VIP in rat TMJ, are believed to be part of the autonomic nervous system and to be involved in the regulation of blood flow in the TMJ (Ichikawa et al, 1989).

Antisera for PGP 9.5 have been used in many studies to detect sensory and autonomic fibres, small nerve endings and corpuscles in a variety of tissues including the TMJ (Ramieri et al, 1990; Morani et al, 1994). Neurospecific markers S-100 protein and PGP 9.5 were used by Morani et al (1994) to demonstrate the innervation of the capsule and disc of human TMJ. Perivascular and interstitial fibres were located in the capsule and bilaminar part of the disc. It was suggested that since some fibres were located in avascular parts of the disc, these fibres were most likely proprioceptive or nociceptive in function.

In the present study, numerous mechanoreceptor nerve endings were labelled by PGP 9.5 in the anterior and lateral part of the capsule in normal sheep TMJ. This is the first report of PGP 9.5 being used as a method for labelling nerve receptors in various tissues. Therefore this new finding suggests the use of PGP 9.5 for labelling different types of neural structures including mechanoreceptors, thus eliminating many limitations that accompany the use of methylene blue or gold chloride techniques. With the gold chloride technique, tissue can not be decalcified and this is a major problem when using joint tissues.

In conclusion, the present study details the appearance and distribution of neural elements in normal, healthy, young adult sheep, and forms a basis for an important part of the present work where the sheep is being used as a model for the study of the effects of

arthritis (Bosanquet and Goss, 1987; Bosanquet et al, 1991a and Ishimaru and Goss, 1992) on the innervation of the joint.

CHAPTER 4

INNERVATION OF THE PRENATAL SHEEP TEMPOROMANDIBULAR JOINT

4.1. SUMMARY	2
4.2 INTRODUCTION	3
4.3 MATERIALS AND METHODS	4
4.3.1. Animals and tissue processing	4
4.3.2. Immunocytochemistry	6
4.3.2.1. Single labelling	6
4.3.2.2. Double and triple labelling	7
4.3.3. Laser scanning confocal microscopy	9
4.3.4. Quantification and statistical analysis	10
4.4. RESULTS	11
4.4.1. General observations	11
4.4.2. Immunohistochemical observations	12
4.4.2.1. Disc	12
4.4.2.2. Capsule	13
4.4.2.3. Synovium	13
4.4.2.4. Bone and periosteum	14
4.4.2.5 Double and triple labelling	14
4.4.2.6. Confocal immunofluorescence microscopy	14
4.4.3. Quantitative data	15
4.5. DISCUSSION	15

4.1. SUMMARY

The density and distribution of sensory and autonomic innervation, containing general neuronal marker protein gene product 9.5 (PGP 9.5), and neuropeptides calcitonin gene related peptide (CGRP), substance P (SP), neuropeptide Y (NPY), vasoactive intestinal peptide (VIP) and the enzyme tyrosine hydroxylase (TH) were examined in the temporomandibular joint (TMJ) of late gestation fetal sheep to determine whether the innervation of the joint at 140 days gestation (full term=157d) differed from that in the mature adult.

Immunofluorescence microscopy was applied to serial sections (25 µm) of the capsule, disc and synovial membrane of ten joints from five fetuses and image analysis was used for the quantitative assessment. The capsule, synovial membrane and the disc contained fibres immunoreactive (IR) to antisera for PGP 9.5, SP and CGRP. NPY- and VIP-IR fibres were only visible in the loose connective tissue of the capsule. No TH-IR nerve fibres were detected in the fetal TMJ. There was no statistically detectable difference between the density of nerve fibres immunoreactive to CGRP or PGP 9.5 antisera in the capsule or disc. Substance P-immunoreactivity (IR) was relatively weak in all samples examined. Scattered branches of CGRP-IR fibres were found deep in the disc proper. The lack of receptor endings, other than free nerve endings in the TMJ of the late fetal sheep, might be a reflection of the functional and anatomical immaturity of the TMJ, as reflected in the immature, gross and microscopic appearance of the disc, the inferior joint compartment and articular surface of the condyle at this stage.

These results demonstrate that the capsule, synovial membrane and disc in the TMJ of fetal sheep at 140 days gestation age are innervated with PGP 9.5-, SP- and CGRP-IR (sensory) fibres, while autonomic fibres are located in the capsule only. The findings

also support the view that the disc is innervated at an early stage of life but at a later stage the density of innervation in the central part of the disc regresses and the innervation remains only peripherally in the adult TMJ disc.

4.2 INTRODUCTION

Previous studies have indicated differences in the innervation of the temporomandibular joint (TMJ) during prenatal and postnatal development in both human and laboratory animals, including guinea pigs, rabbits and rats (Thilander, 1963; Doyle, 1982; Ichikawa et al, 1989). These data are limited and incomplete, but indicate that the greatest density of nerve fibres in the mandibular condyle and disc occurs in the sixth month of gestation in the human and several days after birth in the rat (Ichikawa et al, 1989). The inferior joint cavity appears at 10 weeks of gestation (Moore, 1982), whereas the superior cavity begins to appear in the 12th week of gestation in the human (Yuodelis, 1966). After this time there is a progressive loss of nerve fibres from most of the disc with localisation occurring in the marginal areas of the disc prior to birth.

Recent developments in immunocytochemical methods have permitted a more thorough understanding of the distribution of nerve fibres in a variety of tissues including the TMJ than has been possible with the silver, gold chloride and methylene blue techniques used in the studies referred to above (Fristad et al, 1994). It has also become clear that neuropeptides within the nerves can play an important role in the physiology and metabolism of synovial joints both in normal and pathological conditions (Pereira da Silva and Carmo-Fonseca, 1990 ; Hukkanen et al, 1992a; Kido et al, 1993).

In Chapter 3 it was shown that the peripheral disc of the adult sheep TMJ is innervated by CGRP-immunoreactive nerve fibres and free nerve endings. In addition, encapsulated and unencapsulated endings are found in the disc/capsule junction. In this aspect of the study the density and distribution of nerve fibres immunoreactive with antisera to PGP 9.5, CGRP, SP, NPY, VIP and TH in the TMJ of late gestation fetal sheep were examined to determine the influence of age at 140 days gestation (full term =157d) on the innervation of the temporomandibular joint. Prior to the present study most of these antisera had not been used to examine fetal TMJ tissues. There are no CGRP-IR nerve fibres in the TMJ disc of rats at birth but between days 3 and 10 postpartum CGRP-IR fibres are present in the disc (as free nerve endings) and there is an increase in numbers in the disc and in fibrous tissue around the condyle (Ichikawa et al, 1989). In human fetuses, however, nerve endings in the disc are most numerous at 20 weeks, about the time the superior and inferior joint compartments are fully formed (Melfi, 1994), after which there is a progressive reduction (Ramier et al, 1996).

The prenatal TMJ was studied: (1) to clarify whether the innervation of this tissue prior to birth was different from that of adult animals; (2) to determine whether the joint was fully formed at this stage, like the human TMJ or immature, like the rat TMJ; (3) to determine whether the development of the innervation might be correlated with the stage of maturation of the TMJ.

4.3 MATERIALS AND METHODS

4.3.1. Animals and tissue processing

Fetuses were removed from normal Merino sheep (n=7) sacrificed by intravenous overdose of sodium pentobarbital (Lethabarb, Abbott Laboratories, Australia) at 140

days of gestation as part of another project conducted within the Medical School at the University of Adelaide. All tissues were collected in accordance with ethics approval guidelines for the University of Adelaide.

Temporomandibular joints (n=14) were quickly removed en bloc with a solid blade scalpel the normal fetuses (140 days gestation) and placed in fixative containing 4% paraformaldehyde plus 0.2% picric acid in 0.1M phosphate buffer (PB) pH 7.4 for 24 hrs.

The joints from two animals were then decalcified in a solution containing 10% w/v ethylenediaminetetraacetate (EDTA, disodium salt, Sigma, Australia) and 7.4% w/v polyvinylpyrrolidone (PVP, MW 40000, Sigma, Australia) in 0.1M Tris buffer (PH 6.95) for two weeks at 4° C. The demineralisation process was monitored once per week by using a fine pin. These joints were used for observations of general morphology, not immunocytochemistry.

The joints from the remaining five fetuses were processed for immunostaining. The disc and attached capsule was removed from each of these joints after fixation. When the disc was cut out of the TMJ, the upper surface of the condyle was also included in blocks of tissue from four joints in two animals.

Subsequently, all tissues were rinsed in 20% sucrose in 0.1M PB overnight before cryosectioning. Tissues were then blotted with filter paper and mounted in embedding medium (O.C.T compound, Miles Inc, USA) on metal stubs and frozen in a cryostat (Leitz 1720) at minus 30°C. The decalcified joints were embedded so that sagittal sections could be cut for general observations on the morphology of the joint. The blocks of tissue from the other ten joints were embedded so that horizontal sections could be cut through the disc for the immunostaining. Serial sections (25µm to 35µm)

were cut and mounted on Vectabond (Vector Laboratories, USA)-coated slides and allowed to dry overnight at room temperature.

4.3.2. Immunocytochemistry

4.3.2.1. Single labelling

Sections were processed for indirect immunofluorescence according to Coons et al. (1955). The solution used to dilute the antisera was 1% bovine serum albumin and 0.05% sodium azide in 0.1M phosphate-buffered saline (PBS, pH 7.4) containing 0.3% Triton X100 (Rohmand Haas Co, USA). All incubation of the sections with antisera was carried out at room temperature. The tissue sections were first preincubated for one hour with diluted normal blocking serum which was prepared from the same species as used in the secondary antibody. After the excess serum was blotted, the sections were incubated with rabbit antisera. Details of the neuropeptide rabbit antisera (SP and CGRP) are in Table 4.1. PGP 9.5 antiserum was obtained from Ultraclone, Cambridge, UK. Diluted antisera were applied to sections overnight in a humid chamber at room temperature. After three washes in PBS, the sections were incubated in the dark for one hour with FITC-labelled anti-rabbit IgG (Sigma, Australia) diluted 1:60 in PBS at room temperature. After a further three washes in PBS the sections were sealed with coverslips using mounting medium consisting of PBS and glycerine. Sections were viewed with a BH-2 Olympus fluorescence microscope and photographed with Kodak T-Max 400 film. During the immunohistochemical procedures, control sections were processed in parallel, except that they were incubated in normal serum instead of primary antisera. No immunoreactivity was observed in control sections.

Table 4.1. Primary antibody characteristics

Antisera	code number	Dilution	Host species	Source	References for specificity
PGP 9.5	2582	1/600	rabbit	Ultraclone, Cambridge	Gulbenkian et al (1987)
SP	1657	1/400	rabbit	Hammersmith Hospital	Hökfelt et al (1975)
SP	RMSP-1	1/800	rabbit	R. Murphy	Gibbins & Morris (1987)
CGRP	1204	1/500	rabbit	Hammersmith Hospital	Gibson et al (1984)
CGRP	6006-N	1/2000	rabbit	Peninsula	Kummer et al (1990)
NPY	RMJ-263	1/600	rabbit	Maccarone and Jarrot	Morris et al (1986)
TH	LNC-1	1/2000	rabbit	Incstar	Gibbins & Matthew (1996)
VIP	F1/111	1/1000	rabbit	R. Murphy	Morris & Gibbins (1987)

4.3.2.2. Double and triple labelling

In addition to single labelling, double and triple labelling immunofluorescence was used to visualize more than one antigen simultaneously in a single tissue section, according to the method described by Gibbins et al, 1985; Gibbins and Matthew (1996). One fetal joint was examined for coexistence of SP-, VIP-, TH-, NPY-, CGRP- and PGP 9.5-immunoreactivities. Briefly, after preincubation with normal blocking serum, sections were incubated for 24h with a mixture of two primary antibodies for double labelling, and a mixture of three primary antibodies for triple labelling. Each primary antiserum was raised in a different host species (see Table 4.2 & 4.3).

All antibodies were diluted with hypertonic PBS (1.7% Na Cl) to reduce nonspecific binding of the antibodies to tissue sections. After washing with PBS, the sections were incubated for 1h with two or three species-specific secondary antibodies. The secondary antibodies were raised in donkeys (Jackson Immuno Research Laboratories, USA) and conjugated to 7-amino-4-methylcoumarin-3-acetic acid (AMCA), dichlorotriazinylamino fluorescein (DTAF) or indocarbocyanine (Cy3). These antibodies were also diluted with hypertonic PBS. After a further three washings in PBS the sections were sealed with coverslips using antifade mounting medium (PBS, glycerine). The sections were viewed with an Olympus Vanox fluorescence microscope fitted with filters selective for the red fluorescence of Cy3, the green fluorescence of DTAF or the blue fluorescence of AMCA. All images were captured with an Apple Macintosh computer with a sicon frame-grasber card and running NIH Image software.

All primary and secondary antibodies used here for double and triple labelling have been tested extensively for cross-reactivity (for references see Table 4.1). Combinations of primary and secondary antibodies that were used are summarized in Tables 4.2 & 4.3.

Table 4.2. Antibody combinations used for double-labelling immunofluorescence

Primary antibody combination	Secondary antibody combination
Rat anti-SP	donkey anti-rat-AMCA
Rabbit anti-TH	donkey anti-rabbit-CY3
Rat anti-SP	donkey anti-rat-AMCA
Rabbit anti-VIP	donkey anti-rabbit-CY3
Rat anti-SP	donkey anti-rat-AMCA
Rabbit anti-NPY	donkey anti-rabbit-CY3

Table 4.3 Antibody combinations used for triple-labelling immunofluorescence

Primary antibody combination	Secondary antibody combination
Rabbit anti-VIP	Donkey anti-rabbit-AMCA
Rat anti-SP	Donkey-anti-rat-CY3
Mouse anti-TH	Donkey-anti-mouse-DTAF
Rabbit anti-NPY	Donkey anti-rabbit-AMCA
Rat anti-SP	Donkey anti-rat-CY3
Mouse anti-TH	Donkey anti-mouse-DTAF
Rat anti-VIP	Donkey anti-rabbit-AMCA
Rabbit anti-CGRP	Donkey anti-rat-CY3
Mouse anti-TH	Donkey anti-mouse-DTAF
Rabbit anti-PGP 9.5	Donkey anti-rabbit-AMCA
Rat anti-SP	Donkey anti-rat-CY3
Mouse anti-TH	Donkey anti-mouse-DTAF
Rat anti-SP	Donkey anti-rabbit-AMCA
Rabbit anti-CGRP	Donkey anti-rat-CY3
Mouse anti-TH	Donkey anti-mouse-DTAF

4.3.3. Laser scanning confocal microscopy

Bio-Red 1000 Laser Scanning confocal microscopy was employed, whenever it was a difficult problem to obtain sharp images, using conventional microscopy. By this method it was possible to confirm or to exclude the results obtained by conventional methods in the dense fibrous tissue of the disc.

4.3.4. Quantification and statistical analysis

Each block of tissue (disc plus capsule from one joint) was cut into about 25 sections. From these, three groups of three consecutive sections were randomly selected (9 sections in total) for immunostaining. Each of these consecutive sections was immunostained with antiserum to one of PGP 9.5, CGRP or SP. The group of three consecutive sections that had the cleanest immunolabelling was selected for quantification. From each section, thirty-two fields (chosen as a manageable number of fields) were systematically sampled by dividing the section into 32 regions and selecting one field of view from the centre of each region at a 10x objective magnification. On account of the small size of the fetal disc it was difficult to delineate separate regions (eg anterior, posterior etc) within each section with the fluorescence microscopy, however, capsule and disc were noted.

By using the Video-Image analysis system which included a colour Panasonic camera attached to a BH-2 Olympus microscope, the fluorescent image was analysed using a modified version of the software package, Video Pro 32 (Leading Edge Australia). Immunostained nerve fibres exhibited a bright fluorescence which the Video-image analysis system was programmed to detect and measure the width and number of nerves as well as percentage surface area of immunoreactive nerves were measured.

A general linear model analysis using program 3V from the BMDP statistical software package (Dixon, 1991) was used to analyse the quantitative results. The general linear model is a variation of an analysis of variance, sometimes called a mixed model of analysis of variance because it has fixed effects and random effects. It uses similar F tests.

The analysis used a random effect for sheep and fixed effects for stain, side and stain by side interaction. Data were used as actual values or (i) subjected to a square root transformation or (ii) subjected to a log transformation before being analysed by the model. This was to check the robustness of distributional assumptions. The conclusions were identical. A P value of <0.01 was chosen for determining significance. More details of the general linear model analysis are found in Appendix 2.

4.4. RESULTS

4.4.1. General observations

At 140 days gestation age (term=157 days) the TMJ was not fully developed. The condyle, glenoid fossa, disc and synovial membrane were recognisable but the inferior joint compartment was incomplete (Fig. 4.1a). The superior joint compartment was present but the inferior compartment was confined to a narrow region anteriorly, near the capsule/disc junction (Fig. 4.1a). Over most of the mandibular condyle the disc was continuous with the cellular fibrous tissue on the superior surface of the condyle. Some small clefts indicated the location of the developing inferior joint compartment (Fig. 4.1c). The articular surfaces of the condyle and temporal fossa were composed of dense cellular connective tissue (Figs. 4.1.d, e). The outermost surface of the condyle was covered by a thin band of closely packed cells that was continuous with the synovial villi in the anterior section of the inferior joint cavity and continued onto the inferior and superior aspects of the disc as a slightly thinner layer (Fig. 4.1e). Adjacent and inferior to this cellular layer, a band of fibrous tissue and scattered cells merged with the underlying hyaline cartilage which merged with bone (Figs 4.1d, e).

PLATE 18 Light Microscopy Of The Fetal Sheep TMJ

Figure 4.1a Sagittal section of the temporomandibular joint of a 140-days-old sheep fetus, showing condyle (C), disc (D), temporal fossa (T), anterior capsule (Ca), superior joint cavity (SJC) and inferior joint cavity (IJC). Haematoxylin and eosin stain. Bar: 2mm.

Figure 4.1b Temporomandibular joint of a 140-days-old sheep fetus, showing condyle (C), articular surface of the condyle (AS), disc (D), synovium (S), superior joint cavity (SJC) and inferior joint cavity (IJC). Haematoxylin and eosin stain. Bar: 20 μ m.

Figure 4.1c Temporomandibular joint of a 140-days-old sheep fetus, showing articular surface of the condyle (AS), disc (D), inferior joint cavity (IJC) and cartilage cells of the condyle (CC). Haematoxylin and eosin stain. Bar: 10 μ m.

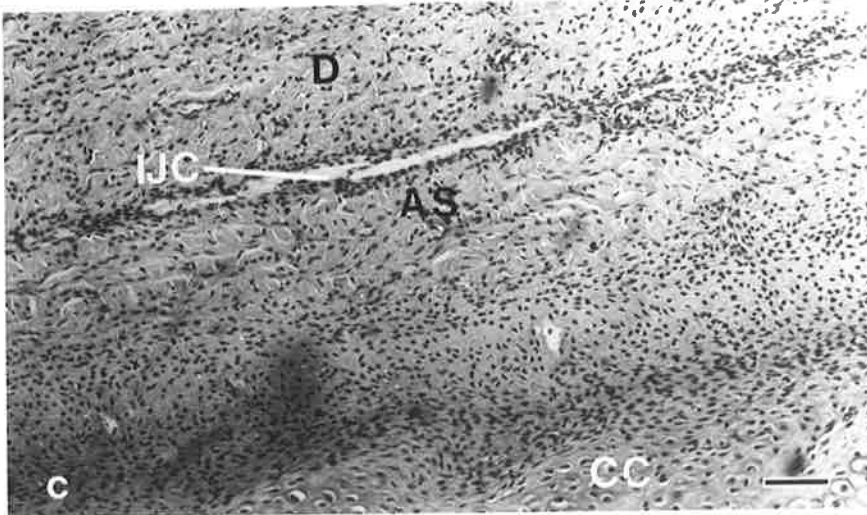
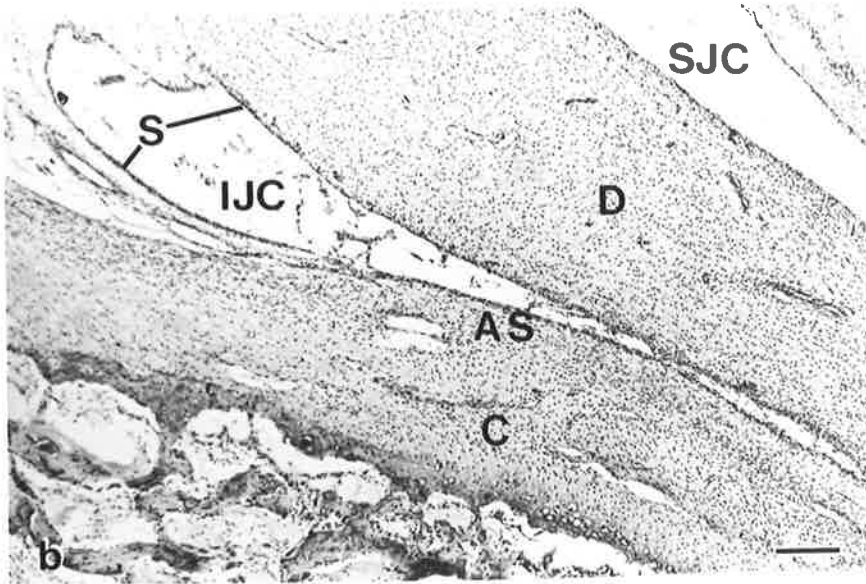
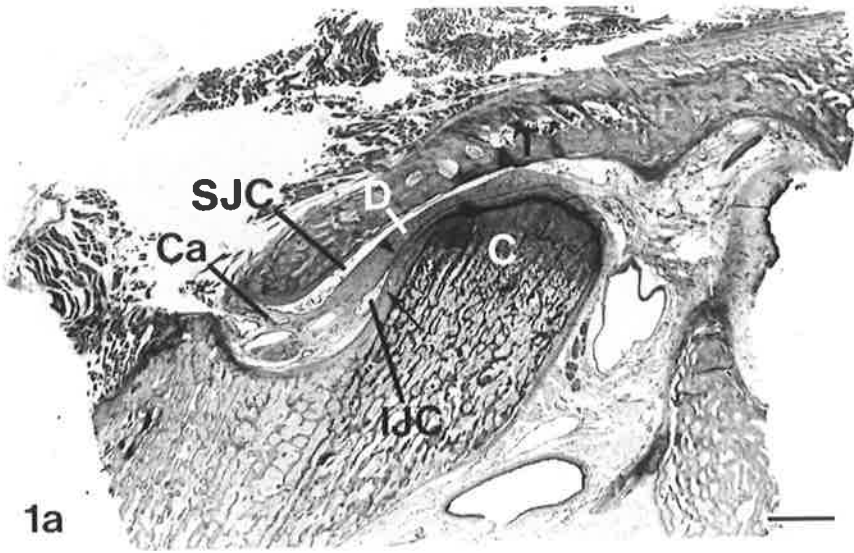


PLATE 19 Light Microscopy Of The Fetal Sheep TMJ

Figure 4.1d Temporomandibular joint of a 140-days-old sheep fetus, showing articular surfaces (AS) of the condyle (C) and temporal fossa (T), disc (D) and superior joint cavity (SJC). Haematoxylin and eosin stain. Bar: 10µm.

Figure 4.1e Temporomandibular joint of a 140-days-old sheep fetus, showing articular surface of the condyle (AS), disc (D), inferior joint cavity (IJC), temporal fossa (T), capsule (Ca) and vessels (V). Haematoxylin and eosin stain. Bar: 10µm.

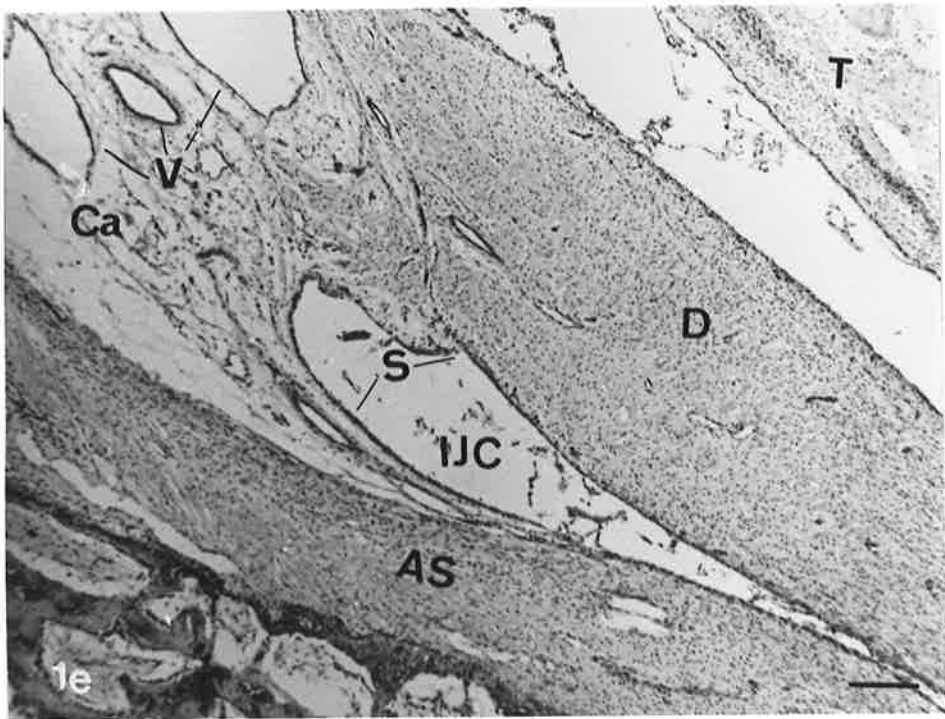
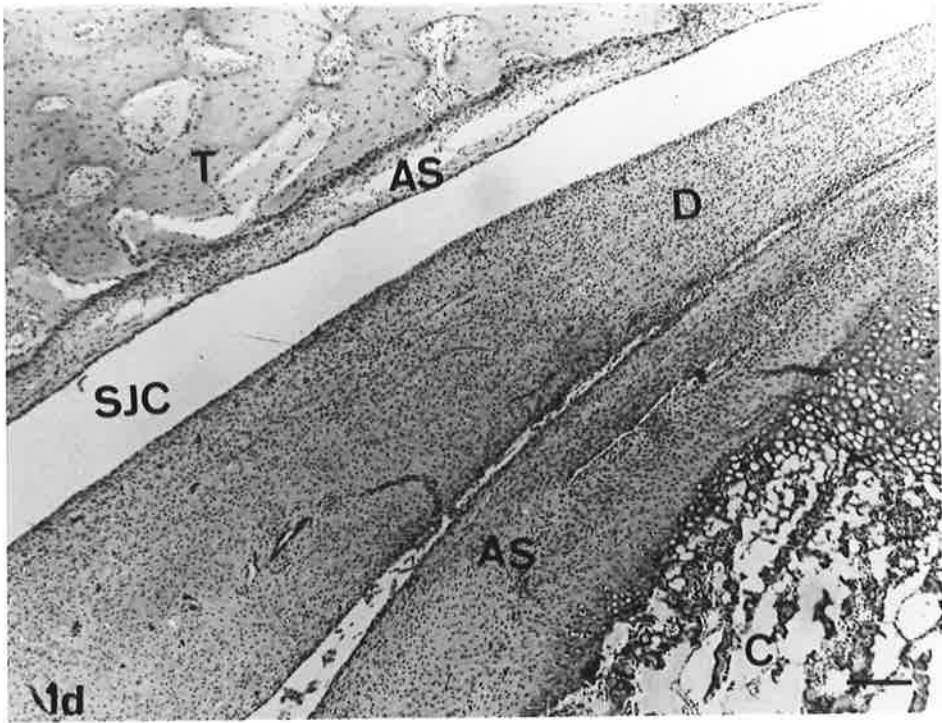
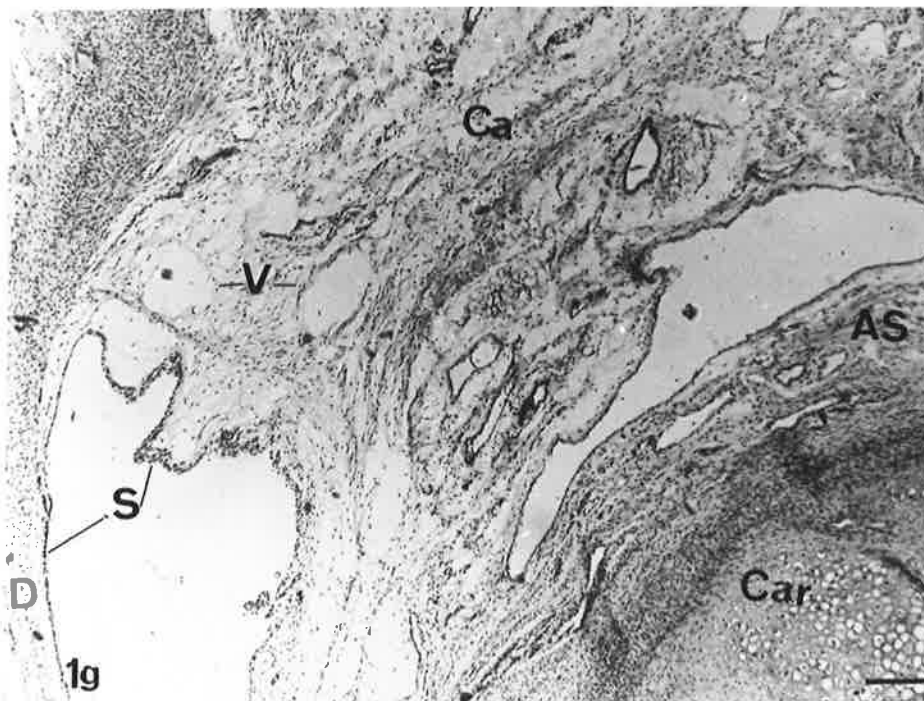
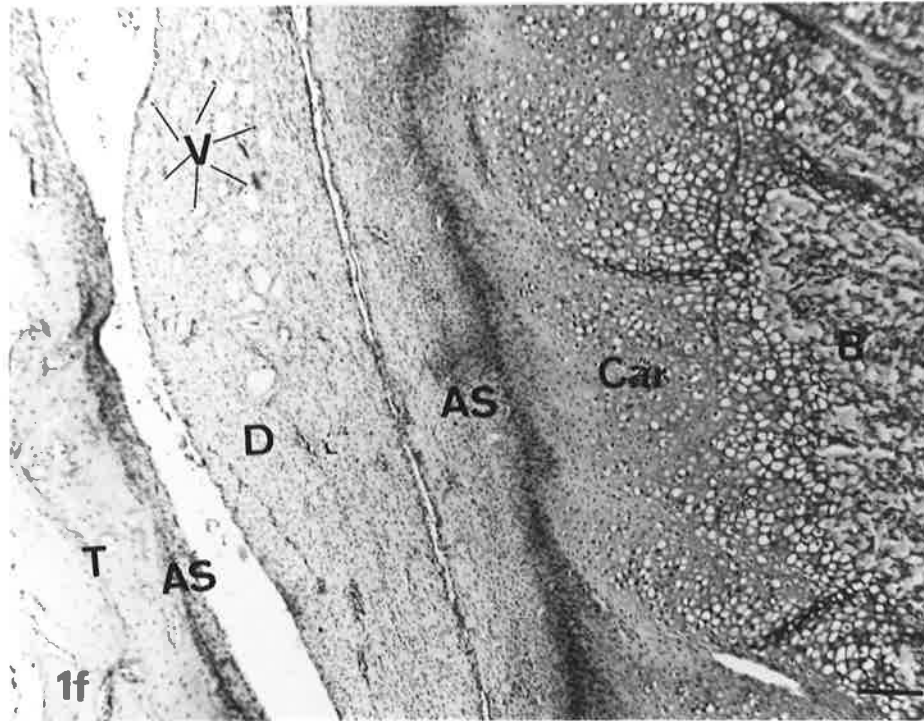


PLATE 20 Light Microscopy Of The Fetal Sheep TMJ

Figure 4.1f Temporomandibular joint of a 140-days-old sheep fetus, showing articular surfaces (AS) of the condyle and temporal fossa (T), disc (D), cartilage (Car) and bone (B) of the condyle. V: vessels in the disc. Haematoxylin and eosin stain. Bar: 10µm.

Figure 4.1g Temporomandibular joint of a 140-days-old sheep fetus, showing articular surface (AS) of the condyle, disc (D), cartilage (Car) of the condyle, capsule (Ca), synovium (S) and vessels (V). Haematoxylin and eosin stain. Bar : 10µm.



The articular disc was also highly cellular. Dense fibrous tissue was located in the moderately cellular central region with highly cellular layers superiorly and inferiorly. Vascularization extended throughout the disc, although, except for enlarged venules in the posterior one fourth of the disc (Fig. 1f), there were only small numbers of narrow vessels scattered through the remainder of the disc. No cartilage cells were visible in the disc. The anterior disc/capsule junction contained many large blood vessels and bundles of nerves. Both the anterior and posterior capsule consisted of loose connective tissue with scattered bundles of collagen fibres, fat cells, bundles of nerve fibres and large blood vessels (Fig. 4.1a) The synovium lining of the peripheral disc was composed of a narrow band of flattened cells while that adjacent to the anterior and posterior capsule consisted of several layers of rounded cells with narrow processes or villi projecting into the superior and inferior joint cavities (Fig. 4.1g).

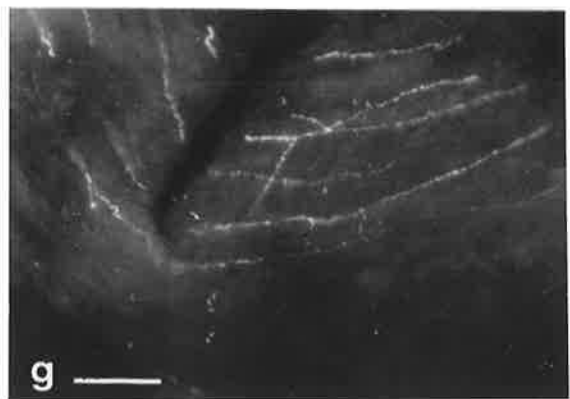
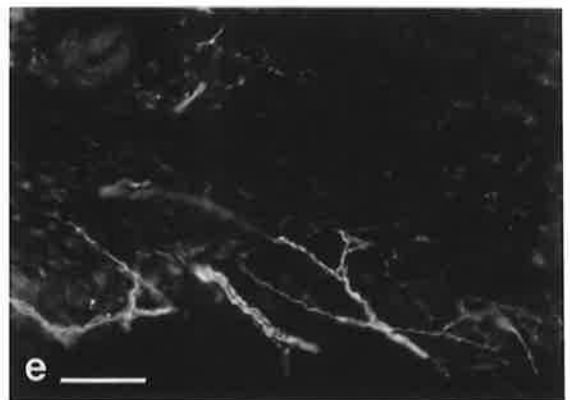
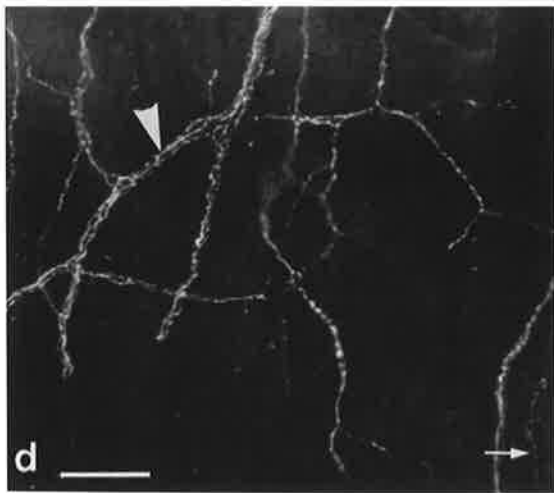
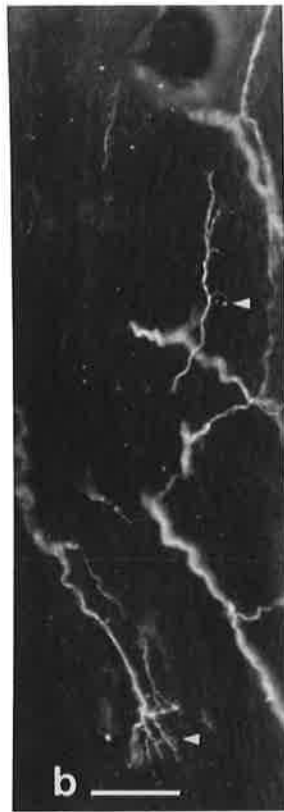
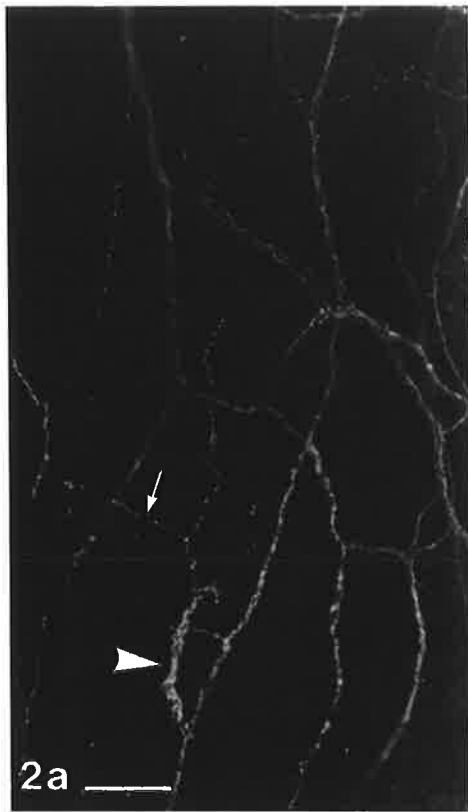
4.4.2. Immunohistochemical observations

4.4.2.1. Disc

PGP 9.5-IR fibres formed interconnecting networks of fibres in the disc. Thin, varicose fibres, thicker, more evenly fluorescent fibres and branching bundles of fluorescent fibres were visible (Figs, 4.2d, e). CGRP-IR nerve fibres formed anastomosing networks or plexuses of thin, strongly fluorescent fibres throughout the disc (Figs 4.2a-c). Some of these fibres displayed varicosities. Many bundles (up to 45 μm diameter) of nerve fibres showed intense CGRP-immunoreactivity. The largest bundles were confined to the periphery of the disc. Nerve fibres up to 7 μm diameter occurred in the central region of the disc. Thin varicose branches of CGRP-IR fibres, which might have represented nerve terminals such as free nerve endings were found throughout the disc. Some CGRP-IR fibres were located adjacent to blood vessels, but many appeared independent of blood vessels. Substance P-immunoreactivity was relatively weak compared to that for PGP 9.5 or CGRP, and did not form an anastomosing network.

**PLATE 21 CGRP-, SP- And PGP9.5 Immunoreactive
Nerve Fibres In Disc Of The Fetal Sheep
TMJ**

Figure 4.2 Disc of a 140-days-old sheep fetus showing CGRP-IR fibres (a,b,c), PGP 9.5-IR fibres (d,e) and substance P-IR fibres (f,g) with single fibres, bundles of fibres (large arrow heads), varicose fibres (arrows) and free nerve endings (small arrow heads). JC: joint cavity. Bars: 100µm.



SP-IR fibres were sparsely distributed throughout the disc, and showed some varicosities (Figs. 4.2f, g). No immunoreactive fibres were seen with antisera to NPY, VIP or TH.

4.4.2.2. Capsule

Many bundles of fibres in the capsule were immunostained with PGP 9.5 antibodies. These fibres were often located near blood vessels and were wavy in appearance (Figs. 4.3d, e). Thin PGP 9.5-IR fibres accompanied blood vessels and others penetrated the connective tissue away from the blood vessels. Bundles of SP-IR fibres branched within the capsule to form thin, varicose fibres (Figs 4.3f, g). In the capsule the CGRP-IR fibres did not form anastomosing networks as in the disc, but rather were spread unevenly throughout the fibrous tissues, often in association with blood vessels (Figs. 4.3a-c). There appeared to be more bundles of CGRP-IR fibres and fewer single fibres in the capsule than in the disc. The CGRP-IR fibres had a characteristically wavy or sinuous appearance. Many thin fibres featured immunofluorescent varicose swellings. Some SP-IR fibres were located in the adventitia of arteries and some of these fibres had thin branches with varicosities (Figs. 4.3f, g). NPY-IR nerve fibres were present in the capsule, however, no fibres were immunoreactive with antiserum to TH.

4.4.2.3. Synovium

PGP 9.5-IR nerve fibres passed parallel to the synovium in the subsynovial tissue, having branched from nerve bundles in the capsule (Figs. 4.4c, d). Thin, intensely fluorescent varicose fibres passed into the synovium, including villous processes, to end just deep to the surface adjacent to the joint cavity. The synovium contained fine CGRP-IR fibres, most of which had varicosities (Figs. 4.4a, b). Some fibres passed parallel to the surface of the synovium adjacent to the joint cavity while others penetrated from deeper subsynovial tissue and ended in the synovium, just below the joint cavity. Synovial villi also contained fine CGRP-IR fibres. Scattered, thin SP-IR

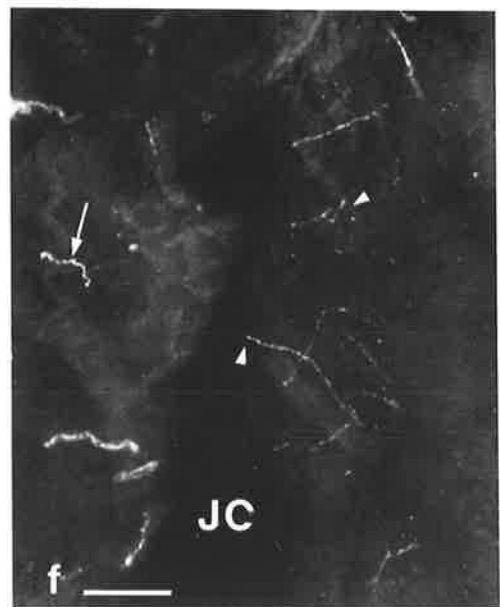
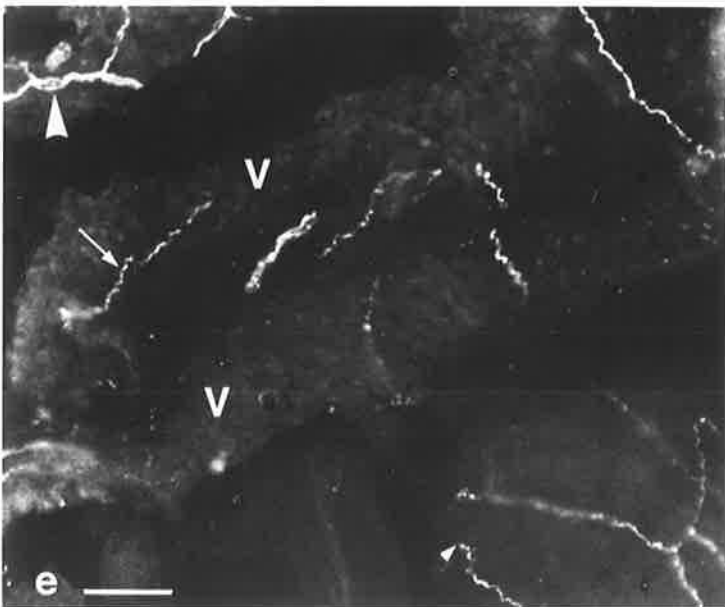
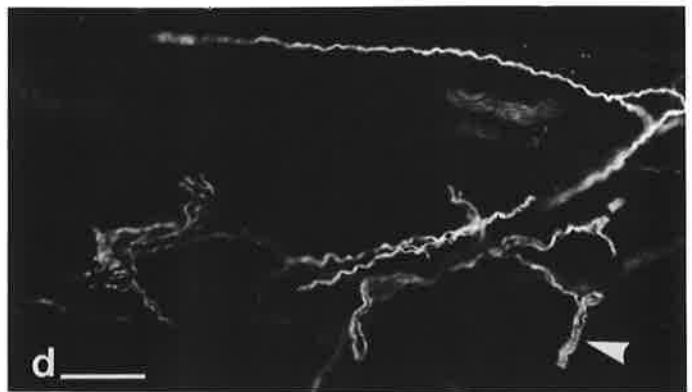
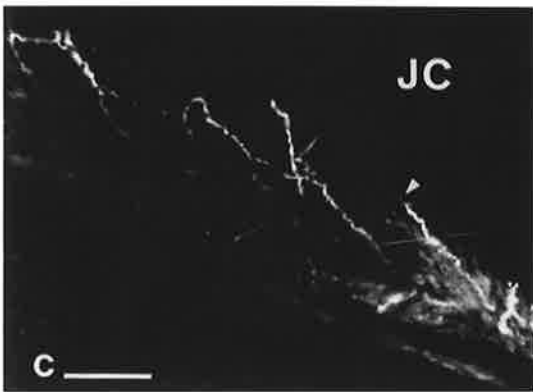
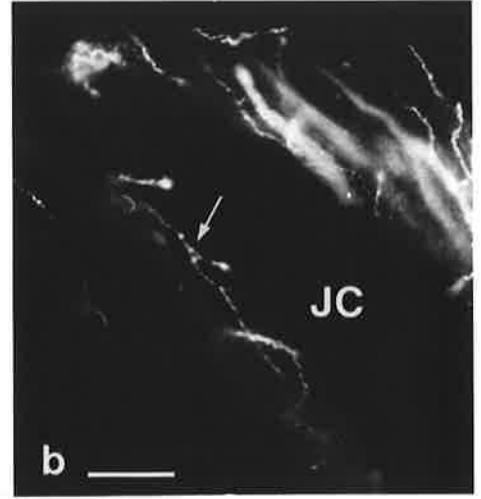
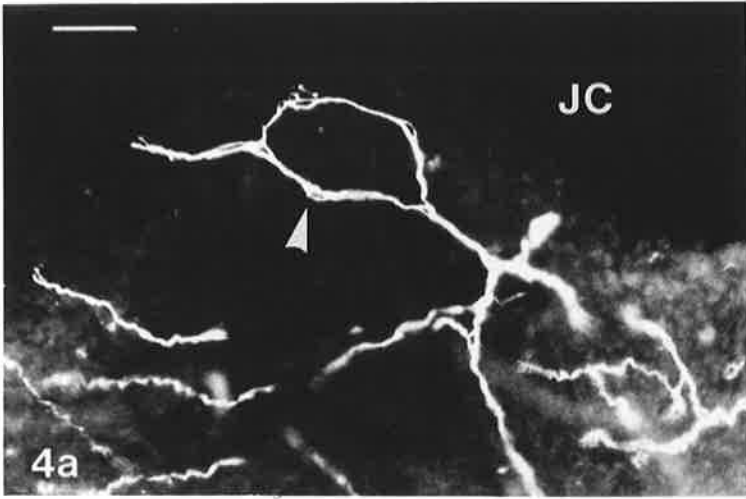
**PLATE 22 CGRP-, SP- And PGP9.5 Immunoreactive
Nerve Fibres In Capsule Of The Fetal Sheep
TMJ**

Figure 4.3 Capsule of a 140-days-old sheep fetus showing CGRP-IR fibres (a,b,c), PGP 9.5-IR fibres (d,e) and substance P-IR fibres (f,g) with single fibres, bundles of fibres (large arrow heads), varicose fibres (arrows) and fibres in the adventitia of arteries (small arrow heads). Bars: 100µm.



**PLATE 23 CGRP-, SP- and PGP9.5 Immunoreactive
Nerve Fibres In Synovium Of The Fetal
Sheep TMJ**

Figure 4.4 Synovium and adjacent capsule of a 140-days-old sheep fetus showing CGRP-IR fibres (**a,b**), PGP 9.5-IR fibres (**c,d**) and substance P-IR fibres (**e,f**) with single fibres, bundles of fibres (large arrow heads), varicose fibres (arrows) and free nerve endings (small arrow heads). JC: joint cavity; V: synovial villus. Bars: 100µm.



fibres passed through the subsynovium (often accompanying blood vessels) to end just below the synovial lining cells (Figs. 4.4e, f). Other thin fibres immunostained with SP antibodies projected into synovial villi. There were no VIP-, NPY- or TH-IR fibres in the synovium.

4.4.2.4. Bone and Periosteum

Blood vessels in the subchondral bone of the condyle were surrounded by fine, varicose fibres immunostained with PGP 9.5 antibodies (Fig. 4.5c). Thin, weakly fluorescent PGP 9.5-IR fibres were visible throughout the subchondral bone. Subchondral bone within the condyle contained thin CGRP-IR fibres and small nerve bundles (Figs. 4.5a, b). Some thin varicose fibres were visible. SP-IR fibres were sparsely distributed in the subchondral bone of the condyle (Fig. 4.5e). Some PGP 9.5-, SP- and CGRP-IR fibres within the bone of the condyle passed parallel to the periosteum and had thin branches extending into the periosteum.

4.4.2.5 Double and triple labelling

Double and triple labelling with different combinations of antibodies to CGRP, SP, NPY, VIP and TH demonstrated the co-existence of CGRP- and SP-IR in some nerve fibres in the disc, capsule and synovial membrane (Fig 4.6). No TH-IR was detected. NPY- and VIP-IR nerve fibres were detected in the capsule, but these fibres were not immunoreactive to any of the other antisera tested (Fig. 4.7).

4.4.2.6. Confocal immunofluorescence microscopy

The details of nerve fibre branching and location of nerve fibres relative to different tissues, especially the synovium and disc, were much clearer using confocal microscopy. Figures 4.8a-c show SP- and CGRP-IR fibres in the disc and entering adjacent synovium.

**PLATE 24 CGRP-, SP- and PGP9.5 Immunoreactive
Nerve Fibres In Condyle Of The Fetal Sheep
TMJ**

Figure 4.5 Condyle of a 140-days-old sheep fetus showing CGRP-IR fibres (**a,b**), PGP 9.5-IR fibres (**c**) and substance P-IR fibres (**e**) with single fibres, bundles of fibres (large arrow heads), varicose fibres (arrows) and free nerve endings (small arrow heads). JC: joint cavity. Bars: 100µm.

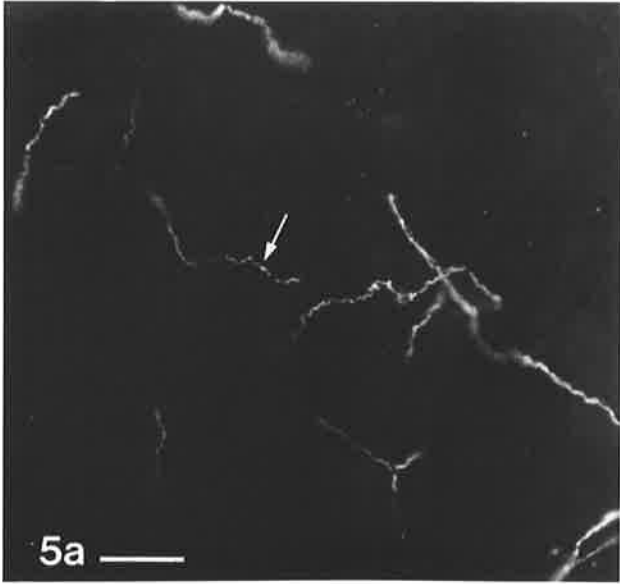


PLATE 25 **Triple Labelling Of NPY- And SP-
Immunoreactive Nerve Fibres In Synovium
Of The Fetal Sheep TMJ**

Figure 4.6 Triple labelled section of synovium (S) and capsule (Ca) of the TMJ of a 140-day-old sheep fetus. (a) TH-IR, (b) SP-IR and (c) CGRP-IR. Arrows indicate fibres immunoreactive for CGRP and SP but not TH. JC: joint cavity. Bars: 50µm.

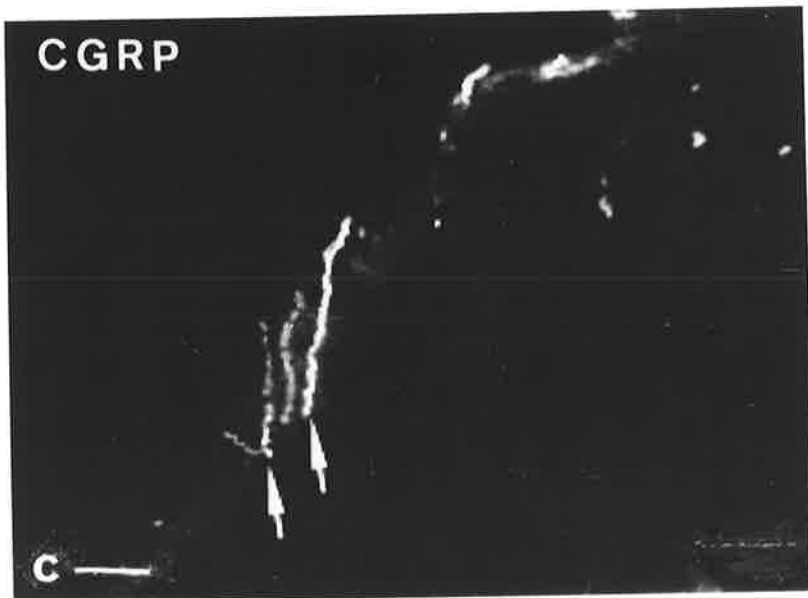
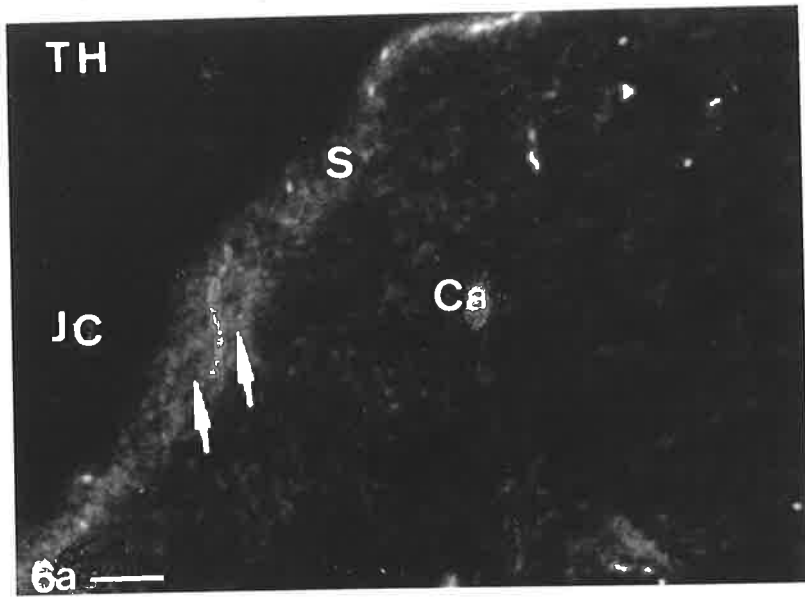
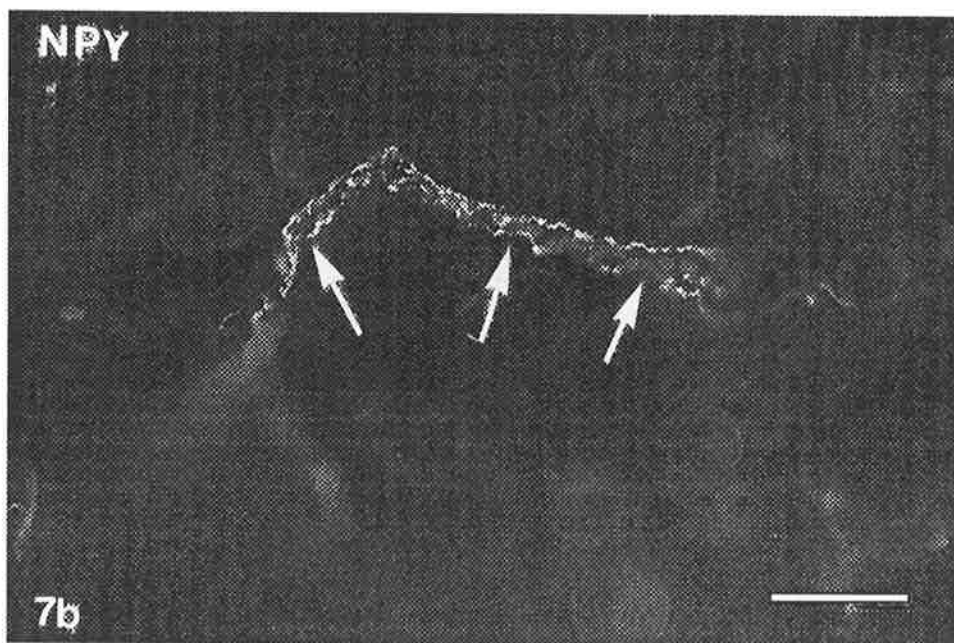
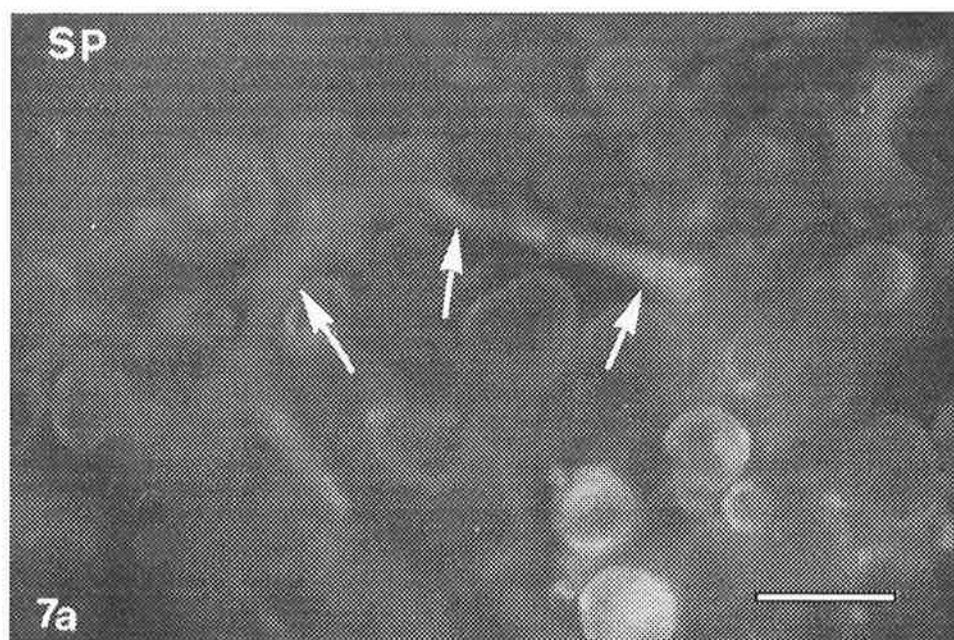


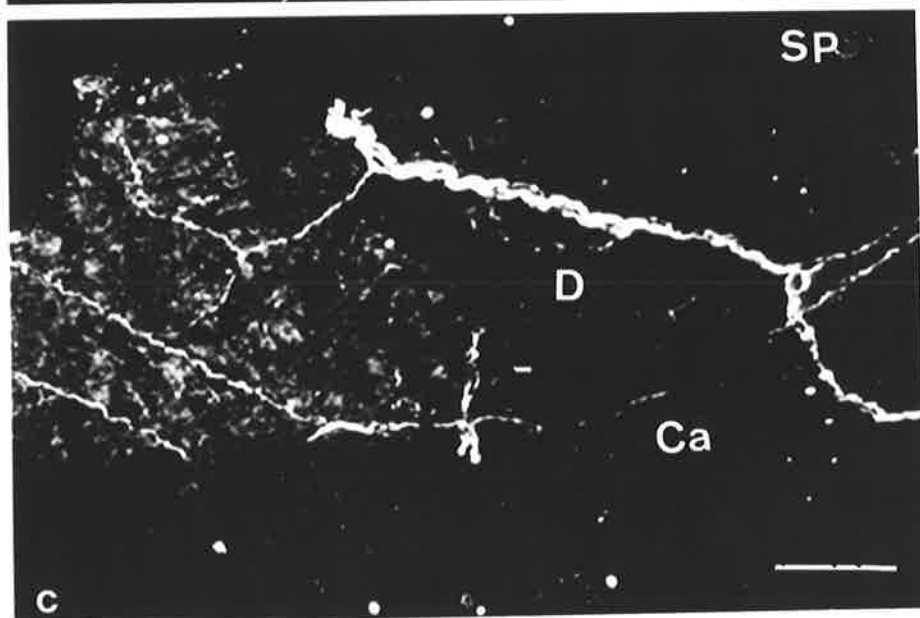
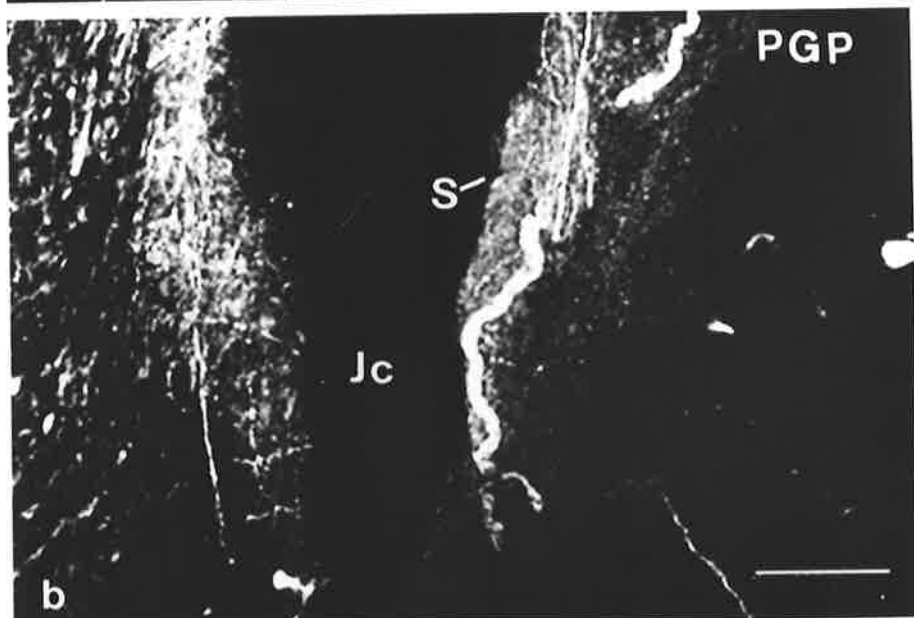
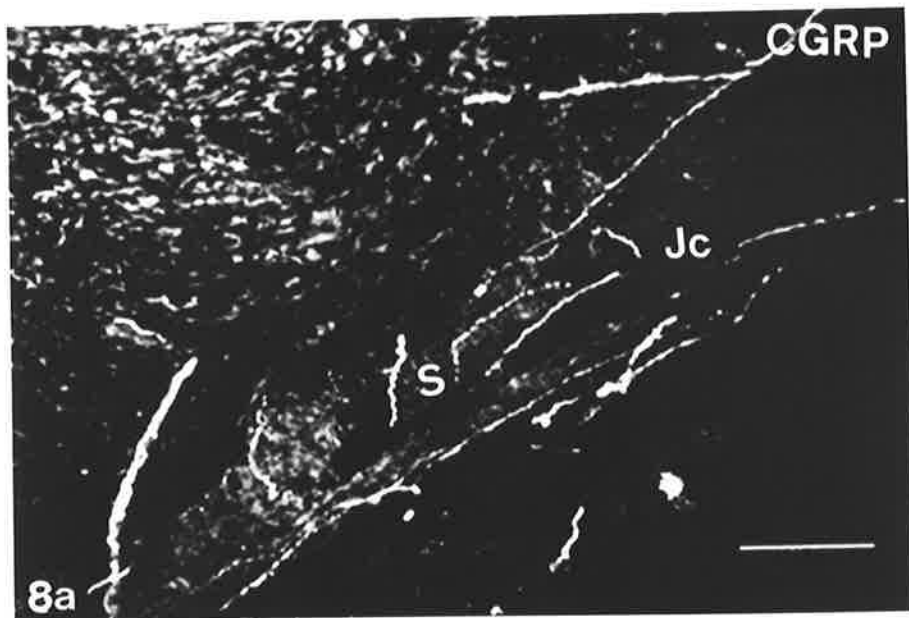
PLATE 26 **Double Labelling Of NPY- And SP-
Immunoreactive Nerve Fibres In Synovium
Of The Fetal Sheep TMJ**

Figure 4.7 Double labelled section capsule of the TMJ of a 140-day-old sheep fetus. (a) SP-IR and (b) NPY-IR. Arrows indicate fibres immunoreactive for NPY but not SP. Bars: 50µm.



**PLATE 27 Laser Scanning Immunofluorescence
Confocal Microscopy Of Nerve Fibres In
Synovium, Disc And Capsule Of The Fetal
Sheep TMJ**

Figure 4.8 Immunoreactive nerve fibres in the TMJ of a 140-days-old sheep fetus as revealed by immunofluorescence confocal microscopy. (a) CGRP-IR, (b) PGP 9.5-IR and (c) SP-IR showing synovium (S), joint cavity (Jc), disc (D) and capsule (Ca). Bars: 100µm.



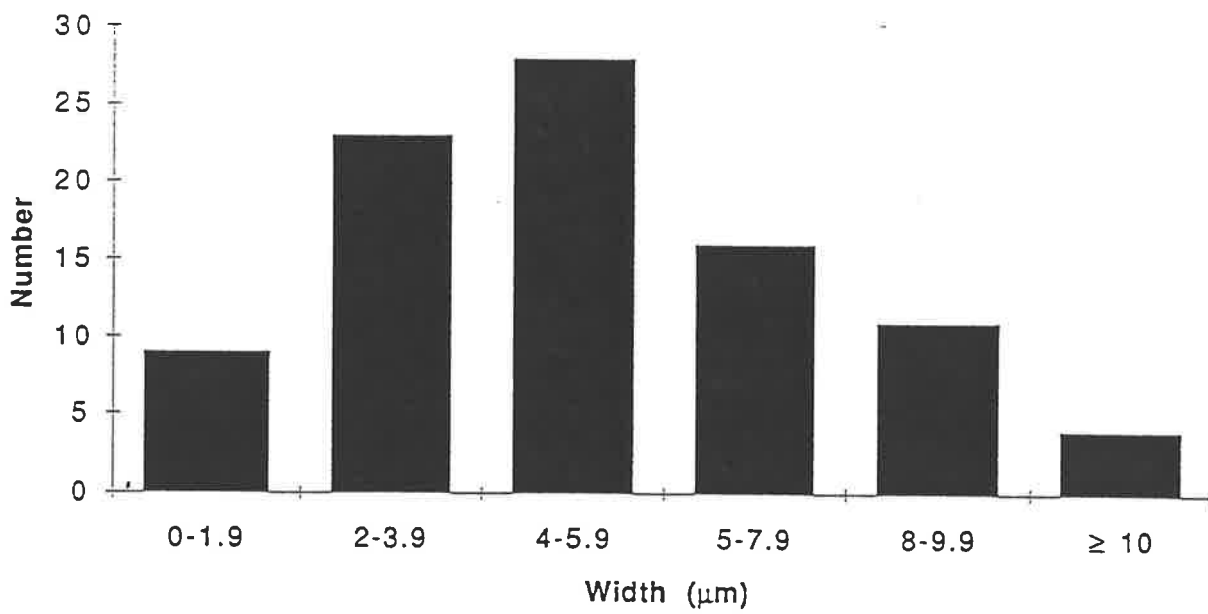


Figure 4.9 Widths of nerves in capsule and disc of TMJ of fetal sheep.

4.4.3 Quantitative Data

Measurements were made for capsule and disc. However, on account of the small size of the fetal temporomandibular joint, and the difficulty in delineating different regions in all sections used for the quantitative analysis (fluorescence microscopy) it was not possible to get sufficient data for the quantitative analysis of the synovium, periosteum or bone. There were no statistically detectable differences ($P > 0.01$) in % surface area (surface area of immunoreactive fibres expressed as a % of the area of tissue examined), number of nerves (single fibres and bundles of fibres) per mm^2 , or width of nerves (single fibres and bundles of fibres) between left and right sides, between capsule and disc or between PGP 9.5 and CGRP stains. The mean (plus standard errors) for % surface area, number of nerves per mm^2 and width of nerves in fetal capsule and disc for CGRP and PGP 9.5 were 0.54% (.080), 2.79/ mm^2 (0.32) and 5.18 μm (0.35) respectively. While few nerves were 10 μm or more in width, about 65% were 6 μm or less in width (Fig. 4.9). Substance P-immunoreactivity was less intense and more scattered than that for PGP 9.5 or CGRP and quantitative data were insufficient for comparison.

4.5. DISCUSSION

Antisera for substance P and CGRP have been used to localise sensory nerve fibres in adult TMJ tissues from rats (Ichikawa et al, 1989; Hukkanen et al. 1992b; Kido et al, 1993), monkey (Johansson et al, 1986), and sheep (see chapter 3 and Tahmasebi Sarvestani et al, 1996). Antisera for PGP 9.5 (a neuron-specific protein) have been used in many studies to detect sensory and autonomic fibres, small nerve endings and corpuscles in a variety of tissues including the TMJ (Ramieri et al, 1990; Morani et al, 1994). While neither VIP- or NPY-immunoreactivity (autonomic fibres) has been

studied in TMJ tissues, VIP- and NPY-immunoreactivity has been measured in joint perfusates in humans and rats (Holmlund et al, 1991). Prior to the present study these antisera had not been used to examine fetal TMJ tissues, however one recent study by Ramieri et al (1996), used antisera for PGP 9.5 and S-100 to investigate the innervation of the human TMJ from 9 weeks of gestation to birth.

Nerve fibres immunoreactive to antisera for PGP 9.5, SP and CGRP were located throughout the capsule, synovium and disc in the present study on the sheep. The CGRP- and PGP 9.5-IR fibres in the disc frequently formed interconnecting networks resembling the networks of type IV fibres described by Wyke (1967). CGRP-immunoreactive fibres were not arranged into networks in the capsule. The arrangement of CGRP-immunofluorescent fibres in the fetal capsule appeared to be similar to the arrangement of CGRP-IR fibres (using the immunoperoxidase technique) reported for capsular tissues of adult sheep TMJ (chapter 3 and Tahmasebi-Sarvestani et al, 1996). Substance P-IR fibres in the disc did not form networks and resembled the CGRP- and PGP 9.5-IR fibres in the capsule, but with lower intensity of fluorescence. Thin varicose branches of PGP 9.5-, substance P- and CGRP-immunoreactive fibres resembled free nerve endings, but no encapsulated receptors were located. Furthermore, the pattern of distribution in the disc is different from that of the adult TMJ disc. The disc of the adult sheep TMJ is innervated only in the peripheral part at the site of attachment to the capsule (chapter 3 and Tahmasebi-Sarvestani et al, 1996). These data support the observations by Thilander (1963) that the TMJ disc is innervated during fetal development but at later ages these nerves degenerate and persist only in the peripheral disc. CGRP- and SP-immunoreactivity suggests that these nerve fibres in fetal sheep TMJ disc are sensory, for nociception and perhaps mechanoreception, and might also have a role in regulation of vascular supply to joint tissues through the release of SP and CGRP in joint tissues (Lembeck and Holzer, 1979; Fischer et al, 1983; Pernow, 1983).

While the development of the TMJ in human and sheep fetuses follows a similar sequence, there are differences in the timing of different developmental events. Thus the joint compartments and disc morphology attain an adult appearance during mid to late gestation in the human but still possess an immature appearance near term in the sheep. Similarly, the innervation is different. Ramieri et al (1996), in their study of human TMJ tissues using antisera for PGP 9.5 and S-100, noted a progressive reduction in the number of nerve endings during the last trimester of fetal development. These authors also found encapsulated corpuscular nerve endings at 20 weeks gestation. In contrast, in the present study of the sheep, no encapsulated corpuscles could be found and the innervation of the disc was more extensive in the sheep than in the human (Ramieri et al, 1996) near-term. The development of the innervation in the rat TMJ is even more delayed than in the sheep. Unlike the fetal sheep TMJ disc, there are no CGRP-IR nerve fibres in the TMJ disc of rats at birth but at day 3 postpartum (pp) some CGRP-IR fibres are present in the disc (as free nerve endings) and capsule, where they are associated with blood vessels (Ichikawa et al, 1989). By day 10 pp there are increased numbers of CGRP-IR fibres in the disc and fibrous tissue around the condyle. In tissues including the intervertebral disc, limb joints, and periodontium, the development of encapsulated and nonencapsulated receptors is correlated with changes in function in different tissues. Thus weightbearing postnatally is believed to influence the distribution of encapsulated receptors in intervertebral discs and the mechanical stimuli associated with tooth eruption and occlusion might be necessary for the maturation of Ruffini endings in periodontium postnatally (Malinsky, 1959; Nakakura-Ohshima et al, 1993). Hence it might be that the lack of receptor endings, other than free nerve endings in the TMJ of the late gestation, fetal sheep used in this study, might be a reflection of the anatomical and perhaps functional immaturity of the TMJ, as reflected in the gross and

microscopic appearance of the disc, the inferior joint compartment and articular surface of the condyle at this stage.

In the adult sheep, TMJ adrenergic nerve fibres were demonstrated in the capsule, synovial membrane and peripheral disc (chapter 3 and Tahmasebi-Sarvestani et al, 1996). Nevertheless the distribution of sympathetic efferent fibres, as determined by NPY-IR, in fetal sheep TMJ, is restricted to the capsule. No NPY- or VIP -IR (autonomic) fibres are present in the disc in fetal or adult TMJ of the rat but these fibres are present in the capsule around blood vessels and in some nerve bundles (Ichikawa et al, 1989). Presumably, the NPY-IR fibres in the fetal sheep TMJ have a vasomotor role, and perhaps, like cutaneous tissues, might cause vasodilation within the joint (Lundberg et al, 1982; Ekblad et al, 1984; Hashim and Tadepalli, 1995).

In conclusion, this investigation has shown that while the development of TMJ in human and sheep fetuses follows a similar sequence, there are differences in the timing of neural and morphological development. The capsule, synovial membrane and disc in the TMJ of fetal sheep at 140 days gestation age are innervated with PGP 9.5-, SP- and CGRP-IR (sensory) fibres, while autonomic fibres are located in the capsule only. The findings also support the view that the disc is innervated at an early stage of life but at a later stage the density of innervation in the central part of the disc regresses and the innervation remains only peripherally in the adult TMJ disc.

CHAPTER 5

THE INFLUENCE OF OSTEOARTHRITIS ON THE INNERVATION OF THE SHEEP TEMPOROMANDIBULAR JOINT

5.1 SUMMARY	2
5.2. INTRODUCTION	3
5.3. MATERIALS AND METHODS	4
5.3.1. Animals	4
5.3.2. Surgical procedures	5
5.3.3. Sample collection	6
5.3.4. Immunocytochemistry	7
5.3.4.1. Tissue processing	7
5.3.4.2. Single labelling	8
5.3.4.3. Double- and triple-labelling	8
5.3.5. Quantification and statistical analysis	9
5.4. RESULTS	10
5.4.1. Morphology of osteoarthrotic temporomandibular joint	10
5.4.2. Immunocytochemical observations	11
5.4.2.1. Normal sheep TMJ tissue	11
5.4.2.2. Arthritic joints	12
5.4.3. Quantitative observations	13
5.5. DISCUSSION	15

5.1 SUMMARY

Painful temporomandibular joint (TMJ) is a common clinical problem. The etiology is multifactorial and pain may be a feature of joint overload, joint injury, internal derangement, degeneration and rheumatoid arthritis. The role of the nervous system in this pain mediation has not been studied for the TMJ but has been in other joints. The purpose of this investigation was to study the effect of experimentally induced TMJ osteoarthritis, or non inflammatory degenerative changes, on the innervation of the sheep joint using indirect immunohistochemistry and image analysis quantification.

Bilateral condylar scarification was performed in eight sheep which were killed at 16 weeks postoperation. Tissues from eight osteoarthrotic joints and four normal joints were processed for the immunostaining with antisera for protein gene product 9.5 (PGP 9.5), substance P (SP), calcitonin gene-related peptide (CGRP), neuropeptide Y (NPY), vasoactive intestinal peptide (VIP) and tyrosine hydroxylase (TH). An additional eight joints were decalcified to study the morphological changes induced by the condylar abrasion.

The osteoarthrotic changes were commonly seen in the anterior and lateral regions of the joint and included fibrosis, peripheral osteophyte formation, sub-cortical cysts and erosion of articular surfaces.

In the osteoarthrotic joints the distribution of PGP 9.5-, CGRP- and SP-IR nerve fibres was similar to that observed for normal, control joints in the capsule, synovium and capsule/disc junction. Immunoreactive nerve fibres contained CGRP- and SP- but not VIP-IR in triple staining. No TH-IR could be found in the capsule, synovial membrane or peripheral part of the disc in double staining with NPY antisera. Nerve fibres immunoreactive to either NPY or VIP antisera were mainly found perivascularly in the

anterior part of the capsule. While the density of PGP 9.5-, CGRP- and SP-IR nerve fibres appeared to be decreased in osteoarthrotic joint capsule, compared to the normal joints, this could not be verified with the image analysis data. The general linear model that was used to examine the quantitative data evaluated the influences of side, stain, region, and individual. There were no statistically detectable differences ($P>0.01$) in the % surface area and number of nerve fibres for either PGP 9.5 or CGRP in arthrotic joints compared with normal control joints. The anterior region of the capsule had a significantly greater density of PGP 9.5- and CGRP-IR nerve fibres than other parts of the capsule in both normal and arthrotic joints and the medial capsule was poorly innervated in all joints. Immunostaining for substance P was always weaker.

5.2. INTRODUCTION

The role of the nervous system in joint diseases has become an important focus for arthritis research in the last 5-10 years. Recent developments in immunocytochemical methods have shown that neuropeptides within articular nerves play an important role in the physiology and metabolism of synovial joints both in normal and pathological conditions. Decreased nerve fibre immunoreactivity to antisera for substance P (SP), calcitonin gene-related peptide (CGRP) and protein gene product 9.5 (PGP 9.5) in inflammatory arthritis have been shown in a variety of joint tissues in humans and experimental animals (Grönblad et al, 1988; Konttinen et al, 1990; Mapp et al, 1990; Hukkanen et al, 1991; Konttinen et al, 1992). There are limited, contradictory data available for the influence of osteoarthritis on joint innervation, for example, while degenerative changes associated with collagenase-induced arthritis have been shown to be associated with reduced SP- and CGRP-IR in periosteum and synovium in mouse knee joint (Buma et al, 1992), osteoarthritis did not deplete nerve fibres immunoreactive for SP or CGRP antisera in human synovium (Grönblad et al, 1988).

Degenerative changes associated with osteoarthritis or rheumatoid arthritis are common in TMJ pathology and often feature pain along with disruption of normal joint movements. In order to gain a better understanding of TMJ pathology the Japan/Australia TMJ research group at the University of Adelaide is using the Merino sheep as an experimental model for TMJ dysfunction in humans (Goss et al, 1995). Bosanquet and Goss (1987) used sheep since this species had many advantages compared to other animal models for studying TMJ pathology. Ishimaru and Goss (1992) used mild condylar scarification in sheep TMJ to induce changes characteristic of osteoarthrosis such as fibrosis, osteophyte formation, subcortical-cysts and articular surface erosion. To better understand the pathological processes associated with arthritis of the TMJ there is a need for detailed information on the innervation of TMJ tissues in normal as well as arthritic joints. The observations regarding innervation of the normal adult TMJ in the sheep are presented in chapter 3. The effects of osteoarthritis on the innervation of TMJ are not known. In the present study osteoarthritis was surgically induced in the sheep by mild condylar scarification. The influence of osteoarthrotic changes on the innervation of the TMJ were investigated using immunohistochemistry and image analysis techniques.

5.3. MATERIALS AND METHODS

5.3.1. Animals

The temporomandibular joints of adult male Australian Merino sheep (about 2 years of age and approximately 60 kg in weight) were studied (n=10). All animals were provided by the Gilles Plains Agriculture Research Centre, Adelaide and had been bred specifically for experimental research. Ethical approval for this study was granted by the Animal Ethics Committees of the University of Adelaide and Institute of Medical and Veterinary Science.

The animals were divided into three groups. In group one, two animals were used as a normal control, with no surgical intervention. In group two, four animals were used with bilateral condylar scarification to study the effects of osteoarthritis on joint morphology. In group three, four animals were used with bilateral condylar sacrifice to study the effects of osteoarthritis on nerve fibres in the TMJ (Table 5.1).

Table 5.1. Number of animals, joints and applied procedure.

Group	Sheep	Joints	Procedure
I	2	4	Normal control, with no surgical involvement
II	4	8	Bilateral condylar sacrifice (effects on joint morphology)
III	4	8	Bilateral condylar scarification (effects on joint innervation)
Total	10	20	

5.3.2. Surgical procedures

All surgical procedures were followed as previously described (Bosanquet and Goss, 1987; Ishimaru and Goss, 1992). The sheep to be operated on were fasted (48 h for solid food and 24 h for drinking water) before operation. General anaesthesia was induced with an injection of between 500 and 1,000 mg thiopentone sodium into the external jugular vein and maintained with 3% halothane/O₂/NO₂ through an orotracheal tube. The preauricular area was shaved and prepared with aqueous antiseptics. The field was isolated with sterile drapes. A preauricular incision was made by scalpel blade and the underlying layers were dissected, by dissecting scissors, to the lateral joint capsule. Bleeding was controlled by application of pressure and ligation of vessels. After the lateral joint capsule was exposed,

the inferior joint space was opened carefully by a horizontal incision through the lateral capsule. After the condylar surface was exposed, mild condylar scarification was performed on the superficial condylar surface with scalpel blade and periosteal elevator. The condylar surface was rinsed with normal saline. Then the joint capsule was closed in a single layer and the overlying tissue was repaired with continuous suture using 4/0 Dexon® (Davis and Geck, Inc. , USA) suture. Black silk sutures (3/0) were used to close the skin incision. A broad spectrum antibiotic of 3.0 mg of Vetspen® (Procaine Penicillin, 300 mg/ml; Glaxovet, Glaxo, Australia Pty ®Ltd.) was administered by three intramuscular injections in the rump. The first injection was given prior to surgery. The two subsequent injections were given on the first and second post-operative days, respectively. All the operated sheep were returned to the field three days after surgery.

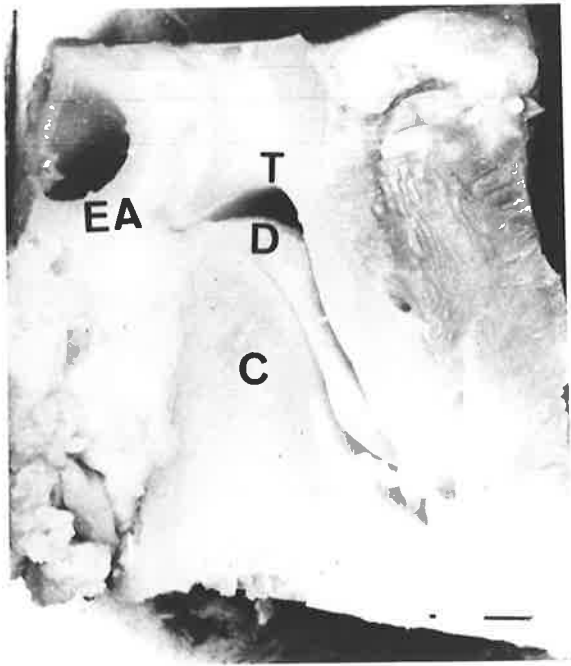
5.3.3. Sample collection

At 120 days following the initial operation, the sheep were reanaesthetized and the TMJ was perfused by an intraarticular injection of Zamboni's fixative (to preserve neuropeptide integrity). Animals were then killed by intravenous overdose of sodium pentobarbitone (Lethabarb, Arnolds of Reading). Immediately, the right and left TMJs were removed 'en bloc' with a band saw and immersed in the same perfused fixative (Zamboni's fixative) for 24 h.

Ten of the joint blocks (two control and eight experimental) were decalcified in a solution containing 9.5% of hydrochloric acid and 1% sodium acetate in saturated ethylenediaminetetracetate (EDTA, Sigma, Australia) for 2 weeks. Prior to decalcification, conventional plain radiographs were used to assess decalcification. Decalcified blocks were sectioned in the sagittal plane into lateral, central, and medial parts (Fig. 5.1). These were then embedded in paraffin, cut at 10µm and stained using haemotoxylin and eosin, Massons

PLATE 28 **A Sagittal Section Of Normal Decalcified
TMJ**

Figure 5.1 Sagittal section of the central part of a decalcified TMJ from a normal adult sheep to show the condyle (C), disc (D), external acoustic meatus (EA) and the temporal fossa (T). Bar: 5mm.



trichrome, alcian blue or van Giesson's method (Drury et al, 1967) for studying the effects of osteoarthritis on the general morphology of the TMJ.

5.3.4. Immunocytochemistry

5.3.4.1. Tissue processing

After fixation, a total of 12 joints (four normal control and eight operated joints) were processed for the indirect immunofluorescence procedure according to Coons et al (1955). For each joint, the disc, capsule and attached synovial membrane were removed intact and divided into anterior, posterior, lateral and medial pieces (Fig. 5.2). These pieces were washed in three changes of 80% ethanol to remove unbound picric acid, and were then cleared in dimethyl sulphoxide (DMSO) before being stored in 0.1mol/l phosphate buffer (PB; pH 7.4) containing 20% sucrose as a cryoprotectant. Pieces of tissue were mounted in tissue tek (Miles Inc, USA) on metal stubs and frozen at -30°C. Cryostat sections (30µm thickness) were mounted on 3-Aminopropyl-Triethoxy-Silane (ATS)-coated slides (Sigma Corporation, Australia) and allowed to dry overnight at room temperature. After treatment with 0.3% Triton-X 100 (Rohmand Haas Co, USA) in PBS, pH 7.4 for thirty minutes, the sections were incubated for 1 h with diluted normal blocking serum which was prepared from the same species in which the secondary antibody was raised.

During immunohistochemical procedures control sections were processed in parallel except that they were incubated in normal serum instead of primary antisera. No immunoreactivity was observed in control sections.

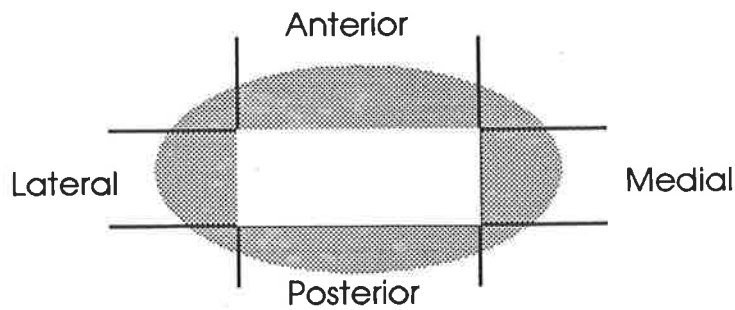


Fig. 5.2. Sample collection from different regions of TMJ disc and attached capsule.

5.3.4.2. Single labelling

For the single labelling method, after the excess serum was blotted, the sections were incubated overnight with antisera for protein gene product 9.5 (PGP 9.5), calcitonin gene-related peptide (CGRP), or substance P (SP) with a dilution of 1:500 in a solution consisting of 1% bovine serum albumen and 0.05% sodium azide in 0.1M PBS. After three washings in PBS for 30 minutes each, the sections were incubated in the dark for 1 h with goat fluoresceine isothiocyanate (FITC)-labeled anti-rabbit IgG (Sigma, USA) diluted to 1:60 in PBS at room temperature. Then the sections were rinsed thoroughly in PBS for 30 minutes and sealed with coverslips using PBS and glycerine. Sections were viewed with an epifluorescence microscope fitted with filters for FITC fluorescence and images were captured and analysed by using the Video-Image analysis system. Some details of the antisera including the immunospecificity of the reaction and cross reactivities are presented in Table 5.2.

5.3.4.3. Double and triple-labelling

In addition to single labelling, double and triple-labelling immunofluorescence (Gibbins, 1990 and 1992) was used to visualize more than one antigen simultaneously in a single tissue section. After preincubation with normal blocking serum, the sections were incubated for 24 h with a mixture of two primary antibodies for double labelling and mixture of three primary antibodies for triple labelling, each raised in a different species

Table 5.2. Primary antibody characteristics.

Antisera	Code N.	Dilution	Host species	Source	References for specificity
PGP 9.5	2582	1/600	rabbit	Ultraclone, Cambridge, UK	Gulbenkian et al (1987)
SP	1657	1/400	rabbit	Hammersmith Hospital	Hökfelt et al (1975)
SP	RMSP-1	1/800	rabbit	R. Murphy	Gibbins & Morris (1987)
CGRP	1204	1/500	rabbit	Hammersmith Hospital	Gibson et al (1984)
CGRP	6006-N	1/2000	rabbit	Peninsula	Kummer et al (1990)
NPY	RMJ263	1/600	rabbit	C. Maccarone and B Jarrot	Morris et al (1986)
TH	LNC-1	1/2000	rabbit	Incstar	Gibbins & Matthew (1996)
VIP	F1/111	1/1000	rabbit	R. Murphy	Morris & Gibbins (1987)

(see Table 5.3 and 5.4). All antibodies were diluted with hypertonic PBS (1.7% NaCl) to reduce nonspecific binding of the antibodies to tissue sections (Grube, 1980). After washing with PBS, the sections were incubated for 1h with two or three species-specific secondary antibodies, which were all raised in donkeys (Jackson Immunoresearch, USA) and were conjugated with 7-amino-4-methylcoumarin-3-acetic acid (AMCA), Dichlorotriazinylamino Fluorescein (DTAF) or Indocarbocyanine (Cy3). These antibodies were also diluted in hypertonic PBS. The sections were viewed with a fluorescence microscope fitted with filters selective for the red fluorescence of Cy3, the green fluorescence of DTAF or the blue fluorescence of AMCA. All images were captured with image analysis and saved in an optic disc.

5.3.5. Quantification and Statistical Analysis

The disc and attached capsule from each of 12 joints (four control and eight arthrotic) was cut into four blocks (anterior, posterior, medial and lateral). Each block was cut into 30 μ m thick sections. From these, three groups of three consecutive sections (9 sections) were randomly selected for immunostaining. Each of these consecutive sections was immunostained with antiserum to one of PGP 9.5, CGRP or SP. The group of three consecutive sections from each block that had the cleanest immunolabelling were selected for quantification. From each section, thirty-two fields (chosen as a manageable number of fields) were systematically sampled by dividing the section into 32 regions and selecting one field of view from the centre of each region at a 10x objective magnification. By using the Video-Image analysis system which included a colour Panasonic camera attached to a BH-2 Olympus microscope, the fluorescent image was analysed using a modified version of the software package, Video Pro 32 (Leading Edge Australia). Immunostained nerve fibres exhibited a bright fluorescence which the Video-image analysis system was programmed to detect. The width and number of nerves as well as the percentage surface area of immunoreactive nerves were recorded.

Table 5.3 Antibody combinations used for double-labelling immunofluorescence.

Primary antibody combination	Secondary antibody combination
Rat anti-SP Rabbit anti-TH	donkey anti-rat-AMCA donkey anti-rabbit-CY3
Rat anti-SP Rabbit anti-VIP	donkey anti-rat-AMCA donkey anti-rabbit-CY3
Rat anti-SP Rabbit anti-NPY	donkey anti-rat-AMCA donkey anti-rabbit-CY3

Table 5.4. Antibody combinations used for triple-labelling immunofluorescence

Primary antibody	Secondary antibody combinations	Primary antibody	Secondary antibody combination
Rabbit anti-VIP	Donkey anti-rabbit-AMCA	Rat anti-VIP	Donkey anti-rabbit-AMCA
Rat anti-SP	Donkey-anti-rat-CY3	Rabbit anti-CGRP	Donkey anti-rat-CY3
Mouse anti-TH	Donkey-anti-mouse-DTAF	Mouse anti-TH	Donkey anti-mouse-DTAF
Rabbit anti-NPY	Donkey anti-rabbit-AMCA	Rabbit anti-PGP 9.5	Donkey anti-rabbit-AMCA
Rat anti-SP	Donkey anti-rat-CY3	Rat anti-SP	Donkey anti-rat-CY3
Mouse anti-TH	Donkey anti-mouse-DTAF	Mouse anti-TH	Donkey anti-mouse-DTAF
Rat anti-SP	Donkey anti-rabbit-AMCA	Rabbit anti-PGP 9.5	Donkey anti-rabbit-AMCA
Rabbit anti-CGRP	Donkey anti-rat-CY3	Rat anti-VIP	Donkey anti-rat-CY3
Mouse anti-TH	Donkey anti-mouse-DTAF	Mouse anti-TH	Donkey anti-mouse-DTAF

A general linear model analysis using program 3V from the BMDP statistical software package (Dixon, 1991) was used to analyse the quantitative results. The general linear model is a variation of an analysis of variance, sometimes called a mixed model of analysis of variance because it has fixed effects and random effects. It uses similar F tests.

The analysis used a random effect for sheep and fixed effects for stain, side region and their interactions. Data were used as actual values or (i) subjected to a square root transformation or (ii) subjected to a log transformation before being analysed by the model. This was to check the robustness of distributional assumptions. The conclusions were identical. A P value of ≤ 0.01 was chosen for determining significance.

5.4. RESULTS

5.4.1. Morphology of osteoarthrotic temporomandibular joint

The articular surfaces of the temporal fossa and the articular condyle of normal, healthy TMJ had a smooth, uniform texture and even margins. The arthrotic joints were characterised by abnormalities mainly in condylar surfaces. Macroscopically, the articulating surface of the glenoid fossa appeared normal (Fig. 5.3b). Erosions and outgrowths were observed on all condylar surfaces, but these deformities were different from one animal to another, even between the left and right joints of the same animal (Fig. 5.3a). Peripheral osteophyte formation, fibrosis and sub-cortical cysts were obvious. The osteoarthrotic changes were commonly seen in the anterior and lateral regions of the condyle (Figs 5.4a, b, c). Only in one joint had these deformities extended into the posterior part of the condyle.

PLATE 29 Articular Surfaces Of The Arthritic TMJ

Figure 5.3 Articular surfaces of the condyle (**a**) and temporal (glenoid) fossa (**b**) from arthritic TMJ. C: condyle; T: temporal (glenoid) fossa. Arrows show erosion of the articular surface. Bars: 5mm (**a**); 2mm (**b**).

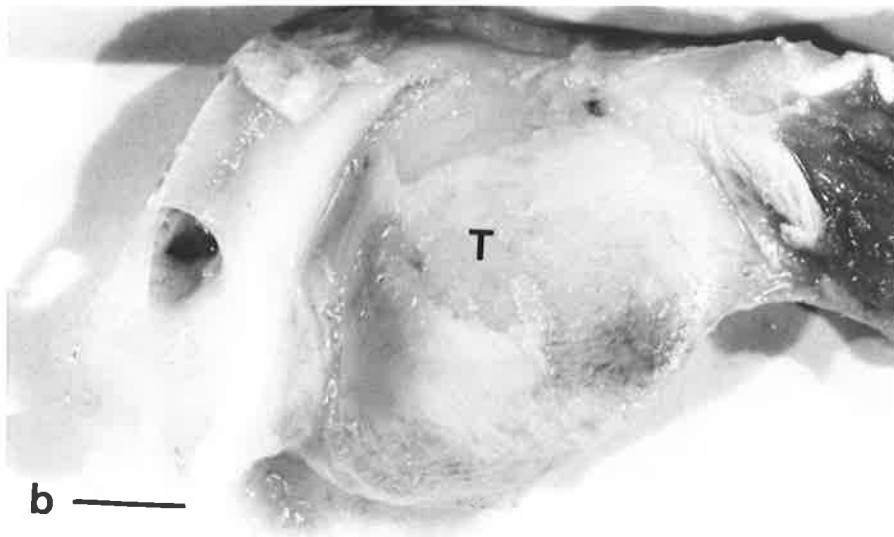
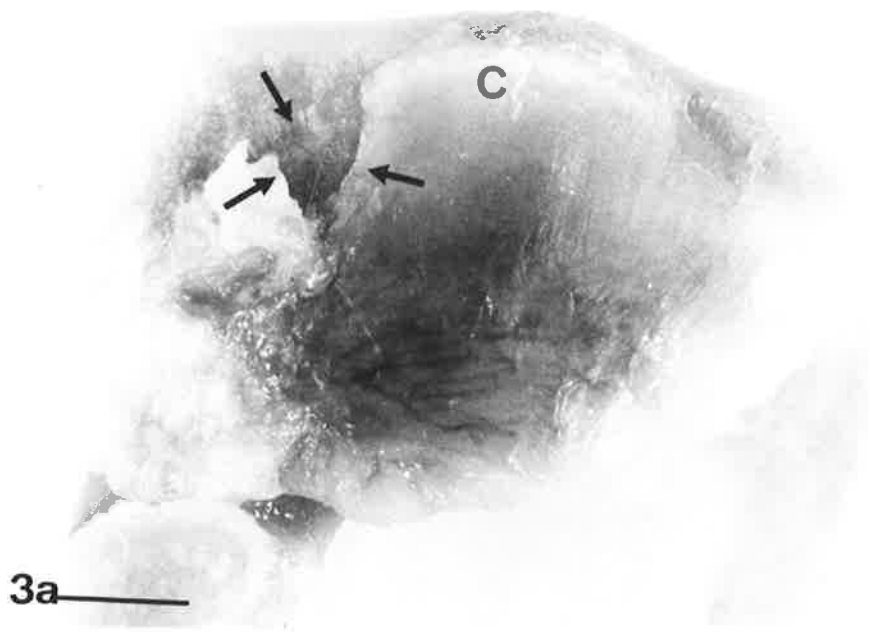


PLATE 30 Articular Surface Of The Arthritic TMJ

Figure 5.4 Lateral (a) and superior (b,c) aspects of the condyle of arthritic TMJ. C: condyle. Arrows indicate areas of sub-cortical cyst and Osteophyte formation of the articular surface. Bar: 2mm.

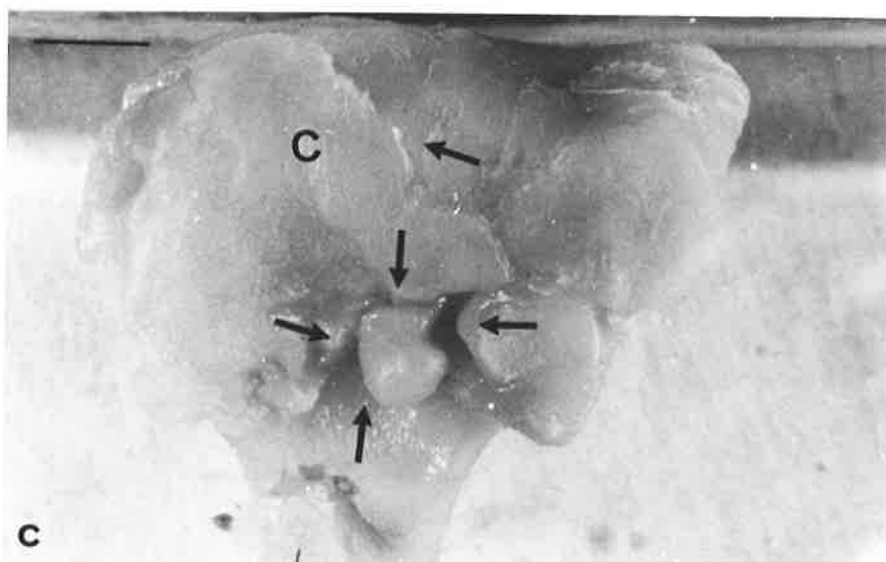
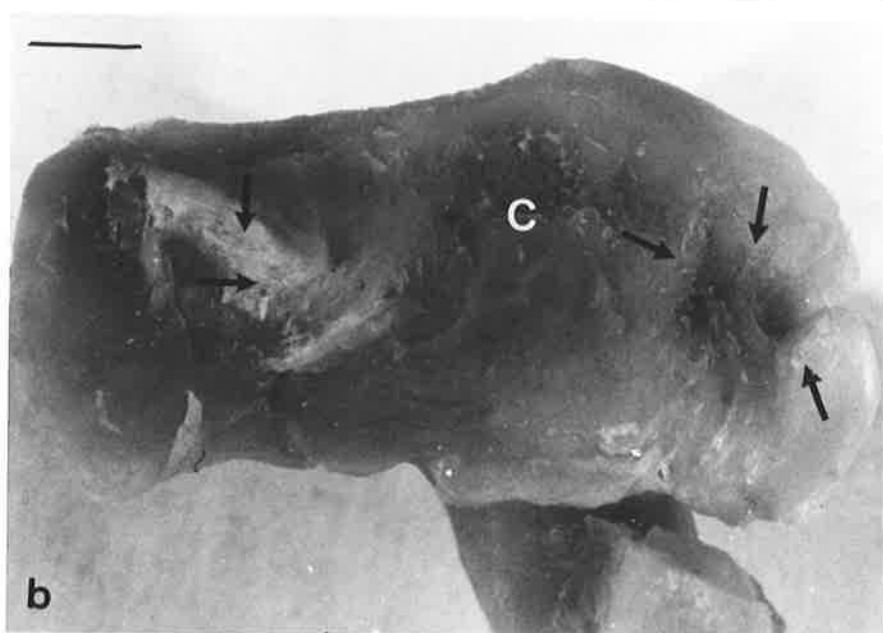
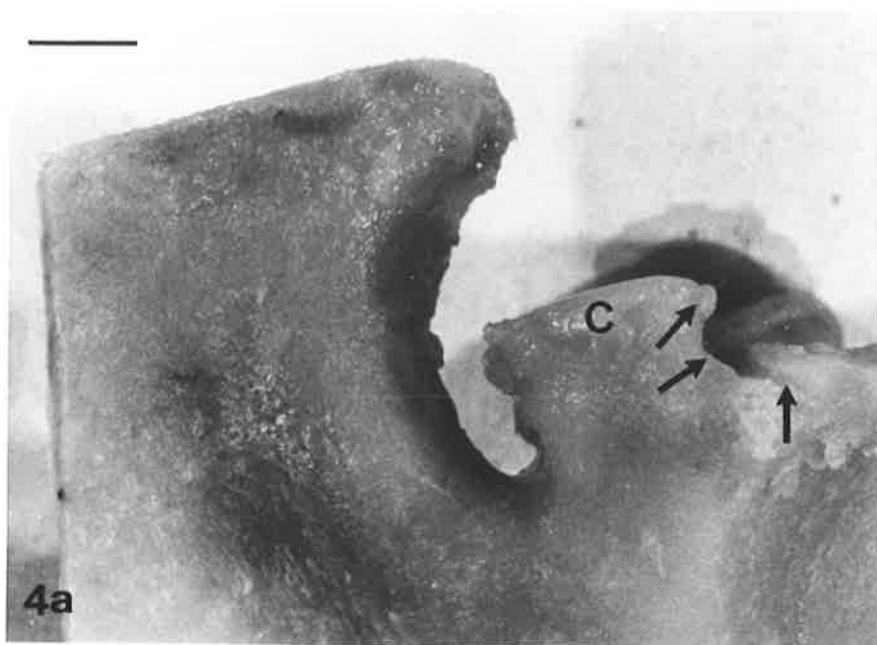
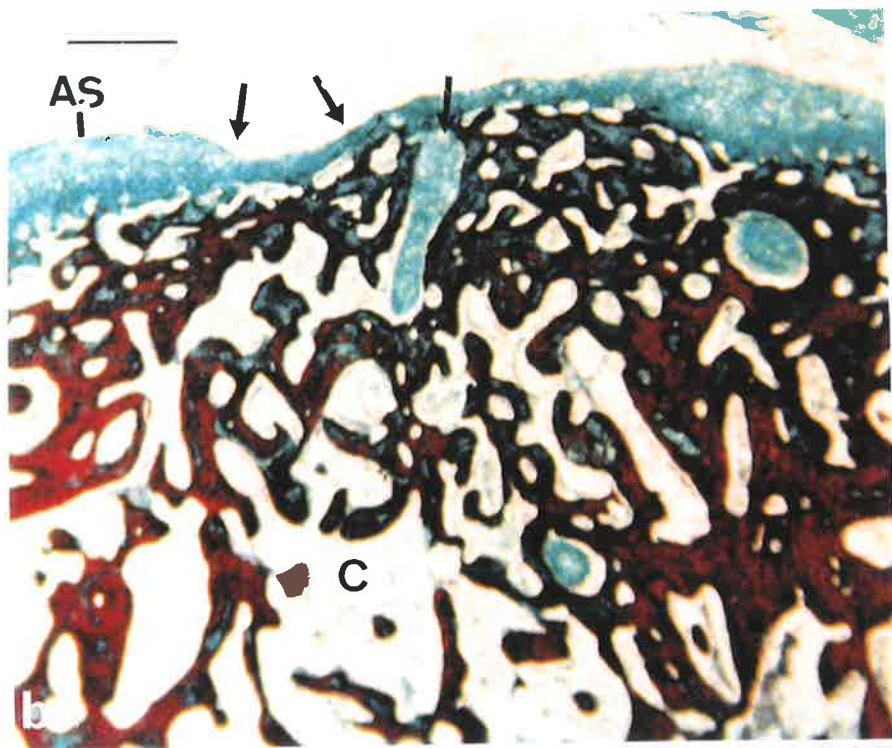
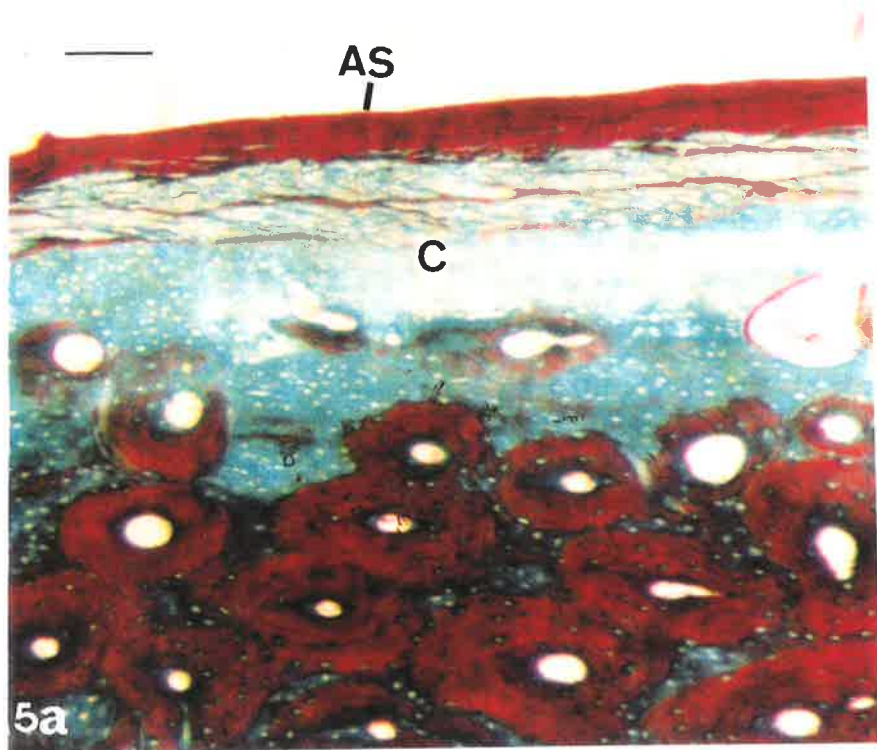


PLATE 31 Histological Sections Of The Normal And Arthritic TMJ

Figure 5.5 Light micrographs of normal (a) and arthritic (b) TMJ stained with Masson's trichrome and Light Green. AS: articular surface; C: condyle. Arrows indicate areas of erosion of the articular surface. Bar: 20 μ m.



Microscopically, fibrosis of bone marrow and trabecular remodelling were obvious (Figs. 5.5a, b). Subcortical cysts were also the common feature in all condylar surfaces (Figs. 5.6a, b, c,d). There was marked proliferation of the synovial connective tissue in the anterolateral parts of two joints, making the joint space narrower (Figs 5.6a, b, c). In one joint the space was completely obliterated by fibrous ankylosis. No disc perforation was present in all joints examined. However, the peripheral parts of the lateral and anterior parts of the discs were either folded or sharply thinned (Figs. 5.7b,c).

5.4.2. Immunocytochemical Observations

5.4.2.1. Normal sheep TMJ tissue

Capsule

In normal control sheep, the anterior part of the TMJ capsule was densely innervated by PGP 9.5- and CGRP-IR nerve fibres. Substance P-IR fibres were less frequently observed. Bundles of PGP 9.5-IR nerves were seen in the deep stroma and joint capsule (Fig. 5.8a,c). Some immunoreactive nerve fibres contained CGRP- and SP- but not VIP-IR in triple staining. No TH-IR could be found in the capsule, in double staining with NPY antisera. Nerve fibres immunoreactive to NPY or VIP antisera were mainly found perivascularly in anterior part of the capsule (Figs 5.9a,b).

Synovium

In the synovium, fibres were located either as plexuses around blood vessels or as free fibres lying parallel to the synovial lining (Fig. 5.9b). Substance P-, CGRP-, and PGP 9.5-IR fibres were often seen immediately beneath the lining synovium, while some fibres even penetrated between the lining synoviocytes. No VIP-, NPY- and TH-IR nerves could be located in the synovium with double and triple labelling methods.

PLATE 32 Histological Sections Of The Arthritic TMJ

Figure 5.6 Light micrographs of arthritic TMJ tissues, showing the degeneration and fragmentation of the articular surface (AS), condyle (C) and the adjacent tissue (a-d). Jc: joint cavity; v: vessel. Arrows indicate areas of chondrocyte proliferation in the lacunae at superficial perforated bone margine of the articular surface (b), peripheral fibrillation of articular surface in (6a,d) and presence of many blood vessels in subsynovial tissue in (e). Bars: 25µm (a); 15µm (b); 10µm (c); 15µm (d) and 20µm (e).

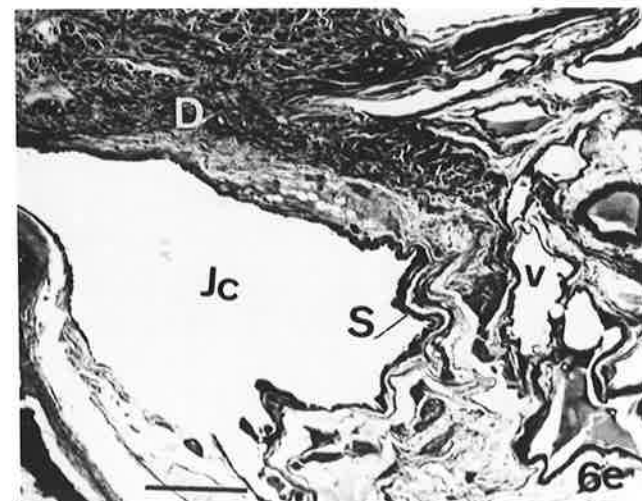
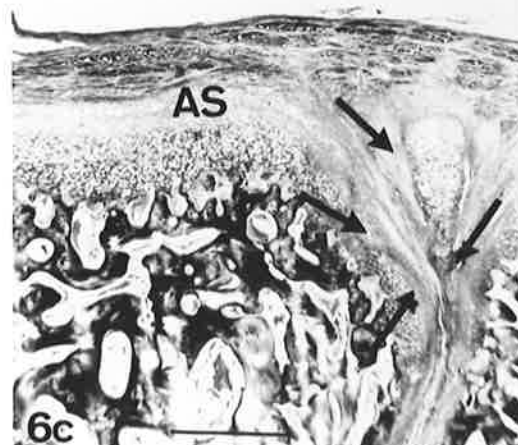
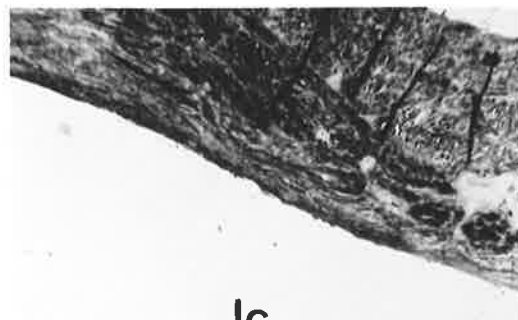
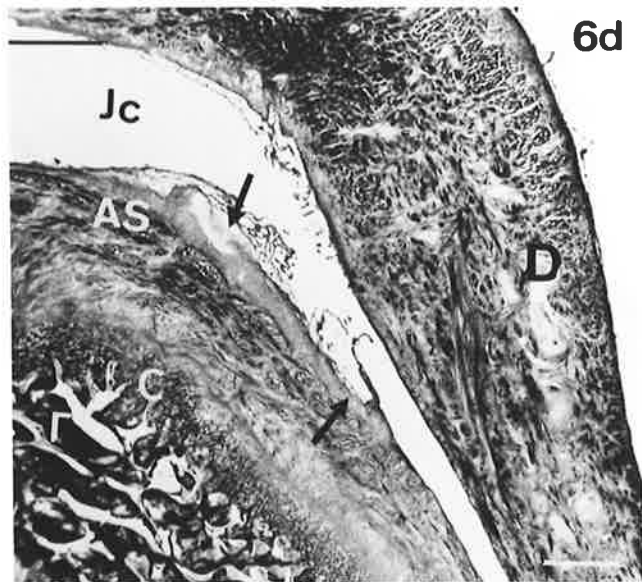
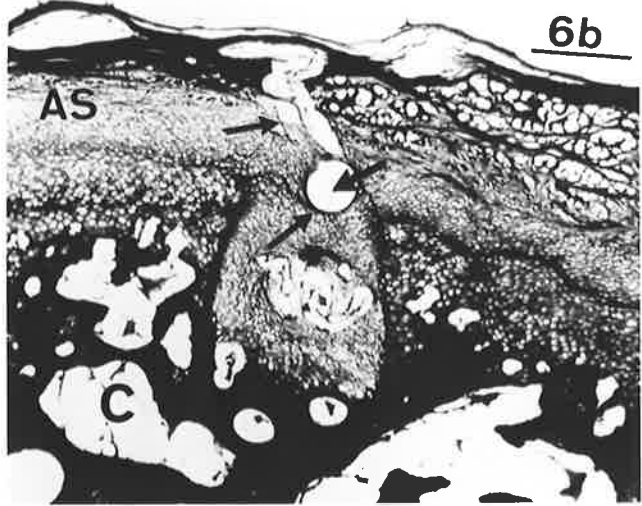
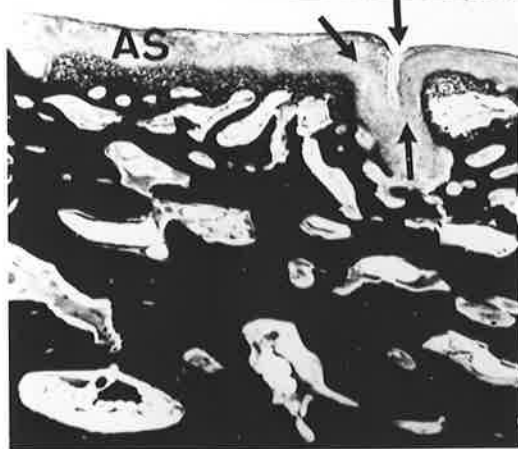
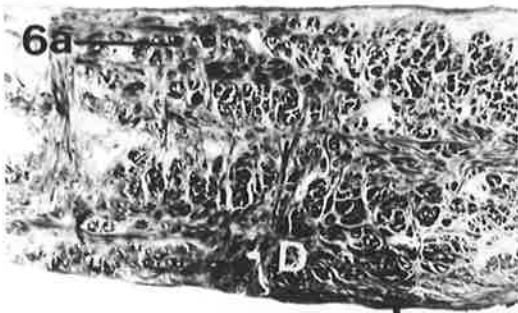


PLATE 33 Histological Sections Of The Normal And Arthritic TMJ

Figure 5.7 Light micrographs of normal histology of the condylar soft tissue layers (a) and arthritic condyle (b,c) stained with Alcian Blue. Articular surface (AS), Proliferative zone of cartilage cells (Ca) and the under layer bone (B) of the condyle. Arrows indicate areas of micro-fracture and lose of the articular surface. Bar: 50µm.

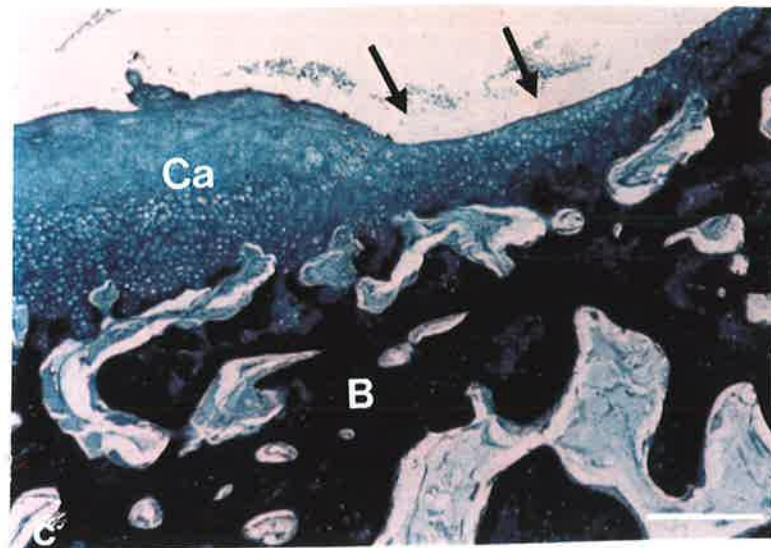
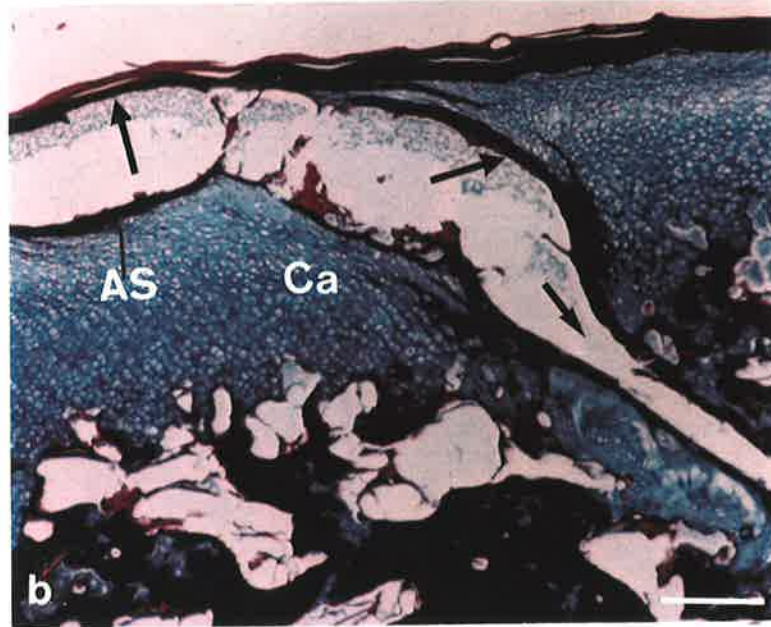
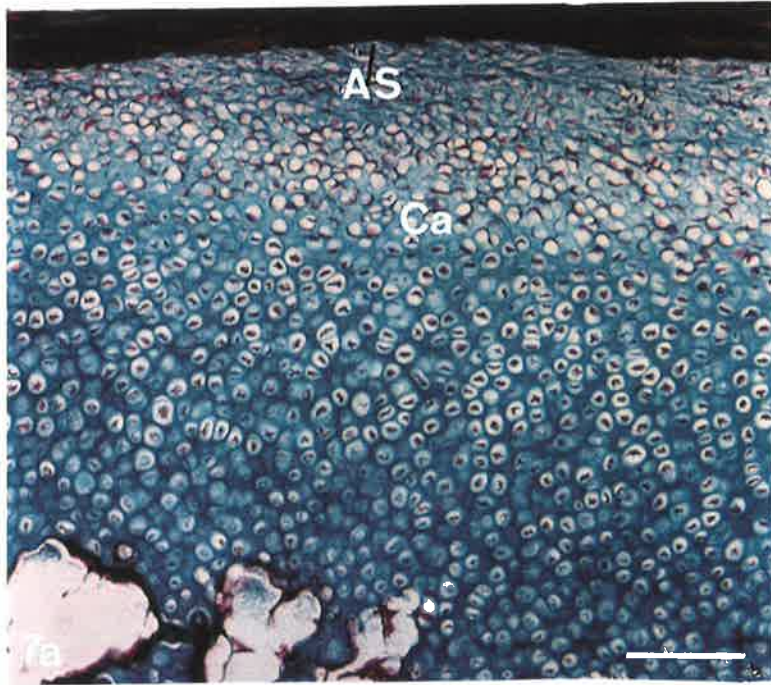
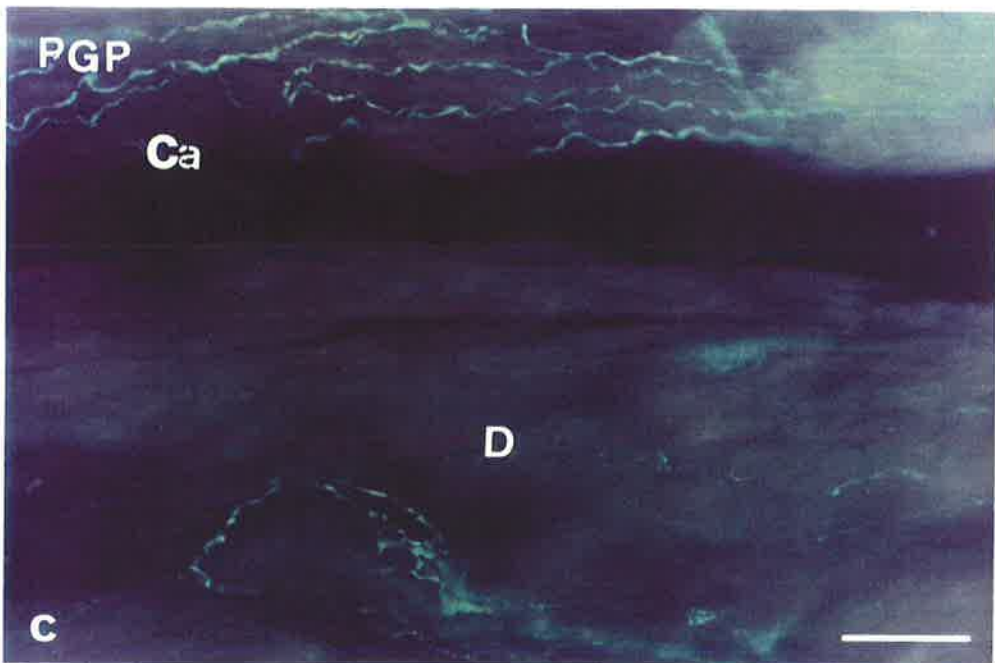
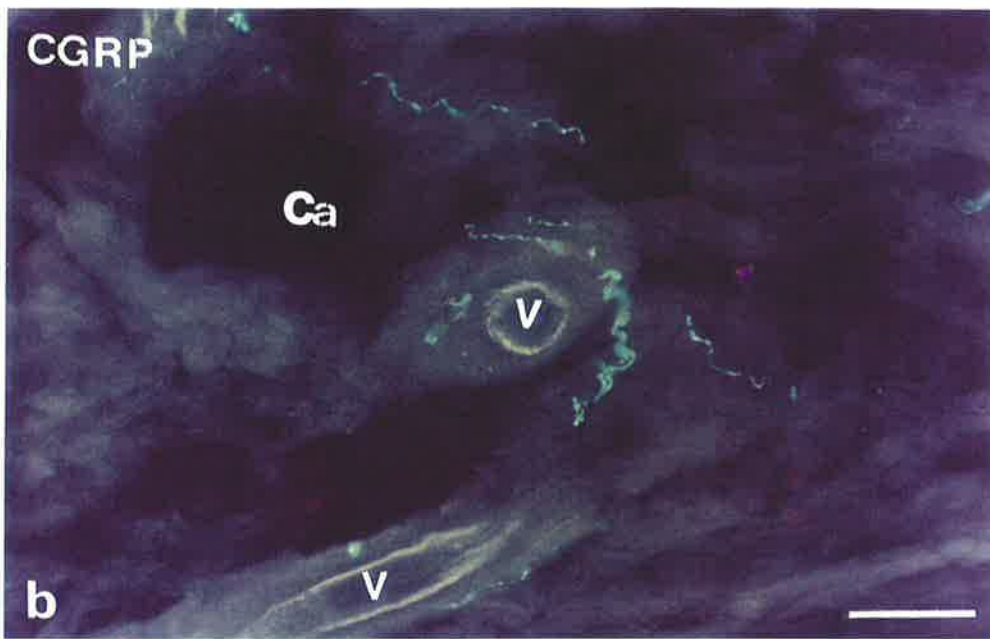
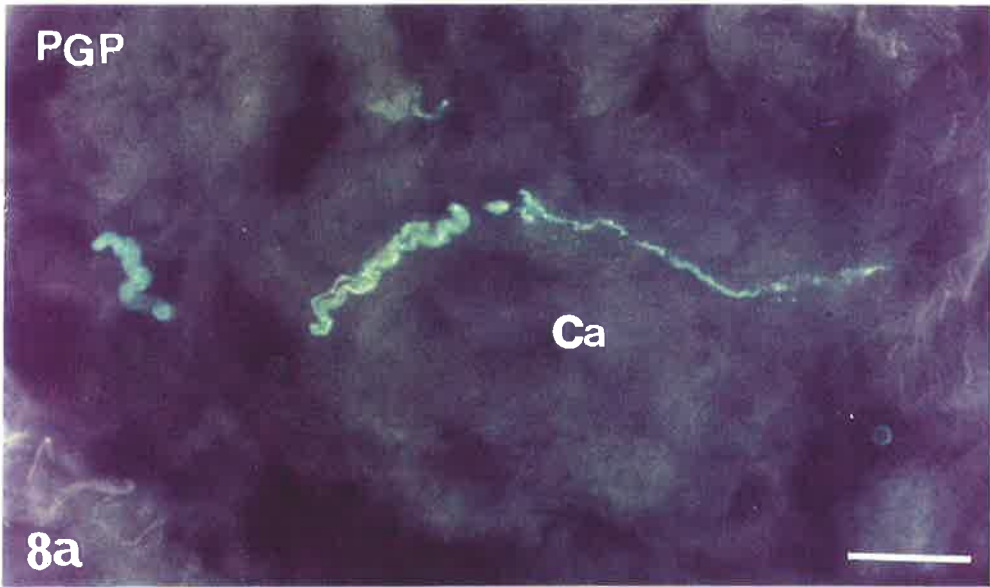


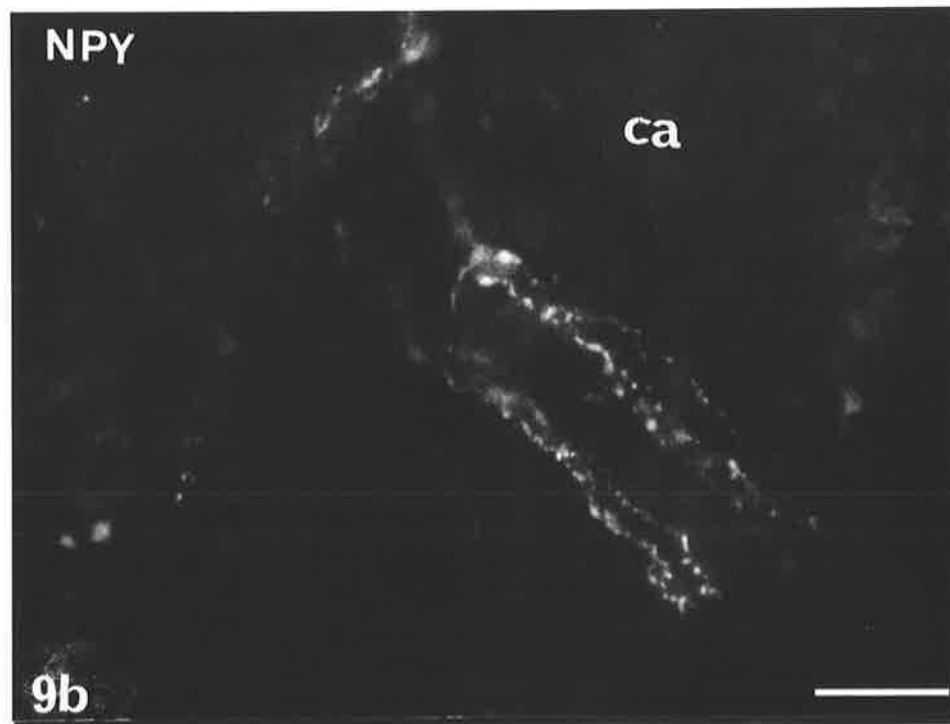
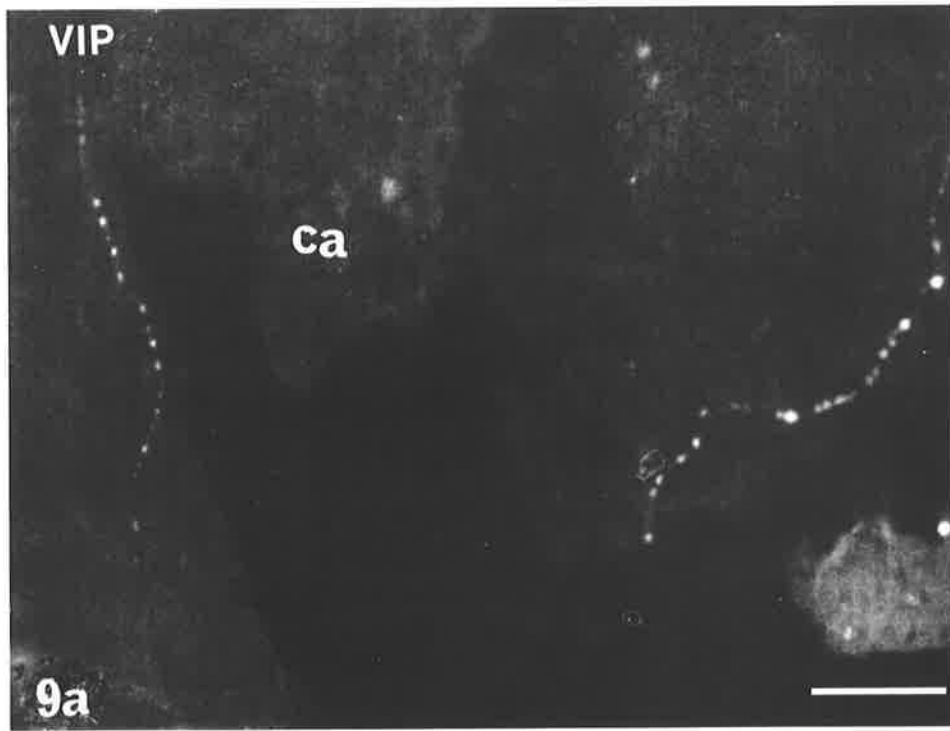
PLATE 34 Immunoreactive Nerve Fibres In Normal TMJ

Figure 5.8 Immunofluorescence micrographs of normal adult TMJ tissues showing PGP 9.5-IR (a,c) and CGRP-IR (b). Ca: capsule; D: disc; V: vessel. Bar: 100 μ m.



**PLATE 35 VIP- and NPY-Immunoreactive Nerve
Fibres In Normal TMJ Capsule**

Figure 5.9 Immunofluorescence micrographs of normal adult TMJ tissues showing VIP-IR (a,) and NPY-IR (b). Ca: capsule. Bar: 20µm.



Disc

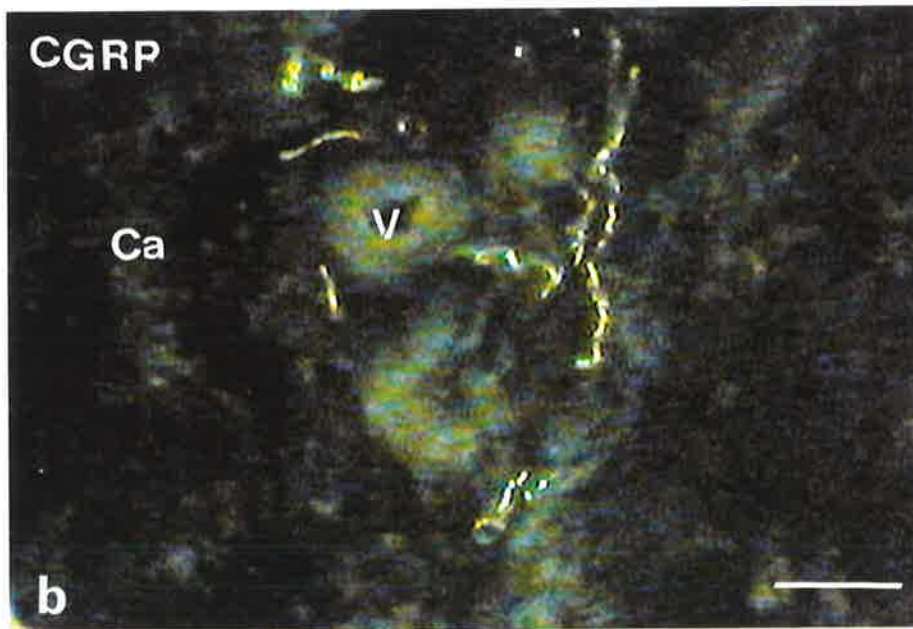
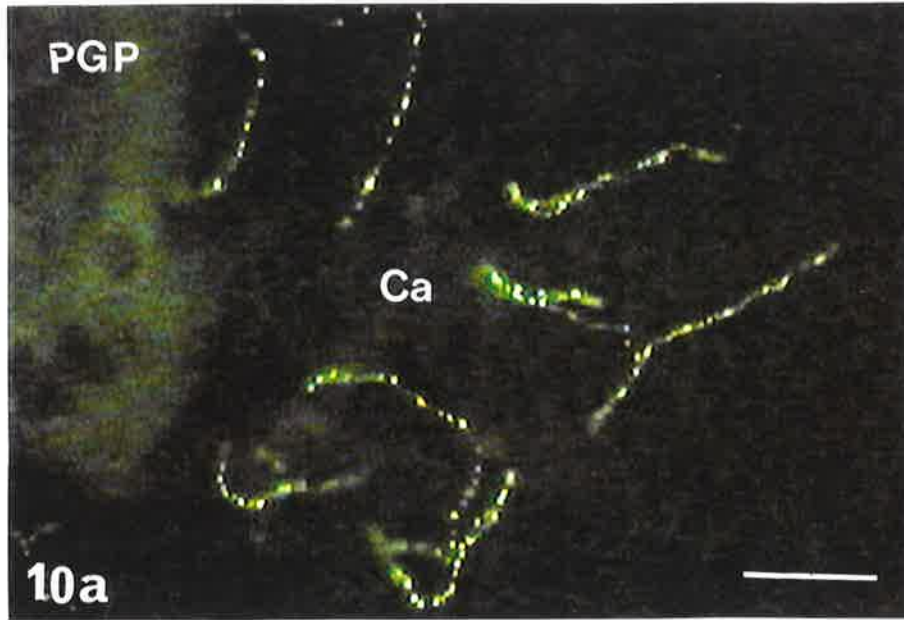
The peridiscal connective tissue was densely innervated. Nerves immunoreactive for PGP 9.5, CGRP and substance P antisera were found in the peripheral part of the disc, at the disc/capsule junction and mainly in the anterior side. Thin varicose fibres were present (see Fig. 5.8c). No TH-, VIP- and NPY-IR could be seen in any parts of the disc.

5.4.2.2. Arthritic joints

Immunoreactivity for PGP 9.5, substance P and CGRP antisera was found consistently in the nerve fibres of anterior, posterior, lateral and to a lesser degree in the medial part of capsule, peripheral disc and synovial tissue of all osteoarthritic TMJs. The anterior part of joint capsule had dense networks, both free and perivascular, of nerve fibres which showed PGP 9.5-, substance P- and CGRP-immunoreactivity. Fibres showing PGP 9.5-IR were predominantly perivascular in their location and exhibited strong immunoreactivity (Figs. 5.10a; 11b,c). Small diameter free nerve endings were seen less frequently and they were generally less strong in their immunoreactivity. Substance P-IR fibres were seen less frequently. Nerve fibres mostly originated from the surrounding connective tissue and terminated at the site of the attachment of the capsule to the disc. The posterior part of the osteoarthritic TMJ capsule had an abundant innervation. Fibres related mostly to the blood vessels. There were some arteries with dense neural plexuses. They appeared to be short and varicose. Veins had fewer fibres (Fig. 5.11a). However, substance P-IR nerve fibres were sparse in this area. The innervation of the lateral part of the osteoarthritic joint was more dense than that in the medial part. In the medial side of the joint the few nerves present showed PGP 9.5- and CGRP-immunoreactivity, and most of these were perivascular. No immunoreactivity for TH antisera could be detected. The distribution pattern of nerve fibres showing immunoreactivity for VIP and NPY antisera resembled that seen for substance P but were found exclusively in perivascular locations. In capsular tissue, numerous CGRP-IR nerve fibres were seen terminating near the insertions of the dense fibrous capsule to the disc (Fig. 5.12b). Nerve fibres, immunoreactive for PGP 9.5 or

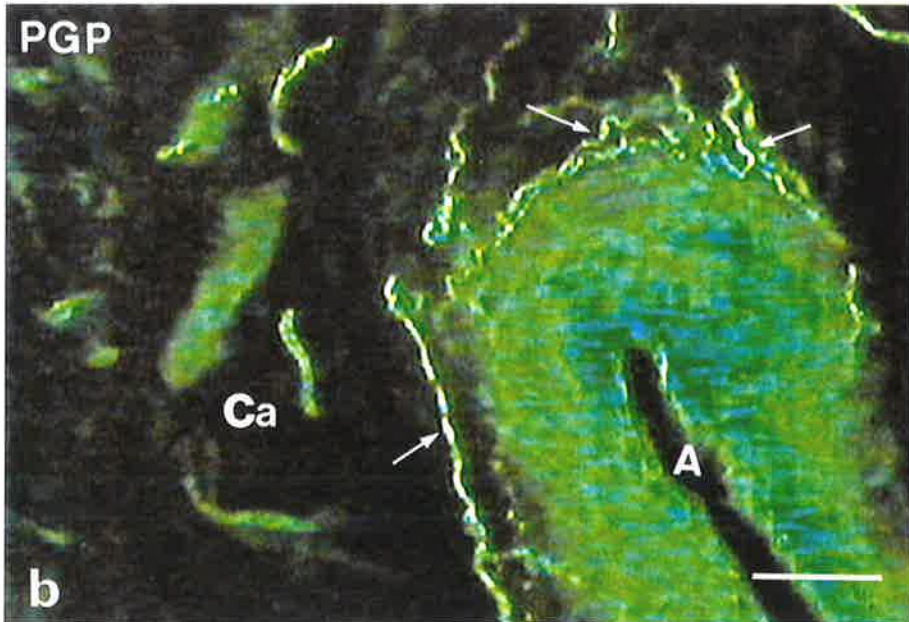
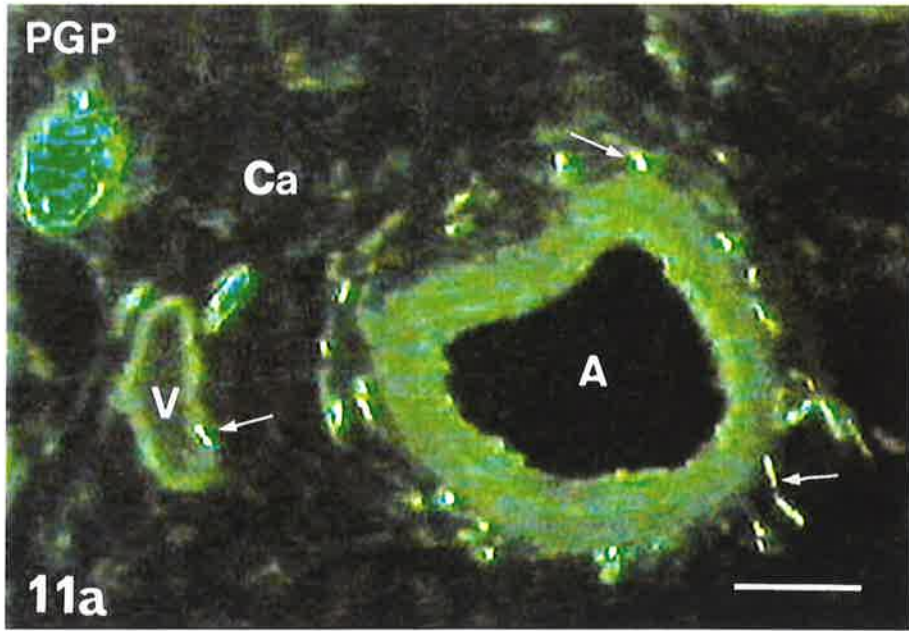
PLATE 36 Immunoreactive Nerve Fibres In Arthritic TMJ

Figure 5.10 Immunofluorescence micrographs of arthritic adult TMJ tissues showing PGP 9.5-IR (a,) and CGRP-IR (b). Ca: capsule; V: vessel. Bar: 20 μ m.



**PLATE 37 Immunoreactive Nerve Fibres In Arthritic
TMJ**

Figure 5.11 Immunofluorescence micrographs of arthritic adult TMJ tissues showing PGP 9.5-IR. Ca: capsule; A: artery V: vein. Arrows indicate nerve fibres accompanying vessels. Bar: 20 μ m.



CGRP antisera, penetrated into the lateral side of the disc in close contact with blood vessels. The synovium had a sparse innervation compared to the capsule and the peripheral disc. Both varicose and non-varicose nerve fibres were observed. Substance P- and CGRP-IR fibres were seen in subintimal synovium and some terminated in between the lining cells (Fig. 5.12a).

There seemed to be fewer nerve fibres in parts of the sheep TMJ that were most affected by the degenerative changes, for example, capsule near osteophytes. In these areas the accumulation of blood vessels and presence of PGP 9.5-IR nerve fibres were seen (Figs. 5.13a, b). The density of PGP 9.5-, CGRP- and SP-IR nerve fibres appeared to be decreased in arthritic joint capsule, compared to the normal joints. Immunoreactive nerve fibres often contained CGRP- and SP- but not VIP-IR in triple staining (Figs 5.14a,b). No TH-IR could be found in the capsule, synovial membrane or peripheral part of the disc in double staining with NPY antisera. Nerve fibres immunoreactive to NPY and VIP antisera were mainly found perivascularly in the anterior part of the capsule.

5.4.3. Quantitative Observations

There were insufficient data to quantify the substance P-immunoreactivities. It was not possible to get sufficient data for a separate quantitative analysis of the synovium so only data for the capsule and synovium are presented together.

Percentage surface area and number of nerve fibres

As a result of the general linear model analysis there were no statistically detectable differences due to joint pathology (arthritis) in % surface area or number of nerve fibres but there were statistically detectable effects due to stain, side and region. Therefore the combined (normal and arthritic) data have been used to estimate the average magnitude of the combination of these statistically significant effects.

PLATE 38 Immunoreactive Nerve Fibres In Arthritic TMJ

Figure 5.12 Immunofluorescence micrographs of arthritic adult TMJ tissues showing CGRP-IR. A: artery; C: capsule; D: disc; JC: joint cavity; S: synovium. Small arrows indicate nerve fibres penetrating the synovium and the larger arrow shows a nerve fibre in the wall of an artery. Bar: 20 μ m.

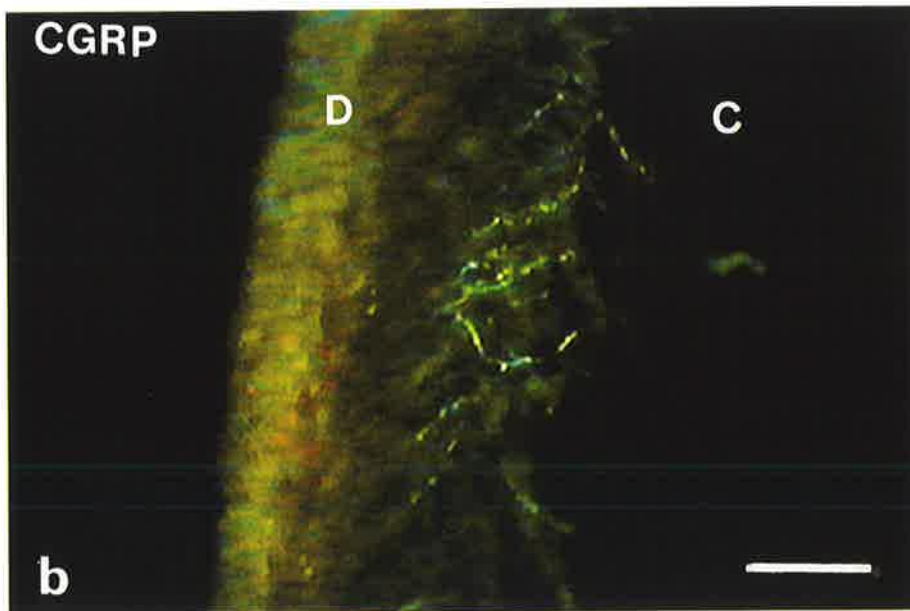
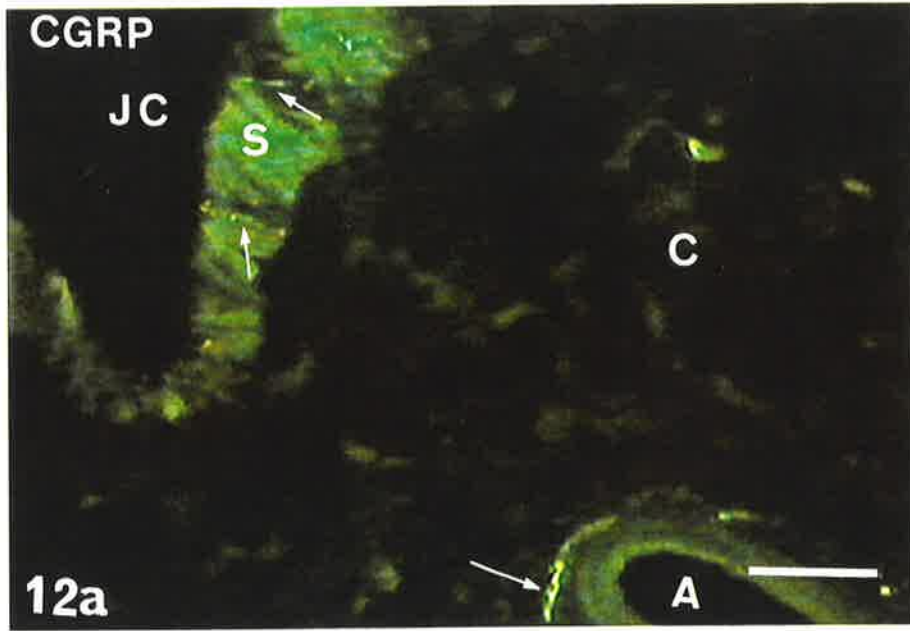
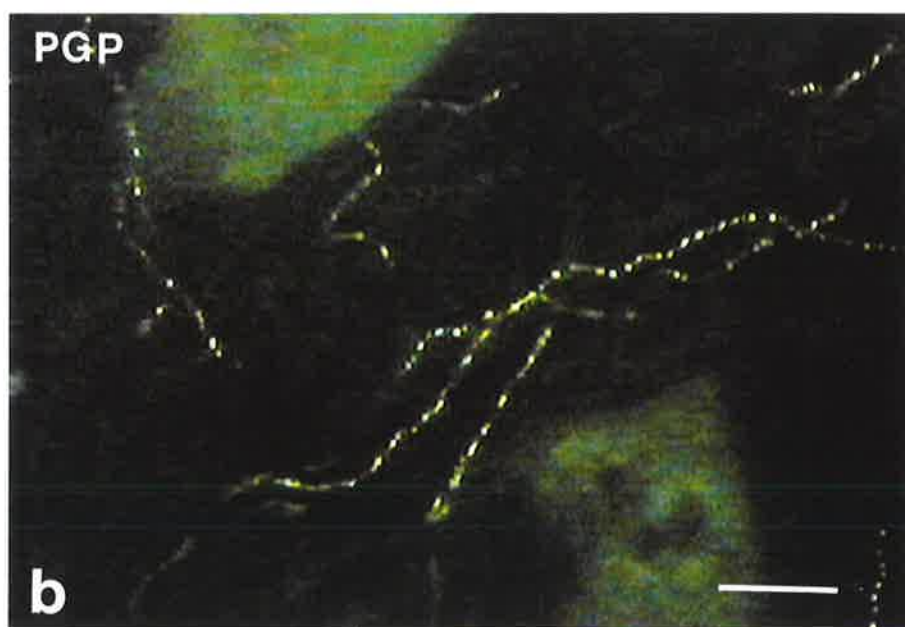
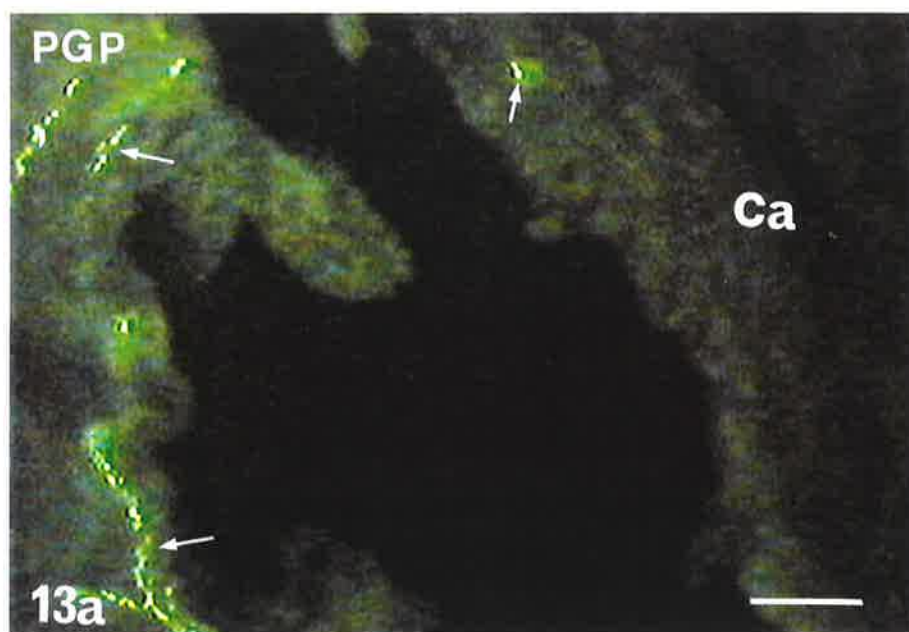


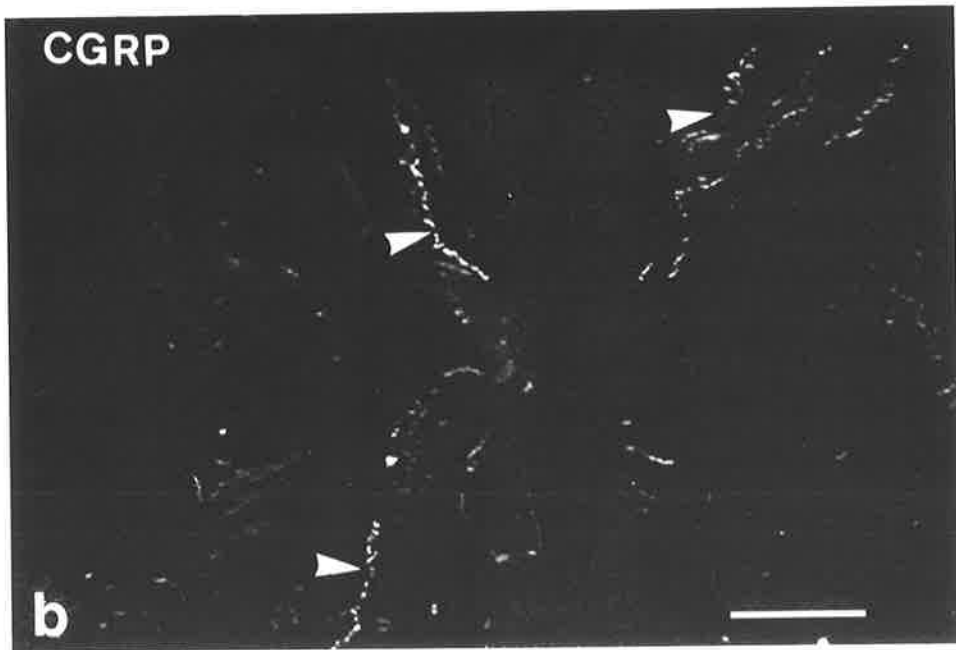
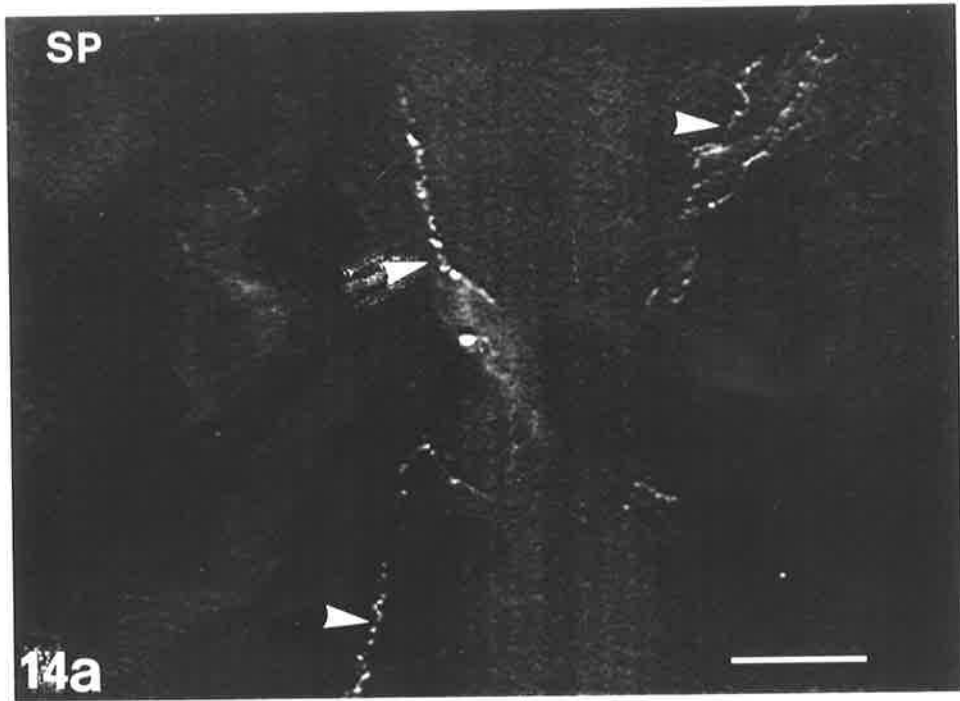
PLATE 39 Immunoreactive Nerve Fibres In Arthritic TMJ

Figure 5.13 Immunofluorescence micrographs of arthritic adult TMJ tissues showing PGP 9.5-IR in capsule near osteophytes. Ca: capsule. Arrows indicate varicose nerve fibres. Bar: 20 μ m.



**PLATE 40 Double Labelling Immunoreactive Nerve
Fibres In Arthritic TMJ**

Figure 5.14 Immunofluorescence micrographs of arthritic adult TMJ tissues showing a section of capsule double labelled with SP antiserum (a) and CGRP antiserum (b). Arrows show nerve fibres immunoreactive to both SP and CGRP antisera. Bar: 20 μ m.



In both normal and arthritic adult TMJ the anterior capsule had the highest density of immunoreactive nerve fibres for both PGP 9.5 and CGRP antisera. The mean percentage surface area and number of immunoreactive nerve fibres for PGP 9.5- and CGRP-IR for anterior, lateral, posterior and medial regions of the capsule (normal TMJ and arthritic TMJ) are shown in Figs. 5.15; 16; 17a, b; 18a, b and Tables 5.5 and 5.6.

There was a side effect in the data for % surface area and number of nerve fibres for PGP 9.5 and CGRP immunoreactivities. Thus the left side had significantly higher values for % surface area and number of nerve fibres than the right side (see Figs. 5.15; 16, 17a,b;18; a, b and Tables 5.5 and 5.6).

There was also a stain effect in the data for % surface area and number of nerve fibres. Hence, values for % surface area and number of nerve fibres for PGP 9.5-immunoreactivity were higher than those for CGRP-immunoreactivity (see Tables 5.5 and 5.6).

Width of nerve fibres

No statistically detectable differences could be found using the general linear model to examine nerve fibre width, so all data were combined to provide a mean width of 5.07 μ m with a standard error of the mean of 0.14 (231 measurements). The distribution of nerve fibre widths showed that 72% of nerve fibres were less than 6 μ m in width and 12% were less than 2 μ m in width (see Fig. 5.19).

CHAPTER 5

Table 5 5. Mean percentage surface area (plus standard error) for all adults (normal and arthritic data combined).

Side	Left	Left	Right	Right
Region	PGP 9.5	CGRP	PGP 9.4	CGRP
Anterior	0.417 (0.036)	0.349 (0.037)	0.314 (0.036)	0.246 (0.037)
Posterior	0.214 (0.037)	0.146 (0.037)	0.111 (0.037)	0.044 (0.038)
Lateral	0.238 (0.037)	0.171 (0.039)	0.136 (0.039)	0.068 (0.042)
Medial	0.167 (0.038)	0.099 (0.041)	0.064 (0.041)	No data

Table 5.6. Mean number of nerve fibres (plus standard error) for all adults (normal and arthritic data combined).

Side	Left	Left	Right	Right
Region	PGP 9.5	CGRP	PGP 9.4	CGRP
Anterior	0.662 (0.060)	0.533 (0.062)	0.488 (0.59)	0.358 (0.062)
Posterior	0.371 (0.061)	0.242 (0.062)	0.196 (0.062)	0.067 (0.063)
Lateral	0.501 (0.061)	0.371 (0.065)	0.326 (0.065)	0.197 (0.069)
Medial	0.302 (0.063)	0.172 (0.068)	0.127 (0.068)	No data

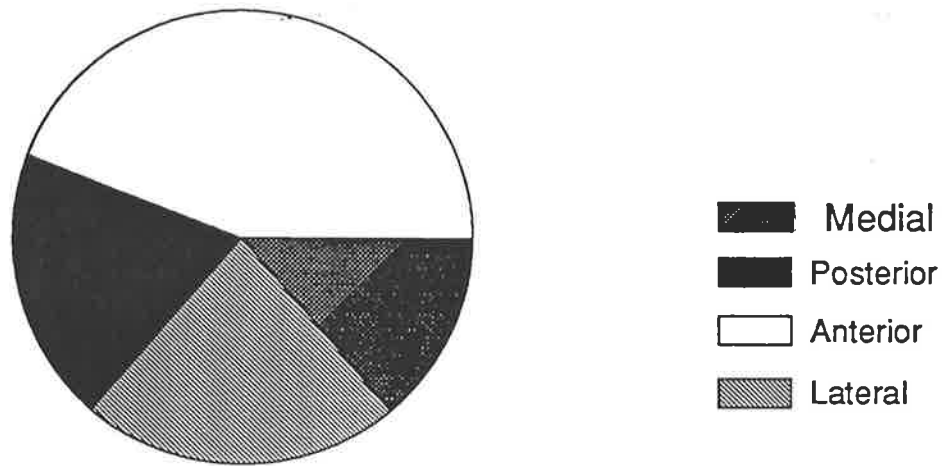


Figure 5.15 Relative distribution of nerve fibres showing PGP 9.5-IR in different regions of the capsule of TMJ in adult sheep (normal and arthritic data combined).

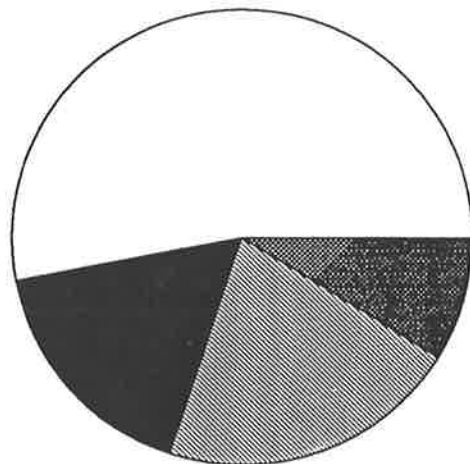


Figure 5.16 Relative distribution of nerve fibres showing CGRP-IR in different regions of the capsule of TMJ in adult sheep (normal and arthritic data combined).

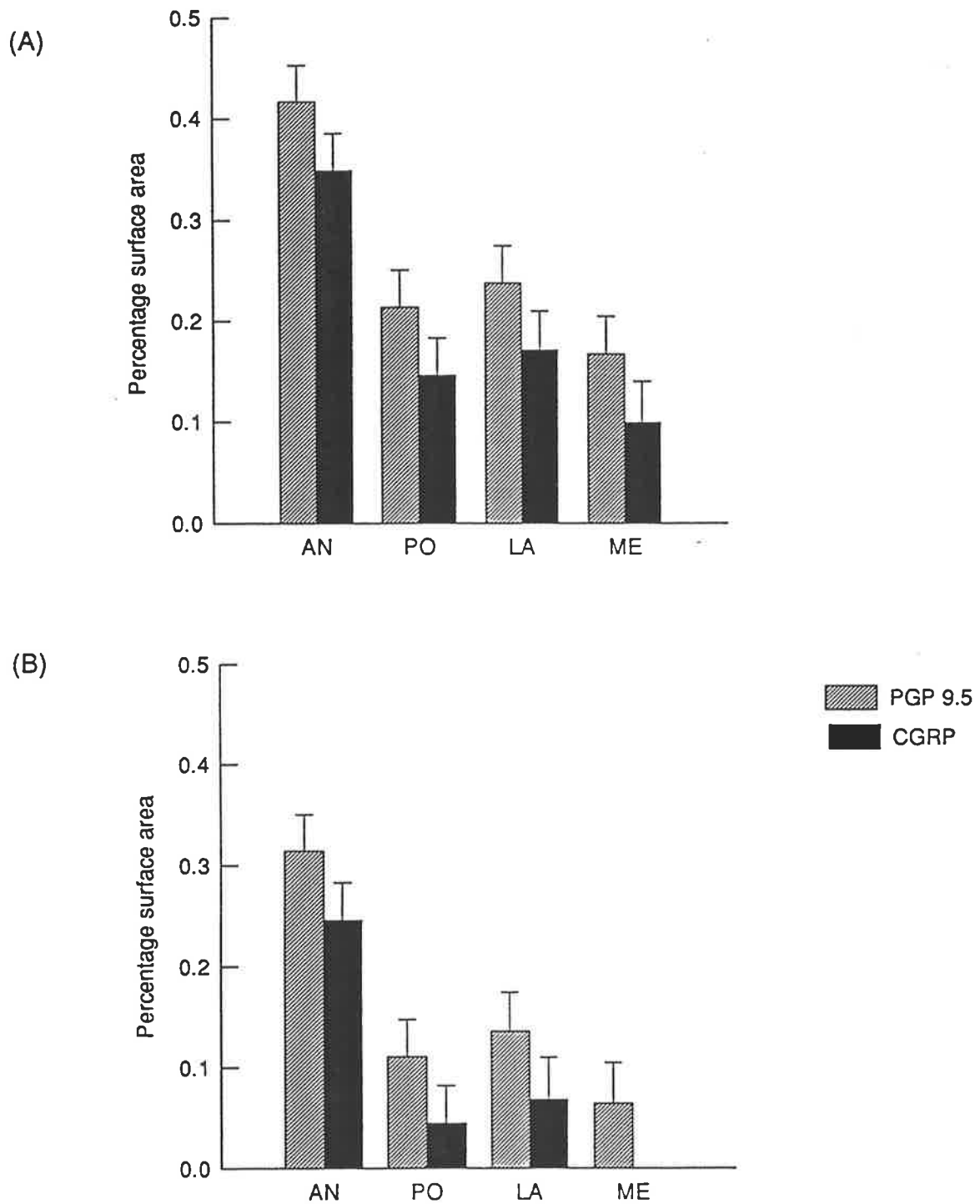
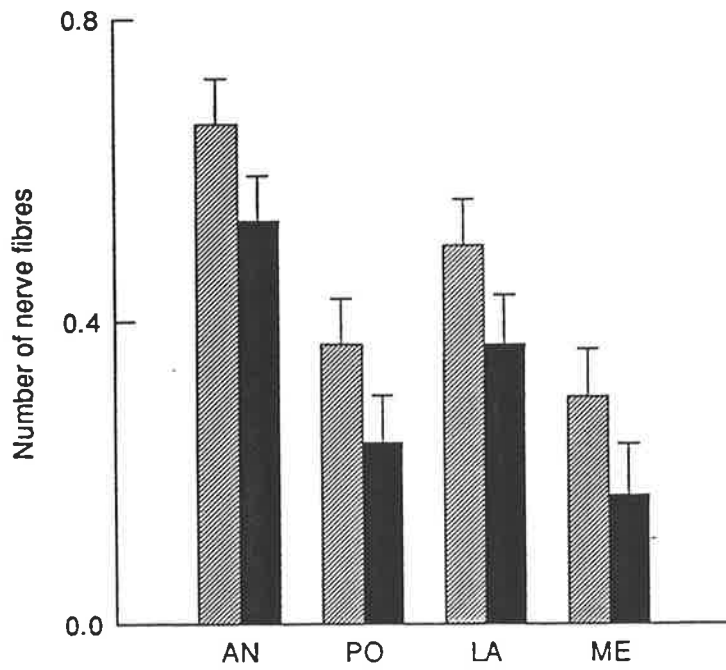


Figure 5.17 Mean plus standard error (SE) percentage surface area in capsule of TMJ of adult sheep (normal and arthritic data combined). A: left, B: right. AN: anterior, PO: posterior, LA: lateral, ME: medial.

(A)



(B)

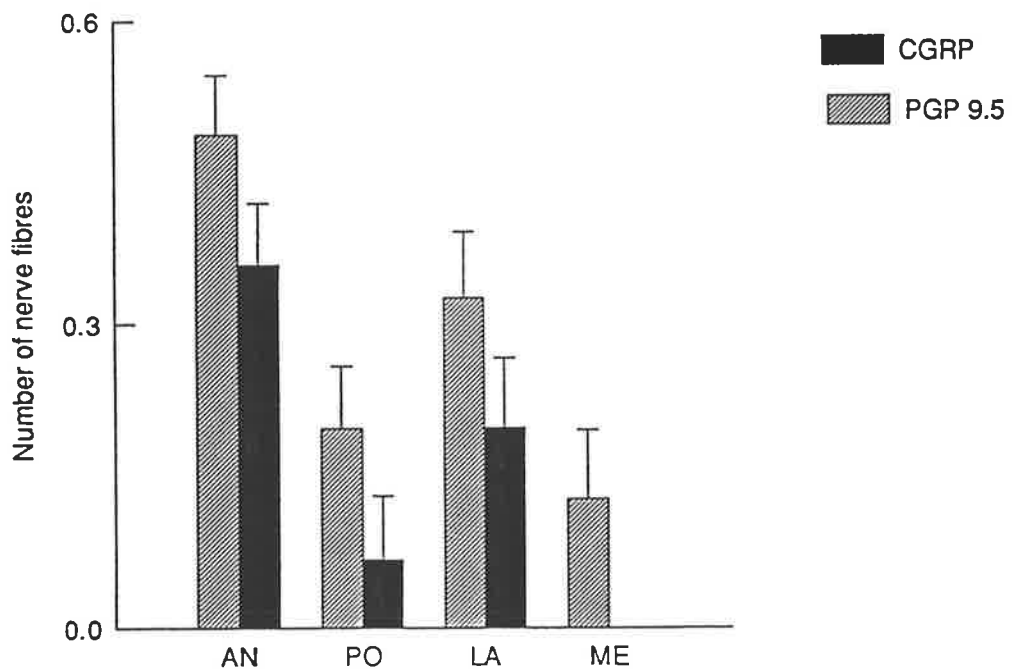


Figure 5.18 Mean plus standard error (SE) number of nerve fibres in capsule of TMJ of adult sheep (normal and arthritic data combined). A: left, B: right. AN: anterior, PO: posterior, LA: lateral, ME: medial.

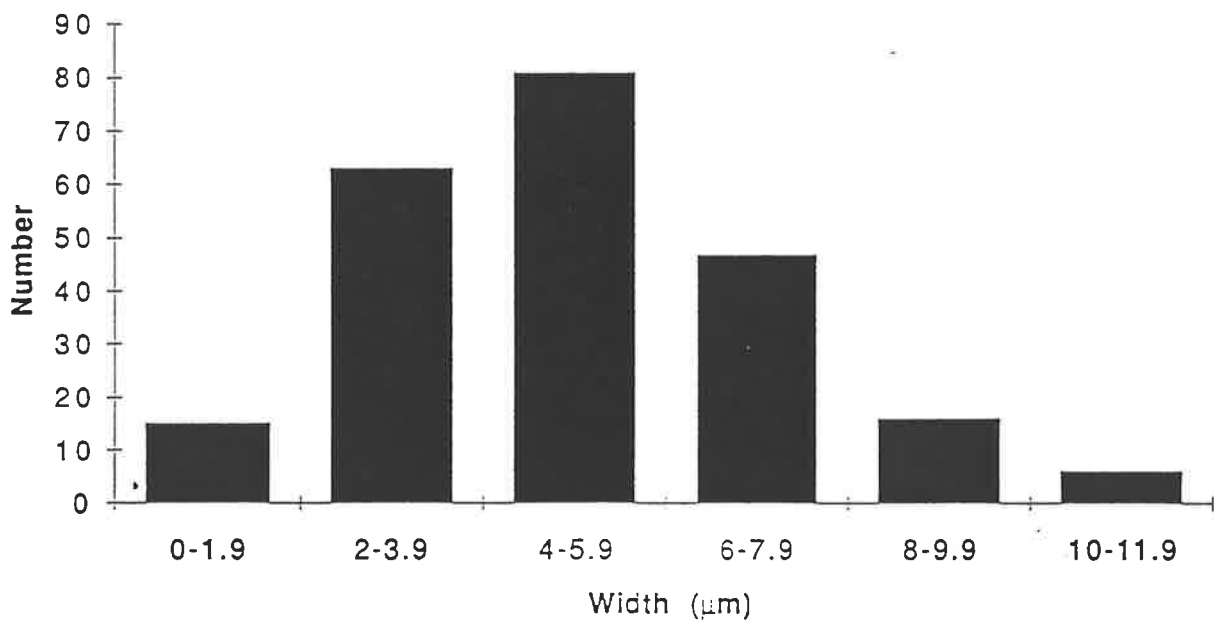


Figure 5.19 Widths of nerves in capsule of TMJ of adult sheep (normal and arthritic data combined).

5.5. DISCUSSION

Many studies have induced osteoarthritis in animal models and only a few have used the TMJ (Ishimaru et al, 1991; Ishimaru and Goss, 1992). Silbermann (1976) used mice to study the osteoarthritic changes in TMJ by an intraarticular injection of steroid. Others like Merjersjo (1984) used the guinea pig to induce osteoarthritis. Yaillen et al (1979) and Helmy et al (1988) both used surgical methods to study osteoarthritic changes in monkey TMJ and finally Bosanquet et al (1991a) used sheep since this species had many advantages compared to other animal models for studying TMJ pathology.

Degenerative changes associated with osteoarthritis are common in human TMJ pathology and often involve pain as well as disruption of normal joint congruity and normal joint movements (Blackwood, 1962; Ogus, 1975). Synovial inflammation, fibrosis, osteophyte formation and various cytoskeletal changes are features of these diseases (Kreutziger and Mahan, 1975). The osteoarthritic-type changes described in the present study (fibrosis, osteophyte formation and subcortical-cysts) resembled the changes reported by Ishimaru and Goss (1992) using the same technique of mild condylar scarification in sheep. In both studies there were variations in the severity of these degenerative changes in different joints.

In the present study qualitative assessments of the effect of experimentally-induced degenerative joint disease (osteoarthritis) on the sheep TMJ suggested that the density of nerve fibres immunoreactive to antisera for PGP 9.5, CGRP and SP was less in the arthritic TMJ capsule than in the normal capsule. In addition, there seemed to be fewer nerve fibres in parts of the sheep TMJ that were most affected by the degenerative changes, for example, capsule near osteophytes. Nevertheless, the general linear model used to analyse the quantitative data was not able to detect any statistically significant effect of arthritis on the % surface areas or numbers of PGP 9.5-, or CGRP-IR nerve fibres in TMJ capsule.

There was a suggestion of a minor decrease in mean % surface areas and numbers of nerve fibres in the arthritic tissues, but the standard errors were too large for statistical significance.

Few comparable data are available for the effects of arthritis on peripheral nerve fibres. Appelgren et al (1991) found levels of SP-, CGRP-, NKA- and NPY-IR higher in human TMJ synovial fluid than from patients with rheumatoid arthritis (RA). Knee joints from patients with rheumatoid arthritis have significantly higher levels of NPY- and CGRP-IR than normal healthy joints (Holmlund et al, 1991). In the same study Holmlund et al (1991) found no differences between the levels of SP-, CGRP-, NPY-, NKA-IR in TM joint fluid from normal, osteoarthritic and mild RA patients, but the levels of these peptides were higher than those in arthritic knee joints. These authors interpreted this to indicate that the TMJ has more dense peptidergic innervation than the knee joints. Inflamed joints (rheumatoid arthritis) contain higher levels of SP and CGRP than synovial fluid from osteoarthritic patients (Hernanz et al, 1993). Menkes et al (1993) reported levels of SP-IR in synovial fluid from patients with rheumatoid arthritis 5 times that in fluid from patients with osteoarthritis (OA). The SP-IR levels in the RA synovium were less than those of OA synovium. These results confirmed a role of SP in joint inflammation and further supported the contention that active secretion of SP into the synovial fluid in the inflamed tissue depletes the SP in the nerve fibres (Menkes et al, 1993).

Support for a role of the sympathetic nerves in arthritis was shown by Ahmed et al (1995) in which there were increased levels of NPY-IR in ankle joint synovium of adjuvant-induced arthritic rats. Lundeberg et al (1996) recorded an increase in the levels of SP, CGRP, NKA and NPY in TMJ fluid of humans bilaterally, following unilateral injection of carrageenan which induced cartilage changes similar to osteoarthritis in humans as well as inflammation. This was interpreted to indicate that carrageenan-induced osteoarthritis activates both sensory and sympathetic nervous systems in the TMJ (Lundeberg et al,

1996). Collagenase-induced osteoarthritis in mouse knee joint was characterised by sclerosis of the subchondral bone, osteophyte formation, synovial proliferation and cartilage abrasion (Buma et al, 1992). While no differences could be found in the innervation of joint capsule and medullary cavity in normal and arthritic joints, at locations where arthritic changes were severe, for example, the periosteum at some locations, and in the synovium, the innervation was depleted (Buma et al, 1992). Grönblad et al (1988) found no difference in the density of nerve fibres immunoreactive to SP and CGRP in the synovium of human patients with normal or osteoarthritic joints, but noted a decrease in IR for these antisera in synovium from rheumatoid (inflammatory) arthritis. Hukkanen et al (1991; 1992a) observed a depletion of nerves immunoreactive for antisera to PGP 9.5, SP and CGRP in the synovium of rat ankle joints with severe adjuvant-induced polyarthritis (inflammatory arthritis). Rheumatoid human synovium from knees and metatarsophalangeal joints have a reduced innervation as determined by PGP 9.5-, SP-, CGRP- and NPY/C-PON-immunoreactivity, compared to normal synovia (Pereira da Silva and Carmo-Fonseca, 1990). Similarly, Kontinen et al (1990; 1992) noted that nerves immunostained by antisera to PGP 9.5, SP and CGRP were depleted in inflammatory arthritic synovium compared to normal synovium and Mapp et al (1989; 1990) noted decreased density of perivascular fibres and weaker immunostaining for PGP 9.5, SP, CGRP and C-PON antisera in arthritic rats compared to normal synovia.

The limited data suggest that while inflammatory arthritis has a marked influence on the density of sensory and autonomic nerve fibres in synovium, the influences on other areas of the joint are not clear. Osteoarthritis may induce some changes in the synovium innervation but this is not consistent in the various studies reviewed. Hence the data presented in this work are consistent with data reported in the literature. If the methodology could be improved to separate the data for the synovium from the deeper capsule, then it might be possible to show a difference in the effect of osteoarthritis on the sheep TMJ.

Antisera for substance P and CGRP have been used to localise sensory nerve fibres in adult TMJ tissues from rats (Ichikawa et al, 1989; Kido et al, 1993), monkey (Johansson et al, 1986), and sheep (Chapter 3). Antiserum for PGP 9.5 (a neuron-specific protein) has been used in many studies to detect sensory and autonomic fibres, small nerve endings and corpuscles in a variety of tissues including the TMJ (Ramieri et al, 1990; Morani et al, 1994). In the sheep TMJ capsule from normal and arthritic animals, more nerve fibres were revealed by PGP 9.5-immunoreactivity than by CGRP-immunoreactivity. It is likely therefore that the additional nerve fibres stained by PGP 9.5 antiserum compared to the CGRP antiserum are autonomic fibres. The review by Schaible and Grubb (1993) showed that 80% of articular nerves are unmyelinated and that 50% of these are sympathetic efferent fibres. Large nerve bundles (branches of the masseteric nerve) innervating the TMJ of the sheep do not contain autonomic nerve fibres (Chapter 3). Schmid (1969) found that autonomic nerve fibers (a branch of the otic ganglion) entered the medial side of the capsule in the human TMJ. He presumed that sympathetic fibres came from a sympathetic plexus of the internal maxillary artery that joined the otic ganglion. Autonomic nerve fibres characteristically form plexuses in the walls of arteries and accompany arterioles and capillaries in joint capsules as well as forming plexuses separate from vessels in the capsule and synovial membrane (Chapter 3). A retrograde tracing study by Widenfalk and Wiberg (1990) revealed an "impressive" number of sympathetic efferents to the TMJ, in the rat, originating from the superior cervical ganglion. These authors hypothesised that nociceptive input from the TMJ could modulate activity in sympathetic efferents, which normally have a vasomotor role.

Both PGP 9.5- and CGRP-immunoreactivity demonstrated that the anterior capsule of the sheep TMJ was more densely innervated than other areas of the capsule in normal and arthritic joints. As discussed in chapter 3 when gold chloride, silver and methylene blue techniques are used, the richest innervation occurs in the posterior/posterolateral part of the TMJ capsule in the cat (Klineberg, 1971), mouse (Dreessen, et al, 1990), monkey (Keller

and Moffett, 1968) and human (Thilander, 1961). Kido et al (1993), using immunocytochemical techniques for the peptides substance P and CGRP, have found the highest density of neural elements in the anterolateral part of the capsule of the rat TMJ. Johansson et al (1986) found substance P-immunoreactive nerve fibres to be sparser in the posterior capsule than other parts of the monkey TMJ. The qualitative observation of normal sheep TMJ (Chapter 3) showed the greatest density of CGRP-immunoreactive fibres (using an immunoperoxidase technique) in the anterior capsule. It seems that the asymmetrical arrangement of nerve fibres in different parts of the joint is characteristic of the TMJ. In addition there appear to be species differences in the distribution of nerve fibres.

Type IV receptors are noncorpuscular endings that belong to small myelinated (<5 or 6µm diam.) A-delta or unmyelinated C-type nerve fibres (Wyke,1967). They are the most numerous of the four categories of receptors found in the temporomandibular joint in humans (Polacek, 1966), cats (Wyke, 1967), rhesus monkey (Keller and Moffett,1968), mouse (Dreessen, et al 1990), rat, guinea pig and rabbit (Franks, 1965). In the present study, the majority of nerve fibres (72%) located in the sheep TMJ. Synovium and capsule were less than 6µm in width. Most of these probably have a nociceptive role and may also serve polymodal mechanoreceptive functions (Dreessen et al, 1990). Some of these fibres would have been unmyelinated sympathetic efferents.

In conclusion this study suggests that while inflammatory arthritis has a marked influence on the density of sensory and autonomic nerve fibres in synovium, the experimentally induced non-inflammatory osteoarthritis in the sheep TMJ broadly maintains a nerve supply similar to normal joints with no statistically significant difference in the density of nerve endings in the synovium and capsule.

CHAPTER 6

GENERAL DISCUSSION

6.1. INTRODUCTION	2
6.2. MORPHOLOGY OF THE SHEEP TMJ	2
6.3. DISTRIBUTION OF NERVES IN SHEEP TMJ	3
6.4. INNERVATION OF THE PRENATAL SHEEP TMJ	5
6.5. THE EFFECTS OF ARTHRITIS ON THE INNERVATION OF THE TMJ	8
6.6. USING SHEEP AS AN ANIMAL MODEL IN THE PRESENT WORK	10
6.7. CONCLUDING REMARKS AND FUTURE DIRECTIONS	12

6.1. INTRODUCTION

This chapter describes the implications of the observations made and the implications for the use of sheep as a model for human TMJ. In addition, the limitations of the work undertaken and future directions are outlined.

6.2. MORPHOLOGY OF THE SHEEP TMJ

The general morphological appearance of the TMJ of the sheep resembles that of other species studied (Chapters 1 and 2). The temporomandibular joint is composed of the mandibular condyle and glenoid fossa of the temporal bone with an articular disc dividing the joint into superior and inferior compartments. In all species studied, including the sheep, the TMJ differs from other synovial joints in that the articular surfaces of the TMJ are lined with loose fibrous connective tissue overlying fibrocartilage (Bosanquet et al, 1991a). This is an important feature because fibrous connective tissue has a greater ability to repair itself than does hyaline cartilage which covers the articular surfaces of most synovial joints (McNeill, 1993). The articular surfaces are subjected to compressive stress and are the first areas to be affected by degenerative disease (Kreutziger and Mahan, 1975).

The TMJ capsule in sheep, like other mammals including humans, consists of inner loose and outer dense connective tissue. The anterior capsule in sheep is well vascularised with loose connective tissue while the posterior capsule is more dense with fewer vessels. However in humans, the posterior capsule has loose connective tissue and

is highly vascular while the anterior part is less vascularised and dense. In the sheep the anterior attachment of the TMJ disc is well vascularised and contains multiple vascular sinusoids, whereas the posterior attachment is fibrous and avascular as reported by Bosanquet and Goss (1987). This was confirmed in the present study except that some adipose tissues and capillaries could be seen in the posterior attachment of the disc. This is again different from the human where the posterior part of disc attachment is surrounded by abundant loose vascular tissue and the anterior part is dense and avascular. As has been reported elsewhere (1.2.1.5) that the morphology of the synovial membrane of most species that have been studied (eg. rabbit, pig, dog, sheep, horse) is similar to that of humans. Nevertheless there are some differences between the synovial membrane of the TMJ and the other joints of the body as reported by Toller (1961) and Moffett (1964). These authors stated that the synovial lining cells in the TMJ are not attached to each other, and there are spaces up to one micron between each of the lining cells. Moffett (1964) also reported that the basement membrane and desmosomal junctions are absent in synovial lining cells in the TMJ. In the present study, ultrastructural observations of the synovial lining cells in sheep TMJ show that the lining cell layers are composed of two to three cuboidal cells which are not attached to each other. However, the lining cells are supported by a thin band of fine connective tissue which is different from that seen in the human TMJ.

6.3. DISTRIBUTION OF NERVES IN SHEEP TMJ

In the sheep TMJ the distribution of neural elements using gold chloride resembles that described for a variety of other animals including cat, mouse, monkey as well as humans, with the greatest density of nerve fibres occurring in the posterior and lateral parts of the capsule (3.4.3). Only Kido et al (1993) using

immunocytochemical techniques for the peptides substance P and CGRP have found the highest density of neural elements in the anterolateral part of the capsule of the rat TMJ. Consideration must be given to the possibility that the techniques used might be highlighting different components or different amounts of the innervation of the TMJ (Fischer et al, 1983; Dressen et al, 1990; Kido et al, 1993). Nevertheless, species differences in the form of the TMJ articulation might account for this asymmetrical arrangement of nerve fibres (Dressen et al, 1990; Kido et al, 1993). Johansson et al (1986) found substance P-immunoreactive nerve fibres to be sparser in the posterior capsule than other parts of the monkey TMJ. Very few nerve endings were seen but there were regular plexi in the arterial adventitia in this region. The distribution of CGRP-IR nerve fibres in the sheep TMJ resembles that described for the rat TMJ in that the greatest density of sensory nerve fibres was found also in the anterior part of the capsule (Chapters 3 & 5). There were more neural elements stained by the gold chloride technique in the posterior and lateral parts of the capsule of the sheep TMJ than by immunolocalisation of CGRP-containing fibres. Since the glyoxylic acid revealed low numbers of autonomic fibres in the posterior and lateral capsule (3.4.4), the discrepancy in the numbers of neural elements revealed by the techniques mentioned previously can not be due to the autonomic innervation. The gold chloride technique revealed proprioceptors as well as free nerve fibres whereas the immunoreactivity for CGRP revealed nerve fibres and very few free nerve endings, but no spray endings. Thus it would seem that while immunoreactivity for CGRP most likely demonstrates the distribution of sensory nerve fibres in the sheep TMJ a more complete picture of the distribution of neural elements including proprioceptors can be gained by using gold chloride.

6.4. INNERVATION OF THE PRENATAL SHEEP TMJ

Several investigators (Baume, 1962; Levy, 1964; Larsen, 1993) have reported that the elements of the TMJ develop and grow at different rates. In humans the TMJ forms between the 6th and 12th weeks and greatest changes occur between the tenth and 12th week. Scott (1951) examined the TMJ of fetal sheep at 36-70 days gestation (full term=157) and found no evidence of TMJ formation up to the 40th day of gestation. In the present study at 140 days gestation, the TMJ in fetal sheep was not fully developed. The condyle, temporal fossa, disc and synovial membrane were recognisable but the inferior joint compartment was incomplete while the superior joint compartment was present. In the human fetus the inferior joint cavity appears at 10 weeks of gestation (Moore, 1982), whereas the superior cavity begins to appear in the 12th weeks of gestation (Yuodelis, 1966). At birth, the rat TMJ is relatively immature (Ichikawa et al. 1989) and is even less developed than that of the sheep at 140 days gestation (Chapter 4).

The human articular disc changes in appearance postnatally from a relatively plane surface in the newborn to a moulded appearance during adolescence in response to changes in the condyle and temporal fossa (Öberg and Carlson, 1979). There are changes in shape, thickness and hardness in different parts of the disc. The disc of adult sheep is convex superiorly and concave inferiorly and it is thicker anteriorly and posteriorly and thinner centrally (Chapter 3). In the present work, at 140 days gestation, the disc did not show any central thinning and the inferior joint compartment was mostly nonexistent. Scattered, narrow clefts indicated where the inferior joint compartment was developing.

In the human knee joint the substance P-immunoreactive nerve fibres appeared at 11 weeks of gestation but CPON- and TH-immunoreactive nerve fibres appeared at 17 weeks of gestation (Hukkanen et al, 1990). The neural structures in the TMJ may be detectable from the end of the 8th week and full development of nerves in different compartments of human TMJ have been seen between the third and the fifth month of gestation (see section 1.5.1). Fetal sheep TMJ is innervated by nociceptive fibres at 140 days gestation (chapter 4). However, only free nerve endings were visible and no receptors were located at this stage of development. Nerve fibres immunoreactive to antisera for PGP 9.5, substance P and CGRP, were located throughout the capsule, synovium and disc at 140 days gestation in the present work. NPY- and VIP-IR were seen only in the capsule perivascularly but not in the disc and synovial membrane. No TH-IR fibres were found in fetal TMJ at 140 days gestation. These findings support the view that the sympathetic neurons develop much later than many other neurons in the peripheral and central nervous systems and reach their targets after birth when nerve growth factor (NGF) is required for their survival (Zhou et al, 1996).

The increase in complexity of nerve endings and nerve fibres in a variety of tissues in late fetal and early postnatal development may be a response to maturation of functionality (Malinsky, 1959). Encapsulated receptors are present at 4 months in knee, hip, talocrural and carpal joints of humans (Malinsky, 1959). The earlier development of the receptors in these joints compared to the TMJ is said to be correlated with earlier functional development of these joints. The marked increase in the number of Ruffini-like endings after eruption of the first molars, in rat periodontal ligament suggests that mechanical stimuli due to tooth eruption and occlusion might be a prerequisite for final differentiation and maturation of periodontal Ruffini endings (Nakakura-Ohshima et al, 1993). Hence it might be that the lack of receptor endings, other than free nerve endings in the TMJ of the fetal sheep used in this study, might be a reflection of the functional

and anatomical immaturity of the TMJ, as reflected in the gross and microscopic appearance of the disc, the inferior joint compartment and articular surface of the condyle at this stage.

Sisask et al (1995) argued that SP and CGRP could regulate blood flow in the fetal and neonatal skeleton because of localisation of SP and CGRP fibres adjacent to blood vessels. CGRP and SP coexist in nerve terminals in cat dental pulp and in trigeminal ganglion cells and produce vasodilatory effects upon antidromic nerve stimulation, ie. these nerve fibres participate in the sensory nerve-induced vascular response in the pulp (Gazelius et al, 1987). Thus the CGRP- and SP-immunoreactivity in the present studies suggests that these nerve fibres in fetal sheep TMJ disc are sensory, for nociception and perhaps mechanoreception, and might also have a role in the regulation of vascular supply to joint tissues through the release of SP and CGRP in joint tissues.

The sensory nerve supply of developing bone (as indicated by CGRP and SP immunoreactivity) prior to birth and in parallel with increasing mineralisation, suggests that CGRP has a sensory influence on developmental processes in the skeleton (Sisask et al, 1995). These neuropeptides might have a role in bone formation and resorption. Substance P may be a trophic factor for the development of the vomeronasal glands in mouse fetus (Nagahara et al, 1995). Consequently, the SP- and CGRP-IR fibres in the fetal sheep TMJ might have an influence on metabolism within joint tissues and therefore on developmental processes in bone and soft tissues within the joint.

Autonomic fibres represent 40% of the fibres in articular nerves (Schaible and Grubb, 1993). In the adult sheep TMJ, adrenergic nerve fibres were demonstrated in capsule, synovial membrane and peripheral disc. Transverse sections of large arteries showed plexiform varicosities embedded in the adventitial sheath (see Chapter 3). Nevertheless

the distribution of sympathetic efferent fibres, as determined by NPY-IR, in the fetal sheep TMJ, is restricted to the capsule. NPY can have inhibitory and stimulatory effects on sympathetic function (Lundberg et al, 1982) and greatly potentiates the vascular response to adrenergic nerve stimulation (Ekblad et al, 1984). NPY-IR fibres are present perivascularly in synovium from various joints (Mapp et al, 1990). Presumably, the NPY-IR fibres in the fetal sheep TMJ have a vasomotor role, and perhaps, like the cutaneous tissue, might cause vasodilation within the joint. Synovium from human knee and metatarsophalangeal joints have NPY/CPON-IR and TH-IR fibres perivascularly (Pereira da Silva and Carmo-Fonseca, 1990). NPY-IR cell bodies are present in sympathetic ganglia, and are usually colocalised with TH-IR (Lindh et al, 1989). However TH-IR was not colocalised with NPY-IR in fetal sheep TMJ tissues (see Chapter 4). VIP-IR fibres have a non-vascular distribution in some tissues, including ankle joint synovium and periosteum of rats, but have a perivascular arrangement in human spondylolysis ligament (Eisenstein et al, 1994; Ahmed et al, 1995). No VIP-IR fibres were found in the synovial membrane and peripheral disc in the present study in the sheep TMJ. The analysis of VIP-, TH- and NPY-IR in this joint was limited to a few sections and perhaps, therefore may not be representative of the joint. Further work is required to thoroughly investigate the distribution of these immunoreactivities.

6.5. THE EFFECTS OF ARTHRITIS ON THE INNERVATION OF THE TMJ

The detailed morphology of TMJ and appearance and distribution of neural elements in healthy, young adult sheep formed a basis for the next part of the study in which the sheep was used as a model for the study of the effects of arthritis (see work by Bosanquet et al, 1991a, b, c; Ishimaru and Goss, 1992; Ishimaru et al, 1991; 1992; 1994)

on the innervation of the joint. Increasing numbers of studies have shown changes in the distribution/density of neural elements in joint tissue as a result of clinical and experimentally induced arthritis (Grönblad et al, 1988; Konttinen et al, 1990; Mapp et al, 1990; Pereira da Silva and Corno-Fonseca, 1990 and Hukkanen et al, 1991). The participation of the nervous system in arthritic pathologies has been acknowledged for many years (Lembeck et al, 1981; Payan et al, 1984; Matucci-Cerinic and Partsch, 1992) Various levels of the nervous system appear to be involved: Large and small diameter afferents, central nervous system circuits and peripheral interactions between sympathetic efferents and nociceptive afferents (Levine et al, 1986). There is strong evidence that bilateral spread of experimental and clinical arthritis is mediated by a neuronal mechanism (Donaldson et al, 1995). Capsaicin sensitive primary afferent neurons and the contained peptides are involved in the maintenance and spread of arthritis. Arthritic changes, especially inflammation involve facilitation of nociceptive reflexes of C- and A- fibres, enhanced excitability and central sensitization (Herrero and Cervero, 1996). Prostaglandins released by synovial cells play an important role in lowering of nociceptive thresholds in inflamed joints (Lotz et al, 1987; Birrell, 1991). One of the actions of SP is to stimulate proliferation of synoviocytes and production of prostaglandins. The neuropeptides CGRP and SP contribute to the development and maintenance of experimentally-induced inflammatory arthritis (Dockray et al, 1992; Woolf et al, 1994). The present study using an experimentally-induced osteoarthrotic model and its effects on joint innervation showed no significant effect on the percentage surface area or number of PGP 9.5- and CGRP-IR nerve fibres in the sheep TMJ. Nevertheless changes could be seen in relation to the morphology of the articular surfaces which showed mild to severe damage. It has been suggested that there is an initial degeneration of bone innervation distal to and in the vicinity of the experimentally induced tibial fracture in rat but seven days after the injury, PGP 9.5- and CGRP-IR nerves have been increased uniformly (Hukkanen et al, 1993). In the

present study the time between initial operation for inducing osteoarthritis and the time of tissue collection was 120 days. Therefore it is possible any nerve degeneration may have been masked by regeneration of nerves as part of healing process within the TMJ. Additional work using antisera to label regenerating nerves (eg. growth-associated protein GAP-43; Li and Dahlström, 1995) is needed to investigate this possibility.

6.6. USING SHEEP AS AN ANIMAL MODEL IN THE PRESENT WORK

Many investigators have tried to find suitable animal models for studying the TMJ (see section 1.9). Sheep and goats have been selected as the most useful animal models in TMJ research based on their availability, the cost and anatomical similarities to the human TMJ (Bosanquet and Goss, 1987; Bermejo et al, 1993; Goss, 1995). The present study on the neurology of the normal fetal, adult and osteoarthrotic TMJ of the Merino sheep has significantly improved the understanding of the structural and neural components of the normal TMJ as well as the influence of pathologies such as degenerative joint disease. The Australian Merino sheep offers many advantages for surgical investigations, including (a) similarity of TMJ size to that of the human, allowing a wide range of surgical techniques, (b) low cost and good availability in Australia (Bosanquet and goss, 1987). Nevertheless there are some limitations for a systematic investigation of peptidergic nerves in the sheep TMJ.

Limitations:

In immunocytochemical work the preservation of the tissue structure and antigens are very critical. Insufficient or delayed fixation may result in loss of antigens and tissue autolysis. In the present work the preparation and collection of the tissue before fixation

was time consuming. At least two people are needed to handle the the animal during sampling. While perfusion fixation is ideal the size of the sheep makes it difficult to perform this intravascularly. Immunolabelling at the level of electron microscopy requires a rapid penetration of fixative via the vascular tree and immobilisation of the protein and peptides throughout the tissue (Hukkanen, 1994). This was difficult to carry out in sheep and possibly that was the major drawback of the immuno-electron microscopy using gold labelling which was carried out during this study with no success. In contrast, perfusion in a small animal, compared to the sheep, is relatively easy to perform.

In addition, for studying the regional distribution and density of immunoreactivity in the sheep TMJ, the joint must be divided into several parts before preparation for sectioning because the joint is so large. Again this would not be a problem in laboratory animals such as rat and mouse in which with one section the complete TMJ can be sectioned, thus reducing the time and cost of antisera for quantitative work. Consequently, with all the advantages and disadvantages of using sheep as an animal model for studying the pathological dysfunction of TMJ in humans, it can be concluded that "the sheep provides a model closely analogous to humans for evaluation of surgical techniques and replacement materials within the TMJ system" (Bosanquet and Goss, 1987). However the high cost of the immunostaining procedures for quantitative studies as well as the difficulties associated with processing tissues from such a large animal are important limitations.

6.7. CONCLUDING REMARKS AND FUTURE DIRECTIONS

Much of the present work in this thesis has been published and the following conclusions can be made:

1. The TMJ of the sheep is innervated by auriculotemporal (posteriorly) plus masseteric and deep temporal branches (anteriorly) of the mandibular division of the trigeminal nerve. Similar observations have been made for TM joints of the human and monkey. Although a branch of the otic ganglion (autonomic nerve) was not found in the sheep TMJ, and sympathetic fibres could not be detected in major nerves entering the joint, the present study detected sympathetic fibres accompanying blood vessels in the capsule, the synovial membrane, and the disc. It is most likely that the sympathetic fibres entered the joint accompanying branches of the maxillary artery.

2. The gold chloride technique in the present study revealed four types of nerve receptors in the sheep TMJ, although the Ruffini endings were the most frequently encountered type. The majority of corpuscular endings were located in the lateral capsule and were concentrated at the capsule-disc junction. In all parts of the TMJ, this junction was more richly innervated by receptors than were adjacent capsular areas. Thus, the lateral capsule and all disc-capsule junction areas must play an important role in static and dynamic mechanoreception. In the present study in the sheep, only Ruffini and Mazzoni endings were located in the peripheral disc of the sheep.

3. While the development of the TMJ in human and sheep fetuses follows a similar sequence, there are differences in the timing of different developmental events. The joint compartments and disc morphology attain an adult appearance during mid to late gestation in the human but still possess an immature appearance near term in the sheep. Similarly, the innervation is different in human TMJ tissues. There is a progressive reduction in the number of nerve endings during the last trimester of fetal development and the presence of encapsulated corpuscular nerve endings at 20 weeks gestation. In contrast, in the present study of the late gestation fetal sheep, no encapsulated corpuscles could be found and the innervation of the disc was more extensive in the sheep than in the human near-term.

4. The pattern of neuropeptide-immunoreactive fibre distribution in the fetal sheep TMJ disc is different from that of the adult TMJ disc. At 140 days gestation the disc is fully innervated by SP-, CGRP- and PGP 9.5-IR fibres, while in adult sheep the disc is innervated only in the peripheral part at the site of attachment to the capsule. This supports the view that the TMJ disc is innervated during fetal development but at later ages these nerves degenerate and persist only in the peripheral disc.

5. The qualitative assessment of the effect of experimentally-induced degenerative disease on the TMJ in the present study suggested that the density of nerve fibres immunoreactive to antisera for PGP 9.5, CGRP and SP was less in the arthritic TMJ capsule than in the normal capsule. In addition, there seemed to be fewer nerve fibres in parts of the sheep TMJ that were most affected by the degenerative changes. Nevertheless, the quantitative data show no statistically significant effect of induced osteoarthritis on the percentage surface areas or number of PGP 9.5- or CGRP-IR nerve fibres in the capsule. Therefore these data suggest that the

experimentally induced non-inflammatory osteoarthritis in the sheep TMJ broadly maintains a nerve supply similar to normal joints.

To the author's knowledge, this work is the first neurological study of TMJ in a control animal model using normal fetal, adult and experimentally-induced osteoarthritis in Merino sheep. Many other parameters still need to be investigated for a better understanding of pain phenomena and involvement of the nervous mechanism in the pathogenesis of TMJ arthritis. Such parameters include localisation of the cells of origin of sensory and sympathetic innervation of the TMJ by using intraaxonal transport methods (Fried et al, 1991) and also finding convergence patterns of afferent information from TMJ to the central nervous system. In addition, the correlation between vascular distribution and synovial structure in association with nerve fibres needs to be determined.

This investigation has provided an anatomical and neurohistological understanding of the TMJ in an animal model as a basis for further studies of the neural mechanisms involved in TMJ pain and in determining the possible roles of both afferent receptor structures and neuropeptides in the pathophysiology of arthritic joints.

CHAPTER 7

REFERENCES

-
- Aherne WA and Dunnill MS (1982) *Morphometry*. Edward Arnold, London.
- Ahmed M, Bjurholm A, Theodorsson E, Schultzberg M and Kreichbergs A (1995) Neuropeptide Y- and vasoactive intestinal polypeptide-like immunoreactivity in adjuvant arthritis: effects of capsaicin treatment. *Neuropeptides*. 29: 33-43.
- Alam P, Alumets J, Hakanson R and Sundler F (1977) Peptidergic (Vasoactive intestinal peptide) nerves in the genito-urinary tract. *Neuroscience*. 2: 751-757.
- Alavizaki M, Shiraishi MA, Rassool FV, Ferrier GJM, MacIntyre I and Legon S (1986) The calcitonin-like sequence of the CGRP gene. *FEBS Letter*. 206: 47-52.
- Allen JM, McGregor GP, Woodhams PC, Polak JM and Bloom SR (1984) Ontogeny of a novel peptide neuropeptide Y (NPY) in rat brain. *Brain Research*. 303: 197-200.
- Allen YS, Adrina TE, Allen JM, Tatemoto K, Crow TJ, Bloom SR and Polak JM (1983) Neuropeptide Y distribution in the rat brain. *Science*. 221: 877-879.
- Amara SG, Jonas V, Rosenfeld MG, Ong ES and Evans RM (1982) Alternative RNA processing in calcitonin gene expression generates mRNA encoding different polypeptide products. *Nature*. 298: 240-244.
- Amara SG, Arriza JL and Leff SE (1985) Expression in brain of a messenger RNA encoding a novel neuropeptide homologous to calcitonin gene-related peptide. *Science*. 229: 1094-1097.

-
- Angel JL (1948) Factors in temporomandibular joint formation. *American Journal of Anatomy*. 83: 223-246.
- Appelgren A, Appelgren B, Eriksson S, Kopp S, Lundeberg T, Nylander M *et al* (1991) Neuropeptides in temporomandibular joint with rheumatoid arthritis. A clinical study. *Scandinavian Journal of Dental Research*. 99: 519-521.
- Atkinson ME and White FH (1992) Early embryology. In: *Principles of Anatomy and Oral Anatomy for Dental Students..* eds. Atkinson ME and White FH, 1st edition, p 92-93. Longman Singapore Publishers (Pty) Ltd, Singapore.
- Avery JK and Bernick S (1994) Structure and function of the temporomandibular joint. In: *Oral Development and Histology*. ed. Avery JK, 2nd edition, p214-225. Thieme Medical Publishers Inc, New York.
- Barber RP, Vaughn JE, Slemmon JR, Salvaterra PM, Roberts E and Leeman SE (1979) The origin distribution and synaptic relationship of substance P axons in rat spinal cord. *Journal of Comparative Neurology*. 184: 331.
- Barcroft J (1941) Evolution of function in the mammalian organism. *Nature*. 147: 762-765.
- Barnett CH, Davis DV and McConnail MA (1961) *Synovial Joints: Their Structure and Mechanisms*. Longmans Green, London.
- Basbaum AI and Livene JD (1991) The contribution of the nervous system to inflammation and inflammatory disease. *Canadian Journal of Physiology and Pharmacology*. 69: 647-651.

-
- Baume LJ (1962) Ontogenesis of the human T.M.J; Development of the condyle. *Journal of Dental Research*. 41: 1327-1336.
- Baume LJ (1969) Cephalo-facial growth patterns and the functional adaptation of the temporomandibular joint structures. *Reproductive Congress European Orthodontal Society*. 1969: 79-98.
- Bell WE (1983) *Clinical Management of Temporomandibular Disorders*. Year Medical Book Publisher, Inc, Chicago.
- Bellinger DH (1948) Present status of arthrosis of the temporomandibular joint. *Journal of Oral Surgery* .6: 9-16.
- Bennett GAJ and Anderson WAD (1971) *Pathology*. 6th edition. The CV Mosby Company, St Louis.
- Bermejo A, Fenoll A, Puchades-orts A, Sanchez-Del-Campo F, Panchon-Ruiz A and Herrera-Lara M (1987) Morphology of the meniscotemporal part of the temporomandibular joint and its biomechanical implications. *Acta Anatomical Journal*. 129: 220-226.
- Bermejo A, Fenoll A, Gonzalez-Siqueros O and Gonzalez-Gonzalez JM (1992) Histological study of the temporomandibular joint capsule: theory of the articular complex. *Acta Anatomica*. 145: 24-28.
- Bermejo A, Gonzalez O and Gonzalez JM (1993) The pig as an animal model for experimentation on the temporomandibular articular complex. *Oral Surgery, Oral Medicine, Oral Pathology*. 75: 18-23.

-
- Bernard GW and Shih E (1990) The osteogenic stimulating effect of neuroactive calcitonin gene-related peptide. *Peptides*. 11: 625-632.
- Birrell GI (1991) PGI₂ induced activation and sensitization of articular mechanoreceptors. *Neuroscience Letters*. 124:5-8
- Bjurholm A, Kreicbergs A, Terenius L, Goldstein M and Schultzberg M (1988) Neuropeptide Y-, tyrosine hydroxylase- and vasoactive intestinal polypeptide-immunoreactive nerves in bone and surrounding tissues. *Journal of the Autonomic Nervous System*. 25: 119-125.
- Bjurholm A, Kreicbergs A, Ahmed M and Schultzberg M (1990) Noradrenergic and peptidergic nerves in the synovial membrane of the sprague-dawley rat. *Arthritis and Rheumatism*. 33: 859-865.
- Bjurholm A, Kreicbergs A, Schultzberg M and Lerner VH (1992) Neuroendocrine regulation of cyclic AMP formation in osteoblastic cell lines. *Journal of Bone Mineral Research*. 7: 1011-1019.
- Billingham ME (1983) Models of arthritis and the search for anti-arthritic drugs. *Pharmacological Therapy*. 21: 389-428.
- Blackwood HJ (1962) Arthritis of the mandibular joint. *British Dental Journal*. 115: 317-326.
- Bosanquet AG and Goss AN (1987) The sheep as a model for temporomandibular joint surgery. *International Journal of Oral and Maxillofacial Surgery*. 16: 600-603.

-
- Bosanquet A, Ishimaru J-I and Goss AN (1991a). Effect of experimental disc perforation in sheep temporomandibular joints. *International Journal of Oral and Maxillofacial Surgery*. 20: 177-181.
- Bosanquet AG, Ishimaru J-I and Goss AN (1991b) Effect of fascia repair of the temporomandibular joint disk of sheep. *Oral Surgery, Oral Medicine, Oral Pathology*. 72: 520-523.
- Bosanquet AG, Ishimaru J-I and Goss AN (1991c) The effect of silastic replacement following diskectomy on sheep temporomandibular joints. *Journal Oral Maxillofacial Surgery*. 49: 1204-1209.
- Bove GM and Light AR (1995) Calcitonin gene-related systed and peripherin immunoreactivity in nerve sheaths. *Somatosensory and Motor Research*. 12: 49-57.
- Brain S D, William T J, Tippins J R et al (1985) Calcitonin gene-related peptide is a potent vasodilator. *Nature*. 313: 54-56.
- Brimijoin S, Lundberg JM, Brodin E, Hokfelt T and Nilsson G (1980) Axonal transport of substance P in the vagus and sciatic nerves of the guinea pig. *Brain Research*. 191: 443-457.
- Buma P, Verschuren C, Versleyen D, Van der Kraan, P and Oestreicher AB (1992) Calcitonin gene-related peptide, substance P and GAP-43/B-50 immunoreactivity in the normal and arthrotic knee joint of the mouse. *Histochemistry* 98: 327-339.
- Carlsson GE, Kopp S and Oberg T (1979) Arthritis and allied diseases. In: *Temporomandibular Function and Dysfunction*. eds. Zarb GA and Carlson GE, p. 269-320. Munksgaard, Copenhagen.

-
- Casatte CA and Barrer JA (1996) Temporomandibular joint (TMJ) innervation: a study with neuronal tracers and immunohistochemistry. *Journal of Dental Research*. 75: 112 (abstract).
- Chang MM and Leeman SE (1970) Isolation of a sialoogic peptide from bovine hypothalamus tissue and its characterization as substance P. *Journal of Biology and Chemistry*. 245: 4784-4790.
- Choukas NC and Sicher H (1960) The structure of the temporomandibular joint. *Oral Surgery, Oral Medicine, Oral Pathology*. 13: 1302-1312.
- Clark R and Wyke B (1973) Contributions of temporomandibular articular mechanoreceptors to the control of mandibular posture: an experimental study. *Journal of Dental Research*. 2: 121-123.
- Conn PM (1994) *Neuroscience in Medicine*. J. B. Lippincott Company, Philadelphia.
- Coons AH, Ledue EH and Connolly JM (1955) Studies on antibody production. A method for the histochemical demonstration of specific antibody and its application to a study of the lymph-immune rabbit. *Journal of Experimental Medicine*. 102: 49-63.
- Crowley CM, Wilkinson TM, Piehslinger E, Wilson D and Czerny C (1996) Correlations between anatomic and MRI sections of human cadaver temporomandibular joints in the coronal and sagittal planes. *Journal of Orofacial Pain*. 10: 199-216.
- Cutlip RC and Cheville NF (1973) Structure of synovial membrane of sheep. *American Journal of Veterinary Research*. 34 : 45-50.

-
- Davies DV (1946) Synovial membrane and synovial fluid of joints. *The Lancet* 7: 815-819.
- De la Torre JC and Surgeon JW (1976) A methodological approach to rapid and sensitive monomine histofluorescence using a modified glyoxylic acid technique: the SPG method. *Histochemistry*. 49: 81-93.
- Di Iulio P (1995) *The Synovial Membrane of the Normal Sheep Temporomandibular Joint*. Honours Thesis, Dept Dentistry, University of Adelaide.
- Dijkgraaf LC, de Bont LGM, Boering G and Liem RSB (1996) Structure of the normal synovial membrane of the temporomandibular joint: A review of the literature. *Journal of Oral and Maxillofacial Surgery*. 54: 332-338.
- Dixon AD (1962) Structure and functional significance of the intraarticular disc of the human temporomandibular joint. *Oral Surgery, Oral Medicine, Oral Pathology*. 15: 48-61.
- Dixon EW (1991) *BMDP Statistics Software Manual* vol 1. University of California Press, Berkeley.
- Dockray GJ, Louis SM and Forster ER (1992) Neuropeptides in experimental arthritis. *Neuropeptides*. 22: 17-18
- Domeij S, Dahlqvist A and Forsgren S (1991) Regional differences in the distribution of nerve fibres showing substance P- and calcitonin gene-related peptide-like immunoreactivity in the rat larynx. *Anatomy and Embryology*. 183: 49-56.

-
- Donnerer J, Schuligoi R and Stein C (1992) Increased content and transport of substance P and calcitonin gene-related peptide in sensory nerves innervating inflamed tissue; evidence for a regulatory function of nerve growth factor in vivo. *Neuroscience*. 49: 693-698.
- Donaldson LF, McQueen DS and Seckl JR (1995) Neuropeptide gene expression and capsaicin-sensitive primary afferents: maintenance and spread of adjuvant arthritis in the rat. *Journal of Physiology*. 486: 473-482.
- Doyle DE (1982) Embryology and evolution. In *Diseases of the Temporomandibular Apparatus - A Multidisciplinary Approach*. eds. Morgan DH , House LR , Hall WP and Vambas SJ, p. 3-7. CV Mosby, St. Louis.
- Dreessen D, Halata Z and Strassmann T (1990) Sensory innervation of the temporomandibular joint in the mouse. *Acta Anatomica Basel*. 139: 154-160.
- Drury RAB and Wallington E.A (1967) *Carlton's Histological Technique*. 4th edition. Oxford University Press, London.
- Dubrul EL (1980) The craniomandibular articulation. In: *Sicher's Oral Anatomy*. 7th edition, Chapter 4. C.V Mosby, St Louis.
- Durkin JF, Heeley JD and Irving JT (1979) *Temporomandibular Joint Function and Dysfunction*. eds. Zarb GA and Carlsson GE, Chapter 2. Munksgaard, Copenhagen.
- Eisenstein SM, Ashton IK, Roberts S, Darby AJ, Kanse P, Menage J and Evans H (1994) Innervation of the spondylosis ligament. *Spine*. 19: 912-916.

-
- Ekblad E, Edvinsson L, Wahlestedt L, Uddmann R, Hakanson R and Sundler F (1984) Neuropeptide Y co-exists and co-operates with noradrenaline in perivascular nerve fibres. *Regulatory Peptides*. 8: 225-235.
- Erspamer V. (1981) The tachykinin peptide family. *Trends in Neuroscience*. 4: 267-269.
- Ferrell WR, Crighton A and Sturrock RD (1992) Position sense at the proximal interphalangeal joint is distorted in patients with rheumatoid arthritis of finger joints. *Experimental Physiology*. 77: 675-680.
- Finn, B (1994) *The Anatomy and Biomechanics of the Masticatory Apparatus in the Australian Merino Sheep*. MSc Thesis. Dept. of Dentistry, University of Adelaide.
- Fischer JA and Born W (1984) Novel peptides from the calcitonin gene: expression, receptor and biological function. *Peptides*. 3: 265-271.
- Fischer LA, Kikkawa DO, Rivier JE, Amara SG, Evans RM, Rosenfeld MG, Vale WW and Brown MR (1983) Stimulation of noradrenergic sympathetic outflow by calcitonin gene-related peptide. *Nature* (London). 305: 505-521.
- Fitzgerald M and Gibson S (1984) The postnatal physiological and neurochemical development of peripheral sensory C fibres. *Neuroscience*. 13: 933-944.
- Franks AST (1975) Studies on the innervation of the temporomandibular joint and lateral pterygoid muscle in animals. *Journal of Dental Research Supplement*. 43: 947-948.
- Freeman MAR and Wyke B (1967) The innervation of the ankle joint: An anatomical and histological study on the cat. *Acta Anatomischer Basel*, 68: 321-333.

-
- Fried K, Arvidsson J, Robertson B and Pfaller K (1991) Anterograde horseradish peroxidase tracing and immunohistochemistry of trigeminal ganglion tooth pulp neurons after dental nerve lesions in the rat. *Neuroscience*. 43: 269-278.
- Fristad I, Heyeraas KJ and Kvinnsland I (1994) Nerve fibres and cells immunoreactive to neurochemical markers in developing rat molars and supporting tissues. *Archives Oral Biology*. 39: 633-646.
- Fromer J and Monroe CW (1966) The morphology and distribution of nerve fibres and endings associated with the mandibular joint of the mouse. *Journal of Dental Research*. 45: 1762-1766.
- Furness JB and Costa M (1975) The use of glyoxylic acid for the fluorescence histochemical demonstration of peripheral stores of noradrenaline and 5-hydroxytryptamine in whole mounts. *Histochemistry*. 41: 335-352.
- Gaywood, I (1989) Neuropeptides. *British Journal of Rheumatology*. 29: 140-141.
- Gazelius B, Edwall B, Algart L, Lundberg JM, Hökfelt T and Fischer JA (1987) Vasodilatory effects and coexistence of calcitonin gene-related peptide (CGRP) and substance P in sensory nerves of cat dental pulp. *Acta Physiologica Scandinavica*. 130: 33-40.
- Gebhart GF (1995) Somatovisceral sensation. In: *Neuroscience in Medicine*. ed. Conn PM, p.433-450. JP Lippincott Company, Philadelphia.
- Gerard MT, Yoon JH, Luyk NH and McMillan MD (1992) Temporalis muscle as a disc replacement in the temporomandibular joint of sheep. *Journal of Oral and Maxillofacial Surgery*. 50: 979-987.

-
- Ghadially FN (1983) *Fine Structure of Synovial Joints*. Butterworths, England.
- Ghosh P, Fraci GM, Sutherland, Taylor Tkf, Pettit GD and Bellenger CR (1983) The effects of postoperative joint immobilization on articular cartilage degeneration following meniscectomy. *Journal of Surgical Research*. 35: 461-473.
- Gibbins IL (1989) Dynorphin-containing pilomotor neurons in the superior cervical ganglion of guinea-pigs. *Neuroscience Letters*. 107: 45-50.
- Gibbins IL (1990) Target-related patterns of co-existence of neuropeptide and vasoactive intestinal peptide, enkephalin and substance P in cranial parasympathetic neurons innervating the facial skin and exocrine glands of guinea-pigs. *Neuroscience*. 38: 541-560.
- Gibbins IL (1992) Vasoconstrictor, vasodilator and pilomotor pathways in sympathetic ganglia of guinea-pigs. *Neuroscience*. 47: 657-672.
- Gibbins IL and Matthew SE (1996) Dendritic morphology of presumptive vasoconstrictor and pilomotor neurons and their relations with neuropeptide containing preganglionic fibres in lumbar sympathetic ganglia of guinea pigs. *Neuroscience*. 70: 998-1012.
- Gibbins IL and Morris JL(1987) Co-existence of neuropeptides in sympathetic, cranial, autonomic and sensory neurons innervating the iris of the guinea-pig. *Journal of the Autonomic Nervous System*. 21: 67-82.

-
- Gibbins I L, Furness J B, Gosta M, MacIntyre I, Hillyard CJ and Girgis S (1985) Colocalization immunoreactivity with substance P in cutaneous, vascular and visceral sensory nerves of guinea pigs. *New Science*. 57: 125-130.
- Gibson SJ, Polak JM, Bloom SR, Sabate IM, Mulberry PM, Ghatol MA, McGregor GP, Morrison JFB, Kelly JS, Evans RM and Rosenfeld MG (1984) Calcitonin gene-related peptide immunoreactivity in the spinal cord of men and of eight other species. *Journal of Neuroscience*. 14: 3101-3111.
- Gibson SJ, Polak JM, Katagiri T, Su H, Weller RO, Brownell DB, Holland S, Hughes JT, Kikujama S, Bloom SR, Steiner TJ, de Belleruche J and Clifford-R F (1988) Calcitonin gene-related peptide messenger RNA is expressed in sensory neurones of the dorsal root ganglia and also in spinal motoneurons in man and rat. *Neuroscience Letters*. 12: 283-288.
- Gigor Z (1971) The morphology of the nerve fibres and receptors in the oral mucous membrane of sheep. *Anatomica Anzeiger*. 128: 84-100.
- Gillbe GV (1973) A comparison of the disc in the craniomandibular joint of three mammals. *Acta Anatomischer*. 86: 394-409.
- Girgis SI, MacDonald DWR, Stevenson JC, Bevis PJR, Lynch C, Wimalawansa SJ, Self CH, Morris HR and MacIntyre I (1985) Calcitonin gene-related peptide: Potent vasodilator and major product of the calcitonin gene. *Lancet*. 11: 14-19.
- Goltzman D and Mitchell J (1985) Interaction of calcitonin gene-related peptide at receptor sites in target tissues. *Science*. 227: 1343-1345.

- Goodman EC and Iversen LL (1986) Calcitonin gene-related peptide: novel neuropeptide. *Life Science* 38: 2169-2178.
- Goss AN (1993) Second international consensus conference on temporomandibular joint surgery. *International Journal of Oral and Maxillofacial Surgery*. 22: 65-70.
- Goss AN. (1995) A comparison of the form and function of the human, monkey, and goat temporomandibular joint. In: *The Sheep as a Model for Temporomandibular Joint Disorders*. eds. Goss AN, Kurita K and McMahon L, p. 10-11. The Japan-Australia Temporomandibular Joint Disorders Research Group 1989-1995, The University of Adelaide.
- Goss AN and Bosanquet AG (1989) An animal model for TMJ arthroscopy. *Journal of Oral and Maxillofacial Surgery*. 47: 537-538.
- Goss AN, Bosanquet AG and Tideman H.(1987) The accuracy of temporomandibular joint arthroscopy. *Journal of Cranio-Maxillo-Facial- Surgery*. 15: 99-105.
- Goss AN, Jones RHB, Kurita K, Ishimaru JI, Ogi N and Handa Y (1992) The sheep temporomandibular joint model: A Japanese/Australian Investigation. *Hospital Dentistry and Oral Maxillofacial Surgery (Tokyo)*. 4: 58-60.
- Goss AN, Kurita K and McMahon L (1995) *The Sheep as a Model for Temporomandibular Joint Disorders* Dept. of Dentistry, University of Adelaide, Adelaide.
- Greenfield BE and Wyke B (1964) The innervation of the cat's temporomandibular joint. *Journal of Anatomy*. 98: 300.

- Greenfield B E and Wyke B (1966) Reflex innervation of the temporomandibular joint. *Nature*. 211: 940-910.
- Griffin CJ, Hawthorn R and Harris R (1975) Anatomy and histology of the human temporomandibular joint. *Monographs in Oral Science*. 4: 1-26.
- Griffin CJ and Sharpe CJ (1962) Distribution of elastic tissue in the human temporomandibular joint meniscus specially in respect to "compression" areas. *Australian Dental Journal*. 7: 72-78.
- Grönblad DM, Leisi P and Munck AM (1984) Peptidergic nerves in human tooth pulp. *Scandinavian Journal of Dental Research*. 92: 319-324.
- Grönblad DM, Konttinen YT, Korkala O, Liesi P, Hukkanen M and Polak JM (1988) Neuropeptides in synovium of patients with rheumatoid arthritis and osteoarthritis. *Journal of Rheumatology*. 15: 1807-1810.
- Grönblad M, Korkala O, Liesi P and Karaharju E (1985) Innervation of synovial membrane and meniscus. *Acta Orthopædica Scandinavica*. 56: 484-486.
- Grube D (1980) Immunoreactivities of gastrin (G-) cells. II. Non-specific binding of immunoglobins to G-cells by ionic interactions. *Histochemistry*. 87: 149-167
- Gu J, Polak JM, Adrian TE, Allen JM, Tatemoto K and Bloom SR (1983) Neuropeptide tyrosine (NPY)- a major cardiac neuropeptide. *Lancet*. 1: 1008-1010.
- Gulbenkian S, Wharton J and Polak JM (1987) The visualization of cardiovascular innervation in the guinea-pig using an antiserum to protein gene peptide 9.5. *Journal of the Autonomic Nervous System*. 18: 235-247.

-
- Hanesch V, Heppelman B and Schmidt RF (1991) Substance P and calcitonin gene-related peptide immunoreactivity in primary afferent neurons of the cat's knee joint. *Neuroscience*. 45: 185-193.
- Hanky GT (1954) Temporomandibular arthrosis. *British Dental Journal*. 97: 249-270.
- Hansson T (1988) Craniomandibular disorders and sequencing their treatment. *Australian Prosthetic Journal*. 2: 9-15.
- Harmar A, Schofield JG and Keen, P (1981) Substance P biosynthesis in dorsal root ganglia: An immunochemical study of (35S) methionine and (3H) proline incorporation in vitro. *Neuroscience*. 6: 1917-1922.
- Hashim MA and Tadepalli AS (1995) Cutaneous vasomotor effects of neuropeptide Y. *Neuropeptides*. 29: 263-271.
- Hatton MN and Swann DA. (1986) Studies on bovine temporomandibular joint synovial fluid. *Journal Prosthetic Dentistry* 56: 635-638.
- Helland MM (1986) Anatomy and function of the temporomandibular joint. In: *Modern Manual Therapy of the Vertebral Column*. (ed. Grieve GP), p64-76. Churchill Livingstone, London.
- Hel G, Ottesen B, Fahrenkrug J, Larsen JJ, Owman C, Sjoberg NO, Stolderg B, Sundler F and Walles B (1981) Vasoactive intestinal polypeptide (VIP) in the human femal reproductive tract : distribution and motor effects. *Biology of Reproduction*. 25:227-234.

-
- Helmy ES, Bays RA and Sharawy M (1988) Osteoarthritis of the temporomandibular joint following experimental disc perforation in *Macaca fascicularis*. *Journal of Oral and Maxillofacial Surgery*. 46: 979-990.
- Helmy ES, Timmis DP, Sharawy MH, Abdelatif O and Bays RA (1990) Fatty change in the human temporomandibular joint disc. Light and electron microscopy study. *International Journal of Oral and Maxiofacial Surgery*. 19: 38-43.
- Henderson B and Edwards JCW. (1987) *The Synovial Lining: In Health and Disease*. Chapman and Hall, London.
- Henderson B, Hardingham T, Blake S, and Lewthwaite J (1993) Experimental arthritis models in the study of the mechanisms of articular cartilage loss in rheumatoid arthritis. *Agents and Action Supplements*. 39: 15-26.
- Hernanz A, De-Miguel E, Romera N, Perez-Ayala C, Gijon J & Arnalich F (1993) Calcitonin gene-related peptide II, substance P and vasoactive intestinal peptide in plasma and synovial fluid from patients with inflammatory joint disease. *British Journal of Rheumatology*. 32: 31-35.
- Herrero JF and Cervero F (1996) Supraspinal influences on the facilitation of rat nociceptive reflexes induced by carrageenan monoarthritis. *Neuroscience Letters*. 209: 21-24.
- Hoheisel U, Mense S and Scherotzke R (1994) Calcitonin gene-related peptide-immunoreactivity in functionally identified primary afferent neurones in the rat. *Anatomy and Embryology*. 189: 41-49.

- Hohmann A, Wilson K and Nelms CR Jr. (1983) Surgical treatment in temporomandibular joint trauma. *Otolaryngology Clinics of North America*. 16: 549-562.
- Hökfelt T, Kellerth JO, Nilsson G and Pernow B (1975) Morphological report for a transmitter role of substance P immuno-histochemical localization in the central nervous system and in some primary sensory neurons. *Science*. 190: 889-890.
- Holmlund A, Ekblom A, Hansson P, Lind J, Lundeberg T and Theodorsson E (1991) Concentrations of neuropeptides substance P, neurokinin A, calcitonin gene-related peptide, neuropeptide Y and vasoactive intestinal polypeptide in synovial fluid of the human temporomandibular joint. *International Journal of Oral and Maxillofacial Surgery*. 20: 228-231.
- Holmlund A and Hellsing G (1988) Arthroscopy of the temporomandibular joint. Occurance and location of osteoarthritis and synovitis in a patient material. *International Journal of Oral and Maxillofacial Surgery*. 17: 36-40.
- Holzer P (1988) Local effector functions of capsaicin-sensitive sensory nerve endings: involvement of tachykinins, calcitonin gene-related peptide and other neuropeptides. *Neuroscience*. 24: 739-768.
- Hromada J and Polacek P (1958) A contribution to the morphology of encapsulated nerve endings in the joint capsule and in the periarticular tissue. *Acta Anatomica*. 33: 187-202.
- Hsu SM, Raine L and Fanger H (1981) Use of avidinbiotin peroxidase complex (ABC) in immunoperoxidase techniques: A comparison between ABC and unlabelled antibody (PAP) procedures. *Journal of Histochemistry and Cytochemistry* 29: 577-580.

-
- Hukkanen MVJ (1994) *Neuropeptides in the central and peripheral nervous system: Their role in the pathophysiology of painful osteoarticular inflammatory disease and trauma in man and animals*. PhD thesis. Royal Postgraduate Medical School.
- Hukkanen M, Mapp PI, Moscoso G, Brewerton DA, Konttinen YT, Blake DR and Polak GM (1990) Innervation of the human knee joint, a study in fetal material. *British Journal of Rheumatology Supplement* No 2 (abstract).
- Hukkanen M, Grönblad M, Rees R, Konttinen YT, Gibson SJ, Hietnen J, Polak JM and Brewerton DA (1991) Regional distribution of mast cells and peptide containing nerves in normal and adjuvant arthritic rat synovium. *Journal of Rheumatology*. 18: 177-183.
- Hukkanen M, Konttinen YT, Rees RG, Gibson SJ, Santavirta S and Polak JM (1992a) Innervation of bone from healthy and arthritic rats by substance P and calcitonin gene related peptide containing sensory fibers. *Journal of Rheumatology*. 19: 1252-1259.
- Hukkanen M, Konttinen YT, Rees RG, Santavirta S, Terenghi G and Polak JM (1992b) Distribution of nerve endings and sensory neuropeptides in rat synovium, meniscus and bone. *International Journal of Tissue Reaction*. 14: 1-10.
- Hukkanen M, Konttinen YT, Santavirta S, Paavolainen P, Gu HX, Terenghi G and Polak JM (1993) Rapid proliferation of calcitonin gene-related peptide-immunoreactive nerves during healing of rat tibial fracture suggests neural involvement in bone growth and remodelling. *Neuroscience*. 54: 969-979.
- Ichikawa H, Wakisaka S, Matsuo S and Akai M (1989) Peptidergic innervation of temporomandibular disk in rat. *Experimenta*. 45: 303-304.

-
- Ishibashi K (1974) Innervation of human temporomandibular joint in adult. *Bulletin Tokyo University of Medicine and Dentistry* 21: 86-88
- Ishimaru J-I and Goss AN (1992) A model for osteoarthritis of the temporomandibular joint. *Journal of Oral Maxillofacial Surgery*. 50: 1191-1195.
- Ishimaru J-I, Kurita K, Handa Y and Goss AN (1991) Temporomandibular joint osteoarthritis: Literature review and experimental animal models. *Hospital Dentistry (Tokyo)* 3: 64-68.
- Ishimaru J-I, Kurita K, Handa Y and Goss AN (1992) Effect of marrow perforation on the sheep temporomandibular joint. *International Journal of Oral Maxillofacial Surgery*. 21: 239-242.
- Ishimaru J-I, Handa Y, Kurita K and Tatematsu N (1993) Establishment for animal model for temporomandibular joint osteoarthritis. *Acta School of Medicine University of Gifu* 41: 453-479.
- Ishimaru J-I, Handa Y, Kurita K and Goss AN (1994) The effect of occlusal loss on normal and pathological temporomandibular joints: an animal study. *Journal of CranioMaxillofacial Surgery*. 22: 95-102.
- Itoh N, Obata K, Yanaihara N and Okamoto H (1983) Human preprovasoactive intestinal polypeptide contains a novel PHI-27-like peptide, PHM-27. *Nature*. 304: 574-549.
- Jackson P and Thompson RJ (1981) The demonstration of new human brain -specific proteins by high-resolution two dimensional polyacrylamide gel electrophoresis. *Journal of Neurological Science*. 49: 429-438

-
- Jackson P, Thomson VM and Thompson RJ (1985) A comparison of the evolutionary distribution of the two neuroendocrine markers, neuron specific enolase and protein gene product 9.5. *Journal of Neurochemistry*. 45: 185-190.
- Jazwinski SM. and Rothschild H (1991) The biology of aging. What is aging? *Journal of American Veterinary Medicine Association*. 141: 1237-1241.
- Johansson A-S, Isacsson G, Isberg A and Granholm A-C (1986) Distribution of substance P-like immunoreactive nerve fibers in temporomandibular joint soft tissues of monkeys. *Scandinavian Journal of Dental Research*. 94: 225-230.
- Johansson A-S, Isberg A and Isacsson G. (1990) A radiographic and histologic study of the topographic relations in the temporomandibular joint region: Implications for a nerve entrapment mechanism. *Journal of Oral and Maxillofacial Surgery*. 48: 953-961.
- Johnson LC (1962) Joint remodelling as the basis for osteoarthritis. *Journal of American Veterinary Medicine Association*. 141:1237-1241.
- Juniper RP (1984) Temporomandibular joint dysfunction. *British Journal of Oral and Maxillofacial Surgery*. 21:1-8.
- Karant SS, Springall DR, Kuhn DM, Levene MM and Polak JM (1991) An immunocytochemical study of cutaneous innervation and the distribution of neuropeptide and protein gene product 9.5 in new and commonly employed laboratory animals. *American Journal of Anatomy*. 191: 369-383.

-
- Kawamura Y (1974) Neurogenesis of mastication. *Frontal and Oral Physiology* 1: 77-120
- Kawamura Y, Majima T and Kato I (1967) Physiologic role of deep mechanoreceptor in temporomandibular joint capsule. *Journal of the Osaka University Dental School*. 7: 63-76.
- Kawamura Y and Majima T (1964) Temporomandibular joint's sensory mechanism controlling activities of the jaw muscles. *Journal of Dental Research*. 43: 150.
- Kawamura Y, Majima T, Kato I. (1990) Physiologic role of deep mechanoreceptor in temporomandibular joint capsule. *Journal of the Osaka University Dental School*. 7: 63-76.
- Keller JH and Moffett BC (1968) Nerve endings in the temporomandibular joint of the Rhesus monkey. *Anatomical Record*. 160: 587-594.
- Kent C and Clark PJ (1991) The immunolocalisation of the neuroendocrine specific protein PGP9.5 during neurogenesis in the rat. *Developmental Brain Research*. 58: 147-150.
- Key JA (1932) The synovial membrane of joints and bursae. In: *Cowdry's Special Cytology*; 2nd edition, p. 10-53. Hoeber, New York.
- Kido MA, Kondo T, Ayasaka N, Terada Y and Tanake T (1991) The peripheral distribution of trigeminal nerve fibres in the rat temporomandibular joint studied by an arterograde axonal transport method with wheat germ agglutinin - horseradish peroxidase. *Archives of Oral Biology*. 36: 391-400.

-
- Kido MA, Kiyoshima T, Kondo T, Ayasaka N, Moroi R, Terada Y and Tanaka T (1993) Distribution of substance P and Calcitonin gene-related peptide-like immunoreactive nerve fibres in the rat temporomandibular joint. *Journal of Dental Research*. 72: 592-598.
- Kitamura H (1974) Development of temporomandibular joint innervation. *Bulletin Tokyo Medical and Dental University* (Suppl.): 83-85.
- Klineberg I (1971) Structure and function of temporomandibular joint innervation. *Annals Royal College of Surgeons England* . 49: 268-288.
- Klineberg IJ, Greenfield BE and Wyke BD (1971) Afferent discharges from temporomandibular articular mechanoreceptors. *Archives of Oral Biology*. 16: 1463-1479.
- Knight AD and Levick JR (1983) The density and distribution of capillaries around a synovial cavity. *Quarterly Journal of Experimental Physiology*. 68: 629-644.
- Kobayashi A, Yoshida N, Tonosaki Y, Kikuchi S and Sugiura Y (1995) Origin of the calcitonin gene-related peptide-immunoreactive nerve fibres in the rat shoulder joint. *Anatomy and Embryology*. 191: 471-476.
- Konttinen YT, Lindy O, Kempainen P, Saari H, Suomalainen K, Vauhkonen M, Lindy S and Sorsa T (1991) Collagenase reserves in polymorphonuclear neutrophil leukocytes from synovial fluid and peripheral blood of patients with rheumatoid arthritis. *Matrix II*: 296-301.

-
- Konttinen YT, Grönbald M, Hukkanen M, Kinnunen E, Santavirta S, Polak JM, Gibson S, Zhao Y, Revell P, Blake D and Rees R. (1989) Pain fibres in osteoarthritis: a review. *Seminars in Arthritis and Rheumatology*. 18: 35-40.
- Konttinen YT, Rees R, Hukkanen M, Grönbald M, Tolvanen E, Gibson S, Polak JM and Brewerton DA (1990) Nerves in inflammatory synovium: immunohistochemical observations on the adjuvant rat model. *Journal of Rheumatology*. 17: 1586-1591.
- Konttinen YT, Hukkanen M, Segerberg M, Rees R, Kempainen P, Sorsa T, Saari H, Polak JM and Santavirta S (1992) Relationship between neuropeptide immunoreactive nerves and inflammatory cells in adjuvant arthritic rats. *Scandinavian Journal of Rheumatology*. 21: 55-59.
- Koritzer RT, Schwartz AH, Harris RR and St Hoyne LE (1992) Previously undescribed disk-capsule innervation: some speculative thoughts for TMD clinicians. *American Journal of Dentofacial Orthopedics*. 102: 109-112.
- Kreutziger KL and Mahan PE (1975) Temporomandibular degenerative joint disease Part 1 Anatomy, pathophysiology and clinical description. *Oral Surgery, Oral Medicine, Oral Pathology*. 40: 165-182.
- Kummer W, Gibbins IL, Stefan P and Kapoor V (1990) Catecholamines and catecholamine-synthesizing enzymes in guinea-pig sensory ganglia. *Cell Tissue Research*. 261: 595-606.
- Kuraishi Y, Nanayama T, Ohno H, Fuji N, Ojala A, Yajima H and Satoh M (1989) Calcitonin gene-related peptide increases in the dorsal root ganglia of adjuvant rat. *Peptides* 10: 447-452.

-
- Larsen WJ (1993) *Human Embryology*. Churchill livingstone, New York.
- Larsson J, Ekblom A, Henriksson K, Lundeberg T and Theodorsson E (1989) Immunoreactive tachykinins, calcitonin gene-related peptide and neuropeptide Y in human synovial fluid from inflamed knee joints. *Neuroscience Letters*. 100: 326-330.
- Larsson LI, Fahrenkrug J, Schaffalitzky de Muchadell O, Sundler F, Hakanson R and Rehfeld JF (1976) Localization of vasoactive intestinal polypeptide (VIP) to central and peripheral neurons. *Proceeding of National Academy of Science USA*. 73: 3197-3200.
- Lembeck F, Donnerer J and Colpaert FC (1981) Increase of substance P in primary afferent nerves during chronic pain. *Neuropeptides*. 1: 175-180.
- Lembeck F & Holzer P (1979) Substance P as neurogenic mediator of antidromic vasodilation and neurogenic plasma extravasation. *Archives of Pharmacology*. 310: 175-183.
- Lever JD and Ford EHR (1958) Histological, histochemical and electron microscopic observation on the synovial membrane. *Anatomical Record*. 132: 525-539.
- Levine JD, Clark.R, Dover M, Helms C, Moskowitz MA and Basbaum AI (1984) Intraneuronal substance P contributes to the severity of experimental arthritis. *Science*. 226: 547-549.

-
- Levine JD, Dardick SJ, Roizen MF, Helms C and Basbaum AI (1986) Contribution of sensory afferents and sympathetic efferents to joint injury in experimental arthritis. *Journal of Neuroscience*. 6: 3423-3429.
- Levine JD,Coderre TJ and Basbaum AI (1988) The peripheralnervous system and the inflammatory process. In: *Proceedings of the Vth World Congress on Pain*. eds. Dubner R, Gebhardt GF and Bond MR, p. 33-43. Elsevier Science Publishers, New York.
- Levy BM (1964) Embryological development of the temporomandibular joint. In: *The Temporomandibular Joint*. ed. Sarnat BG, 2nd edition. p 34-47. Thomas, Springfield.
- Li JY, How X-E, and Dohlström AB (1995) GAP-43 and its relation to autonomic and sensory neuron in sciatic nerve and gastronemius muscle in the rat. *Journal of the Autonomic Nervous System*. 50: 299-309
- Linder JE (1978) A simple and reliable method for the silver impregnation of nerves in paraffin sections of soft and mineralized tissues. *Journal of Anatomy*. 127: 543-551.
- Lindh B, Lundberg JM and Hökfelt T (1989) NPY-, galanin-, VIP/PHI-, CGRP- and substance P-immunoreactive neuronal subpopulations in cat autonomic and sensory ganglia and their projections. *Cell and Tissue Research*. 256: 259-273.
- Liven E (1993) Diarthroses in the mouse: from different cellular structure to similar joint appearance. *Anatomical Record*. 236: 351-354.

-
- Lotz M, Carson D and Vaughan J H (1987) Substance P activation of rheumatoid synoviocytes. Neural pathway in the pathogenesis of arthritis. *Science*. 235: 893-895.
- Lundberg JM, Hökfelt T, Schultzberg M, Uvnas-Wallensten K, Kohler C and Said SI (1979) Occurance of vasoactive intestinal polypeptide (VIP)-like immunoreactivity in certain acetylcholinesterase staining. *Neuroscience*. 4: 1539-1559.
- Lundberg JM, Hökfelt T, Änggard A, Uvnas-Wallensten K, Brimijoin S, Brodin E and Fahrenkrug J (1980) Peripheral peptide neurons: distribution, axonal transport, and some aspects on possible function. *Advances in Biochemistry and Psychopharmacology*. 22: 25-36.
- Lundberg JM, Terenius L, Hökfelt T, Martling CR, Tatemoto K, Mutt V, Polak J, Bloom S and Goldstein M (1982) Neuropeptide Y (NPY)-like immunoreactivity in peripheral noradrenergic neurons and effects of NPY on sympathetic function. *Acta Physiologica Scandinavica*. 116: 477-480.
- Lundberg JM, Terenius L, Hökfelt T and Goldstein M. (1983) High levels of neuropeptide Y in peripheral noradrenergic neurons in various mammals including man. *Neuroscience*. 42: 167-172.
- Lundeberg T, Alstergren P, Applegren A, Appelgren B, Carleson J, Kopp S and Theodorsson E (1996) A model for experimentally induced temporomandibular joint arthritis in rats: effects of carrageenan on neuropeptide-like immunoreactivity. *Neuropeptides* .30: 37-41.
- Mahan PE (1980) The temporomandibular joint in function and pathofunction. In: Solberg WK Clark GT

-
- Malinsky J (1959) The ontogenetic development of nerve terminations in the intervertebral discs of man. *Acta Anatomischer, Basel*. 38: 96-113.
- Mapp PI, Kidd BL and Merry P (1989) Neuropeptides are found in normal and inflamed human synovium. *British Journal of Rheumatology*. 28:8.
- Mapp PI, Kidd BL, Gibson SJ, Terry JM, Revell PA, Ibrahim NBN, Blake DR, Polak JM. (1990) Substance P-, calcitonin gene-related peptide- and C-flanking peptide of neuropeptide Y-immunoreactive fibres are present in normal synovium but depleted in patients with rheumatoid arthritis. *Neuroscience* 37: 143-153.
- Mapp PI, Valsh DA, Garrett NE, Kidd BL, Cruwys SC, Polak JM and Blake DR (1994) Effect of three animal models of inflammation on nerve fibres in the synovium. *Annals of the Rheumatic diseases*. 53: 240-246.
- Markowitz HA and Gerry RG (1949) Temporomandibular joint disease. *Oral Surgery, Oral Medicine & Oral pathology*. 2: 1309-1337.
- Marlier L, Poulat P, Rajaofetra N and Privata A (1991) Modifications of serotonin-, substanceP- and C-flanking peptide of neuropeptide Y-immuoreactive fibres are present in normal synovium but depleted in patients with rheumatoid arthritis. *Neuroscience*. 37: 143-153.
- Matucci-Cerinic C and Partsch G (1992) The contribution of the peripheral nervous system and the neuropeptide network to the development of synovial inflammation. *Clinical and Experimental Rheumatology*. 10: 211-215.

-
- May ND (1970) *The Anatomy of the Sheep*. 3rd edition. University of Queensland Press, Brisbane.
- McCarthy PW and Lawson SN (1990) Cell type and conduction velocity of rat primary sensory neurons with calcitonin gene-related peptide-like immunoreactivity. *Neuroscience*. 34: 623-632.
- McKay GS, Yemm R and Cadden W (1992) The structure and function of the temporomandibular joint. *British Dental Journal*. 5:126-127.
- McNeil C (1993) Anatomy of the masticatory system. In: *Temporomandibular Disorders*.. ed. McNeil C, p. 11-19. Quintessence Publishing Co, Inc, Chicago.
- Meachim G (1963) The effect of scarification of articular cartilage in the rabbit. *Journal of Bone and Joint Surgery*. 45: 150-155.
- Meek WD, Raber BT, McClain OM, McCosh JK and Baker BB (1991) Fine structure of the human synovial lining cell in osteoarthritis: its prominent cytoskeleton. *Anatomical Record*. 231: 145-155.
- Melfi RC (1994) Temporomandibular joint. In *Permar's Oral Embryology and Microscopic Anatomy*. 9th edition, p. 259-269. Lea and Febiger, Philadelphia:
- Merjersjo C and Kopp S (1984) Long term development after treatment of mandibular dysfunction and osteoarthrosis. A clinical-radiographic follow up and an animal experimental study. *Swedish Dental Journal*. 22: 1-10.

-
- Miller WA (1988) Evolution and comparative anatomy of vertebrate masticatory systems. In :*A Text book of Occlusion*. ed Mohl ND, p.27-41. Quintessence Publishing Co, Chicago.
- Moffett BC (1957) The prenatal development of the human temporomandibular joint. *Contributions to Embryology*. 36: 19-23.
- Moffett BC, Johnsson LC, McCabe JB and Askew HC.(1964) Articular remodelling in adult human temporomandibular joint. *American Journal of Anatomy*. 115: 119-141.
- Moore KL (1982) *The Developing Human Clinically Oriented Embryology*. 3rd edition. Saunders, Philadelphia.
- Morani V, Previgliano V, Schierano GM and Ramieri G (1994) Innervation of the human temporomandibular joint capsule and disc as revealed by immunohistochemistry for neurospecific markers. *Journal of Orofacial Pain*. 8: 36-41.
- Morris HR, Panico M, Etienne T, Tippins J, Girgis SI and Macintyre I (1984) Isolation and characterisation of human calcitonin gene-related peptide. *Nature*. 308: 746-748.
- Morris JL, Gibbins IL and Murphy R (1986) Neuropeptide Y like immunoreactivity is absent from most perinsular noradrenergic axons in a marsupial, the brush-tailed possum. *Neuroscience Letters*. 62: 31-37.
- Morris JL and Gibbins IL (1987) Neuronal colocalization of peptides, catecholamines and catecholamines-synthesizing enzymes in the guinea-pig paracervical ganglia. *Journal of Neuroscience*. 7: 3117-3130.

-
- Moskowitz RW (1984) Introduction In: *Diagnosis and Management* ed. Moskowitz RW, p. 29-42. WB saunders, Philadelphia.
- Moskowitz RW and Davis W (1970) Experimentally induced corticosteroid arthropathy. *Arthritis Rheumatology*. 13: 236-243.
- Moskowitz RW and Davis W, Sammarco J, Martens M, Baker J, Mayor M, Burstein AH and Frankel VH (1973) Experimentally induce degenerative lesions following partial miniscetomy in the rabbit. *Arthritis Romatology*. 16:397-405
- Muir C and Goss AN (1990) The radiological morphology of painful temporomandibular joints. *Oral Surgery*. 70: 355-359.
- Murphy TR (1959) The axis of the masticatory stroke in sheep. *Australian Dental Journal* 4: 104-111.
- Murray DG (1964) Experimentally induced arthritis using intraarticular papain. *Arthritis Rheumatology*. 7: 211-219.
- Nakakura-Ohshima K, Maeda T, Sato O and Takano Y (1993) Postnatal development of periodontal innervation in rat incisors; an immunohistochemical study using protein gene product 9.5 antibody. *Archive of Histology and Cytology*. 56 (4) :385-398.
- Nagahara T, Matsuda A, Kadota T and Kishida R (1995) Development of substance P immunoreactivity in the mouse verneronasal organ. *Anatomy and Embryology*. 192: 107-115

-
- Naraine PA (1994) *Ontogeny and Distribution of Osteoarticular Peptide-containing Nerve Endings the Early Development of the Human Knee Joint*. PhD Thesis, University of London.
- Noble HW (1979) Comparative Functional Anatomy of the Temporomandibular Joint In : *Temporomandibular Joint Function and Dysfunction*, eds. Zarb GA and Carlsson GE, p. 15-41. CV Mosby, St Louis.
- Nolte J (1993) *The Human Brain An Introduction to its Functional Anatomy*. 3rd edition. Mosby Year Book, St Louis.
- O' Dell NL, Sharawy M, Pennington CB and Maslow RK (1989) Distribution of putative elastic fibres in rabbit temporomandibular joint tissues. *Acta Anatomischer, Basel*. 135: 239-244.
- Öberg T, Carlsson EG and Fajers CM (1971) The temporomandibular joint. A morphologic study on a human autopsy material. *Acta Odontologica Scandinavica*. 29: 349-355.
- Öberg T and Carlsson EG (1979) Macroscopic and microscopic anatomy of the temporomandibular joint. In: *Temporomandibular Joint Function and Dysfunction* eds. Zarb GA and Carlsson GE, p101-118. CV Mosby, St Louis.
- Ogus H (1975) Rheumatoid arthritis of the temporomandibular joint. *British Journal of Oral Surgery*. 12: 275-284.
- Ogutcen-Toller M and Juniper RP (1993) The embryologic development of the human lateral pterygoid muscle and its relationships with the temporomandibular joint disc and Meckel's cartilage. *Journal of Oral Maxillofacial Surgery*. 51: 772-778.

-
- Parsons FG (1899) The joints of mammals compared with man. *Journal of Anatomy*. 34: 4-68.
- Payan DG. (1989) Neuropeptides and inflammation. The role of substance P. *Annals of Review Medicine*. 40: 341-52.
- Payan DG, Levine JD and Goetzl EJ (1984) Modulation of immunity and hypersensitivity by sensory neuropeptides. 132: 1601-1604.
- Pearse AG and Polak JM. (1975) Immunocytochemical localization of substance P in mammalian intestine. *Histochemistry*. 41: 373-375.
- Pereira de Silva JA and Carmo-Fonseca J (1990) Peptide containing nerves in human synovium: immunohistochemical evidence for decreased innervation in rheumatoid arthritis. *Journal of Rheumatology*. 17: 1592-1599.
- Pernow B (1983) Substance P. *Pharmacological Reviews*. 35: 85-141.
- Philips TW and Gurr K.(1989) A preconditioned arthritis hip model. *Journal of Arthroplasty*. 4: 193-197.
- Piper PJ, Said SI and Vane JR (1970) Effects on smooth muscle preparations of unidentified vasoactive peptides from intestine and lung. *Nature*. 225 : 1144-1146.
- Polacek P (1966) Receptors of the joints: their structure, variability and classification. *Acta Facultatis Medicae University Brunensis*. 23: 1-107.

-
- Polak JM, Steel JH, Suburo AM, Hukknen M, Terenghi G, Sundaresan M, Wharton J, Facer P, Bishop AE, Hitchcock RJI and Moscoso (1991) Developmental patterns of neuronal peptides and hormones in central and peripheral nervous and neuroendocrine system of the human fetus. *Developmental Pathology Society 21st Autumn Meeting*. Institute of Psychiatry, King's College London, 26 September 1991. Abstract.
- Polak JM and Bloom SR (1989) *Regulatory Peptides*. Birkhauser Verlag, Switzerland.
- Ramieri G, Anselmetti GC, Baracchi F, Panzica GC, Viglietti-Panzica C, Modica R and Polak JM (1990) The innervation of human teeth and gingival epithelium as revealed by means of an antiserum for protein-gene product 9.5 (PGP 9.5). *American Journal of Anatomy*. 189: 146-154.
- Ramieri G, Bonardi G, Morani V, Panzica GC, Del Tetto F, Arisio R and Preti G (1996). Development of nerve fibres in the temporomandibular joint of the human fetus. *Anatomy and Embryology*. 194: 57-64.
- Rees LA (1954) The structure and function of the mandibular joint. *British Dental Journal*. 96: 125-133.
- Roberts G W and Allen S (1986) Immunocytochemistry of brain peptides In: *Immunocytochemistry. Modern Methods and Applications*. eds. Polak JM and Van Noorden S, 2nd Edition.p.349-389 John Wright, Bristol.
- Rocubado M (1983) Arthrokinematics of the temporomandibular joint. *Dental Clinics of North America*. 27: 573-576.
- Romph JH, Capre NF and Gatipon GB (1979) Trigeminal nerve and temporomandibular joint of the cat: a horseradish peroxidase study. *Experimental Neurology*. 65: 99-106.

-
- Rosenfeld MG, Amara SG and Evans RM (1984) Alternative RNA processing: Determining neuronal phenotype. *Science*. 225: 1315-1320.
- Rosenfeld MG, Mermodij, Amara SG, Swanson LW, Sawchenko PE, RiverJ, Vaie WW and Evans RM (1983) Production of a novel neuropeptide encoded by the calcitonin gene via tissue specific RNA processing. *Nature*. 304: 129-135.
- Said SI and Mutt V (1970) Polypeptides with broad biological activity. Isolation from the small intestine. *Science*. 169: 1217-1218.
- Said SI (1980) Peptides common to the nervous system and gastrointestinal tract. *Frontiers in Neuroendocrinology*. 6: 293-332.
- Said SI. (1982) *Vasoactive Intestinal Polypeptide*. Raven Press, N.Y.
- Salter RB and Field P (1960) The effect of continuous compression on living articular cartilage. *Journal Bone Joint Surgery*. 42A: 31-49.
- Samuel EP (1952) The autonomic and somatic innervation of the articular capsule. *Anatomical Record*. 113: 53-70.
- Schaible HG HG and Grubb BP (1993) Afferent and spinal mechanisms of joint pain. *Pain*. 55: 5-54.
- Schmid F (1969) On the nerve distribution of the temporomandibular joint capsule. *Oral Surgery, Oral Medicine, Oral Pathology*. 28: 63-66.

-
- Scott JH and Dixon AD (1972) In: *Anatomy for Students of Dentistry*. 3rd edition. Churchill Livingstone, New York.
- Scott JH (1951) The development of joints concerned with early jaw movements in sheep. *Journal of Anatomy*. 85: 36 -45
- Serra MC, Bazzoni F, Bianca VD, Greskowiak M and Rossi F (1988) Activation of human neutrophils by substance P. Effect of oxidative metabolism, exocytosis, cytosolic Ca⁺⁺ concentration and inositol phosphate formation. *Journal of Immunology*.141: 2118-2124.
- Sharawy M, Bhussy BR and Suarez FR (1984) Temporomandibular joint. In: *Orban's Oral Histology and Embryology*. ed Bhaskar SN, 9th edition. p.395-404. Mosby, St Louis.
- Sharpe CJ, Gee E and Griffin CJ (1965). The osteogenic potential of the human condyle. *Australian Dental Journal*. 10: 287-291.
- Sheppard MN, Polak JM, Allen JM and Bloom SR (1984) Neuropeptide tyrosine (NPY): a newly discovered peptide is present in the mammalian respiratory tract. *Thorax*. 39: 326-330.
- Shu S, Ju G and Fan L (1988) The glucose oxidase-DAB-nickle method in peroxidase histochemistry of the nervous system. *Neuroscience Letters* 85: 169-171.
- Sicher H (1951) In: *Temporomandibular Joint*. (ed. Sarnat BG). Thomas, Springfield, Illinois.

-
- Silberman M (1976) Experimentally induced osteoarthritis in the temporomandibular joint of the mouse. *Acta Anatomischer, Basel* 96: 9-24.
- Silva DG (1969) Further ultrastructural studies on the temporomandibular joint of the guinea pig. *Journal Ultrastructure Research*. 26: 148-162.
- Sisask G, Bjurholm A, Ahmed M and Kreicbergs A (1995) Ontogeny of sensory nerves in the developing skeleton. *Anatomical Record*. 243: 234-240.
- Sison S and Grossman JD (1961) *The Anatomy of the Domestic Animals*. 4th edition. WB Saunders and Company, Philadelphia.
- Skoglund S (1956) Anatomical and physiological studies of knee joint innervation in the cat. *Acta Physiologica Scandinavica*. 36: 1-101.
- Skoglund S (1973) Joint receptors and kinaesthesia In: *Handbook of Sensory Physiology Vol. II Somatosensory System*. ed. Iggo A, p.111-136. Springer-Verlag, Berlin.
- Smith GD, Harmar AJ, McQueen DS and Seckl JR (1992) Increase in substance P and CGRP, but not somatostatin content of innervating dorsal root ganglion in adjuvant monoarthritis in the rat. *Neuroscience Letters*. 137: 257-260.
- Snell RS (1992) *Clinical Neuroanatomy for Medical Students*. 3rd edition. Little, Brown and Company, London.
- Solberg KW (1986) Temporomandibular disorders: Functional and radiological considerations. *British Dental Journal* 160: 195-300.

- Stjernquist M, Emson P, Owen C, Sjoberg F, Sundler F and Tatemoto K (1983) Neuropeptide Y in the female reproductive tract of the rat. Distribution of nerve fibres and motor effects. *Neuroscience Letters* .39: 279-284.
- Storey A (1976) Temporomandibular joint receptors. In: *Mastication* .ed. Anderson DJ and Matthews B, p.50-57. John Wright and Sons Ltd, Bristol.
- Storris TJ (1974) A variation of the auriculotemporal syndrome. *British Journal of Oral Surgery*. 2: 236-240.
- Ström D, Holm S, Clemensson E, Haraldson T and Carlsson GE (1988) Gross anatomy of the craniomandibular joint and masticatory muscles of the dog. *Archives of Oral Biology*. 33: 597-604.
- Symons NBB (1952) The development of the human mandibular joint. *Journal of Anatomy, London*. 86: 326-333.
- Tahmasebi-Sarvestani A, Tedman RA and Goss AN (1996) Neural structures within the sheep temporomandibular joint. *Journal of Orofacial Pain* 10: 217-231.
- Tahmasebi-Sarvestani A, Tedman RA and Goss AN (1997) Distribution and co-existence of neuropeptides in nerve fibres in the temporomandibular joint of late gestation fetal sheep. *Journal of Anatomy* (accepted for publication).
- Tatemoto K, Carlquist M and Mutt V (1982) Neuropeptide Y-a novel brain peptide with structural similarities to peptide YY and pancreatic polypeptide. *Nature*. 296: 659-660.
- Thilander B (1961) Innervation of the temporomandibular joint capsule in man. *Royal Schools of Dentistry Stockholm and Umea Transactions*. 7: 1-67.

-
- Thilander B (1963) Innervation of the temporomandibular disc in man. *Acta Odontologica Scandinavica*. 22: 151-156.
- Thompson RG, Doran JF, Jackson P, Schillon AP and Rode J (1983) PGP 9.5- a new marker for vertebrate neurons and neuroendocrine cells. *Brain Research*. 278: 224-228.
- Toller PA.(1961) Osteoarthritis of the mandibular condyle. *British Dental Journal*. 134: 223-231.
- Toller PA.(1973) Osteoarthritis of the mandibular condyle. *British Dental Journal*. 134: 223-231.
- Toller PA and Glynn.N (1976) *Degenerative Disease of the Joint*. Scientific Foundation of Dentistry, London.
- Trias A (1961) Effect of persistent pressure on the articular cartilage. *Journal of Bone and Joint Surgery*. 43B: 376.
- Uddman R, Alumets J, Edvinsson L, Hakanson R & Sundler F (1978) Peptidergic (VIP) innervation of the esophagus. *Gastroenterology*. 75: 5-8.
- Uddman R, Edvinsson L, Ekblad E, Håkansson R and Sundler F (1986) Calcitonin gene-related peptide (CGRP): Perivascular distribution and vasodilatory effects. *Regulatory Peptides*. 15: 1-23.
- Uddman R, Grunditz T and Sundler F (1986) Calcitonin gene-related peptide: a sensory transmitter in dental pulps. *Scandinavian Journal of Dental Research*. 94: 219-224.

-
- Von Euler V S and Gaddum J H (1931) An unidentified depressor substance in certain tissue extracts. *Journal Physiology*. 72: 577-583
- Walker P, Grouzmann E, Burnier M and Waeber B (1991) The role of neuropeptide Y in cardiovascular regulation. *Trends in Pharmacological Sciences*. 12: 111-115.
- Walsh DA, Mapp PI, Wharton RAD, Kidd BL, Revell PA, Blake DR and Polak JM (1992) Localisation and characterisation of substance P binding to human synovial tissue in rheumatoid arthritis. *Annals of Rheumatic Diseases*. 51: 313-317.
- Warwick R and Williams PL (1973). *Gray's Anatomy*. 35th British Edition. Saunders, Philadelphia.
- Weihe E, Reinecke M and Forssmann WG (1984) Distribution of vasoactive intestinal polypeptide-like immunoreactivity in the mammalian heart. Interrelation with neurotensin-and substance P-like immunoreactive nerves. *Cell Tissue Research*. 236: 527-540.
- Wharton J, Polak JM, Bloom SR, Will JA, Brown MR and Pearse AG (1979) Substance P-like immunoreactive nerves in mammalian lung. *Investigation Cell Pathology*. 2 : 3-10.
- Wharton J, Polak JM, McGregor G, Bishop AE & Bloom SR (1981) The distribution of substance P-like immunoreactive nerves in the guinea pig heart. *Neuroscience*. 6: 2193.-98.
- Widenfalk B (1991) Sympathetic innervation of normal and rheumatoid synovial tissue. *Scandinavian Journal of Reconstructive Hand Surgery*. 25: 31-33.

-
- Widenfalk B and Wiburg M (1990) Origin of sympathetic and sensory innervation of the temporomandibular joint. A retrograde axonal tracing study in the rat. *Neuroscience Letters*. 109: 30-35.
- Wiesnfeld-Hallin Z, Hokfelt T, Lundberg JM, Forssmann WG, Reinecke M, Tschopp FA and Fischer JA (1984) Immunoreactive calcitonin gene-related peptide and substance P co-exist in sensory neurons to the spinal cord and interact in spinal behavioral responses of the rat. *Neuroscience Letters*. 52: 199-204.
- Wilkinson TM and Crowley CM (1994) A histologic study of retrodiscal tissues of the human temporomandibular joint in the open and closed position. *Journal Orofacial Pain*. 8: 7-17.
- Wink CS, St Onge M, Zimny ML (1992) Neural elements in the human temporomandibular articular disc. *Journal of Oral Maxillofacial Surgery*. 50: :334-337.
- Woolf CJ and Doubell PT (1994) The pathophysiology of chronic pain-increased sensitivity to low threshold A β -fibre inputs. *Current Opinion in neurobiology*. 4: 525-534.
- Wyke G (1967) The neurology of joints. *Annals of the Royal College of Surgeons, England*. 41: 25-50.
- Wyke B. (1981) Articular Neurology. *Physiotherapy*. 58: 94-99.

-
- Yailen DM, Shapiro PA, Luschei ES, Feldman GR.(1979) Temporomandibular joint meniscectomy-effect on joint structure and masticatory function in *Macaca fascicularis*. *Journal of Oral and maxillofacial Surgery*. 7: 255-230.
- Yung JP, Carpenter P, Margulles-Bonnet R and Meunissier, M (1990) Anatomy of the temporomandibular joint and related structures in the frontal plane.*Journal of Craniomandibular Practice* 8: 101-107.
- Yuodelis R (1966) The morphogenesis of the human temporomandibular joint and its associated structures. *Journal of Dental Research*. 45: 182-191.
- Zamboni L and De Martine C (1967) Buffered picric-acid formaldehyde: a new rapid fixative for electron microscopy. *Journal Cell Biology*. 35: 148A.
- Zhou XF, OI MT, Reid J, Vahaviolos AP, Tafreshi and Rush RA (1996) Evidence that neurotrophin 3 is a target-derived neurotrophic factor for sympathetic neurons in rat. *Proceedings of the Australian Neuroscience Society*. 7: 17-3
- Zimny C (1988) Mechanoreceptors in articular tissues. *American Journal of Anatomy*. 182: 16-32.
- Zimmy ML, St Onge M and Schutte M (1985) A modified gold chloride method of the demonstration of nerve endings in frozen sections. *Stain Technology*. 60: 305-306.
- Zimmy ML and St Onge M (1987) Mechanoreceptors in the temporomandibular disk (abstract no. 1048). *Journal of Dental Research*. 66: 237.

CHAPTER 8

APPENDICES

APPENDIX 1

Zamboni's fixative

0.2 M phosphate buffer.

Solution A- dissolve 31.2g $\text{NaH}_2\text{PO}_4 \cdot 2\text{H}_2\text{O}$ in 800ml distilled water, then adjust volume to 1 litre.

Solution B- dissolve 28.4g NaH_2PO_4 anhydrous in 800ml distilled water, then adjust volume to 1 litre.

1. Take 77ml solution B and add 23ml of solution A until pH is 7.2-7.4 (pH can be adjusted by adding small amounts of either A or B: solution A= pH acid; solution B= alkaline)
2. The above solution should be diluted 1:1 with distilled water to obtain 0.1 M solution before dissolving paraformaldehyde.
3. Dissolve 20g paraformaldehyde in 800ml of 0.1M phosphate buffer with heat (max 60° C) and stir until solution is clear. Adjust the volume to 1 litre and leave to cool.

Mix the following:

85 ml of 2% paraformaldehyde in 0.1M phosphate buffer (pH 7.4) and 15ml saturated picric acid

Store at +4° C.

APPENDIX 2

SUMMARY OF STATISTICS USED FOR TMJ ANALYSIS

A general linear model analysis using program 3V from the BMDP statistical software package (Dixon, 1991) was used to analyse the quantitative results. The analysis used a random effect for sheep and fixed effects for stain, side, region, arthritis and interactions between stain, side, region and pathology (arthritis vs normal). To test for robustness of distributional assumptions, the analysis was done on both the log scale and after a square root transformation. The conclusions were identical.

The general linear model is a variation of an analysis of variance, sometimes called a mixed model of analysis of variance because it has fixed effects and random effects. It uses similar F tests.

The model utilises the following formula:

$$Y_{ijklmn} = \mu + A_i + S_j + P_m + (St)_k + R_l + (S.St)_{jk} + (S.R)_{jl} + \dots + E$$

where:

i denotes animal (number)

j denotes side (L or R)

k denotes stain (PGP 9.5 or CGRP)

l denotes region (anterior, posterior, medial, lateral)

m denotes experiment (normal or arthritis)

n denotes number of observations for a particular combination of features eg side, stain, region, experiment

A represents animals

S represents side

P represents experiment

St represents stain

R represents region

S.St represents the potential combination effect of side and stain or side/stain interaction

S.R represents the potential combination effect of side and region or side/region interaction

E represents the random error (nature's variation)

Fixed effects are side, stain, region and experiment ie they are repeatable

Random effects are animal because they are individuals selected from a larger population and E

E is assumed to be normally distributed about a zero mean with variance (sigma squared) σ^2

Animals are also assumed to be normally distributed about a zero mean

Program 3V calculates a numerical value for each item as well as sigma squared and sigma a squared

These are estimates and subject to error and the error is used in the statistical test of whether the effect is truly there ie is the estimate for each parameter statistically different from zero using F tests. F tests are done on degrees of freedom that reflect the parameter and sample size for that parameter.

Data were (i) used as actual values, (ii) subjected to a square root transformation or (iii) subjected to a log transformation before being applied to the model. This was to check the normality assumptions for animals and sigma